Liposomal Nanomedicine with Short Chain Sphingolipids Modulate Tumor Cell Membrane Permeability and Improve Chemotherapy

Lília Raquel Cordeiro Pedrosa

ISBN: 978-94-6169-549-9

© Lília Raquel Cordeiro Pedrosa, 2014

No part of this thesis may be reproduced, stored or transmitted in any form by any means without prior written permission from the author.

Financial support for printing of this thesis was obtained from KWF Kankerbestrijding, Ceronco Biosciences B.V.

Printing by Optima Grafische Communicatie, Rotterdam, The Netherlands

Cover Design: Miguel Taborda

Liposomal Nanomedicine with Short Chain Sphingolipids Modulate Tumor Cell Membrane Permeability and Improve Chemotherapy

Liposomale nanomedicijnen met kort-ketenige sfingolipiden moduleren tumorcel membraan permeabiliteit en verbeteren chemotherapie

Thesis

to obtain the degree of Doctor from the Erasmus University Rotterdam
by command of the rector magnificus Prof.dr. H.A.P. Pols
and in accordance with the decision of the Doctorate Board

The public defense shall be held on
Wednesday 10 September 2014 at 11.30 hours

By

Lília Raquel Cordeiro Pedrosa
born in Coimbra, Portugal

Erasmus MC
University Medical Center Rotterdam

DOCTORAL COMMITTEE

Promoters:

Prof.dr. A.M.M. Eggermont

Prof.dr. M. Verheij

Other members:

Prof.dr.ir. M. Hendriks-de Jong

Prof.dr. C.C. Baan

Prof.dr. G. Storm

Copromoter:

Dr. G.A. Koning

"i carry your heart with me(i carry it in
my heart)i am never without it(anywhere
i go you go,my dear;and whatever is done
by only me is your doing, my darling)
here is the deepest secret nobody knows

(here is the root of the root and the bud of the bud
and the sky of the sky of a tree called life, which grows
higher than soul can hope or mind can hide)
and this is the wonder that's keeping the stars apart

i carry your heart (i carry it in my heart)."

Eu levo o teu coração comigo (eu o levo
no meu coração) eu nunca estou sem ele (a qualquer lugar
que eu vá, meu bem, e o que quer que seja feito
por mim somente é o que tu farias, minha querida)

aqui está o mais profundo segredo que ninguém sabe
(aqui é a raiz da raiz e o botão do botão
e o céu do céu de uma árvore chamada vida, que cresce
mais alto do que a alma possa esperar ou a mente possa esconder)
e isso é a maravilha que está mantendo as estrelas distantes

Eu levo o teu coração (eu o levo no meu coração).

e.e.cummings

To my mother,
à minha mãe

CONTENTS

CHAPTER 1

General Introduction
and Aim of the Thesis

INTRODUCTION

Chemotherapy

According to WHO statistics, cancer causes approximately 7.9 million deaths worldwide each year. Breast and prostate cancer are the most commonly occurring cancers among women and men, respectively in both Europe and US [1, 2]. Despite advances in prevention, early diagnosis, and therapy, prognosis for a majority of the cancer patients remains poor. Cancer treatment consists of a multimodal approach which may include a combination of surgery, chemotherapy, radiation therapy, hormone therapy, targeted therapies and immune therapy depending on tumor and patient characteristics [3]. Conventional chemotherapy uses cytotoxic or cytostatic drugs to suppress tumor growth. Chemotherapeutic drugs can be divided in several groups depending on their mechanisms of action. Alkylating agents (Nitrosoureas, Cyclophosphamide and Platinum drugs) are able to directly damage the DNA [4]; Antimetabolites (5-fluorouracil (5-FU), Cytarabine, Capecitabine or Methotrexate) interfere with DNA and RNA synthesis and induce cell death at S-phase of the cell cycle [5]; Topoisomerase inhibitors such as Topotecan and Etoposide interrupt DNA replication in tumor cells [6]; Alkaloids, also known as mitotic inhibitors (Taxanes or Vinca Alkaloids), disrupt mitotic processes by interfering with microtubular dynamics required for proper mitotic function resulting in cell cycle blockade and apoptosis [7, 8]. Antitumor antibiotics are natural products produced from Streptomyces bacteria and interfere with cellular processes inhibiting DNA/RNA synthesis. As subgroups, antitumor antibiotics include anthracyclines (Doxorubicin or Daunorubicin, Idarubicin) [9], anthracenediones (Mitoxantrone) [10, 11], Chromomycines (Dactinomycin) [12], Bleomycin [13] and Mitomycin C [14].

Hormonal agents such as corticosteroids and sex hormones like Tamoxifen [15] and Leuprolide [16] are also applied in chemotherapy. Corticosteroids are mainly used in supportive care to relieve pain or reduce immune responses. It can also be synergetic with other drugs inducing apoptosis. Examples are dexamethasone, hydrocortisone, prednisone or methylprednisolone [17].

Anthracyclines, from the class of antitumor antibiotics continue to play an important role in the treatment of many forms

of cancer, including hematological malignancies and solid tumors [18]. Anthracyclines are derived from Streptomyces bacteria and display strong anti-tumor activity. They are red-colored aromatic compounds that may occur in variety of forms with structural differences in the aglycone moiety or sugar residues [9]. Most widely used anthracyclines are daunorubicin, approved for acute lymphoblastic and myeloblastic leukemia [19], epirubicin, for gastric and breast cancer treatment [19]. Idarubicin is used for acute myelogeneous leukemia [19] and valrubicin for early bladder cancer [20]. Finally, Doxorubicin (Dox), also named Adriamycin, is applied in cervical, endometrial, prostate and pancreatic cancer, head and neck, adrenal cortex, bone, lung and breast cancer and other malignancies such as multiple myeloma and soft tissue sarcoma [21]. Dox acts on tumor cells through multiple pathways including intercalation between adjacent base pairs of the DNA double helix, binding to DNA-associated enzymes such as topoisomerase, an enzyme involved in control of DNA topology through breaking and rejoining double-stranded DNA and formation of free radicals that induce membrane damage by lipid peroxidation [9, 22].

Despite Dox clinical efficacy, its application is dose limited by severe toxicity. Acute toxicity involves myelosuppression, nausea, vomiting, mucositis and alopecia. Yet, chronic cardiomyopathy and congestive heart failure represents the most important clinically reported toxicity for Dox [23, 24]. Cardiotoxicity is a cumulative dose-dependent toxicity, which prevents continued use of Dox in cancer patients and its use in patients at cardiac risk.

Mitoxantrone (MTO), commercialized as Novantrone has gained importance in the treatment of metastatic breast cancer over the use of anthracyclines [25, 26] due to its similar therapeutic activity and lower drug toxicity at equal doses [27, 28]. MTO cardiotoxicity was demonstrated to be absent in pre-clinical studies. Yet, in clinical trials it has been shown to have an anthracycline-like cardiotoxicity profile mainly by MTO cumulative dosing or when prior Dox therapy is administrated [29].

MTO is a synthetic anthracycline related compound of the anthracenedione class and the most potent of many ametantrone derivatives [25, 30, 31]. Ametantrone analogues differ from one another in the position of side chain or functionalities on the

chromophore group displaying different biological activities [11]. MTO is used mainly in the treatment of recurrent breast cancer [26], prostate cancer [32] leukemia [33] and multiple sclerosis [34]. Similarly to Dox, nuclear DNA is the major target for MTO [35-37]. MTO binding to DNA induces DNA condensation, inhibiting replication and RNA transcription. MTO is also a potent inhibitor of topoisomerase II [31]. Leucopenia is the dose-limiting adverse effect by MTO chemotherapy. Also non-hematological adverse effects are described like nausea, vomiting, diarrhea, abdominal pain, stomatitis, infections and alopecia [30]. Generally, the safety and efficacy of conventional intravenous chemotherapy is severely limited by its toxicity. The systemic toxicity of cytotoxic drugs is related to their large volume of distribution, which brings the drug not only to the tumor site, but also to the majority of other healthy organs and tissues. In addition, their general short circulation half-life limits tumor accumulation and requires administration of high drug doses to achieve sufficient therapeutic efficacy, contributing however also to toxicity. Insufficient uptake of chemotherapeutic agents across the cell membrane of tumor cells represents a final important obstacle in clinical cancer chemotherapy success.

The complex and heterogeneous composition of the plasma membrane and the presence of caveolae and lipid rafts composed of high levels of sphingolipids, make the plasma membrane a mosaic-like patchwork [38, 39] with a differentiated lipid distribution. This lipid complexity makes the cell membrane selectively permeable and affects drug passage for various classes of drugs. In cancer cells the lipid membrane composition is subject to alterations in relation to the normal healthy cells with differentiated levels of major classes of lipids – phosphatidylcholine (PC), phosphatidylethanolamine (PE), phosphatidylserine (PS), sphingomyelin (SM), phosphatidylinositol (PI) [40]. In addition, differences in membrane lipid profile of drug sensitive and resistant cells were described to affect membrane fluidity and induce changes in sphingolipid content in drug resistant cells [41]. In resistant vinblastine leukemic T-lymphoblasts, cells displayed elevated cholesterol and phospholipid levels and an increase in multidrug transporters/ lipid ratio in relation to membranes of sensitive cells, suggesting that multidrug transporters overexpression can be influenced by

their lipid environment [40, 42]. Sphingolipids and cholesterol play also a crucial role as constituents of caveolae and membrane rafts [43]. These microdomains have specific functions in lipid trafficking, cell signaling and provide lodging for proteins involved in mechanisms of multidrug resistance that act as drug pumps [38, 44]. Drug pumps such as the transmembrane protein P-glycoprotein and multidrug resistance – associated protein (MRP) belong to the protein superfamily denominated by ABC-transporters and compete actively with inward passive drug transport across the membrane [45, 46].

In summary, clinical success of chemotherapy is hampered by several factors such as suboptimal dosing due to systemic toxicity, rapid drug clearance from the circulation, low levels of drug accumulating in tumors and limited drug traversal across the tumor cell membrane, leading to an unfavorable therapeutic index. Decreasing toxicity to healthy tissues and increasing drug accumulation in tumors and delivery across the tumor cell membrane represent major challenges to improve cancer chemotherapy.

Nanoparticle-based drug delivery technologies are emerging as powerful chemotherapeutic modalities in cancer therapy [47-49]. For example, liposomes are well described to decrease drug toxicity profiles by limiting normal tissue exposure to the drug, which remains encapsulated in the nanoparticle and thereby confined to the blood circulation. Liposomal drug delivery can improve drug accumulation in the target tumor tissue by reducing fast drug clearance rates relative to free drug and by virtue of the enhanced permeability and retention (EPR) mediated tumor accumulation described for nano-sized drug delivery systems [50].

To overcome the final barrier, the tumor cell membrane, the use of short chain sphingolipids (SCS) represents a promising way to improve drug delivery by targeting and modulating tumor cell membrane permeability.

Liposomes as drug delivery systems

Application of liposomal drug carrier technology is one of the best-known and developed ways to improve the therapeutic index of anticancer drugs [47, 51].

Liposomes are nanovesicles with a membrane composed of phospholipids (PLs) enclosing a hydrophilic interior (Fig. 1).

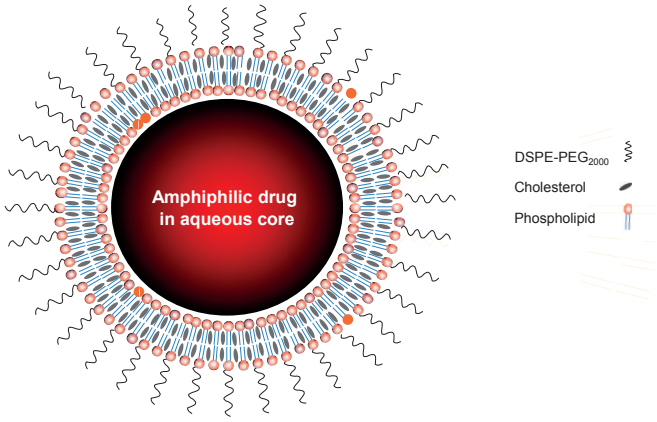

Figure 1 - Liposome illustration

PLs are amphipathic compounds with a polar phosphate headgroup and lipophilic acyl chains.

PLs are classified based on polar headgroup composition, backbone, acyl chain length and the degree of saturation of the acyl chains. Two main classes of phospholipids exist depending on whether they contain a glycerol (phosphoglycerol lipids) or a sphingosine backbone (sphingomyelin). For liposomal formulation mainly glycerophospholipids are used. However, a sphingomyelin/cholesterol composition is successfully used for the formulation of liposomal vincristine, commercially named as Marqibo [52]. Glycerophospholipids consist of two chains of fatty acids that via ester bonds at the sn1 and sn2 positions are connected to a glycerol backbone with a polar phosphate head group, like phosphatidylcholine (PC), phosphatidylserine (PS), phosphatidylethanolamine (PE) and phosphatidylglycerol (PG) at the sn3 position (Fig. 2).

Phospho-sphingolipids are part of a class of sphingolipids that contain a sphingoid long-chain base (e.g. sphingosine) linked to a fatty acid molecule through an amide bond, constituting the ceramide unit (Fig. 3). Sphingomyelin and glycosphingolipids both belong to the class of sphingolipids, but differ in the ceramide attached head group being a phosphocholine or carbohydrate, respectively. Like PLs, sphingolipids are amphipathic compounds and at a cellular level associated with signaling pathways that influence cell proliferation, senescence, inflammatory responses and apoptosis [53]. Effector molecules from the sphingolipid family include ceramide, sphingosine and sphingosine-1-phosphate [54].

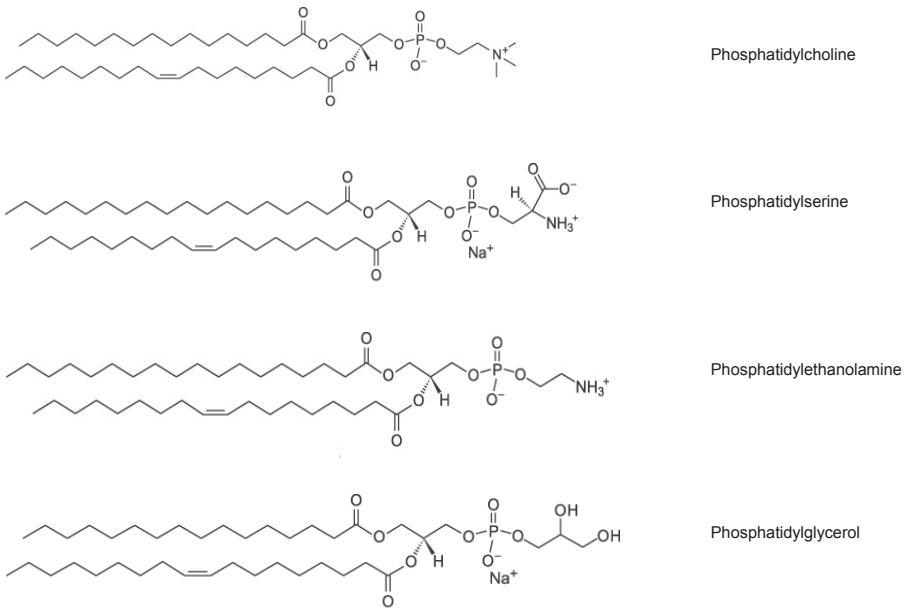

Figure 2 - Molecular structures of glycerophospholipids. Molecular structures were designed in Chem Draw Ultra 8.0

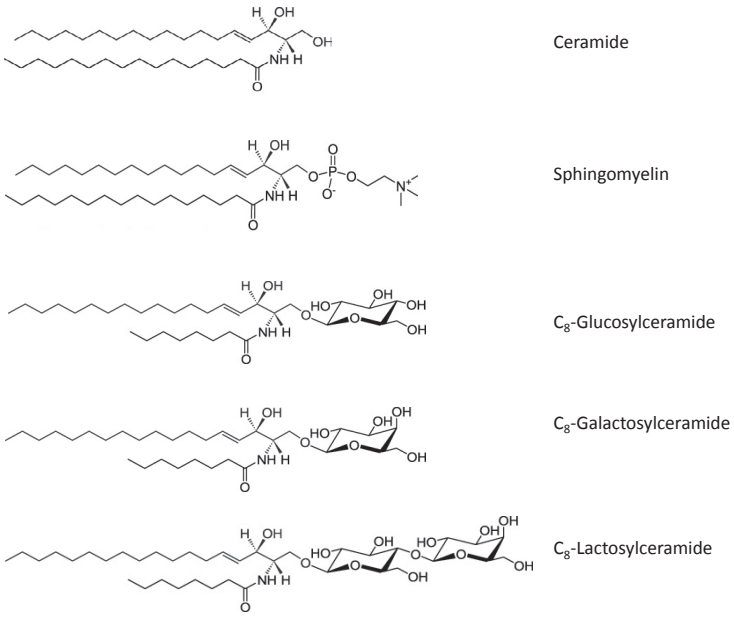

Figure 3 - Molecular structures of ceramide and sphingomyelin and short chain glycosphingolipids (C_8-Glucosylceramide, C_8-Galactosylceramide and C_8-Lactosylceramide). Molecular structures were designed in Chem Draw Ultra 8.0

In aqueous medium, PLs can be cationic, anionic or zwitterionic, depending on the pH of the solution. For instance, PC is zwitterionic and can form lamellar structures independent of pH. In contrast, PE at physiologic pH presents a zwitterionic headgroup unable to form lamellar structures, but at strongly basic pH, the respective headgroup is charged and able to form lamellar structures [55]. Bilayers are formed because of the amphipathic character of phospholipids, which align their hydrophobic tails together to form an inner layer shielded from water while the polar head groups hydrated by water provide a thin shell at the outer layers, mimicking cell membrane architecture [56, 57].

Liposomes are biocompatible carriers existing in unilamellar or multilamellar morphology with one or more bilayers, respectively. Multilamellar liposomes can be converted to unilamellar vesicles by freeze-thaw, sonication or extrusion [58] of different size and broad range of pharmaceutical applications [59-61].

Originally, Gregoriadis and Rymann introduced the concept of liposomal drug delivery by entrapping drugs and change their *in vivo* distribution to improve efficacy and drug safety [62]. Liposomes with a hydrophilic core sealed by a PL bilayer were used to entrap either hydrophilic drugs in the liposomal core or lipophilic drugs in the bilayer. PLs can consist of different head and tail groups that affect the surface charge and bilayer permeability of the liposomes. The surface charge of liposomes can be tailored in order to modulate electrostatic repulsion and stabilization against liposome fusion [63].

The first liposome-entrapped drug formulations were cytosine arabinose, amphotericin B and Dox [47]. The latter is described as the first nanoliposomal formulation achieving FDA-approval [64]. Further liposomal optimization for drug delivery included incorporation of cholesterol and poly(ethylene glycol) (PEG)-lipids (DSPE-PEG_{2000}) into the liposomal bilayer. Cholesterol is an amphipathic compound able to incorporate itself in the phospholipid liposomal bilayer enhancing the liposomal membrane stability by forming a highly ordered and rigid membrane [47, 65]. Yet, DSPE-PEG_{2000} is a non-biodegradable polymer linked to a lipid anchor with a very low toxicity profile that provides a steric barrier at the liposome surface. Its flexible chains form “brush” or “mushroom” configurations depending on the length and density

of PEG-lipids [66, 67], extending out from the surface thereby preventing interaction of liposomes with opsonins and subsequent uptake by phagocytic cells. Liposomes composed of DSPE-PEG_{2000} are known as "stealth liposomes", and have good solubility properties in aqueous media [68, 69], preventing liposomal clearance by cells of the Mononuclear Phagocytic System (MPS) in spleen and liver (Kupffer cells) by inhibition of nanocarrier recognition [70-72]. Thereby, liposomal drugs remain longer in circulation and by virtue of the enhanced permeability and retention effect (EPR) in solid tumors, liposomes are able to accumulate at the tumor site for drug delivery [50, 70, 73]. The EPR effect results in the extravasation of macromolecules or nanoparticles through the characteristic leaky tumor vasculature. The leaky tumor vasculature is generated by immature and disorganized angiogenic vessels that contain large endothelial cell-cell gap openings of 100-800 nm in contrast to 6 nm in healthy tissue [73]. The leakiness of tumor vasculature is variable between tumors or within a tumor, and liposomal extravasation is size-dependent and described to be optimal at sizes of 150 nm or less [73]. Vascular permeability regulating factors such are bradykinin, nitrogen monoxide (NO), prostaglandins, vascular endothelial growth factors (VGF or VEGF), tumor necrosis factor alpha (TNF-α) facilitate the EPR effect in tumor tissue. In normal healthy tissue these factors are not activated [50]. Besides the defective architecture of tumor vasculature, an impaired lymphatic drainage in the tumor favors the retention of macromolecules and nanoparticles in tumor tissue. Yet, the intrinsic heterogeneity of tumors and tumor vasculature [74, 75] causes heterogeneous nanoparticle accumulation and drug distribution and will thus exert limited efficacy in less accessible sites. In addition, relatively large nanoparticles such as liposomes will not penetrate deeply into tumor interstitium [76] limiting efficacy at sites located at further distance from supplying vessels [77]. To circumvent this problem, strategies such as mild hyperthermia [78, 79] or use of TNF-α [80] may be applied to improve tumor vessel permeability to liposomes for a better tumor response.

Liposomes should also be biocompatible, meaning not interacting with blood components or blood vessels, not expressing antigenicity or be cleared out by the reticulum endothelial system and not be subject to cell lysis [50, 81]. In this view, liposome surface

charge is important and should be neutral or weakly negative, since particles with high negative charges are taken up by the liver and positively charged particles bind to the luminal surface of vessels, proteins or blood cells causing rapid clearance as well [50].

Currently, several different liposome-based drugs have been approved for clinical use and many more are in different stages of clinical development [47, 82]. Approved and commercially available are DaunoXome (liposomal daunorubicin), Ambisome (liposomal amphotericin B), Visudyne (liposomal verleporfin), Depocyt (liposomal cytarabine), DepoDur (liposomal morphine sulphate) and Doxil/Caelyx, Lipo-Dox, Myocet for liposomal doxorubicin. Examples of liposomal formulations in clinical development are LEP-ETU (liposomal paclitaxel), Marqibo (liposomal vincristine), ThermoDox (liposomal Dox), Lipoplatin (liposomal cisplatin), Alocrest (liposomal vinorelbine) and Brakiva (liposomal topotecan) [47, 82].

Liposomal Chemotherapy

Liposomal Doxorubicin

Caelyx (in Europe) also known as Doxil (in USA) is a PEGylated "stealth" liposomal formulation of Dox (PLD) and the most often applied liposomal chemotherapeutic drug formulation worldwide. Dox encapsulation in liposomes can improve its anti-tumor activity [83-85]. Dox, an amphipathic weak base is encapsulated in liposomes by a remote loading method [70, 86]. Dox loading into liposomes composed of hydro soy phosphatidylcholine (HSPC), cholesterol and DSPE-PEG_{2000} [59] is based on a transmembrane ammonium sulphate gradient. During remote loading at a temperature above the phase transition of the main phospholipid, for HSPC above 56°C, unprotonated Dox from the extraliposomal neutral pH environment passes the liposomal bilayer reaching the low pH liposome core where it gets protonated and precipitates with sulphate ions.

Dox molecular intercalation occurs with itself and sulphate anions and intraliposomal precipitation promotes continuous inward doxorubicin transport resulting in high levels of entrapped drug. The highly concentrated Dox content can be visualized by Cryo-TEM as electron dense nanocrystalline fibers in the liposomal core resulting in non-spherical, rod-like structures [70, 87].

By encapsulating Dox in PEGylated liposomes its volume of distribution is lowered, circulation half-life is enhanced and severe side effects such as cardiotoxicity and myelosupression are circumvented, enabling administration of higher doses and improving therapeutic outcome [88-90]. However, a new dose limiting side effect has been observed; palmar-plantar erythrodysesthesia (PPE) also named hand-foot syndrome. This toxicity is caused by accumulation of PLD in the skin and subsequent slow drug release, causing local toxicity [91, 92]. PLD is currently approved for AIDS-related Kaposi's sarcoma [93], refractory ovarian cancer [94], myeloma [95] and metastatic breast cancer [96, 97] treatment. In addition, PLD is applied clinically in prostate [98, 99], head and neck [100] and ovarian cancer treatment [101]. PLD presents a favorable pharmacokinetic profile and small size of 80-90 nm [70], enabling extravasation through leaky vasculature and accumulation within the tumor. Yet, it was demonstrated that liposomal tumor uptake was heterogeneous among different tumor types and even among different patients with the same tumor type [102]. Importantly, liposomal delivery of Dox content into tumor cells remains a major challenge. PLD is characterized by high stability due to use of rigid phospholipids and cholesterol, which efficiently prevents drug release in circulation, but also is a major cause for slow and suboptimal drug delivery into tumor cells upon accumulation in the tumor area [59, 80, 103]. The mechanism of liposomal drug release and intracellular delivery are still largely unknown. Some authors suggest drug release in the interstitial space by liposomal degradation followed by intracellular Dox diffusion [59, 80]. Others proposed a role for tumor associated macrophages (TAM) in drug release from liposomes [104], whereas it has also been described that tumor uptake of liposomal drugs does not correlate with the presence of TAM [105, 106]. Seynhaeve *et al.* described that in addition to passive release, PLD may be taken up by tumor cells and upon intracellular liposomal degradation slowly render bioavailable Dox reaching the nucleus, effecting anti-tumor activity [80]. However, PLD is neutrally charged and due to the PEGylated surface liposomal uptake is unlikely to be a very efficient process. Therefore, inadequate and uncontrolled Dox release in combination with the tumor cell membrane barrier are important factors limiting

intracellular drug bioavailability and therapeutic success of PLD in cancer patients.

Myocet is a non-PEGylated liposomal (NPLD) formulation of Dox citrate complex composed of phosphatidylcholine and cholesterol [107] and has been used clinically in breast cancer combined with cyclophosphamide [47]. Myocet is a formulation of conventional liposomes and its pharmacokinetic and toxicity profile differs from PLD. The absence of DSPE-PEG_{2000} and a larger average particle size (~ 190 nm) than PLD favors clearance of NPLD by the RES [108]. In addition, liposomal stability might be affected by plasma proteins, which interact with liposomes resulting in lipid exchange and subsequently liposomal rupture and release of entrapped drug contents [109]. In terms of toxicity, leukopenia is the dose limiting toxicity and PPE or hand-foot syndrome is rarely observed in contrast to PLD [99], which likely reflects the differences in circulation time [110]. Importantly, cardiac and gastrointestinal toxicity were prevented upon liposomal encapsulation in comparison to free Dox [110, 111]. In terms of efficacy NPLD was shown to have at least similar anti-tumor activity as conventional Dox [112].

Liposomal Mitoxantrone

Although MTO has been developed as a less toxic alternative to Dox, it still exerts considerable toxicity [36, 113], for which liposomal encapsulation could offer a solution. Different preparation methods have been described for MTO containing liposomes [114-116]. Remote loading of chemotherapeutic drugs into small unilamellar vesicles (SUVs) is of proven advantage in terms of high entrapment levels and safety in the preparation procedure [86] and proved efficacious for MTO as well [114, 115, 117].

Yet, progress into clinical application of MTO-liposomes has been limited to a Phase I study of a non PEGylated formulation containing MTO and composed of DOPC, cholesterol and cardiolipin in a molar ratio of 90:5:5 in patients with leukemia, breast, stomach, liver and ovarian cancer [82]. Although novel PEGylated and more stable formulations have been developed, these so far have not been applied clinically [115-117]. Like Dox, MTO encounters similar drawbacks as a liposomal formulation for which improvement of drug bioavailability and intracellular delivery remain major challenges to improve liposomal chemotherapy.

Strategies to Improve (Liposomal) Drug Bioavailability

Liposomes are versatile carriers that offer several strategies for improved drug bioavailability. Passive targeting describes the process of intratumoral liposome accumulation depending on the EPR effect. In addition, liposomes can be coupled to active targeting ligands to direct these specifically to cell surface receptors that are specific for or overexpressed by cancer cells [118, 119]. Optimal use of active targeting will result in similar liposome biodistribution and accumulation at the target tissue as non-targeted liposomes [120, 121], but has the benefit of improved receptor-mediated liposomal uptake by tumor target cells and intracellular drug delivery of molecules that are not able to cross the cell membrane autonomously [122]. Antibodies are the most commonly used biomolecules applied as active targeting ligands against tumor associated antigens [123-125]. Also hormones [126], folate [127] or peptides [128-131] which are directed towards normal cellular receptors that are overexpressed in certain tumor cells [48] are in development for active liposomal targeting application.

Another attractive strategy to improve drug bioavailability uses triggered release to induce a stable carrier to release its content [132]. Tumor specific triggers can be remote or local. Remote triggering involves application of ultrasound [133], UV or visible light [134] and mild heat (39-43°C) [78, 79, 132, 135] to the tumor to induce liposomal drug release. Thus far, the most successful application of triggered drug release, which currently is in clinical phase III, is the combination of hyperthermia and ThermoDox, a thermosensitive liposomal formulation containing Dox that releases drug in response to mild hyperthermia [136, 137].

Local triggers may involve specific enzymes overexpressed in the tumor such as phospholipase C [138], phospholipase A2 [139], matrix metalloproteinases [140] or pH differences in combination with specific liposome design for local activation of liposomal release of bioavailable drug into the tumor microenvironment [77, 141].

Importantly, mechanisms of trigger-specific release from liposomal delivery systems in most cases involve modifications that have a liposome membrane destabilizing effect which compromises the systemic stability of the carrier and counteracts the diminished toxicity that liposomal encapsulation normally offers.

Nevertheless, even after applying most of the above strategies for improved drug bioavailability, drugs are still confronted with an additional barrier, i.e. the plasma membrane.

Short chain sphingolipids and cell membrane

As mentioned earlier, the cell membrane represents a final strong and limiting barrier for drug passage and intracellular drug influx due to its dynamic complexity and lipid heterogeneity [38]. The lipidic arrangement of the cell membrane involves a majority of sphingo- and glycerophospholipids (SM, PC, PS, PI and PE) next to cholesterol [142, 143] with an asymmetric distribution between the exoplasmic leaflet enriched in SM and PC [143] and the cytoplasmic leaflet preferentially containing the aminophospholipids, PS and PE [143]. The inward movement of PC and SM from the outer to the inner leaflet of the plasma membrane is a slow process under normal conditions mainly because of cholesterol and SM packing. Cholesterol interacts with membrane phospholipids and sphingolipids, affecting membrane condensation with increased packing density of the phospholipids [144]. For PS and PE a rapid and active ATP-dependent protein-mediated transport from the outer to the inner leaflet provides the basis of the asymmetry [145]. Once lipid asymmetry is established it is maintained by membrane passive lipid flip-flop between membrane leaflets with protein-lipid interactions and protein mediated transport such are flippases, floppases and scramblases [145, 146]. Flippases are mainly responsible for the transport of PS from the outer monolayer to the cytoplasmic leaflet. Floppases selectively catalyze the efflux of cholesterol and PC. Scramblases, which are ATP-energy independent, but calcium activated upon cell stimulation, are non-specific for phospholipid distribution between membrane leaflets [147]. Maintenance of cell membrane asymmetry is crucial in cellular homeostasis. For instance, PS exposure at the plasma membrane is an important signal both in the recognition and phagocytosis of apoptotic cells and in the activation of blood coagulation [148].

In addition to their role in cell membrane structure, ceramides and other sphingolipids, participate in a variety of cellular signaling pathways. Examples include regulating differentiation, proliferation, interplay with proteins and programmed cell death [54, 149].

Sphingolipids have a sphingosine backbone where the functional amino group at position C2 is acylated with a fatty acid. Ceramide has a free functional hydroxy group (-OH) at position C1, whereas in sphingomyelin this position is O-linked to a charged head group (phosphocholine). In glycosphingolipids such as glucosyl- or galactosylceramide the C1 hydroxy group is linked to a sugar moiety (Fig. 3).

When interacting with phospholipid monolayers or bilayers, ceramides are described to increase the molecular order of phospholipids [150], to induce lateral phase separation, domain formation [151] and transient nonlamellar structures in the membrane. Also transbilayer lipid motion [152, 153] and membrane permeability [154] are processes modulated by ceramides [155]. On the other hand, cell membrane microdomains (lipid rafts and caveolae) are formed on the basis of the auto-organizing properties of sphingolipids [39, 44] both with themselves and in association with cholesterol [156] contributing to local differences in lipophilicity, membrane fluidity, and lipid packing affecting cellular transmembrane permeability [38].

The short chain sphingolipid (SCS) analogues N-hexanoyl-sphingomyelin and N-octanoyl-glucosylceramide (GC) have been described to enhance membrane traversal of amphiphilic drugs, such as Dox, improving intracellular delivery [157]. The underlying mechanism has been studied extensively and studies thus far indicated that it did not involve aspecific detergent-like membrane disruption, enhanced endocytosis, or decreased ABC transporter mediated efflux nor involved natural lipid rafts [157]. Therefore, SCS are thought to enhance tumor cell membrane permeability, by the potential of glycosphingolipids to form specific permeable microdomains that contribute to amphiphilic drug uptake enhancement. SCS are proposed as a novel drug delivery approach enhancing drug bioavailability at the tumor site through the use of nanoscaled liposomes carrying both the lipid and the drug [158-160].

It is hypothesized that upon cellular contact, SCS spontaneously relocate from the liposomal to the plasma membrane where they self-organize into specific microdomains. The short acyl chains of the SCS lead to imperfect lipid packing and hence create local differences in membrane fluidity and lipophilicity. This sequence

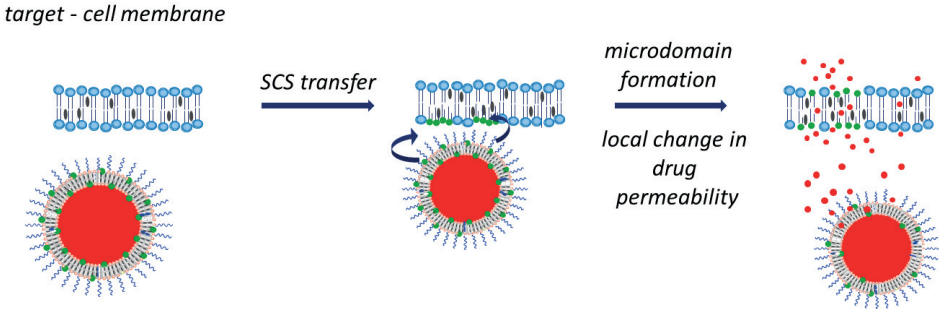

Figure 4 - Illustration of hypothesized SCS mechanism of action. SCS from the liposome bilayer are transferred to tumor cell membranes creating domains with enhanced drug permeability. Next, improved intracellular drug influx across the cell membrane occurs in the permeabilized membrane areas

of events likely leads to changes in membrane permeability and promotes transmembrane diffusion of amphiphilic drugs (Fig. 4).

AIM OF THE THESIS

The aim of the work described in this PhD thesis is to develop and apply nano targeted drug delivery systems for different cytostatics (Dox and MTO) and different lipids (C_8-GluCer, C_8-GalCer and C_8-LacCer) with improved drug delivery. Pharmaceutical optimization and development of new formulations, which benefit from reduced toxicity through nanoliposomal drug encapsulation and enhanced cellular drug delivery by short chain sphingolipid (SCS)-mediated tumor cell membrane permeabilization, are presented together with exploration of the mechanism behind the potential of SCS as drug uptake enhancers.

From the available SCS with proven drug enhancing properties, glycosphingolipids of N-acyl short chain of 8 carbons: C_8-glucosylceramide (C_8-GluCer), C_8-galactosylceramide (C_8-GalCer) or C_8-lactosylceramide (C_8-LacCer) (Fig. 3) were selected for insertion into the nanoliposomal bilayer for co-delivery with chemotherapeutic drugs to tumor cells. Two different amphiphilic cytotoxic agents were tested in parallel, Dox and MTO.

At first, optimization of SCS-nanoliposomes containing Dox, a critical step towards development of this formulation for clinical application, is performed for C_8-GluCer enriched Dox

liposomes [158]. Alongside, novel Dox-nanoliposomal formulations with different synthetic glycosphingolipids C_8-Galcer and C_8-LacCer are developed. MTO is chosen as a second drug to formulate in SCS-nanoliposomes. These liposomes underwent pharmaceutical development to obtain optimal C_8-GluCer and C_8-GalCer enriched MTO co-delivery formulations. Different drug loading methods, drug to phospholipid (D:PL) ratios and SCS content are investigated. Furthermore, co-delivery of the respective drug and SCS to tumor cells is tested *in vitro* and *in vivo* to evaluate the drug uptake enhancing properties of the formulations and subsequent anti-tumor activity.

Studies on drug pharmacokinetics and biodistribution together with intravital optical imaging and immunohistochemistry aimed to get a better understanding of intratumoral liposome and drug accumulation and the cellular fate of the carrier and drug content. SCS transfer and effects on tumor and non-tumor cell membranes are studied to determine possible tumor-cell type specificity of this therapeutic approach. Additionally the drug delivery mechanism was addressed by model-membrane studies, live-cell confocal microscopy and click chemistry to monitor in detail the intracellular fate of the nanoliposomes, SCS and drug.

OUTLINE OF THE THESIS

This thesis first describes the continued use of SCS to improve Dox delivery. Whereas previous work identified the positive effect of various SCS on intracellular uptake of Dox [157] and resulted in one functional SCS-liposomal Dox formulation [158, 159], **Chapter 2** describes further optimization of established and novel SCS enriched Dox-liposomes. Drug loading efficiency was optimized and liposomal drug stability was investigated. Different SCS such as C_8-GalCer and C_8-LacCer were tested for incorporation in PLD and based on these findings, a novel C_8-GalCer PEGylated liposomal formulation of Dox was established, and tested for improved drug delivery and Dox efficacy *in vitro* both in tumor and non-tumor cells. New insights in the mechanism of action are presented upon studying the fate of the drug, the lipids and the liposomal carrier.

To broaden the application of this SCS drug delivery technology we set out to formulate MTO as another important chemotherapeutic drug in SCS liposomes. **Chapter 3** describes novel SCS-enriched liposomal MTO formulations based on C_8-GluCer and C_8-GalCer bilayer enrichment. These optimally designed nanocarriers are studied *in vitro* and *in vivo*. Stability and release kinetics in serum were analyzed together with cellular MTO uptake and cytotoxicity to normal and tumor cells when formulated in standard or SCS enriched liposomes. The drug delivery mechanism involved a transfer of SCS to the cell membrane, independently of drug transfer and without nanoliposome internalization. Intratumoral MTO delivery in a MCF-7 breast carcinoma orthotopic model was studied and correlated to macrophage presence and tumor vessel localization. Novel SCS-liposomes containing MTO were studied *in vivo* and described in **Chapter 4**. MTO formulations from chapter 3 were tested for efficacy in a MDA-MB-231 breast carcinoma orthotopic model. After establishing the MTD, single and multiple doses of MTO-liposomes were tested for efficacy. MTO pharmacokinetics and biodistribution after 24h of a single i.v. administration were described for SCS enriched liposomes containing MTO and standard liposomes (MTOL). Intratumoral MTO uptake was studied in time by intravital microscopy for standard and SCS enriched liposomes. Intratumoral MTO distribution over normoxic and hypoxic areas in the tumor were investigated as well.

It is hypothesized, that a dynamic biophysical mechanism at the plasma membrane is responsible for the enhanced drug delivery properties of SCS upon their insertion into the tumor cell membrane. The modulation of tumor cell membrane lipid composition by SCS may result in specific porous domains in the cell membrane increasing cellular drug influx. **Chapter 5** provides novel insights into the mechanism of action of SCS. Firstly, fluorescent C_6-NBD Galactosyl-Ceramide was used for glycolipid tracing in tumor and normal cells. To confirm these studies click chemistry was applied to post-incubation label, image and quantify C_8-GluCer in tumor and normal cells. Assays assessing lipid transbilayer motion or flip-flop were performed to further understand the effect exerted by C_8-GluCer and C_8-GalCer in free or liposomal form in both cells and model membranes mimicking cell membrane lipid composition. Finally, pore formation was studied in model membranes by assessing

SCS-induced leakage of DTX or dextran. All results are combined and summarized in a schematic representation proposing the working mechanism behind SCS mediated liposomal drug delivery.

Chapter 6 discusses the results of this thesis and places these in a broader context. It also describes future perspectives of this novel drug delivery technology and its translation into clinical application.

REFERENCES

1. Ferlay J, Steliarova-Foucher E, Lortet-Tieulent J, Rosso S, Coebergh JW, Comber H, Forman D, Bray F, Cancer incidence and mortality patterns in Europe: Estimates for 40 countries in 2012. Eur J Cancer, 2013. 49(6):1374-1403.
2. Society AC, Cancer Facts & Figures 2013. Atlanta; American Cancer Society, 2013.
3. Maughan K, Treatment of Breast cancer. Am Fam Physician, 2010.
4. Fu D, Calvo JA, Samson LD, Balancing repair and tolerance of DNA damage caused by alkylating agents. Nat Rev Cancer, 2012. 12(2): 104-20.
5. Kaye SB, New antimetabolites in cancer chemotherapy and their clinical impact. Br J Cancer, 1998. 78 Suppl 3:1-7.
6. Hand, K, Topoisomerase II inhibitors. Update Cancer Ther, 2008. 3(1):13-26.
7. Jiang N, Wang X, Yang Y, Dai W, Advances in mitotic inhibitors for cancer treatment. Mini Rev Med Chem, 2006. 6(8):885-95.
8. Perez E, Microtubule inhibitors: Differentiating tubulin-inhibiting agents based on mechanisms of action, clinical activity, and resistance. Mol Cancer Ther, 2009. 8(8): 2086-95.
9. Minotti G, Menna P, Salvatorelli E, Cairo G, Gianni L, Anthracyclines: molecular advances and pharmacologic developments in antitumor activity and cardiotoxicity. Pharmacol Rev, 2004. 56(2): 185-229.
10. Weiss R, Mitoxantrone: its development and role in clinical practice. Oncology (Williston Park), 1989. Jun;3(6):135-41.
11. Awasthi P, Dogra S, Awasthi LK, Barthwal R, Molecular modeling study of interaction of anthracenedione class of drug mitoxantrone and its analogs with DNA tetrameric sequences. Adv Exp Med Biol, 2011. 696: 385-400.
12. Wobbes T, Eibergen R, Oldhoff J, Koops HS, Results of retroperitoneal lymph node dissection and postoperative adjuvant chemotherapy with dactinomycin in the treatment of retroperitoneal metastases of nonseminomatous testicular germ cell tumors. Cancer, 1983. 51(6):1076-9.
13. Kawai K, Akaza H, Bleomycin-induced pulmonary toxicity in chemotherapy for testicular cancer. Expert Opin Drug Saf, 2003. 2(6): 587-96.
14. Volpe A, Racioppi M, D'Agostino D, Cappa E, Filianoti A, Bassi PF, Mitomycin C for the treatment of bladder cancer. Minerva Urol Nefrol, 2010. 62(2):133-44.
15. Davies C, Pan H, Godwin J, Gray R, Arriagada R, Raina V, et al Long-term effects of continuing adjuvant tamoxifen to 10 years versus stopping at 5 years after diagnosis of oestrogen receptor-positive breast cancer: ATLAS, a randomised trial. Lancet, 2013. 381(9869): L805-16.
16. Schweizer MT, Huang P, Kattan MW, Kibel AS, de Wit R, Sternberg CN, Epstein JI, Eisenberger MA, Adjuvant leuprolide with or without docetaxel in patients with high-risk prostate cancer after radical

prostatectomy (TAX-3501): important lessons for future trials. Cancer, 2013. 119(20):3610-8.
17. Dorff TB, Crawford ED, Management and challenges of corticosteroid therapy in men with metastatic castrate-resistant prostate cancer. Ann. Oncol, 2013. 24(1):31-8.
18. Nadas J, Sun D, Anthracyclines as effective anticancer drugs. Expert Opin Drug Discov, 2006;1(6):549-68.
19. Cortés-Funes H, Coronado C,Role of anthracyclines in the era of targeted therapy. Cardiovasc Toxicol, 2007;7(2):56-60.
20. Kuznetsov DD, Alsikafi NF, O'Connor RC, Steinberg GD, Intravesical valrubicin in the treatment of carcinoma in situ of the bladder. Expert Opin Pharmacother, 2001;(2):1009-13.
21. Tacar O, Sriamornsak P, Dass CR, Doxorubicin: an update on anticancer molecular action, toxicity and novel drug delivery systems. J Pharm Pharmacol, 2013;65(2):157-70.
22. Gewirtz DA, A critical evaluation of the mechanisms of action proposed for the antitumor effects of the anthracycline antibiotics adriamycin and daunorubicin. Biochem Pharmacol, 1999; 57(7):727-741.
23. Campos S, Liposomal Anthracyclines: Adjuvant and Neoadjuvant Therapy for Breast Cancer. The Oncologist, 2003; 8(supplement 2):10-16.
24. Thigpen JT, Innovations in anthracycline therapy: overview. Commun Oncol, 2005. 2 (Suppl. 1)(1):3-7.
25. Cristofanilli M, Holmes FA, Esparza L, Valero V, Buzdar AU, Neidhart JA, Hortobagyi GN, Phase I/II trial of high dose mitoxantrone in metastatic breast cancer: the M.D. Anderson Cancer Center experience. Breast Cancer Res Treat, 1999. 54(3):225-233.
26. Pusztai L, Holmes FA, Fraschini G, Hortobagyi GN, Phase II study of mitoxantrone by 14-day continuous infusion with granulocyte colony-stimulating factor (GCSF) support in patients with metastatic breast cancer and limited prior therapy. Cancer Chemother Pharmacol. 1999; 43(1):86-91.
27. Cook AM, Chambers EJ, Rees GJ, Comparison of mitozantrone and epirubicin in advanced breast cancer. Clin Oncol, 1996. 8:363-366.
28. Smith LA, Cornelius VR, Plummer CJ, Levitt G, Verrill M, Canney P, Jones A, Cardiotoxicity of anthracycline agents for the treatment of cancer: systematic review and meta-analysis of randomised controlled trials. BMC Cancer, 2010;10:337.
29. Gharib MI, Burnett AK, Chemotherapy-induced cardiotoxicity: current practice and prospects of prophylaxis. Eur J Heart Fail, 2002; 4(3): 235-42.
30. Dunn CJ, Goa KL, Mitoxantrone: a review of its pharmacological properties and use in acute nonlymphoblastic leukaemia. Drugs Aging, 1996. 9(2):122-47.
31. White RJ, Durr FE, Development of mitoxantrone. Investigational New Drugs, 1985.3(2):85-93.
32. Taylor DJ, Parsons CE, Han H, Jayaraman A, Rege K, Parallel screening of FDA-approved antineoplastic drugs for identifying sensitizers of TRAIL-induced apoptosis in cancer cells. BMC Cancer, 2011. 1(11):470.

33. Parker C, Waters R, Leighton C, Hancock J, Sutton R, Moorman AV, Ancliff P, Morgan M, Masurekar A, Goulden N, Green N, Révész T, Darbyshire P, Love S, Saha V, Effect of mitoxantrone on outcome of children with first relapse of acute lymphoblastic leukaemia (ALL R3): an open-label randomised trial. Lancet, 2010. 11;376(9757): 2009-17.
34. Minagar A, Current and future therapies for multiple sclerosis. Scientifica (Cairo), 2013.
35. Fox E, Mechanism of action of mitoxantrone. Neurology, 2004. 63(12 suppl 6):S15-S18.
36. Faulds D, Balfour JA, Chrisp P, Langtry HD, Mitoxantrone. A review of its pharmacodynamic and pharmacokinetic properties, and therapeutic potential in the chemotherapy of cancer. Drugs, 1991. 41(3):400-449.
37. Hajihassan Z, Rabbani-Chadegani A, Studies on the binding affinity of anticancer drug mitoxantrone to chromatin, DNA and histone proteins. J Biomed Sci, 2009. 16:31.
38. Nicolson G, The Fluid—Mosaic Model of Membrane Structure: Still relevant to 3 understanding the structure, function and dynamics of biological 4 membranes after more than 40 years. Biochim Biophys Acta, 2013. 1838(6):1451-66
39. Rajendran L, Simons K, Lipid rafts and membrane dynamics. J Cell Sci, 2005.118(Pt 6):1099-102.
40. Hendrich AB, Michalak K, Lipids as a target for drugs modulating multidrug resistance of cancer cells. Curr Drug Targets, 2003. 4(1): 23-30.
41. Callaghan R, Stafford A, Epand RM, Increased accumulation of drugs in a multidrug resistant cell line by alteration of membrane biophysical properties. Biochim Biophys Acta, 1993. 1175(3):277-82.
42. May GL, Wright LC, Dyne M, Mackinnon WB, Fox RM, Mountford CE, Plasma membrane lipid composition of vinblastine sensitive and resistant human leukaemic lymphoblasts. Int J Cancer, 1988. 42(5): 728-33.
43. Anderson RG, The Caveolae Membrane System. Annu.Rev.Biochem, 1998. 67:199-225.
44. Reeves VL, Thomas CM, Smart EJ, Lipid rafts, caveolae and GPI-linked proteins. Adv Exp Med Biol, 2012. 729:3-13.
45. Regev R, Yeheskely-Hayon D, Katzir H, Eytan GD, Transport of anthracyclines and mitoxantrone across membranes by a flip-flop mechanism. Biochem Pharmacol. 2005 Jul 1;70(1):161-9.
46. Germann UA, Pastan I, Gottesman MM, P-glycoproteins: mediators of drug resistence. Semin Cell Biol, 1993. 4(1):63-76.
47. Allen TM, Cullis PR, Liposomal drug delivery systems: from concept to clinical applications. Adv Drug Deliv Rev, 2013. 65(1):36-48.
48. Perche F, Torchilin VP, Recent trends in multifunctional liposomal nanocarriers for enhanced tumor targeting. J Drug Deliv, 2013;2013: 705265.
49. Mattheolabakis G, Rigas B, Constantinides PP, Nanodelivery strategies in cancer chemotherapy: biological rationale and

pharmaceutical perspectives. Nanomedicine (Lond), 2012.7(10): 1577-90.
50. Maeda H, Nakamura H, Fang J, The EPR effect for macromolecular drug delivery to solid tumors: Improvement of tumor uptake, lowering of systemic toxicity, and distinct tumor imaging in vivo. Adv Drug Deliv Rev, 2013. 65(1):71-9.
51. Deshpande PP, Biswas S, Torchilin VP, Current trends in the use of liposomes for tumor targeting. Nanomedicine (Lond), 2013. 8(9): 1509-28.
52. Pathak P, Hess R, Weiss MA, Liposomal vincristine for relapsed or refractory Ph-negative acute lymphoblastic leukemia: a review of literature. Ther Adv Hematol, 2014. 5(1):18-24.
53. Tirodkar TS, Voelkel-Johnson C, Sphingolipids in apoptosis. Exp Oncol, 2012. 34(3):231-42.
54. Hannun YA, Obeid LM, Principles of bioactive lipid signalling: lessons from sphingolipids. Nat Rev Mol Cell Biol, 2008. 9(2): 139-50.
55. Seddon J, Structure of the inverted hexagonal (HII) phase, and non-lamellar phase transitions of lipids. Biochim Biophys Acta, 1990. 1031(1):1-69.
56. Bangham A, Surrogate cells or Trojan horses. The discovery of liposomes. Bioessays. 1995;17(12):1081-8.
57. Bangham AD, Standish MM, Watkins JC, Diffusion of univalent ions across the lamellae of swollen phospholipids. J Mol Biol, 1965. 13(1):238-52.
58. Mayer LD, Hope MJ, Cullis PR, Vesicles of variable sizes produced by a rapid extrusion procedure. Biochim Biophys Acta, 1986. 858(1): 161-8.
59. Drummond DC, Meyer O, Hong K, Kirpotin DB, Papahadjopoulos D, Optimizing Liposomes for Delivery of Chemotherapeutic Agents to Solid Tumors. Pharmacol Reviews, 1999. 51(4):691-744.
60. Kohli AG, Kierstead PH, Venditto VJ, Walsh CL, Szoka FC, Designer lipids for drug delivery: From heads to tails J Control Release. 2014;S0168-3659(14)00280-6.
61. Akbarzadeh A, Rezaei-Sadabady R, Davaran S, Joo SW, Zarghami N, Hanifehpour Y, Samiei M, Kouhi M, Nejati-Koshki K, Liposome: classification, preparation, and applications. Nanoscale Res Lett, 2013. 8(1):102.
62. Gregoriadis G and Ryman BE, Liposomes as carriers of enzymes or drugs: a new approach to the treatment of storage diseases. Biochem J, 1971. 124(5): 58P.
63. Ulrich AS, Biophysical aspects of using liposomes as delivery vehicles. Biosci Rep. 2002;22(2):129-50.
64. Barenholz Y, Doxil®-the first FDA-approved nano-drug: lessons learned. J Control Release, 2012. 160(2)117-34.
65. Lee SC, Lee KE, Kim JJ, Lim SH, The effect of cholesterol in the liposome bilayer on the stabilization of incorporated Retinol. J Liposome Res, 2005. 15(3-4):157-66.

66. Needham D, McIntosh TJ, Lasic DD, Repulsive interactions and mechanical stability of polymer-grafted lipid membranes. Biochim Biophys Acta, 1992. 1108 (1): 40-8.
67. Papisov MI, Theoretical considerations of RES-avoiding liposomes: Molecular mechanics and chemistry of liposome interactions. Adv Drug Deliv Rev, 1998. 32(1-2):119-138.
68. Torchilin VP, Omelyanenko VG, Papisov MI, Bogdanov AA Jr, Trubetskoy VS, Herron JN, Gentry CA, Poly(ethylene glycol) on the liposome surface: on the mechanism of polymer-coated liposome longevity. Biochim Biophys Acta, 1994. 1195(1):11-20.
69. Immordino ML, Dosio F, Cattel L, Stealth liposomes: review of the basic science,rationale, and clinical applications, existing and potential. Int J Nanomedicine, 2006. 1(3):297–315.
70. Gabizon A, Shmeeda H, Barenholz Y, Pharmacokinetics of Pegylated Liposomal Doxorubicin: Review of Animal and Human Studies. Clin Pharmacokinet, 2003.42(5):419-36.
71. Woodle MC, Lasic DD, Sterically stabilized liposomes. Biochim Biophys Acta, 1992.1113(2):171-99.
72. Harrington KJ, Rowlinson-Busza G, Syrigos KN, Uster PS, Vile RG, Stewart JS, Pegylated Liposomes Have Potential as Vehicles for Intratumoral and Subcutaneous Drug Delivery. 2000. 2528-2537.
73. Brown JM, Giaccia AJ, The Unique Physiology of Solid Tumors: Opportunities (and Problems) for Cancer Therapy. Cancer Res, 1998.58(7):1408-16.
74. Nakasone ES, Askautrud HA, Kees T, Park JH, Plaks V, Ewald AJ, Fein M, Rasch MG, Tan YX, Qiu J, Park J, Sinha P, Bissell MJ, Frengen E, Werb Z, Egeblad M, Imaging Tumor-Stroma Interactions during Chemotherapy Reveals Contributions of the Microenvironment to Resistance. Cancer Cell, 2012.21(4):488-503.
75. Kostarelos K, Emfietzoglou D, Papakostas A, Yang WH, Ballangrud A, Sgouros G, Binding and interstitial penetration of liposomes within avascular tumor spheroids. Int J Cancer, 2004. 112(4):713-21.
76. Simões S, Moreira JN, Fonseca C, Düzgüneş N, de Lima MC, On the formulation of pH-sensitive liposomes with long circulation times. Adv Drug Deliv Rev, 2004. 7:947-65.
77. Manzoor AA, Lindner LH, Landon CD, Park JY, Simnick AJ, Dreher MR, Das S, Hanna G, Park W, Chilkoti A, Koning GA, ten Hagen TL, Needham D, Dewhirst MW, Overcoming Limitations in Nanoparticle Drug Delivery: Triggered, Intravascular Release to Improve Drug Penetration into Tumors. Cancer Res, 2012.72(21):5566-75.
78. Li L, ten Hagen TL, Bolkestein M, Gasselhuber A, Yatvin J, van Rhoon GC, Eggermont AM, Haemmerich D, Koning GA, Improved intratumoral nanoparticle extravasation and penetration by mild hyperthermia. J Control Release, 2013.167(2):130-7.
79. Seynhaeve AL, Hoving S, Schipper D, Vermeulen CE, de Wiel-Ambagtsheer Ga, van Tiel ST, Eggermont AM, Ten Hagen TL, Tumor Necrosis Factor α Mediates Homogeneous Distribution of Liposomes in Murine Melanoma that Contributes to a Better Tumor Response. Cancer Res, 2007.67(19):9455-62.

80. Maeda H, Bharate GY, Daruwalla J, Polymeric drugs for efficient tumor-targeted drug delivery based on EPR-effect. Eur J Pharm Biopharm, 2009. 71(3):409-19.
81. Chang HI, Yeh MK, Clinical development of liposome-based drugs: formulation, characterization, and therapeutic efficacy. Int J Nanomedicine, 2012.7:49-60.
82. Gabizon A, Goren D, Cohen R, Barenholz Y, Development of liposomal anthracyclines: from basics to clinical applications. J Control Release, 1998.53(1-3):275-9.
83. Mayer LD, Bally MB, Cullis PR, Uptake of adriamycin into large unilamellar vesicles in response to a pH gradient. B Biochim Biophys Acta, 1986.857(1):123-6.
84. Mayer LD, Bally MB, Cullis PR, Wilson SL, Emerman JT, Comparison of free and liposome encapsulated doxorubicin tumor drug uptake and antitumor efficacy in the SC115 murine mammary tumor. Cancer Lett, 1999. 53(2-3):183-90.
85. Haran G, Cohen R, Bar LK, Barenholz Y, Transmembrane ammonium sulfate gradients in liposomes produce efficient and stable entrapment of amphipathic weak bases. Biochim Biophys Acta, 1993.1151(2):201-15.
86. Li X, Hirsh DJ, Cabral-Lilly D, Zirkel A, Gruner SM, Janoff AS, Perkins WR, Doxorubicin physical state in solution and inside liposomes loaded via a pH gradient. Biochim Biophys Acta, 1998. 9; 1415(1):23-40.
87. Gabizon A, Emerging Role of Liposomal Drug Carrier Systems in Cancer Chemotherapy. J Liposome Res, 2003.13(1):17-20.
88. Vail DM, Amantea MA, Colbern GT, Martin FJ, Hilger RA, Working PK, Pegylated Liposomal Doxorubicin: Proof of Principle Using Preclinical Animal Models and Pharmacokinetic Studies. Semin Oncol, 2004. 31(6 Suppl 13):16-35.
89. Farr KP, Safwat A, Palmar-plantar erythrodysesthesia associated with chemotherapy and its treatment. Case Rep Oncol, 2011. 4(1):229-35.
90. von Moos R, Thuerlimann BJ, Aapro M, Rayson D, Harrold K, Sehouli J, Scotte F, Lorusso D, Dummer R, Lacouture ME, Lademann J, Hauschild A, Pegylated liposomal doxorubicin-associated hand-foot syndrome: recommendations of an international panel of experts. Eur J Cancer, 2008. 44(6):781-90.
91. Northfelt DW, Dezube BJ, Thommes JA, Miller BJ, Fischl MA, Friedman-Kien A, Kaplan LD, Du Mond C, Mamelok RD, Henry DH, Pegylated-liposomal doxorubicin versus doxorubicin, bleomycin, and vincristine in the treatment of AIDS-related Kaposi's sarcoma: results of a randomized phase III clinical trial. J Clin Oncol, 1998. 16(7): 2445-2451.
92. Tejada-Berges T, Granai CO, Gordinier M, Gajewski W, Caelyx/Doxil for the treatment of metastatic ovarian and breast cancer.Expert Rev Anticancer Ther, 2002.2(2):143-50.
93. Hussein MA, Anderson KC, Role of liposomal anthracyclines in the treatment of multiple myeloma. Seminars in oncology, 2004.31: 147-160.

94. O'Brien ME, Wigler N, Inbar M, Rosso R, Grischke E, Santoro A, Catane R, Kieback DG, Tomczak P, Ackland SP, Orlandi F, Mellars L, Alland L, Tendler C, CAELYX Breast Cancer Study Group.Reduced cardiotoxicity and comparable efficacy in a phase III trial of pegylated liposomal doxorubicin HCl (CAELYX,Doxil) versus conventional doxorubicin for first-line treatment of metastatic breast cancer. Ann Oncol, 2004. 15(3):440-449.
95. Alberts DS, Liu PY, Wilczynski SP, Clouser MC, Lopez AM, Michelin DP, Lanzotti VJ, Markman M, Southwest Oncology Group, Randomized trial of pegylated liposomal doxorubicin (PLD) plus carboplatin versus carboplatin in platinum-sensitive (PS) patients with recurrent epithelial ovarian or peritoneal carcinoma after failure of initial platinum-based chemotherapy (Southwest Oncology Group Protocol S0200). Gynecol Oncol, 2008.108(1):90-4.
96. Harris KA, Harney E, Small EJ, Liposomal doxorubicin for the treatment of hormone-refractory prostate cancer. Clin Prostate Cancer, 2002. 1(1):37-41.
97. Alberts DS, Muggia FM, Carmichael J, Winer EP, Jahanzeb M, Venook AP, Skubitz KM, Rivera E, Sparano JA, DiBella NJ, Stewart SJ, Kavanagh JJ, Gabizon AA, Efficacy and safety of liposomal anthracyclines in phase I/II clinical trials. Semin Oncol, 2004.31(6 Suppl 13):53-90.
98. Caponigro F, Comella P, Budillon A, Bryce J, Avallone A, De Rosa V, Ionna F, Comella G, Phase I study of Caelyx (doxorubicin HCL, pegylated liposomal) in recurrent or metastatic head and neck cancer. Ann Oncol, 2000.11(3):339-42.
99. Ferrandina G, Corrado G, Licameli A, Lorusso D, Fuoco G, Pisconti S, Scambia G, Pegylated liposomal doxorubicin in the management of ovarian cancer. Ther Clin Risk Manag,2010. 6:463–483.
100. Laginha KM, Verwoert S, Charrois GJ, Allen TM, Determination of Doxorubicin Levels in Whole Tumor and Tumor Nuclei in Murine Breast Cancer Tumors. Clin Cancer Res, 2005.11(19 Pt 1):6944-9.
101. Harrington KJ, Mohammadtaghi S, Uster PS, Glass D, Peters AM, Vile RG, Stewart JSW, Effective Targeting of Solid Tumors in Patients With Locally Advanced Cancers by Radiolabeled Pegylated Liposomes. Clin Cancer Res, 2001.7(2):243-54.
102. Laginha KM, Verwoert S, Charrois GJR, Allen TM, Determination of Doxorubicin Levels in Whole Tumor and Tumor Nuclei in Murine Breast Cancer Tumors. Clin Cancer Res, 2005.11(19 Pt 1):6944-9.
103. Storm G, Steerenberg PA, Emmen F, van Borssum WM, Crommelin DJ, Release of doxorubicin from peritoneal macrophages exposed in vivo to doxorubicin-containing liposomes. Biochim Biophys Acta, 1988. 965(2-3):136-45.
104. Banciu M, Schiffelers RM, Storm G, Investigation into the Role of Tumor-Associated Macrophages in the Antitumor Activity of Doxil. Pharmaceutical Research, 2008.25(8):1948-1955.
105. Mayer LD, Dougherty G, Harasym TO, Bally MB, The Role of Tumor-Associated Macrophages in the Delivery of Liposomal Doxorubicin to Solid Murine Fibrosarcoma Tumors. J Pharmacol Exp Ther. 1997.280(3): 1406-14.

106. Charrois GJ, Allen TM, Drug release rate influences the pharmacokinetics, biodistribution, therapeutic activity, and toxicity of pegylated liposomal doxorubicin formulations in murine breast cancer. Biochim Biophys Acta, 2004. 1663(1-2):167-77.
107. Maurer N, Fenske DB, Cullis PR, Developments in liposomal drug delivery systems. Expert Opin Biol Ther, 2001.1(6):923-47.
108. Leonard RC, Williams S, Tulpule A, Levine AM, Oliveros S, Improving the therapeutic index of anthracycline chemotherapy: focus on liposomal doxorubicin (Myocet). Breast, 2009.18(4):218-24.
109. Waterhouse DN, Tardi PG, Mayer LD, Bally MB, A comparison of liposomal formulations of doxorubicin with drug administered in free form: changing toxicity profiles. Drug Saf, 2001.24(12):903-20.
110. Rigacci L, Mappa S, Nassi L, Alterini R, Carrai V, Bernardi F, Bosi A, Liposome-encapsulated doxorubicin in combination with cyclophosphamide, vincristine, prednisone and rituximab in patients with lymphoma and concurrent cardiac diseases or pre-treated with anthracyclines. Hematol Oncol, 2007.25(4):198-203.
111. Batist G, Ramakrishnan G, Rao CS, Chandrasekharan A, Gutheil J, Guthrie T, Shah P, Khojasteh A, Nair MK, Hoelzer K, Tkaczuk K, Park YC, Lee LW, Reduced cardiotoxicity and preserved antitumor efficacy of liposome-encapsulated doxorubicin and cyclophosphamide compared with conventional doxorubicin and cyclophosphamide in a randomized, multicenter trial of metastatic breast cancer. J Clin Oncol, 2001. 19(5):1444-54.
112. Chugun A, Uchide T, Tsurimaki C, Nagasawa H, Sasaki T, Ueno S, Takagishi K, Hara Y, Temma K, Mechanisms Responsible for Reduced Cardiotoxicity of Mitoxantrone Compared to Doxorubicin Examined in Isolated Guinea-Pig Heart Preparations. J Vet Med Sci, 2008.70: 255-264.
113. Lim HJ, Masin D, Madden TD, Bally MB, Influence of Drug Release Characteristics on the Therapeutic Activity of Liposomal Mitoxantrone. J Pharmacol Exp Ther, 1997.281(1):566-73.
114. Li C, Cui J, Wang C, Li Y, Zhang H, Wang J, Li Y, Zhang L, Zhang L, Guo W, Wang Y, Encapsulation of mitoxantrone into pegylated SUVs enhances its antineoplastic efficacy. European journal of pharmaceutics and biopharmaceutics : official journal of Arbeitsgemeinschaft fur Pharmazeutische Verfahrenstechnik e.V, 2008.70(2):657-665.
115. Pinto AC, Moreira JN, Simões S, Liposomal imatinibŞmitoxantrone combination: Formulation development and therapeutic evaluation in an animal model of prostate cancer. The Prostate, 2011.71(1):81-90.
116. Haran G, Cohen R, Bar LK, Barenholz Y, Transmembrane ammonium sulfate gradients in liposomes produce efficient and stable entrapment of amphipathic weak bases. Biochim Biophys Acta, 1993.1151(2):201-215.
117. Chang CW, Barber L, Ouyang C, Masin D, Bally MB, Madden TD, Plasma clearance, biodistribution and therapeutic properties of mitoxantrone encapsulated in conventional and sterically stabilized liposomes after intravenous administration in BDF1 mice. Br J Cancer, 1997.75(2):169-177.

118. Couvreur P, Nanoparticles in drug delivery: past, present and future. Adv Drug Deliv Rev, 2013.65(1):21-3.
119. Koning GA, Krijger GC, Targeted multifunctional lipid-based nanocarriers for image-guided drug delivery. Anticancer Agents Med Chem, 2007.7(4):425-40.
120. Koning GA, Morselt HW, Gorter A, Allen TM, Zalipsky S, Kamps JA, Scherphof GL, Pharmacokinetics of differently designed immunoliposome formulations in rats with or without hepatic colon cancer metastases. Pharm Res, 2001. 18(9):1291-8.
121. Koning GA, Storm G, Targeted drug delivery systems for the intracellular delivery of macromolecular drugs. Drug Discov Today,2003.8(11): 482-3.
122. Danhier F, Feron O, Préat V, To exploit the tumor microenvironment: Passive and active tumor targeting of nanocarriers for anti-cancer drug delivery. J Control Release, 2010.148(2):135-46.
123. Sofou S, Sgouros G, Antibody-targeted liposomes in cancer therapy and imaging. Expert Opin Drug Deliv, 2008.2(5):189-204.
124. Kirpotin DB, Drummond DC, Shao Y, Shalaby MR, Hong K, Nielsen UB, Marks JD, Benz CC, Park JW, Antibody targeting of long-circulating lipidic nanoparticles does not increase tumor localization but does increase internalization in animal models. Cancer Res,2006. 66(13): 6732-40.
125. Laginha KM, Moase EH, Yu N, Huang A, Allen TM, Bioavailability and therapeutic efficacy of HER2 scFv-targeted liposomal doxorubicin in a murine model of HER2-overexpressing breast cancer. J Drug Target, 2008.16(7):605-10.
126. Paliwal SR, Paliwal R, Mishra N, Mehta A, Vyas SP, A novel cancer targeting approach based on estrone anchored stealth liposome for site-specific breast cancer therapy. Curr Cancer Drug Targets, 2010.10(3):343-53.
127. Gabizon A, Horowitz AT, Goren D, Tzemach D, Shmeeda H, Zalipsky S, In vivo fate of folate-targeted polyethylene-glycol liposomes in tumor-bearing mice. Clin Cancer Res, 2003.9(17):6551-9.
128. Zhang J, Jin W, Wang X, Wang J, Zhang X, Zhang Q, A novel octreotide modified lipid vesicle improved the anticancer efficacy of doxorubicin in somatostatin receptor 2 positive tumor models. Mol Pharm, 2010;7(4):1159-68.
129. Danhier F, Le Breton A, Préat V, RGD-based strategies to target alpha(v) beta(3) integrin in cancer therapy and diagnosis. Mol Pharm, 2012.9(11):2961-73.
130. Zhao H, Wang JC, Sun QS, Luo CL, Zhang Q, RGD-based strategies for improving antitumor activity of paclitaxel-loaded liposomes in nude mice xenografted with human ovarian cancer. J Drug Target, 2009.17(1):10-8.
131. Schiffelers RM, Koning GA, ten Hagen TL, Fens MH, Schraa AJ, Janssen AP, Kok RJ, Molema G, Storm G, Anti-tumor efficacy of tumor vasculature-targeted liposomal doxorubicin. J Control Release, 2003.91(1-2):115-22.

132. Bibi S, Lattmann E, Mohammed AR, Perrie Y, Trigger release liposome systems: local and remote drug delivery? J Microencapsul, 2012.29: 262-276.
133. Ueno Y, Sonoda S, Suzuki R, Yokouchi M, Kawasoe Y, Tachibana K, Maruyama K, Sakamoto T, Komiya S, Combination of ultrasound and bubble liposome enhance the effect of doxorubicin and inhibit murine osteosarcoma growth. Cancer Biol Ther, 2011.12(4):270-7.
134. Yavlovich A, Singh A, Blumenthal R, Puri A, A novel class of photo-triggerable liposomes containing DPPC:DC(8,9)PC as vehicles for delivery of doxorubcin to cells. Biochim Biophys Acta, 2011;1808(1): 117-26.
135. Li L, ten Hagen TL, Schipper D, Wijnberg TM, van Rhoon GC, Eggermont AM, Lindner LH, Koning GA, Triggered content release from optimized stealth thermosensitive liposomes using mild hyperthermia. J Control Release, 2010.143(2):274-9.
136. Staruch R, Chopra R, Hynynen K, Localised drug release using MRI-controlled focused ultrasound hyperthermia. Int J Hyperthermia, 2011.27(2):156-171.
137. Poon RT, Borys N, Lyso-thermosensitive liposomal doxorubicin: an adjuvant to increase the cure rate of radiofrequency ablation in liver cancer. Future Oncol, 2011.7(8):937-45.
138. Kim CK, Lim SJ, Liposome immunoassays using phospholipase C or alkaline phosphatase. Methods Enzymol, 2003.373:260-77.
139. Davidsen J, Jørgensen K, Andresen TL, Mouritsen OG, Secreted phospholipase A(2) as a new enzymatic trigger mechanism for localised liposomal drug release and absorption in diseased tissue. Biochim Biophys Acta, 2003.1609(1):95-101.
140. Sarkar N, Banerjee J, Hanson AJ, Elegbede AI, Rosendahl T, Krueger AB, Banerjee AL, Tobwala S, Wang R, Lu X, Mallik S, Srivastava DK, Matrix metalloproteinase-assisted triggered release of liposomal contents. Bioconjug Chem, 2008.19(1):57-64.
141. Leite EA, Souza CM, Carvalho-Júnior AD, Coelho LG, Lana AM, Cassali GD, Oliveira MC, Encapsulation of cisplatin in long-circulating and pH-sensitive liposomes improves its antitumor effect and reduces acute toxicity. Int J Nanomedicine, 2012.7: 5259–5269.
142. Temmerman K, Nickel W, A novel flow cytometric assay to quantify interactions between proteins and membrane lipids. J Lipid Res, 2009.50(6):1245-54.
143. Zachowski A, Phospholipids in animal eukaryotic membranes: transverse asymmetry and movement. Biochem J, 1993.294 (Pt1):1-14.
144. Ohvo-Rekilä H, Ramstedt B, Leppimäki P, Slotte JP, Cholesterol interactions with phospholipids in membranes. Prog Lipid Res, 2002.41(1):66-97.
145. Pomorski T, Hrafnsdóttir S, Devaux PF, van Meer G, Lipid distribution and transport across cellular membranes. Semin Cell Dev Biol, 2001.12(2):139-48.
146. Daleke DL, Regulation of transbilayer plasma membrane phospholipid asymmetry. J Lipid Res, 2003.44(2):233-42.
147. Borst P, Zelcer N, van Helvoort A, ABC transporters in lipid transport. Biochim Biophys Acta, 2000.1486(1): 128-44.

148. Fadeel B, Xue D, The ins and outs of phospholipid asymmetry in the plasma membrane: roles in health and disease. Crit Rev Biochem Mol Biol, 2009.44(5):264-77.
149. Holthuis JC, Pomorski T, Raggers RJ, Sprong H, Van Meer G, The organizing potential of sphingolipids in intracellular membrane transport. Physiol Rev, 2001. 81(4):1689-723.
150. Goñi FM, Alonso A, Effects of ceramide and other simple sphingolipids on membrane lateral structure. Biochim et Biophys Acta, 2009.1788(1):169-177.
151. Hsueh YW, Giles R, Kitson N, Thewalt J, The effect of ceramide on phosphatidylcholine membranes: a deuterium NMR study. Biophys J, 2002. 82(6):3089-95.
152. Contreras FX, Villar AV, Alonso A, Kolesnick RN, Goñi FM, Sphingomyelinase Activity Causes Transbilayer Lipid Translocation in Model and Cell Membranes. J Biol Chem,2003.278(39):37169-74.
153. Contreras FX, Basañez G, Alonso A, Herrmann A, Goñi FM, Asymmetric Addition of Ceramides but not Dihydroceramides Promotes Transbilayer (Flip-Flop) Lipid Motion in Membranes. Biophys J, 2005.88(1):348-59.
154. Siskind LJ, Fluss S, Bui M, Colombini M, Sphingosine Forms Channels in Membranes That Differ Greatly from Those Formed by Ceramide. J Bioenerg Biomembr, 2005.37(4):227-36.
155. Goñi FM, Alonso A, Biophysics of sphingolipids I. Membrane properties of sphingosine, ceramides and other simple sphingolipids. Biochim Biophys Acta, 2006.1758(12):1902-21.
156. London M, Erwin L, Ceramide selectively displaces cholesterol from ordered lipid domains (rafts): implications for lipid raft structure and function. J Biol Chem, 2004.279(11):9997-10004.
157. Veldman RJ, Zerp S, van Blitterswijk WJ, Verheij M, N-hexanoyl-sphingomyelin potentiates in vitro doxorubicin cytotoxicity by enhancing its cellular influx. Br J Cancer, 2004.90(4):917-925.
158. Veldman RJ, Koning GA, van Hell A, Zerp S, Vink SR, Storm G, Verheij M, van Blitterswijk WJ, Coformulated N-Octanoyl-glucosylceramide Improves Cellular Delivery and Cytotoxicity of Liposomal Doxorubicin. J Pharmacol Exp Ther, 2005.315(2):704-10.
159. van Lummel M, van Blitterswijk WJ, Vink SR, Veldman RJ, van der Valk MA, Schipper D, Dicheva BM, Eggermont AM, ten Hagen TL, Verheij M, Koning GA, Enriching lipid nanovesicles with short-chain glucosylceramide improves doxorubicin delivery and efficacy in solid tumors. FASEB J, 2009.25(1):280-289.
160. van Hell AJ, Melo MN, van Blitterswijk WJ, Gueth DM, Braumuller TM, Pedrosa LR, Song JY, Marrink SJ, Koning GA, Jonkers J, Verheij M, Defined lipid analogues induce transient channels to facilitate drug-membrane traversal and circumvent cancer therapy resistance. Sci Rep, 2013.3:1949.

CHAPTER 2

Improving intracellular doxorubicin delivery through nanoliposomes equipped with selective tumor cell membrane permeabilizing short chain sphingolipids

Lília R. Cordeiro Pedrosa, Albert van Hell, Regine Süss, Wim van Blitterswijk, Ann L.B Seynhaeve, Wiggert A. van Cappellen, Alexander M.M Eggermont, Timo ten Hagen, Marcel Verheij and Gerben A. Koning

Pharm Res. 2013;30(7):1883-95

ABSTRACT

Purpose: To improve nanoliposomal-doxorubicin (DoxNL) delivery in tumor cells using liposome membrane-incorporated short chain sphingolipids (SCS) with selective membrane-permeabilizing properties. DoxNL bilayers contained synthetic short chain derivatives of known membrane microdomain-forming sphingolipids; C_8-glucosylceramide (C_8-GluCer) C_8-galactosylceramide (C_8-GalCer) or C_8-lactosylceramide (C_8-LacCer).

Methods: DoxNL enriched with C_8-GluCer or C_8-GalCer were developed, optimized and characterized with regard to size, stability and drug retention. *In vitro* cytotoxic activity was studied in a panel of human tumor cell lines and normal cells. Intracellular Dox delivery was measured by flow cytometry and visualized by fluorescence microscopy. For a further understanding of the involved drug delivery mechanism confocal microscopy studies addressed the cellular fate of the nanoliposomes, the SCS and Dox in living cells.

Results: C_8-LacCer-DoxNL aggregated upon Dox loading. In tumor cell lines SCS-DoxNL with C_8-GluCer or C_8-GalCer demonstrated strongly increased Dox delivery and cytotoxicity compared to standard DoxNL. Surprisingly, this effect was much less pronounced in normal cells. Nanoliposomes were not internalized and SCS transfer from the nanoliposomal bilayer to the cell membrane preceded cellular uptake and subsequent nuclear localization of Dox.

Conclusion: C_8-GluCer or C_8-GalCer incorporated in DoxNL selectively improved intracellular drug delivery through transfer to tumor cell membranes by local enhancement of cell membrane permeability.

INTRODUCTION

Insufficient uptake of chemotherapeutic agents by tumor cells remains an important limitation in clinical cancer treatment. Several factors play a role such as suboptimal dosing due to systemic toxicity, rapid drug clearance from circulation and limited drug traversal across the tumor cell membrane. Here we addressed these hurdles using advanced drug delivery technologies. Liposomes, small nanovesicles composed of phospholipids, cholesterol and poly(ethylene glycol) (PEG)-lipids, are used to entrap the chemotherapeutic agent prolonging systemic drug concentrations and reducing dose-limiting toxicities [1]. In addition, nanoliposomes (NL), due to their small size (< 100 nm), can accumulate in tumor tissue by virtue of the enhanced permeability and retention effect (EPR) [2-5]. In this study nanoliposomal delivery is combined with a novel strategy using short chain sphingolipids (SCS) to enhance transmembrane drug transport [6-8].

Sphingolipids are key molecules for assembly of microdomains in the cell membrane, [9-11]. Evidence exists that SCS self-association may lead to domain or channel formation in the membrane [12] and may explain the enhanced passage of amphiphilic drugs across cell membranes [6]. In this study we exploited this property of SCS to develop PEGylated-nanoliposomal doxorubicin (DoxNL) formulations.

Dox is a chemotherapeutic agent whose mode of action includes intercalation between adjacent base pairs of the DNA double helix, binding to DNA-associated enzymes such as topoisomerase, and effects on membranes [13, 14]. DoxNL (Caelyx/Doxil) increased drug accumulation in solid tumors and reduced dose-limiting toxicities such as myelosuppression and cardiotoxicity [15-17]. DoxNL is currently approved for use in AIDS-related Kaposi's sarcoma [18], refractory ovarian cancer [19], myeloma [20] and metastatic breast cancer [16, 18, 21]. Although DoxNL, due to its favorable pharmacokinetic profile and small size accumulates in tumors, its ability to deliver the Dox content to its active site intracellularly (bioavailability) remains a main issue. DoxNL is characterized by high stability to prevent drug release in circulation, causing slow and suboptimal drug delivery to tumor cells upon accumulation in the tumor area [22, 23]. The inadequate Dox release together with its slow intracellular uptake likely are

main reasons for the limited efficacy increase of DoxNL in cancer patients [16, 18]. In order to improve intracellular Dox delivery we combined nanoliposomal drug delivery with the concept of tumor cell membrane modulation (TCMM) using SCS.

Regarding the mechanism of enhanced drug delivery from SCS enriched nanoliposomes we hypothesize that they transfer spontaneously from the NL bilayer to cell membranes creating enhanced cellular accessibility for amphiphilic compounds by the formation of specific domains with increased drug permeability or transient pores which improve drug influx. The aim of this study is to further optimize and explore SCS-based nanoliposomal drug delivery using various synthetic SCS and investigate the involved drug delivery mechanism.

MATERIALS AND METHODS

Materials

Hydrogenated soy phosphatidylcholine (HSPC) and distearylphosphatidylethanolamine (DSPE)-PEG_{2000} were from Lipoid (Ludwigshaven, Germany). Short chain sphingolipids, C_8-glucosylceramide (C_8-GluCer), C_8-galactosylceramide (C_8-GalCer), C_8-lactosylceramide (C_8-LacCer) and fluorescent lipid NBD PE (1,2-dipalmitoyl-sn-glycero-3-phosphoethanolamine-N-(7-nitro-2-1,3-benzoxadiazol-4-yl) (ammonium salt) and C_6-NBD-Galactosylceramide N-[6-[(7-nitro-2-1,3-benzoxadiazol-4-yl)amino] hexanoyl]-D-galactosyl-ß1-1'-sphingosine were from Avanti Polar Lipids (Alabaster, AL, USA).

Polycarbonate filters were from Northern Lipids (Vancouver, BC, Canada) and PD-10 Sephadex columns were from GE Healthcare (Diegem, Belgium). Dox-HCl (Dox) was from Pharmachemie (Haarlem, The Netherlands). Cholesterol, HEPES (2-[4-(2-hydroxyethyl) piperazin-1-yl] ethanesulfonic acid), trichloroacetic acid (TCA), acetic acid, Triton-X, sulforhodamine B (SRB) were from Sigma Aldrich (Zwijndrecht, The Netherlands). Hoechst was from Molecular Probes (Leiden, The Netherlands). PBS was from Boom and FACS flow fluid from BD Biosciences.

Preparation of SCS-NL

Nanoliposomes were formulated of HSPC/ Cholesterol/ DSPE-PEG2000 in a molar ratio of 1.85: 1: 0.15. Liposomes of 85-100 nm in diameter were prepared by lipid film hydration and extrusion at 65°C. Drug loading was based on ammonium sulfate gradient method [24]. To the mixture of lipids, 0.05, 0.1 or 0.15 mol of SCS was added per mole of total amount of lipid (including cholesterol) and liposomes were formulated as described previously [24]. Dox was added to liposomes in different drug to phospholipid ratios (w/w) - 0.25:1, 0.2:1, 0.15:1 and 0.1:1 for 1h at 65°C. Non-encapsulated Dox was separated by ultracentrifugation at 29000 rpm in a Beckman ultracentrifuge (Ti50.2 rotor). The liposome pellet was resuspended in buffer containing 135 mM NaCl, 10 mM HEPES, pH 7.4.

Size and polydispersity index (pdi) were determined by light scattering using a Zetasizer Nano ZS (Malvern Instruments, Malvern, UK). Lipid concentration was measured by phosphate assay [25].

NBD-PE was incorporated in the formulation at 0.25 mol% of total lipid as a stable fluorescent bilayer marker. Studies assessing the fate of liposomal SCS used a similar mol% of bilayer incorporated C6-NBD-Galactosyl Ceramide.

Loading efficiency

After separation of free non-encapsulated Dox from nanoliposomal encapsulated Dox, the amount of entrapped Dox was measured by fluorimetry (λExitation 475 nm; λ Emission 590 nm). Total amount of drug was measured after entire liposome solubilization with 1% (v/v) Triton in water to a sample from stock liposomal Dox.

Stability

Long-term storage conditions stability (4°C) was based on size, pdi and Dox content measurements for a period of at least 6 months. All measurements were performed in triplicate. Dox content was measured by fluorimetry (λExitation 475 nm; λ Emission 590 nm), after separation of free/entrapped drug by gel filtration chromatography. Stability at 37°C, in the presence and absence of serum was studied for a period of 24 hours by fluorimetry. Total drug release was measured after entire liposomal solubilization by adding 1% (v/v) of Triton-X. The percentage of drug content was calculated following the formula:

[100 – (Fluorescencesample – blank)/ (Fluorescencetotal release – blank)] x 100

Cryo-transmission electron microscopy (TEM)

Cryo-TEM was used to characterize the detailed structure of the liposomal formulations (non-enriched, 10 mol% C_8-GluCer and 10 mol% C_8-GalCer-NL) of Dox and the physical state of the encapsulated drug, as previously described [26, 27]. The freezing was performed in a cooling chamber, which was permanently cooled with liquid nitrogen. A sample droplet was placed on a microperforated copper grid and blotted by a filter paper to result in a thin liquid film. The grid was plunged into liquid ethane for immediate freezing. A Leo 912 Omega TEM microscope (Carl Zeiss NTS GmbH, Oberkochen, Germany) was used.

Cell Culture

In vitro anti-tumor activity was studied towards a panel of human tumor cell lines: BLM and Mel 57 melanomas, MCF-7 and SKBR-3 breast carcinoma and ASPC-1 and Panc-1 pancreatic carcinomas. All tumor cell lines were cultured in Dulbeccos's modified Eagle medium, supplemented with 10% fetal calf serum and 4 mM L-glutamine. HUVEC were isolated by collagenase digestion using the method described by Jaffe et al [28] and cultured in HUVEC medium containing human endothelial serum free medium (Invitrogen), 20% heat inactivated newborn calf serum (Cambrex), 10% heat inactivated human serum (Cambrex), 20 ng/ml human recombinant epidermal basic fibroblast growth factor (Peprotech EC Ltd), 100 ng/ml human recombinant epidermal growth factor (Peprotech EC Ltd) in fibronectin (Roche Diagnostics) coated flasks. Fibroblasts (3T3) were purchased from Biowhitakker and cultured in Dulbeccos's modified Eagle medium containing nutrient mixture F12, supplemented with 10% fetal calf serum and 4 mM L-glutamine.

Cells were subcultured weekly by trypsinization when a confluency of 80-90% was achieved and maintained in a water saturated atmosphere of 5% CO2 at 37°C.

Cell toxicity

All cell lines were plated in flat bottom 96 well-plates. Tumor cells were seeded at cell densities obtained from respective tumor

growth curves to ensure use of cells in their log-phase of growth. BLM and Mel 57 melanoma cells were seeded at a density of $3x10^3$ and $6x10^3$ cells/ well, respectively. $1.25x10^4$ cells/ well were used for breast carcinoma cells MCF-7 and SKBR3. For ASPC-1 and Panc-1 pancreatic carcinoma cell lines $6x10^3$ cells/ well were seeded. HUVEC and 3T3 fibroblast cells were seeded at a density of $1x10^4$ cells/ well and $5x10^3$ cells/ well, respectively, in order to achieve the same confluency.

After 24h, cells were exposed to serial concentrations of Dox-liposomal formulations (SCS enriched and non-enriched) in culture medium for 24h.

Cell survival was determined by measuring total cellular protein levels using the sulforhodamine-B (SRB) assay [29]. Cells were washed twice with PBS, incubated with 10% trichloric acetic acid (1 hour, 4°C) and washed again. Cells were stained with 0.4% SRB (Sigma) for 15 min, washed with 1% acetic acid. After drying, protein-bound SRB was dissolved in TRIS buffer (10 mM, pH 9.4) and absorbance was measured at a wavelength of 540 nm in a plate reader. Cell survival was calculated as a percentage relative to control (untreated cells), which was set at 100%.

IC50 was determinate for each Dox liposomal formulation, by plotting the cell survival observed for each concentration versus the log of the concentration and fitting a non linear regression curve using GraphPad Prism software v5.0. All experiments were performed in triplicates and were repeated at least 3 times, independently.

Cell survival quantification was complemented by evaluation of cellular morphology. Following the same cellular concentration from SRB assay, BLM, Mel 57, MCF-7, SKBR3, Panc-1 and ASPC-1 cells were plated in a 24 well plate and allow to growing for 24h. The cells were treated with Dox (1 µM, 10 µM or 100 µM) in its non-enriched and enriched (C_8-GluCer and C_8-GalCer) liposomal form. After 24h cell morphology was examined with a 10x N.A 0.30 Plan Neofluar objective lens using an inverted Zeiss Axiovert 100M microscope equipped with an Axiocam digital camera (Carl Zeiss).

Intracellular drug uptake by flow cytometry

Intracellular Dox levels in BLM, MCF-7 and ASPC-1 cells were measured by flow cytometry. Cells were seeded on flat bottom 24

well plates at a final concentration of $6x10^4$ cells/ well and incubated for 24h. Non-enriched and SCS-enriched-DoxNL, with C_8-GluCer or C_8-GalCer, diluted in growth medium were added in a drug concentration of 1 µM and 10 µM, after which cells were incubated for 1, 4 and 24h. After incubation, cells were washed twice to discard non-incorporated drug and trypsinized for 2 min. Cell suspensions were washed twice in medium and resuspended in PBS. Cellular uptake was measured on Becton Dickinson FACScan using Cell Quest software. Excitation was set at 488 nm and detection by FL2 detector channel.

Intracellular drug uptake by fluorescence microscopy

MCF-7, BLM and ASPC-1 cells in a concentration of $1x10^5$ cells/ well were seeded on a cover glass coated with 0.1% collagen and incubated for 24h. Hoechst (1:100) was added for 20 min cells and washed twice before adding 10 µM of Dox in form of non enriched-DoxNL or SCS-enriched DoxNL. Cells were incubated at 37°C for 1 and 4h and using fluorescence microscopy intracellular drug uptake was evaluated in living cells, using a filter set consisting of a 450 - 490 nm band pass excitation filter for Hoechst and a 510 nm beam splitter and a 520 – 543 nm long pass excitation filter for Dox. Cells were imaged using a 40x oil immersion objective.

Intracellular drug uptake by confocal microscopy

BLM melanoma, MCF-7 breast carcinoma and ASPC-1 pancreatic carcinoma cell lines cells were cultured on a cover glass of 25 mm diameter coated with 0.1% collagen and incubated for 24h in cultured medium. Cell density was $1x10^5$ cells for BLM melanoma cells, MCF-7 breast carcinoma and ASPC-1 pancreatic carcinoma cells. Non-enriched liposomal Dox and SCS enriched liposomal Dox was added in a concentration of 10 µM. Cells were incubated for 4h. Dox uptake was studied using a Zeiss LSM 510 META confocal microscope using 488 argon laser for NBD-PE (500-550 nm band pass filter), a 405 nm Diode laser for Hoechst (420-480 nm band pass filter) and a 543 nm Helium-Neon laser for Dox (560-615 nm band pass filter). Images of the different incubations were taken using identical settings for laser power and photomultipliers.

Intracellular fate of SCS and Doxorubicin

Labelled NBD-C6-GalCer-DoxNL was followed in time in BLM melanoma cells ($1x10^5$ cells) during treatment for 40 min. A Leica SP5 (Leica Mannheim) confocal microscope was used with 488 nm excitation and BP 500-550 nm emission of the SCS and 561 nm excitation and BP 570 nm-650 nm emission for Dox with a 63x plan apo (na 1.4) lens. Six optical planes were recorded with an interval of 1.22 µm and a pinhole at 1 airy unit.

Doxorubicin was giving by direct excitation with the 488 excitation line, a crosstalk in the SCS emission channel. The amount of crosstalk was measured (35%) and the SCS images were corrected for this crosstalk. To remove some photon noise from the images, a Gaussian filter was applied to the time-lapse images with ImageJ (Rasband, W.S., ImageJ, U. S. National Institutes of Health, Bethesda, Maryland, USA, http://imagej.nih.gov/ij/, 1997-2011). To increase the weak SCS signal a contract stretch was performed.

Statistics

Statistical analysis was performed using the ANOVA test. P-values less than 0.05 were considered statistically significant. All parametric values are expressed as mean ± standard error of the mean (SEM). Calculations were performed using GraphPad Prism v5.0.

RESULTS

Optimizing C_8-GluCer-DoxNL

C_8-GluCer-DoxNL with optimal density of the SCS at 10 mol% [8] were optimized with regard to drug loading. Formulations were loaded at Dox:PL ratios of 0.25:1, 0.2:1, 0.15:1 or 0.1:1 (w/w). The size of the final liposomes after loading was smaller than 100 nm and the pdi ≤0.1 and a loading efficiency > 90% was achieved at a Dox:PL ratio of 0.1:1 for both C_8-GluCer-DoxNL and DoxNL (table 1). To study the effect of Dox:PL ratio on *in vitro* anti-tumor efficacy, 10 mol% C_8-GluCer–DoxNL loaded with the different Dox:PL ratios were tested in human BLM melanoma (Fig. 1A) and human MCF-7 breast carcinoma (Fig. 1B) cell lines. Treatment with 10 mol% C_8-GluCer–DoxNL for 24h, decreased cell viability at increasing DoxNL

Table 1 - Characterization of C_8-GluCer enriched liposomes loaded at different drug to phospholipid mass ratios

Drug:PL $(w/w)_i$	SCS-DoxNL	Size (nm) ±SEM	pdi ±SEM	% Load ±SEM
0.25:1	Non-enriched	109 ± 6.7	0.08 ± 0.01	79 ± 4.1
	10% C_8-GluCer	99 ± 5.7	0.08 ± 0.01	74 ± 4.6
0.2:1	Non-enriched	95 ± 4.9	0.1 ± 0.03	68 ± 10.2
	10% C_8-GluCer	98 ± 7.8	0.19 ± 0.04	69 ± 10.9
0.15:1	Non-enriched	89 ± 3.7	0.09 ± 0.01	92 ± 2.0
	10% C_8-GluCer	86 ± 2.4	0.09 ± 0.02	78 ± 8.2
0.1:1	Non-enriched	89 ± 2.0	0.07 ± 0.01	96 ± 5.7
	10% C_8-GluCer	84 ± 1.1	0.07 ± 0.01	91 ± 5.0

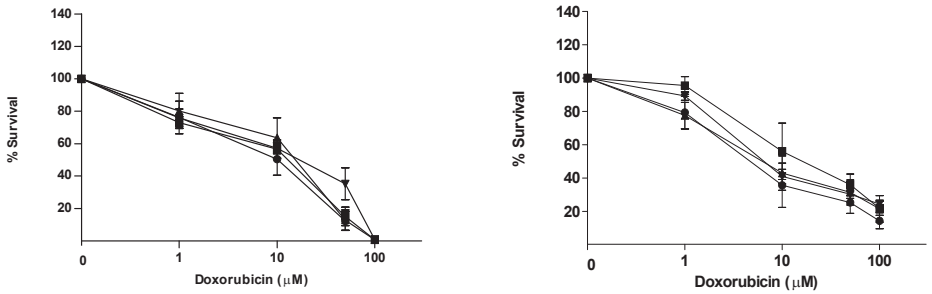

Figure 1 - *In vitro* efficacy study of C_8-GluCer-DoxNL loaded with doxorubicin at different Dox:PL ratios (w/w), 0.25: 1 (●), 0.2:1 (■), 0.15:1 (▲) and 0.1:1 (▼). Different Dox:PL loading ratios did not affect the efficacy of enriched C_8-GluCer-DoxNL in (A) BLM, melanoma and (B) MCF-7 breast carcinoma cell line when incubated for 24h at 37°C. Cell survival was analyzed by SRB assay and values represent the mean ± SEM, n ≥3

concentration, but was not affected by different Dox:PL ratios in either cell line (Fig. 1 and Supplemental table 1).

To assess C_8-GluCer-DoxNL stability, drug retention was studied during long-term storage at 4°C and under cell culture conditions at 37°C in the presence of 10% FCS. During long-term storage, C_8-GluCer-DoxNL had similar stability as DoxNL, showing a minor release of ≤ 10% Dox over 6 months (table 2). Also under culture conditions (37°C with 10% FCS), C_8-GluCer-DoxNL efficiently retained more than 90% of their contents (table 2 and Supplemental Fig. 1), and was comparable to DoxNL.

Novel DoxNL enriched with C_8-GalCer or C_8-LacCer

In addition to C_8-GluCer, two other short chain C_8-glycosphingolipids, with galactosyl (C_8-GalCer) and lactosyl (C_8-LacCer) head groups, (Fig. 2) were evaluated as possible alternative SCS to enhance drug

Table 2- Characterization and stability of different glycoceramide-enriched liposomes

Drug:PL (w/w)i	SCS-DoxNL	Size (nm) ±SEM	pdi ±SEM	%Load ±SEM	% Encapsulated Dox (after 6 months at 4°C) ±SEM	% Encapsulated Dox (after 15h at 37°C) ±SEM
0.1:1	Non-enriched	89 ± 2.0	0.07 ± 0.01	96 ± 5.7	91 ± 4.4	91 ± 9.1
	10% C_8-GluCer	84 ± 1.1	0.07 ± 0.01	91 ± 5.0	88 ± 5.3	98 ± 1.9
	10% C_8-GalCer	92 ± 4.0	0.09 ± 0.02	96 ± 2.8	91 ± 3.3	100 ± 9.5
	10% C_8-LacCer	482 ± 36.2	0.47 ± 0.07	9 ± 2.9	nd *	nd
0.2:1	10% C_8-GalCer	93 ± 4.0	0.16 ± 0.05	98 ± 9.5	nd	nd
	10% C_8-LacCer	395 ± 29.0	0.58 ± 0.07	7 ± 2.9	nd	nd

* nd – not determined

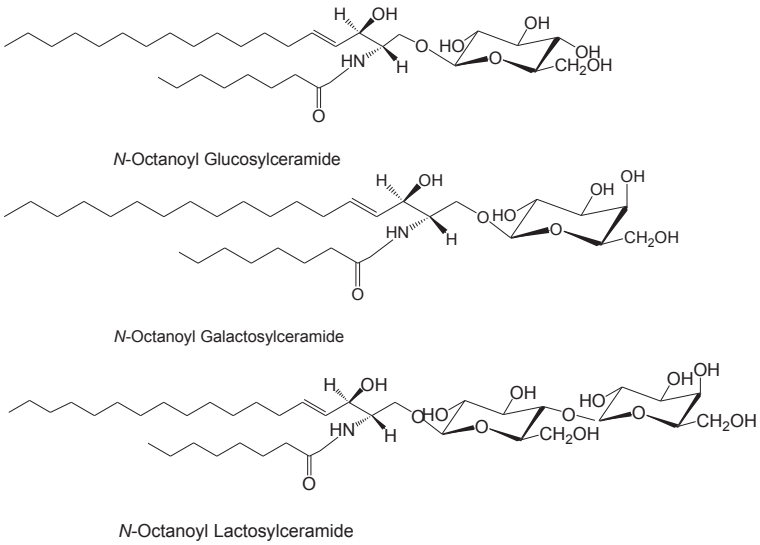

Figure 2 - Short chain sphingolipid molecular structures C_8-GluCer and C_8-GalCer differ in the position of one hydroxyl group in the sugar moiety position, which is equatorial or axial, respectively. C_8-LacCer presents a more complex sugar moiety. Chem Draw v8.0 was used to draw molecular structures

uptake from DoxNL. Formulations were characterized with regard to size, pdi, loading efficiency and stability. At a SCS density of 10 mol% and loaded with Dox at a 0.1:1 Dox:PL (w/w) ratio, C_8-GalCer-DoxNL presented ideal size (<100 nm) and pdi (<0.1), high loading efficiency and a long-lasting stability. At a higher Dox:PL ratio of 0.2:1, Dox loading of C_8-GalCer-DoxNL was still >90%, but pdi increased to 0.16 (table 2). In contrast, C_8-LacCer-DoxNL could not be prepared successfully at either ratio as they strongly aggregated immediately upon Dox loading, resulting in large particle size, pdi and low drug loading efficiency.

Upon long-term storage at 4°C and under cell culture conditions at 37°C in the presence of 10% FCS, C_8-GalCer-DoxNL had similar stability profile as DoxNL, showing a minor release of ≤ 10% Dox

Table 3 - Optimal density of C_8-GalCer-enriched pegylated DoxNL

Drug:PL 0.1:1 $(w/w)_i$	Size (nm) ± SEM	pdi ± SEM	% Load ± SEM
0% C_8-GalCer-DoxNL	89 ± 2.0	0.07 ± 0.01	96 ± 5.7
5% C_8-GalCer-DoxNL	84 ± 1.2	0.06 ± 0.01	97 ± 4.3
10% C_8-GalCer-DoxNL	92 ± 4.0	0.09 ± 0.02	96 ± 2.8
15% C_8-GalCer-DoxNL	83 ± 3.2	0.06 ± 0.01	103 ± 1.1

over 6 months (table 2) and no changes in particle size or pdi (table 2 – thesis supplemental data). Under culture conditions (37°C with 10% FCS) C_8-GalCer–DoxNL efficiently retained more than 90% of their contents (table 2 and Supplemental Fig. 1), comparable to both C_8-GluCer-DoxNL and DoxNL.

Optimal C_8-GalCer enriched DoxNL

C_8-GalCer-DoxNL was prepared at different SCS densities and at a Dox:PL initial mass ratio of 0.1:1. Densities of C_8-GalCer up to 15 mol% did not negatively affect size, pdi or drug loading of the DoxNL (table 3). *In vitro* efficacy studies on MCF-7 breast, human BLM melanoma and ASPC-1 pancreatic carcinoma cells (Fig. 3 and supplemental table 3) demonstrated that a density of 10 mol% resulted in the strongest anti-tumor activity in all cell lines. A higher density of 15 mol% did not further increase efficacy relative to 10 mol%.

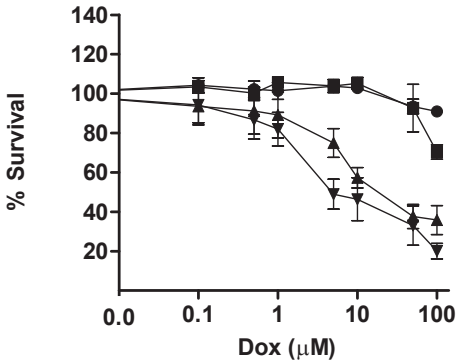

Figure 3 - *In vitro* efficacy study in MCF-7, breast carcinoma cell line incubated with different density of C_8-GalCer in DoxNL, 0 mol% (●), 5 mol% (■), 10 mol% (▲) and 15 mol%(▼) in a Dox:PL mass ratio of 0.1:1. 15 mol % content of C_8-GalCer did not give additional cytotoxicity compared to 10 mol% content. Values represent the mean ± SEM (n_>3)

Transmission Electron Microscopy of SCS-DoxNL

Non-enriched DoxNL and DoxNL enriched with C_8-GluCer or C_8-GalCer were analyzed by cryogenic Transmission Electron Microscopy (cryo-TEM) (Fig. 4). DoxNL were round shaped, uniform in size and most particles were characterized by an intraliposomal gel like precipitate of Dox. C_8-GluCer-DoxNL and C_8-GalCer-DoxNL, which had a normal round shape before Dox-loading (data not shown), were

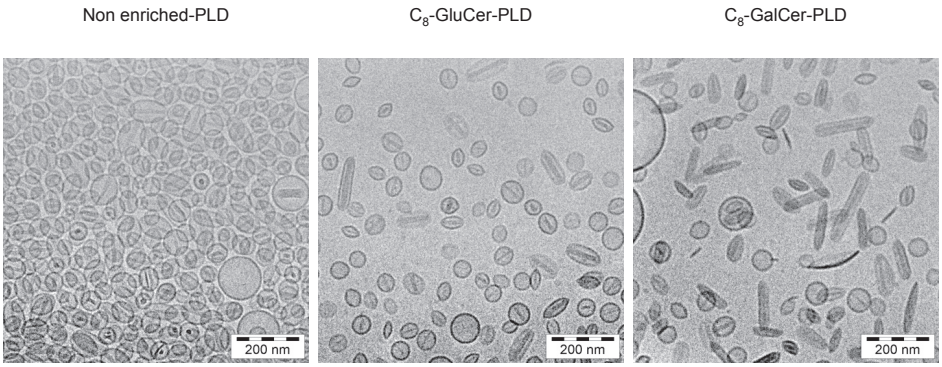

Figure 4 - Cryo-TEM images of HSPC/Chol/PEG liposomes with or without SCS, loaded with doxorubicin in a Dox:PL ratio of 0.1:1. A clear drug precipitate is visible inside liposomes. SCS-enriched DoxNL have more elongated rod-like structures upon loading with Dox. The bar in the micrograph represents 200 nm. A 12500x magnification was used

observed as round and rod-shaped vesicles after Dox-loading. Round vesicles were observed with and without Dox precipitate, rod-shaped particles all contained the typical Dox precipitate and had a width of approximately 40 nm and varied in length between 100 and 200 nm. In the C_8-GalCer-DoxNL formulation occasionally more elongated rod-like particles with a length of up to 500 nm were observed. SCS-enriched-DoxNL exert selective cytotoxicity towards tumor cells.

In vitro drug efficacy of the optimized SCS-enriched DoxNL was tested in a panel of human tumor cell lines, including BLM and Mel57 melanoma, MCF-7 and SKBR3, breast and Panc-1 and ASPC-1 pancreatic carcinoma, as well as in normal cells: endothelial cells (HUVEC) and 3T3 fibroblasts. In all tumor cell lines, C_8-GluCer-DoxNL and C_8-GalCer-DoxNL exerted increased cytotoxicity, compared to DoxNL during 24h incubation. IC50 values of tumor cell treatments with both SCS-enriched formulations dropped significantly by 5 to 50-fold in comparison with DoxNL and commercially available Doxil, $P<0.05$ (table 4 and Supplemental Fig. 2A). Despite the fact that SCS-enrichment of DoxNL increased toxicity towards Mel57 and Panc-1 cell lines, the differences were somewhat less pronounced as compared to the other tumor cell lines. No major differences were observed between C_8-GluCer-DoxNL and C_8-GalCer-DoxNL efficacy towards the various tumor cell lines. Strikingly, cytotoxicity of SCS-DoxNL towards normal endothelial cells and fibroblasts was much less pronounced, with IC50 values that are either indifferent between SCS-DoxNL or DoxNL or show a slight drop of less than 2-fold.

Table 4 - *In vitro* cytotoxicity (IC50,μM) of SCS-enriched-DoxNL and standard PEGylated liposomal doxorubicin in tumor and non-tumor cell lines

	IC_{50} (μM)			
	Doxil	Non enriched DoxNL	10% C_8-GluCer DoxNL	10% C_8-GalCer DoxNL
Tumor cells				
BLM	>150	>150	10.0 ± 2.2*	9.1 ± 0.4*
Mel 57	>150	>150	31.0 ± 7.2*	34.1 ± 18.2*
MCF-7	>150	>150	10.8 ± 2.3*	6.9 ± 2.0*
SKBR-3	>150	>150	3.1 ± 0.9*	5.3 ± 4.5*
Panc-1	>150	>150	29.2 ± 7.1*	25.4 ± 3.3*
ASPC	>150	>150	10.1 ± 1.6*	23.1 ± 17.3*
Non-Tumor cells				
HUVEC	>150	>150	>150	87.7 ± 7.1
3T3	>150	>150	101.7 ± 17.4	103.3 ± 8.6

At least three independent experiments were performed and values represent the mean ± SEM. * $P < 0.05$ versus non enriched-PLD.

In HUVEC, C_8-GluCer-DoxNL showed a toxicity profile comparable to DoxNL and Doxil. On the other hand, C_8-GalCer-DoxNL had a somewhat more pronounced toxicity towards HUVEC than C_8-GluCer-DoxNL at high drug concentrations. In turn, C_8-GluCer-DoxNL showed to be of equally low toxicity to fibroblasts as C_8-GalCer-DoxNL with comparable IC50 values. Empty SCS-NL were tested on MCF-7 breast carcinoma cell line and no toxicity was caused by the presence of C_8-GluCer or C_8-GalCer in the liposomal bilayer (data not shown) at equimolar lipid concentrations to SCS-DoxNL.

In vitro drug efficacy was qualitatively confirmed by evaluating cellular morphology after treatment with free Dox, Doxil, non-enriched and SCS-enriched-DoxNL (Supplemental Fig. 2B). All other tested tumor cell lines showed similar results as the BLM melanoma cell line (data not shown).

Quantification of SCS-enriched-DoxNL potential as drug uptake enhancers

The effect of SCS enrichment of DoxNL on intracellular Dox uptake was quantified by flow cytometry. BLM melanoma, MCF-7 breast carcinoma and ASPC-1 pancreatic carcinoma cell lines were treated with DoxNL, C_8-GluCer-DoxNL or C_8-GalCer-DoxNL at drug concentrations of 10 or 1 μM incubated for 1, 4 or 24h (Fig. 5A and Supplemental Fig. 4A, respectively). Intracellular drug uptake increased in time for both SCS-DoxNL formulations in all

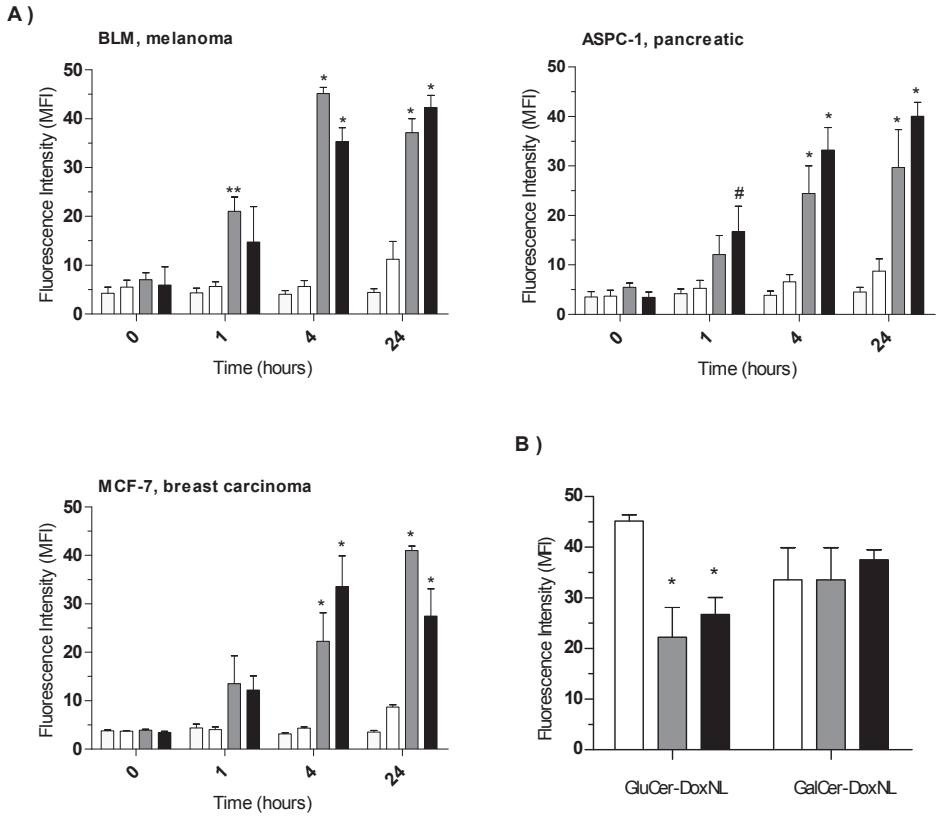

Figure 5 - Intracellular Dox uptake after treatment with DoxNL, 10 µM was quantified by flow cytometry in BLM melanoma, MCF-7 breast carcinoma and ASPC-1 pancreatic carcinoma (A). Doxorubicin was formulated in non-enriched-DoxNL (open), 10% C_8-GluCer-DoxNL (dark grey) and 10% C_8-GalCer-DoxNL (black). Fluorescence of non-treated cells was measured as a control (light grey). At least three independent experiments were performed and values represent the mean ± SEM; *, $P<0.001$; **, $P<0.01$ and #, $P<0.05$ versus non enriched-DoxNL at the same time point. (B) Overview of Dox uptake by 3 different tumor cell lines incubated with 10 µM C_8-GluCer or C_8-GalCer-DoxNL after 4 h of incubation. C_8-GalCer-DoxNL gives similar results in all three cell lines, C_8-GluCer seemed to increase Dox uptake in BLM (open) cells when compared to MCF-7 (dark grey) and ASPC-1 (black) cells

cell lines, whereas only minor drug uptake was observed in cells incubated with DoxNL for 24h. At all drug concentrations and incubation times tested, SCS-DoxNL induced higher intracellular drug levels than DoxNL. Upon incubation with 10 µM SCS-DoxNL a high intracellular drug uptake was achieved after 4h, with little to no increase in uptake upon prolonging the incubation to 24h. This is caused by cytotoxicity effects affecting drug uptake measurements at 24h. At a 10-fold lower concentration, which causes much less cytotoxicity during 24h, drug levels continued

to increase up to 24h (Supplemental Fig. 4). Whereas C_8-GalCer after 4h of incubation at 10 µM gives similar results in all three cell lines, C_8-GluCer seemed to increase Dox uptake in BLM cells (45.2 ± 1.2) to a higher extent than MCF-7 (22.3 ± 5.9) and ASPC-1 cells (24.4 ± 3.9) (Fig. 5B). A similar trend can be seen at 1 µM, where C_8-GluCer improves Dox delivery to BLM more strongly than C_8-GalCer (Supplemental Fig. 4B).

Fluorescence microscopic imaging of intracellular drug delivery

Evaluation of intracellular drug uptake by life cell fluorescence microscopy (Fig. 6) supported the outcome of flow cytometry measurements. After 4h of incubation, non-enriched DoxNL still did not show considerable intracellular drug delivery, whereas both SCS-enriched DoxNL established high intracellular Dox levels. Similar to the observations obtained by flow cytometry, BLM cells showed increased Dox uptake from C_8-GluCer-DoxNL compared to C_8-GalCer-DoxNL. Dox from SCS enriched-DoxNL showed faint cytoplasmic

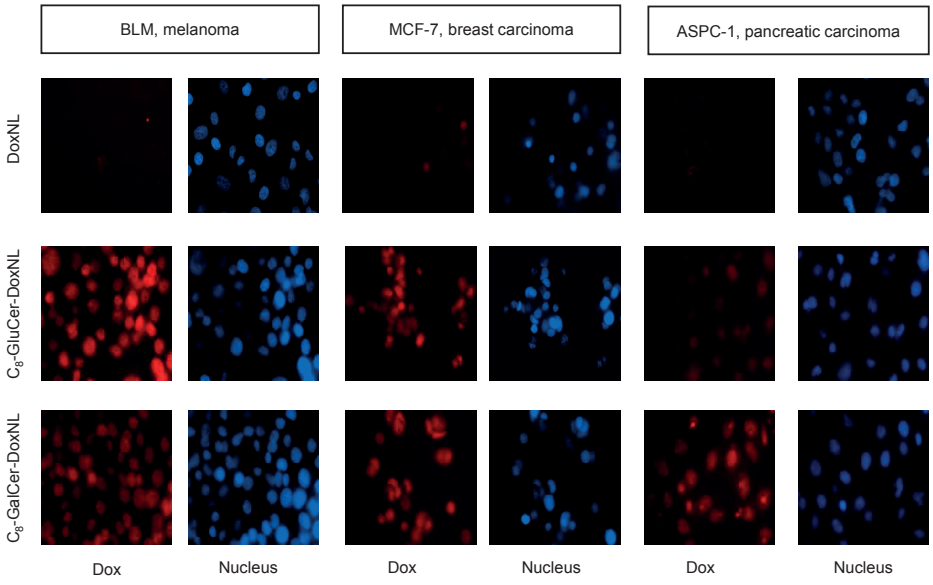

Figure 6 - Fluorescence microscopy images of BLM, melanoma cell line (A), MCF-7 breast carcinoma cell line (B) and ASPC-1, pancreatic carcinoma cell line (C), after 4h of treatment with 10 µM of doxorubicin formulated in standard non-enriched, C_8-GluCer or C_8-GalCer enriched nanoliposomes. Nucleus was stained with Hoechst (blue). Doxorubicin is fluorescent by itself (red). At least three independent experiments were performed

staining, and mainly accumulated in the nucleus as confirmed by a Hoechst co-staining.

Cellular fate of SCS-NL and Doxorubicin

Confocal microscopy experiments were performed to further confirm the intracellular localization of Dox and nanoparticles. After 4h incubation, both enriched DoxNL achieved high intracellular drug levels. Dox accumulated in the nucleus to a high extent, whereas also cytoplasmic Dox was observed. Liposome internalization was not observed by MCF-7, breast carcinoma cells (Fig. 7), BLM melanoma or ASPC-1 pancreatic carcinoma cell lines (Supplemental Fig. 3). The absence of tumor cell DoxNL internalization was evidenced by the lack of cell associated liposomal bilayer marker NBD-PE, which was found extracellularly surrounding the cells whereas at the same time Dox showed some cytoplasmic staining and high levels in the nucleus.

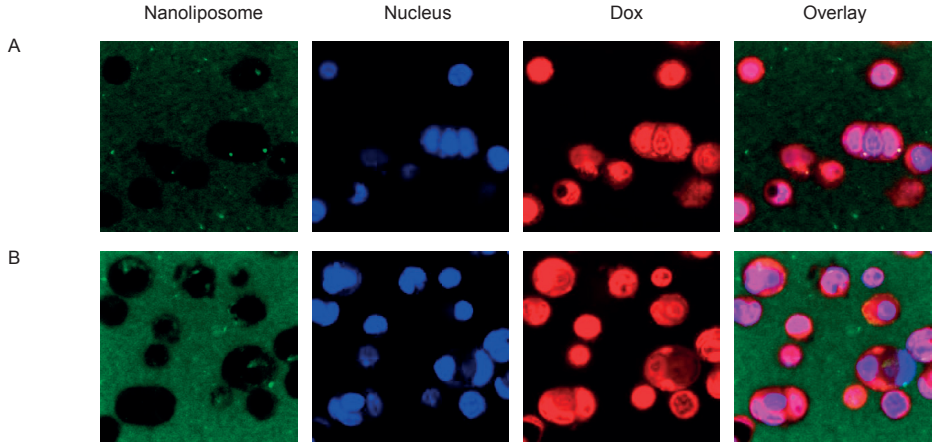

Figure 7 - Intracellular-localization of NBD-PE-labeled liposomes (green) and Dox (red) in MCF-7 breast carcinoma cell line by confocal microscopy. Treatment was added (10 µM Dox) in the form of C_8-GluCer-DoxNL (A) or C_8-GalCer-DoxNL (B) and after 4h of incubation at 37°C, nuclear (blue) and cytoplasmic drug uptake were analyzed

Intracellular localization of SCS and Doxorubicin

Time-lapse confocal microscopy experiments were performed directly after starting the incubation of cells with SCS-enriched liposomes to further study the intracellular localization of Dox and SCS. Three-dimensional reconstructions of cellular stacks in time were used to create a movie representing cellular uptake of the SCS, Dox and their co-localization in time (Supplemental Movie1 – digital version).

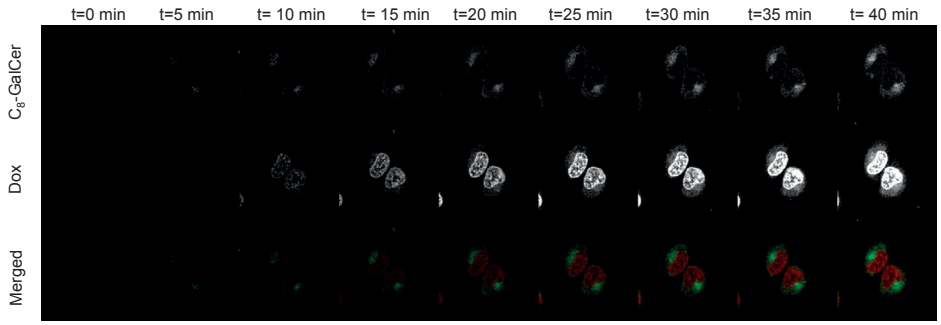

Figure 8 - Localization of SCS and Dox in the plasma membrane by confocal microscopy. Directly after BLM melanoma cell treatment, 5 µM with NBD labeled-SCS liposomes containing doxorubicin, the green fluorescent labelled-C_8-GalCer was followed in time and separately from Dox. The SCS accumulates previously to Dox in the plasma membrane and after Dox accumulates in the nucleus very rapidly

In time, fluorescently labeled SCS were observed to transfer from the DoxNL bilayer to the cell membrane (Fig. 8). This transfer was observed already at 5 minutes after start of the incubation and preceded cellular Dox uptake, which was observed only at 10 min after adding liposomes to the cells. Doxorubicin entered the cell and prominently accumulated in the nucleus within the subsequent 30 min. In addition, appreciable Dox-levels were detected in the cytoplasm at 25-40 min (Fig. 8).

SCS transferred to the cell membrane were later also found intracellular in the cytoplasm, but were not associated with the nucleus or with its membrane.

DISCUSSION

The use of SCS-enriched nanoliposomes to improve drug-cell membrane traversal is a novel drug delivery concept and represents an advanced and versatile technology to enhance Dox delivery into tumor cells and thereby its efficacy as a chemotherapeutic drug. Previously, we were able to demonstrate that DoxNL enriched with C_8-GluCer strongly enhanced Dox delivery and subsequent anti-tumor efficacy both in vitro and in vivo [6, 30, 31]. In the present study a further optimization and characterization of C_8-GluCer-DoxNL was performed, in terms of drug loading, liposome size, pdi, drug entrapment efficiency and morphology, all representing important criteria for translation of this formulation towards

future clinical application. In addition, DoxNL with other synthetic short chain glycosphingolipids were studied for drug uptake enhancement, of which C_8-GalCer, but not C_8-LacCer appeared promising and displayed similar drug uptake enhancing properties as C_8-GluCer. Drug uptake enhancement by SCS-DoxNL significantly increased *in vitro* antitumor activity towards various human tumor cell lines. This effect was observed to a much lesser extent in normal endothelial cells and fibroblasts, demonstrating an important preference of this drug delivery process for tumor cells. Finally, we were able to demonstrate that enhanced Dox delivery by SCS-Dox-NL was not related to uptake of the nanoliposomes as such by the tumor cells, but was preceded by a rapid and apparently critical transfer of the SCS from the nanoliposomal bilayer to the cell membrane. A similar transfer process was proposed previously by Zolnik co-workers for the apoptosis-inducing N-hexanoyl-d-erythrosphingosine (C6-ceramide) [1, 32]. In the present study we demonstrated that the C_8-GluCer or C_8-GalCer upon their transfer to the tumor cell membrane do not affect cell survival in the absence of Dox, but are able to potentiate Dox cytotoxicity.

Optimal loading of Dox (>90% encapsulation efficiency) in DoxNL enriched with 10 mol% C_8-GluCer or C_8-GalCer was obtained at a Dox:PL initial mass ratio of 0.1:1 resulting in homogeneous particles (pdi < 0.1) with a size between 80 and 100 nm, which is considered ideal for efficient extravasation through leaky tumor vasculature [1, 32]. For SCS-DoxNL higher Dox:PL ratios caused somewhat less efficient drug loading, but did not affect drug efficacy towards BLM, melanoma and MCF-7 breast carcinoma cell lines (Fig. 1A).

This result suggests that the quantity of SCS used at the highest Dox:PL ratio of 0.25:1 was sufficient to induce maximal enhancement of drug uptake. This is in accordance with Veldman et al. who demonstrated that uptake of Dox, added to cells in free form, reached saturation upon treating these cells with increasing concentrations of C6-sphingomyelin [1, 32]. Moreover, the higher quantity of SCS, in enriched liposomal formulations with lower Dox:PL mass ratios did not induce additional toxicity by the SCS. This correlates well with the finding that cytotoxicity is related to doxorubicin treatment and not to the SCS.

Formulation of C_8-LacCer in Dox-NL was unsuccessful. Despite the fact that C_8-LacCer enriched-NL could be prepared, Dox loading

of these NL resulted in strong aggregation and low loading efficiency. Likely, the more complex sugar moiety of C_8-LacCer in comparison to C_8-GluCer or C_8-GalCer (Fig. 2) interfered with the liposomal membrane preventing a stable transmembrane ammonium sulfate gradient.

Whereas density of C_8-GalCer did not affect DoxNL size, pdi and Dox loading, *in vitro* drug efficacy was improved only for the 10 and 15 mol% enriched formulations in comparison to standard DoxNL. Since 10 mol% C_8-GalCer-DoxNL were equally effective as those with 15 mol%, we concluded that the former loaded at an initial Dox:PL mass ratio of 0.1:1 represented the optimal C_8-GalCer-DoxNL formulation. With a 10 mol% SCS-density and a 0.1:1 Dox:PL (w/w) loading ratio this optimal C_8-GalCer-DoxNL has similar characteristics as the optimal C_8-GluCer-DoxNL [1, 32].

Stability studies under storage or cell culture conditions demonstrated both SCS-DoxNL formulations provided high stability and did not reveal significant differences between C_8-GluCer or C_8-GalCer enriched and standard DoxNL. Cryo-TEM elucidated a typical Dox precipitate inside all DoxNL [26] with a more prominent rod-shaped morphology for SCS-Dox-NL than Dox-NL. Apparently the presence of SCS in the bilayer of DoxNL is responsible for the change in shape of the nanoparticles during Dox-loading, as SCS-liposomes before loading were round-shaped and after loading all rod-shaped particles did contain a clear Dox precipitate. Liposomal bilayers, when enriched with SCS, seemingly are more flexible or deformable. It remains speculative whether this enhanced flexibility of enriched liposomal bilayers contributes to the improved intracellular Dox delivery.

Both C_8-GluCer-DoxNL and C_8-GalCer-DoxNL significantly increased cytotoxicity in comparison to standard DoxNL and clinically applied DoxNL (Doxil/Caelyx) in all tumor cell lines tested. Stable Dox entrapment in Doxil is known to reduce toxic side effects related to free Dox. However, this high stability in combination with the low tumor cell membrane permeability for DoxNL strongly limits drug delivery and efficacy [22]. It is at this point that drug delivery is improved when using SCS-DoxNL. Enrichment of DoxNL with C_8-GluCer or C_8-GalCer did not affect Dox release for up to 24h in cell culture medium containing 10% of serum (table 2 and supplemental data, Fig. 1), but was in a similar period

able to improve *in vitro* drug efficacy, due to SCS potential as drug uptake enhancer. Remarkably, the *in vitro* cytotoxic effect of SCS-DoxNL was much less pronounced on endothelial cells and fibroblast demonstrating a cell-type dependency and specificity of the SCS-drug delivery process in favor of tumor cells. In addition, this finding holds promise that SCS-DoxNL during circulation will not readily affect the normal endothelial lining of healthy blood vessels. Upon accumulation at the tumor site, SCS can act as a tumor cell membrane selective drug permeabilizer. In this context, similar results using SCS and Dox administered in free form were reported by Veldman et al. with cultured rat cardiac myoblasts [6]. For yet unknown reasons, non-tumor cells are not highly susceptible towards the sphingolipid analogue mediated drug uptake enhancement, when compared to tumor cells.

The increased *in vitro* efficacy of SCS-DoxNL coincided with an increased and rapid intracellular drug delivery in different tumor cell lines as demonstrated by fluorescence microscopy and flow cytometry. Already within 1h notable differences in cellular Dox fluorescence were measured between SCS-enriched and non-enriched DoxNL, in favor of the former. These differences appeared maximal after 4h of incubation reaching up to 5-8-fold more Dox delivered using SCS-DoxNL and remained high until 24h. In these drug uptake studies some variation between the sensitivity of various tumor cell lines towards SCS- DoxNL was observed. Dox uptake after incubation for 4h with C_8-GluCer-DoxNL was higher in BLM melanoma than after C_8-GalCer-DoxNL. This difference was not observed with MCF-7 breast and ASPC-1 pancreatic carcinoma. These observations were confirmed by living cell fluorescence microscopy and suggest a difference in the potential of C_8-GluCer versus C_8-GalCer as drug uptake enhancers and that even among tumor cells certain cell specificity for each distinct SCS exists. Future studies will investigate whether differences in cell membrane lipid composition can explain the differences in SCS-mediated drug uptake in normal and tumor cells. An important question is how Dox is transported from the liposomes into the cell. Seynhaeve et al. concluded that, in addition to passive release, DoxNL may be taken up completely by tumor cells upon long-term incubations, followed by intracellular degradation, after which released Dox enters the nucleus [23]. Others suggested that liposomes can be degraded in the interstitial

space followed by uptake of the released drug by tumor cells [4, 5, 33-35]. Our living cell confocal microscopy studies using SCS-DoxNL with a fluorescent bilayer marker, showed virtually no internalization of the nanoliposomal carrier by MCF-7, ASPC-1 or BLM cell lines during 4h of incubation, whereas at the same time high levels of Dox where detected intracellularly in the nucleus and to a lesser extent in the cytoplasm. Therefore intracellular Dox delivery using SCS-NL is not dependent on internalization of the nanocarrier as such. By contrast, transfer of the SCS from the nanoliposomal bilayer to the tumor cell membrane was demonstrated to occur rapidly and to precede Dox influx. Together these data demonstrate that the selective transfer of the SCS to the tumor cell membrane promotes Dox internalization. Transfer of liposomal bilayer constituents to tumor cell membranes has been described previously for a lipophilic prodrug of 5-fluorodeoxyuridine and the anti-angiogenic drug fumagillin [37-39].

It remains to be seen whether the SCS transfer also enhances drug release from the liposomes. The transfer of SCS from the rod-shaped liposomal bilayer to the cell membrane when in close proximity may well be responsible for a locally enhanced release of Dox from the particles in which the SCS stabilized rod-like shape is deformed causing local content release at the sites of SCS transfer. The released content is then taken up more rapidly due to SCS induced permeability of the cell membrane. Pinnaduwage and Huang referred to a similar delivery process by liposomes that upon direct contact with a membrane-bound antigen, rapidly and spontaneously destabilize, releasing entrapped contents [40].

CONCLUSION

The findings presented here identified, C_8-GluCer and C_8-GalCer, as specific SCS to improve the therapeutic potential of nanoliposomal Dox by selectively enhancing cellular membrane permeability of tumor cells to Dox upon their transfer to the cell membrane. Optimized formulations of SCS-Dox-NL were developed, which will now undergo *in vivo* evaluation to investigate if they are able to overcome the current issue of limited Dox bioavailability related to DoxNL.

ACKNOWLEDGEMENTS

This work was financed by the Dutch Cancer Society.

REFERENCES

1. Gabizon A, Shmeeda H, Barenholz Y, Pharmacokinetics of Pegylated Liposomal Dox: Review of Animal and Human Studies, Clin Pharmacokinet 2003;42(5):419-36.
2. Koning GA, Krijger GC, Targeted Multifunctional Lipid Based Nanocarriers for Image Guided Drug Delivery, Anti Cancer Agents Med Chem 2007;7(4):425-40.
3. Maeda H, Wu J, Sawa T, Matsumura Y, Hori K, Tumor vascular permeability and the EPR effect in macromolecular therapeutics: a review, J. Control Release 2000;65(1-2): 271-84.
4. Mayer D, Nayar R, Thies RL, Boman NL, Cullis PR, Bally MB, Identification of vesicle properties that enhance the antitumor activity of liposomal vincristine against murine L1210 leukemia. Cancer Chemother Pharmacol 1993;33(1):17-24.
5. Mayer LD, Bally MB, Cullis PR, Wilson SL, Emerman JT, Comparison of free and liposome encapsulated Dox tumor drug uptake and antitumor efficacy in the SC115 murine mammary tumor. Cancer Lett. 1999;53(2-3):183-90.
6. Veldman RJ, Zerp S, van Blitterswijk WJ, Verheij M, N-hexanoyl-sphingomyelin potentiates in vitro Dox cytotoxicity by enhancing its cellular influx. Br. J. Cancer 2004; 90(4):917-25.
7. Veldman RJ, Koning GA, van Hell A, Zerp S, Vink SR, Storm G, Et al, Coformulated N-Octanoyl-glucosylceramide Improves Cellular Delivery and Cytotoxicity of Liposomal Dox. J Pharmacol Exp Ther 2005; 315(2):704-710.
8. van Lummel M, van Blitterswijk WJ, Vink SR, Veldman RJ, van der Valk MA, Schipper D, et al, Enriching lipid nanovesicles with short-chain glucosylceramide improves Dox delivery and efficacy in solid tumors. FASEB J 2011;25(10):280-9.
9. Jacobson K, Mouritsen OG, Anderson RG, Lipid rafts: at a crossroad between cell biology and physics. Nat Cell Biol 2007;9(1):7-14.
10. Anderson RG, The Caveolae Membrane System. Annu Rev Biochem 1998;67: 199-225.
11. Masserini M, Ravasi D, Role of sphingolipids in the biogenesis of membrane domains. Biochim Biophys Acta 2001;1532(3):149-61.
12. Siskind LJ, Colombini M, Sphingosine Forms Channels in Membranes That Differ Greatly from those by Ceramide. J Bioenerg Biomembr 2005;37(4):227-36.
13. Bodley A, Liu LF, Israel M, Seshadri R, Koseki Y, Giuliani FC, Kirschenbaum S, Silber R, Potmesil M, DNA Topoisomerase II-mediated Interaction of Dox and Daunorubicin Congeners with DNA. Cancer Res 1989;49(21):5969-78.
14. Gewirtz DA, A critical evaluation of the mechanisms of action proposed for the antitumor effects of the anthracycline antibiotics adriamycin and daunorubicin. Biochem Pharmacol 1999;57(7);727-41.
15. Rahman AM,Yusuf SW, Ewer MS, Anthracycline-induced cardiotoxicity and the cardiac-sparing effect of liposomal formulation. Int J Nanomedicine 2007;2(4):567-83.

16. O'Brien ME, Wigler N, Inbar M, Rosso R, Grischke E, Santoro A, Et al, CAELYX Breast Cancer Study Group, Reduced cardiotoxicity and comparable efficacy in a phase III trial of pegylated liposomal Dox HCl (CAELYX/DoxilÂ®) versus conventional Dox for first-line treatment of metastatic breast cancer. Ann Oncol 2004;15(3):440-49.
17. Torchilin VP, Omelyanenko VG, Papisov MI, Bogdanov AA Jr, Trubetskoy VS, Herron JN Et al, Poly (ethylene glycol) on the liposome surface: on the mechanism of polymer-coated liposome longevity. Biochim Biophys Acta 1994;1195(1):11-20.
18. Northfelt DW, Dezube BJ, Thommes JA, Miller BJ, Fischl MA, Friedman-Kien A Et al, Pegylated-liposomal Dox versus Dox, bleomycin, and vincristine in the treatment of AIDS-related Kaposi's sarcoma: results of a randomized phase III clinical trial. J Clin Oncol 1998; 16(7):2445-2451.
19. Tejada-Berges T, Granai CO, Gordinier M, Gajewski W, Caelyx/Doxil for the treatment of metastatic ovarian and breast cancer. Expert Rev Anticancer Ther 2002; 2 (2): 143-150.
20. Hussein MA, Anderson KC, Role of liposomal anthracyclines in the treatment of multiple myeloma. Semin Oncol 2006;31(6 Suppl 13): 147-160.
21. Alberts DS, Liu PY, Wilczynski SP, Clouser MC, Lopez AM, Michelin DP, Et al, Randomized trial of pegylated liposomal Dox (PLD) plus carboplatin versus carboplatin in platinum-sensitive (PS) patients with recurrent epithelial ovarian or peritoneal carcinoma after failure of initial platinum-based chemotherapy (Southwest Oncology Group Protocol S0200). Gynecol Oncol 2008;108(1);90-94.
22. Seynhaeve AL, Hoving S, Schipper D, Vermeulen CE, Wiel-Ambagtsheer G, van Tiel ST, Et al, Tumor Necrosis Factor A Mediates Homogeneous Distribution of Liposomes in Murine Melanoma that Contributes to a Better Tumor Response. Cancer Res 2007;67(19):9455-9462.
23. Laginha KM, Verwoert S, Charrois GJ, Allen TM, Determination of doxorubicin levels in whole tumor and tumor nuclei in murine breast cancer tumors. Clin Cancer Res. 2005 Oct 1;11(19 Pt 1):6944-9.
24. Judson I, Radford JA, Harris M, Blay JY, van Hoesel Q, le Cesne A Et al Randomised phase II trial of pegylated liposomal doxorubicin (DOXIL/CAELYX) versus doxorubicin in the treatment of advanced or metastatic soft tissue sarcoma: a study by the EORTC Soft Tissue and Bone Sarcoma Group. Eur J Cancer 2001;37(7):870-7.
25. Haran G, Cohen R, Bar LK, Barenholz Y, Transmembrane ammonium sulfate gradients in liposomes produce efficient and stable entrapment of amphipathic weak bases. Biochim Biophys Acta 1993; 1151(2):201-215.
26. Rouser G, Fkeischer S, Yamamoto A, Two dimensional thin layer chromatographic separation of polar lipids and determination of phospholipids by phosphorus analysis of spots. Lipids 1970;5(5): 494-496.
27. Li X, Hirsh DJ, Cabral-Lilly D, Zirkel A, Gruner SM, Janoff AS, Et al, Dox physical state in solution and inside liposomes loaded via a pH gradient. Biochim Biophys Acta 1998; 1415(1):23-40.

28. Maurer-Spurej E, Wong KF. Maurer N, Fenske DB, Cullis PR, Factors influencing uptake and retention of amino-containing drugs in large unilamellar vesicles exhibiting transmembrane pH gradients. Biochim Biophys Acta 1999;1416(1-2):1-10.
29. Jaffe EA, Becker CG, Minick CR, Culture of Human Endothelial Cells Derived from Umbilical Veins. Identification by morphologic and immunologic criteria. J. Clin. Invest 1973;52(11):2745-2756.
30. Skehan P, Storeng R, Scudiero D, Monks A, McMahon J, Vistica D, Et al, New Colorimetric Cytotoxicity Assay for Anticancer-Drug Screening. J Natl Cancer Inst 1990; 82(13):1107-1112.
31. Zolnik BS, Stern ST, Kaiser JM, Heakal Y, Clogston JD, Kester M, Et al, Rapid distribution of Liposomal Short Chain Ceramide in vitro and in vivo. Drug Metab Dispos 2008;36(8):1709-1715
32. Charrois GJ, Allen TM, Rate of biodistribution of STEALTH liposomes to tumor and skin: influence of liposome diameter and implications for toxicity and therapeutic activity. Biochim Biophys Acta 2003; 1609(1):102-8.
33. Bandekar A, Karve S, Chang M, Mu Q, Rotolo J, Sofou S. Antitumor efficacy following the intracellular and interstitial release of liposomal doxorubicin. Biomaterials 2012;33:4345-52.
34. Forssen EA, Coulter DM, Proffitt RT, Selective in Vivo Localization of Daunorubicin Small Unilamellar Vesicles in Solid Tumors. Cancer Res 1992;52(12):3255-3261.
35. Gabizon AA, Selective Tumor Localization and Improved Therapeutic Index of Anthracyclines Encapsulated in Long-Circulating Liposomes. Cancer Res 1992;52(4): 891-896.
36. Perez-Soler R, Ling YH, Zou Y, Priebe W, Cellular pharmacology of the partially non-cross-resistant anthracycline annamycin entrapped in liposomes in KB and KB-V1 cells. Cancer Chemother Pharmacol 1994; 34(2):109-118.
37. Koning GA, Morselt HW, Velinova MJ, Gorter A, Allen TM, Zalipsky S, Et al,Selective transfer of a lipophilic prodrug of 5-fluorodeoxyuridine from immunoliposomes to colon cancer cells Biochim Biophys Acta 1999; 1420 (1-2): 153-67.
38. Koning GA, Gorter A, Scherphof GL, Kamps JA, Antiproliferative effect of immunoliposomes containing 5-fluorodeoxyuridine-dipalmitate on colon cancer cells. Br J Cancer 1999;80(11):1718-25.
39. Cyrus T, Winter PM, Caruthers SD, Wickline SA, Lanza GM, Magnetic resonance nanoparticles for cardiovascular molecular imaging and therapy.Expert Rev Cardiovasc Ther 2005;3(4):705-15.
40. Pinnaduwage P, Huang L, Stable Target-Sensitive immunoliposomes. Biochemistry 1992;31:2850-2855.

CHAPTER 3

Short chain glycoceramides promote intracellular mitoxantrone delivery from novel nanoliposomes into breast cancer cells

Lília R. Cordeiro Pedrosa, Timo L.M. ten Hagen, Regine Süss, Albert van Hell, Alexander M.M Eggermont, Marcel Verheij, Gerben A. Koning

Pharm Res. submitted

ABSTRACT

Purpose: To improve therapeutic activity of mitoxantrone (MTO)-based chemotherapy by reducing toxicity through encapsulation in nanoliposomes and enhancing intracellular drug delivery using short chain sphingolipid (SCS) mediated tumor cell membrane permeabilization.

Methods: Standard (MTOL) and nanoliposomes enriched with the SCS, C_8-Glucosylceramide or C_8-Galactosylceramide (SCS-MTOL) were loaded by a transmembrane ammonium sulphate gradient and characterized by DLS and cryo-TEM. Intracellular MTO delivery was measured by flow cytometry and imaged by fluorescence microscopy. *In vitro* cytotoxicity was studied in breast carcinoma cell lines. Additionally, live cell confocal microscopy addressed the drug delivery mechanism by following the intracellular fate of the nanoliposomes, the SCS and MTO. Intratumoral MTO localization in relation to CD31-positive tumor vessels and CD11b positive cells was studied in an orthotopic MCF-7 breast cancer xenograft.

Results: Stable SCS-MTOL were developed increasing MTO delivery and cytotoxicity to tumor cells compared to standard MTOL. This effect was much less pronounced in normal cells. The drug delivery mechanism involved a transfer of SCS to the cell membrane, independently of drug transfer and not involving nanoliposome internalization. MTO was detected intratumorally upon MTOL and SCS-MTOL treatment, but not after free MTO, suggesting an important improvement in tumor drug delivery by nanoliposomal formulation. Nanoliposomal MTO delivery and cellular uptake was heterogeneous throughout the tumor and clearly correlated with CD31-positive tumor vessels. Yet, MTO uptake by CD11b positive cells in tumor stroma was minor.

Conclusions: Nanoliposomal encapsulation improves intratumoral MTO delivery over free drug. Liposome bilayer-incorporated SCS preferentially permeabilize tumor cell membranes enhancing intracellular MTO delivery.

INTRODUCTION

Mitoxantrone (MTO) is an anthracenedione, a group of synthetic chemotherapeutic drugs. It is the most potent of many ametantrone derivatives that were identified in a quest for synthetic anthracyclin-related compounds with potential chemotherapeutic activity [1, 2]. Due to their chemical similarity to the naturally occurring antitumor antibiotics, such as the anthracyclines doxorubicin and daunorubicin and related drugs such as bleomycin and mitomycin-C, MTO exerts similar mechanisms of action and antitumor activity. However, lower cardiotoxicity as side effect has been described for MTO [3-5].

MTO has gained importance in the treatment of metastatic breast cancer over the use of anthracyclines [6, 7] due to its similar therapeutic activity, which is exerted with less severe gastrointestinal toxicity, cardiotoxicity and alopecia at equally myelosuppressive doses [8]. Numerous studies on the mechanism of action of MTO indicate that nuclear DNA is the major target for this drug [9-12]. Binding of MTO to DNA causes DNA condensation, inhibits replication and RNA transcription. MTO is also a potent inhibitor of topoisomerase II, an enzyme involved in control of DNA topology through breaking and rejoining double-stranded DNA [2, 3]. More recently it was proven that MTO binds to chromatin and produces a compact structure, a finding which is in good agreement with the inhibitory effects on DNA replication and RNA transcription [12, 13]. Despite the improved toxicity profile of MTO compared to anthracyclines, significant side effects still remain [6, 7].

It is well established that the therapeutic index of anticancer agents can be improved through application of liposomal drug carrier technology [14]. Encapsulation in liposomes may reduce toxic side effects and increase drug levels in tumors [15-17]. Liposomes are rationally designed to entrap drugs while in circulation, thereby reducing the exposure of healthy tissue and selectively delivering them locally in the tumor by virtue of the enhanced permeability and retention effect [17]. Sterically stabilized liposomes exhibit extended blood circulation time, which together with their small size of <100 nm can result in tumor accumulation [17, 18]. However the slow drug release, the presence of the tumor cell membrane

barrier and thus limited intracellular drug bioavailability after liposome accumulation in the tumor, represent important factors limiting efficacy of liposomal chemotherapy [19-23].

Previously, we reported that short chain sphingolipids (SCS), like C_8-glucosylceramide (C_8-GluCer) or C_8-galactosylceramide (C_8-GalCer) can significantly potentiate intracellular drug uptake of free or liposome-encapsulated drugs and thereby enhance their efficacy, [24-28]. It is hypothesized, that a dynamic biophysical mechanism is responsible for the enhanced drug delivery properties of SCS upon their insertion into the tumor cell membrane [27, 28]. The modulation of tumor cell membrane lipid composition by SCS may result in specific pore domains in the cell membrane, increasing cellular drug influx [28, 29]. In the current study we broaden the application of this novel drug delivery strategy targeting the plasma membrane lipid composition to MTO. The aim is to develop novel effective liposomal MTO formulations, which benefit from reduction in toxicity through liposomal encapsulation and the SCS-mediated cellular drug uptake enhancement. We therefore co-formulated both SCS and MTO in the same lipid nanovehicle for co-delivery to tumor cells thereby improving therapeutic activity of MTO based chemotherapy.

Here we developed an optimal loading method for liposomal MTO with high drug loading efficiency and stability. Next, we investigated intracellular drug delivery using these SCS-enriched liposomal MTO in comparison to non-enriched liposomal MTO and finally addressed intratumoral MTO localization in a breast carcinoma model.

MATERIAL AND METHODS

Materials & reagents

Hydrogenated soy phosphatidylcholine (HSPC) and distearylphosphatidylethanolamine (DSPE)-PEG_{2000} were from Lipoid (Ludwigshaven, Germany). Short chain sphingolipids, C_8 Glucosyl(ß) Ceramide (d18:1/8:0) D-glucosyl-ß-1,1' N-octanoyl-D-erythro-sphingosine (C_8-GluCer), C_8 Galactosyl(ß) Ceramide (d18:1/8:0) D-galactosyl-ß-1,1' N-octanoyl-D-erythro-sphingosine (C_8-GalCer), C_6-NBD Galactosyl Ceramide N-[6-[(7-nitro-2-1,3-benzoxadiazol-4-yl)amino]hexanoyl]-D-galactosyl-ß1-1'-sphingosine and 16:0

Liss Rhod PE 1,2-dipalmitoyl-sn-glycero-3-phosphoethanolamine-N-(lissamine rhodamine B sulfonyl) (ammonium salt) were from Avanti Polar Lipids (Alabaster, AL, USA).

Polycarbonate filters were from Northern Lipids (Vancouver, BC, Canada) and PD-10 Sephadex columns were from GE Healthcare (Diegem, Belgium). Cholesterol, HEPES (2-[4-(2-hydroxyethyl) piperazin-1-yl] ethanesulfonic acid), trichloroacetic acid (TCA), acetic acid, Triton-X, sulforhodamine B (SRB) were from Sigma Aldrich (Zwijndrecht, The Netherlands). DAPI nuclear dye, diamidino-2-phenylindole was from Molecular Probes (Leiden, The Netherlands). PBS was from Boom and FACS flow fluid from BD Biosciences. Mitoxantrone dihydrocchloride, $2mg \cdot Kg^{-1}$ (OnKotrone) was from Baxter.

Liposome formulation

Liposomes were formulated of HSPC/ cholesterol/ DSPE-PEG_{2000} in a molar ratio of 1.85: 1: 0.15. To the mixture of lipids 0.1 mol of SCS was added per mole of total amount of lipid (including cholesterol).

Liposomes of 85-100nm in diameter were prepared by lipid film hydration and extrusion method using a thermobarrel extruder, Northern Lipids, Vancouver, Canada at 65°C [30].

Lipids were dissolved in chloroform methanol (9:1 v/v), mixed and a lipid film was created under reduced pressure on a rotary evaporator and subsequently dried under a stream of nitrogen. To optimize drug loading efficiency different loading methods were tested in parallel to different drug to phospholipid ratios (D:PL) (w/w) as described in literature for MTO liposomal loading [31-33]. A transmembrane pH gradient driven loading procedure was tested at a D:PL ratio of 0.08 (w/w) at 65°C as described by Lim et al [33]. Additional drug loading methods were based on ammonium sulfate gradient method [30] at 65°C considering different D:PL loading ratios (w/w) of 0.08 and 0.036 [31, 32]. Finally, lipid film was hydrated by addition of 250 mM of $(NH_4)_2SO_4$, pH 5.5 and liposomes were sized by sequential extrusion through 100-, 80-, and 50 nm polycarbonate filters (Northern Lipids, Vancouver, Canada). Non encapsulated $(NH_4)_2SO_4$ was removed by gel filtration chromatography using PD-10 Sephadex column (GE Healthcare, Diegem, Belgium), eluted with 135 mM NaCl, 10 mM Hepes buffer, pH 7.4.

Empty liposomes were heated at 65°C for 10min and MTO was added to liposomes in each respective drug to D:PL (w/w). After loading and separation of free from entrapped liposomal drug, size and polydispersity index (pdi) were determined by light scattering using a Zetasizer Nano ZS (Malvern Instruments, Malvern, UK). Lipid concentration was measured by phosphate assay [34].

After separation of free non-encapsulated MTO from liposome-encapsulated MTO, the amount of entrapped drug was measured by fluorimetry ($\lambda_{excitation}$ 607 nm; $\lambda_{emission}$ 684 nm) and measured after entire liposome solubilization with 1% (v/v) Triton in water to a calibration curve from stock MTO, 2mg·Kg^{-1}. Loading efficiency was calculated as a percentage of recovered amounts of drug entrapped in the liposome, in relation to the initial amount of drug added for loading.

Fluorescent labelled liposomes and fluorescent labelled SCS liposomes were prepared using fluorescent lipid Rhodamine and C6-NBD Galactosyl Ceramide, respectively, at 0.1% and 0.25 mol% of total amount of lipid.

Stability

Long-term storage conditions

Long-term storage conditions stability at 4°C was based on size, pdi and MTO content measurements for a period of at least 1 year. All measurements were performed in triplicate. MTO content was measured as reported in previous section after separation of free drug by gel filtration chromatography.

Short-term storage conditions, 37°C

Stability studies of non-enriched (standard) and SCS-enriched-MTO liposomal formulations were performed for 24h at 37°C, in the absence and presence of 10% or 50% human serum. MTO release was quantified as described in previous section. Total drug release was measured after entire liposomal solubilization by adding 1% (v/v) of Triton-X in water and human serum as blank was subtracted from sample release and total release measurements. Values were presented as percentage of liposomal drug content and calculated following the formula:

$$\% \text{ Entrapped MTO} = 100 - [(\text{Fluorescence}_{sample} - \text{blank}) * 100 / (\text{Fluorescence}_{total\ release} - \text{blank})]$$

Cryo-transmission electron microscopy (TEM)

Cryo-TEM was used to characterize the detailed structure of the liposomal formulations (non-enriched, C_8-GluCer and C_8-GalCer-MTOL) of MTO and the physical state of the encapsulated drug. The freezing was performed in a cooling chamber which was permanently cooled with liquid nitrogen. A sample droplet was placed on a microperforated copper grid and blotted by a filter paper to result in a thin liquid film. The grid was plunged into liquid ethane for immediate freezing. A Leo 912 Omega TEM microscope (Carl Zeiss NTS GmbH, Oberkochen, Germany) was used.

Cell culture

All tumor cell lines were cultured in Dulbeccos's modified Eagle medium, supplemented with 10% fetal calf serum and 4 mM L-glutamine. HUVEC were isolated by collagenase digestion using the method described by Jaffe *et al.* [35] and cultured in HUVEC medium containing human endothelial serum free medium (Invitrogen), 20% heat inactivated newborn calf serum (Cambrex), 10% heat inactivated human serum (Cambrex), 20 ng/ml human recombinant epidermal basic fibroblast growth factor (Peprotech EC Ltd) and 100 ng/ml human recombinant epidermal growth factor (Peprotech EC Ltd) in fibronectin (Roche Diagnostics) coated flasks. Fibroblasts (3T3) were purchased from Biowhitakker and cultured in Dulbeccos's modified Eagle medium containing nutrient mixture F12, supplemented with 10% fetal calf serum and 4 mM L-glutamine.

***In vitro* drug efficacy**

Human breast carcinoma cells, MCF-7 and SKBR3 (1.25×10^4 cells/well) were plated in flat bottom 96 well plates. After 24h at 37°C, cells were exposed to serial concentrations of MTO-liposomal formulations and free MTO in culture medium for 24h.

Cell survival was determined by measuring total cellular protein levels using the sulforhodamine-B (SRB) assay [36]. Cells were washed twice with PBS, incubated with 10% trichloric acetic acid (1h, 4°C) and washed again. Cells were stained with 0.4% SRB (Sigma) for 15min and washed with 1% acetic acid. After drying,

protein-bound SRB was dissolved in TRIS buffer (10 mM, pH 9.4) and absorbance was measured at a wavelength of 540 nm in a plate reader. Cell survival was calculated as a percentage relative to control (untreated cells), which was set at 100%.

IC_{50}, the concentration that inhibits 50% of cellular growth, was determined for each MTO liposomal formulation, by plotting the cell survival observed for each concentration versus the log concentration and non-linear regression curve fitting using GraphPad Prism software v5.0. In all experiments incubations were performed in triplicate at least with three different batches.

Intracellular MTO delivery measured by flow cytometry

Cells were seeded on flat bottom 24 well plates at a final concentration of $6x10^4$ cells/ well and allowed to adhere for 24h. Non-enriched and SCS-MTOL, diluted in growth medium were added resulting in a final drug concentration of 10 µM, and incubated for 4 and 24h. After incubation, cells were washed twice to discard non-incorporated drug and trypsinized for 2min. Cell suspensions were washed twice in medium and resuspended in PBS. Cellular fluorescence representing drug uptake was analyzed with a Becton Dickinson FACScan using Cell Quest software by the fluorescent signal detected in the FL4 channel after excitation at 635nm. Per analysis 10000 cells were counted.

Intracellular fate of SCS and drug

Fluorescently labelled NBD-C_6-GalCer-MTOL were added to SKBR-3 breast carcinoma cells ($1x10^5$ cells) in 10% serum medium and incubated for 2h at 37°C. A Zeiss LSM Meta confocal microscope was used for live cell imaging with 488nm excitation and BP 505-530nm emission for the SCS and 543nm excitation and BP 550-615nm emission for Rhodamine labelled liposomes. MTO was imaged at 633nm excitation and LP 650nm emission, with a 63x plan apo (n.a. 1.4) oil lens.

Intratumoral MTO delivery

MTO delivery and intratumoral fate was evaluated 24h after a single i.v administration of MTO, $5mg \cdot Kg^{-1}$ in form of MTO and C_8-Glucer or C_8-Galcer-MTOL in a MCF-7 breast carcinoma tumor model, implanted orthotopically [37]. Tumors with a diameter of 8 to 10 mm were

excised, immediately snap-frozen in liquid nitrogen and stored at –80°C until further analysis. The endothelial cells of blood vessels and tissue macrophages were stained immunohistochemically, using the same frozen sections as for MTO imaging. As during sample preparation, fixation and staining, MTO fluorescence will be partly lost, cryo-sections before staining were used for measuring MTO fluorescence intensity without further contact of the sections with solvents. After MTO imaging, cryostat sections of 5μm were air dried and fixed with acetone for 5min. After Tris Buffer Saline (TBS) washing and blocking step with 10% Normal Goat Serum (ABD Serotec) in 1%BSA (Sigma) for 10min, sections were incubated with primary antibody, rat anti mouse monoclonal CD31 (BD Pharmingen) for endothelial cells of blood vessels staining, in 1%BSA for 1h at room temperature. Thereafter, sections were washed with TBS and incubated for 30min with goat anti rabbit Alexa Fluor 488 secondary antibody (In vitrogen) in 1%BSA/PBS. For macrophages staining, after Tris Buffer Saline (TBS) washing and blocking, step sections were incubated with primary antibody, rat anti mouse monoclonal anti-CD11b (eBioscience) in 1%BSA for 1h at room temperature. After washing, sections were incubated with goat anti rabbit Alexa Fluor 488 secondary antibody (Invitrogen) in 1%BSA/PBS for 30min. After washing, sections were covered with DAPI 1:1000 for nuclear staining. Imaging was performed with a Leica SP5 microscope for MTO at 633nm 670 LP, previously to staining.

Statistics

Statistical analysis was performed using the ANOVA test. P-values less than 0.05 were considered statistically significant. All parametric values are expressed as mean ± standard error of the mean (SEM). Calculations were performed using GraphPad Prism v5.0.

RESULTS

Formulation of glycoceramide-MTO nanoliposomes

Non-enriched-MTOL (standard MTOL) and SCS-MTOL formulations were prepared using two different buffers to hydrate the lipid film to create a gradient for subsequent drug loading at different lipid:PL ratios. Liposomes prepared in citrate buffer presented

size <100 nm and pdi <0.1, but when loaded with MTO in a D:PL (w/w) of 0.08 [33] the loading efficiency was <10% (Supplemental table 1) and preparations displayed visible liposomal aggregation for non-enriched and SCS-MTOL (data not shown). When ammonium sulfate loading was used, MTO loading efficiency increased to 70% [31, 32] (Supplemental table 1) and no particle aggregation was observed (data not shown). MTOL loaded by ammonium sulfate gradient method at a final D:PL (w/w) of 0.07 resulted in maximal MTO drug loading of 100% for SCS-MTOL whereas MTOL had 75% MTO entrapped. These optimized formulations had a size of around 85nm in diameter with a high level of homogeneity indicated by a pdi <0.1 (table 1), regardless of the presence or absence of C_8-GalCer or C_8-GluCer and were used for further experiments. No lipid loss from nanoparticles was observed during loading procedure.

MTO is retained in SCS enriched-MTOL

Long-term storage conditions

C_8-GluCer or C_8-GalCer-MTOL showed a stability profile similar to MTOL. Weekly assessment of particle size, pdi and entrapped drug levels revealed 6-19% MTO release from liposomes, which occurred in the first week of storage. After this initial release which was equal between MTOL and C_8-GalCer-MTOL, but lower for C_8-GluCer-MTOL, liposomes retained their drug contents up to 1 year. Particle size and pdi remained constant up to 1 year at 4°C (Fig. 1 and table 1).

Stability under *in vitro* cell culture and *in vivo* conditions

Under cell culture conditions at 37°C in the absence and presence of 10% of serum, or upon the presence of 50% human serum in Hepes buffer at 37°C, C_8-GluCer and C_8-GalCer–MTOL efficiently retained high levels of their drug contents up to 24h (Fig. 2). In the absence of serum at 37°C, SCS-MTOL and MTOL retained 100% of their drug content (Fig. 2A). In 10% of human serum at 37°C, both SCS-MTOL displayed initial drug release of 10-15% in the first hour (Fig. 2B, insert) and a more gradual release of another 5-10% up to 24h, similar to MTOL (Fig. 2B). When exposed to 50% human serum at 37°C, mimicking the conditions in blood circulation, SCS-MTOL showed an initial release of around 20% of drug (Fig. 2C, insert),

Table 1 – Characterization of optimized MTO-nanoliposomes

MTOL	D:PL$(w/w)_{initial}$	D:PL$(w/w)_{extrusion}$ ±SEM	D:PL$(w/w)_{final}$ ±SEM	Size (nm) ±SEM	Pdi ±SEM	%Load ±SEM	Entrapped MTO ≥1 year, 4°C ±SEM	Size (nm) ≥1 year, 4°C ±SEM
Non-enriched	0.045	0.075 ± 0.014	0.068 ± 0.005	86 ± 0.7	0.06 ± 0.00	75 ± 4.8	84 ± 4.3	91 ± 1.0
C_8-GluCer	0.045	0.078 ± 0.014	0.070 ± 0.004	84 ± 0.7	0.08 ± 0.01	96 ± 3.3	94 ± 5.7	87 ± 1.3
C_8-GalCer	0.045	0.088 ± 0.016	0.073 ± 0.003	84 ± 1.5	0.07 ± 0.01	93 ± 4.2	81 ± 5.7	85 ± 1.2

More than 3 independent batches were formulated for each formulation and each measurement was performed in triplicate

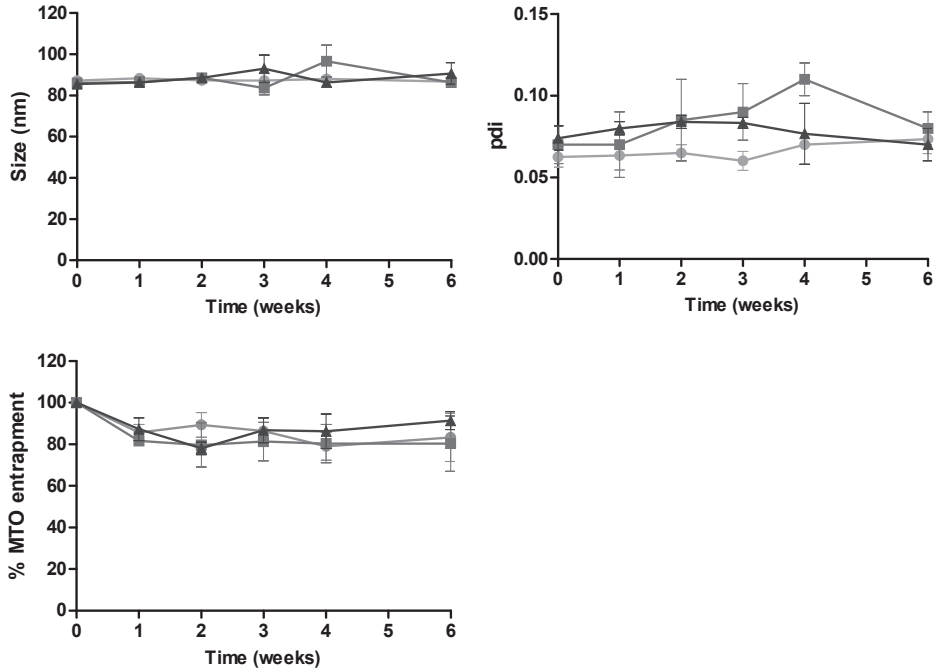

Figure 1 - Stability at 4°C during 6 weeks of different MTO-containing SCS-enriched liposomes (non-enriched (●), C_8-GluCer (■) and C_8-GalCer-MTOL (▲)). Liposomal drug content, size and pdi were analyzed. Three independent experiments were performed testing at least three independent batches and values represent the mean ± SEM

followed by a phase with minimal release up to 24h. Non-enriched-MTOL showed a more gradual and continuous drug release of 25-30% during 24h (Fig. 2C).

Morphology of nanoliposomes containing MTO by cryo-Transmission Electron Microscopy

Cryogenic transmission electron microscopy (cryo-TEM) analysis of MTOL formulations demonstrated an intraliposomal crystallized gel-like form of MTO visible in the hydrophilic core of all formulations (Fig. 3). All three liposomal formulations presented a homogeneous population of uniformly round-shaped vesicles with sizes confirming DLS measurements.

***In vitro* liposomal MTO efficacy is enhanced by SCS**

In vitro efficacy of liposomal MTO formulations was tested towards human MCF-7 and SKBR3, breast carcinoma cell lines. In both cell lines, C_8-GluCer and C_8-GalCer-MTOL exerted increased cytotoxicity

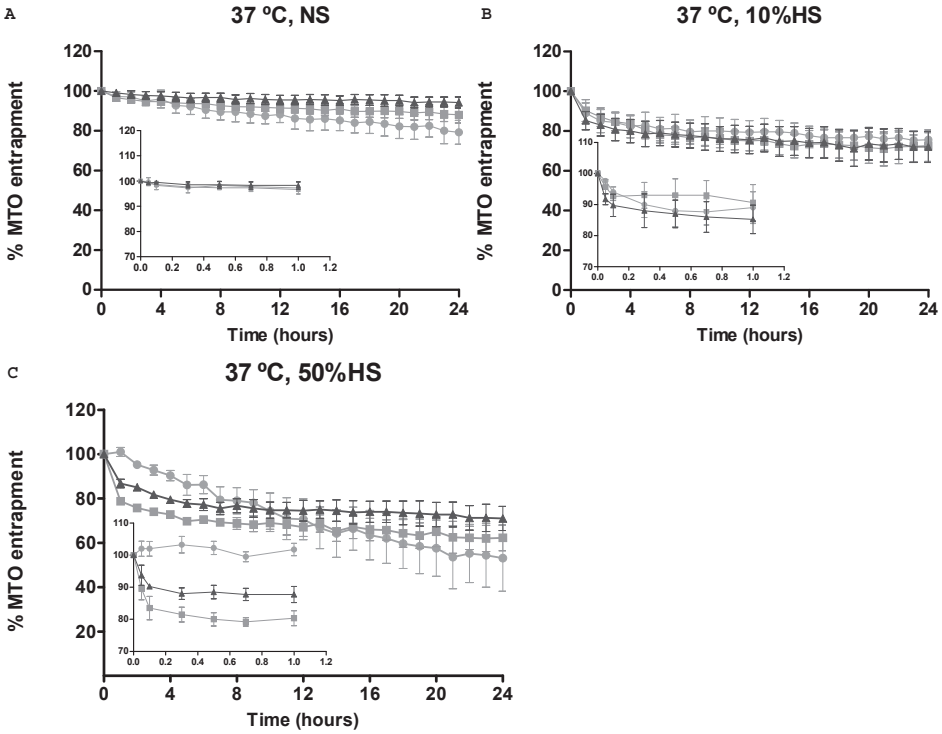

Figure 2 - Liposomal drug content stability at 37°C in absence (A) and presence of 10% (B) or 50% (C) human serum of non-enriched MTOL (●) C_8-GluCer-MTOL (■) and C_8-GalCer-MTOL (▲) for 24h. Graph inserts represent MTO release within the first hour. At least three independent batches from each formulation were tested and values represent the mean ± SEM

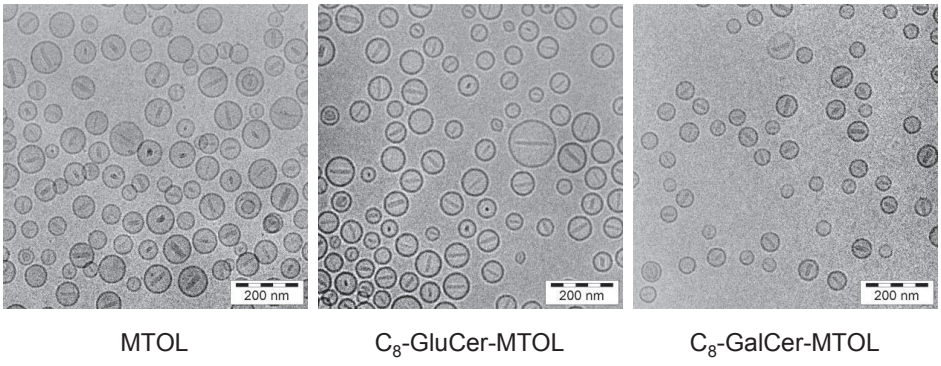

Figure 3 - Cryo-TEM images of liposomes with or without SCS. A clear MTO precipitate is visible inside liposomes. SCS-MTOL are uniform in size and shape and comparable to non-enriched-MTOL. The bar represents 200 nm. A 12500x magnification was used

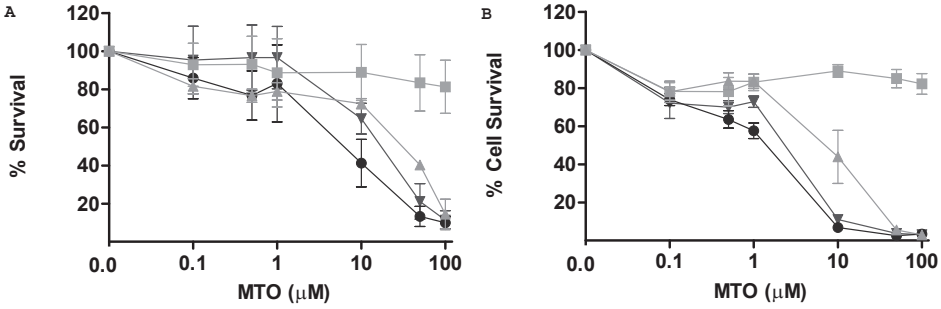

Figure 4 - *In vitro* drug efficacy toward breast carcinoma tumor cells, MCF-7 and SKBR-3. Cells were treated with Free MTO (●) non-enriched-MTOL (■) C_8-GluCer-MTOL (▲) and C_8-GalCer-MTOL (▼) for 24h at 37°C. Cell survival was quantified by colorimetric SRB assay. Values represent the mean ± SEM of at least 3 independent experiments, testing at least three independent batches

Table 2 – *In vitro* cytotoxicity (IC50, μM) of Free MTO, non-enriched and SCS-MTOL in breast carcinoma cell lines

	IC_{50} (μM)			
	MTO	MTOL	C_8-GluCer-MTOL	C_8-GalCer-MTOL
Tumor cells				
MCF-7	8.3 ± 6.3*	>200	16.1 ± 3.6*	14.8 ± 5.6*
SKBR3	1.0 ± 0.2*	>200	6.2 ± 2.5*	1.6 ± 0.3*

At least three independent experiments were performed and values represent the mean ± SEM.
*P<0.05 vs Non enriched MTO-L

compared to non-enriched MTOL after a 24h incubation time at 37°C (Fig. 4). At concentrations of 10 μM and higher, SCS-MTOL had significantly higher anti-tumor activity than MTOL ($p<0.05$). IC_{50} values of both SCS-enriched formulations were over 100-fold lower than non-enriched MTOL and approached IC_{50} concentrations achieved for free MTO in SKBR3 and MCF-7 carcinoma cells (table 2).

Breast carcinoma cells demonstrate higher sensitivity to C_8-GalCer mediated MTO uptake

MTO uptake was measured by flow cytometry in SKBR-3 breast carcinoma cells and compared to human endothelial cells (HUVEC) and fibroblasts (3T3). Cells were treated with non-enriched MTOL, C_8-GluCer or C_8-GalCer–MTOL for 4 or 24h at a concentration of 10 μM MTO. The presence of C_8-GluCer or C_8-GalCer in the liposomal bilayer enhanced intracellular drug uptake in SKBR-3 tumor cells at both time points (Fig. 5). Remarkably, C_8-GalCer increased intracellular drug levels 12-15 fold compared to non-enriched liposomes

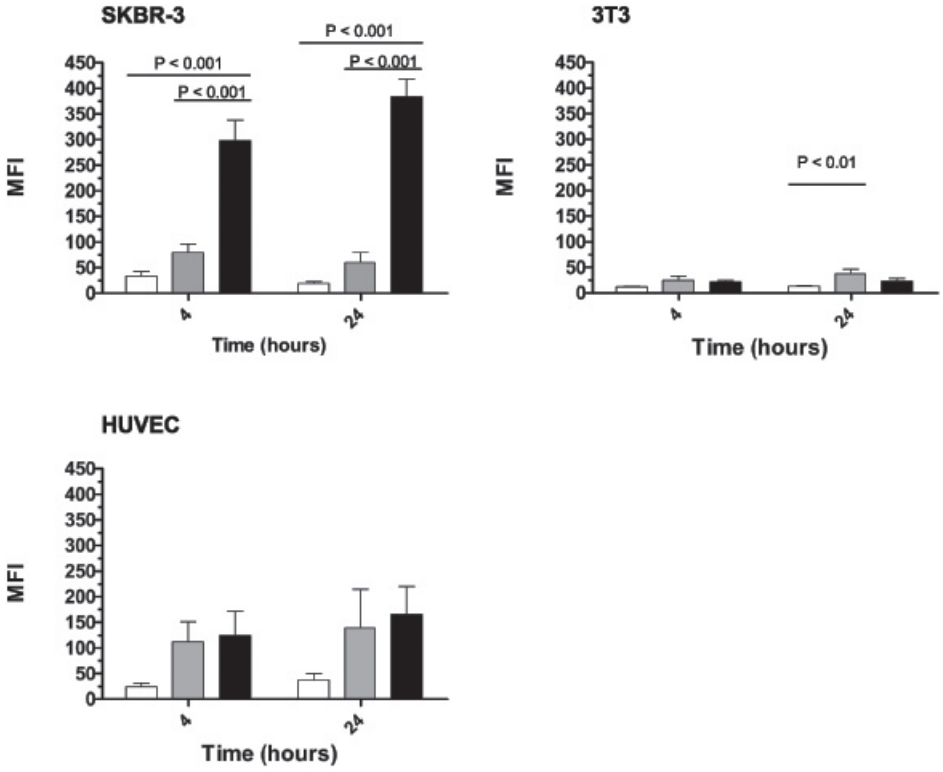

Figure 5 - Intracellular MTO uptake after treatment with MTO liposomes (10 μM), quantified by flow cytometry in breast carcinoma cells (SKBR3) and non-tumor endothelial cells (HUVEC) and fibroblasts (3T3). MTO was formulated in non-enriched liposomes (open), C_8-GluCer-MTOL (grey) and C_8-GalCer-MTOL (black). At least three independent experiments were performed and values represent the mean ± SEM

($p<0.001$), whereas C_8-GluCer enhanced drug uptake 3-fold, but not significantly in relation to non-enriched liposomes ($p>0.05$). The increased drug levels observed in SKBR-3 cells treated with C_8-GalCer-MTOL correspond to the *in vitro* cytotoxicity data (Fig. 4).

Drug uptake enhancement by SCS was much less pronounced in non-tumor cells. In human endothelial cells (HUVEC) no significant differences were distinguished between MTOL and C_8-GluCer or C_8-GalCer-MTOL treatments neither after 4h or 24h ($p>0.05$). Fibroblast (3T3) had much lower MTO uptake compared to tumor cells. C_8-GluCer-MTOL induced higher MTO uptake ($p<0.01$) than MTOL after 24h, whereas C_8-GalCer-MTOL treatment did not yield differences in drug uptake compared to MTOL.

Intracellular fate of nanoliposomes, SCS and MTO

To study the intracellular fate of MTO, SCS and the liposomal nanocarrier, confocal microscopy was performed 2h after incubation of cells with MTOL containing NBD-GalCer and/or Rho-PE and by using the intrinsic fluorescent nature of the drug molecule. Fluorescently labelled NBD-GalCer was observed to transfer from the liposomal to the cell membrane (Fig. 6A). MTO from SCS-MTOL was internalized and localized mainly in the nucleus. C_8-GluCer or C_8-GalCer-MTOL delivered high intracellular MTO levels compared to MTOL, which did not show detectable MTO uptake after 2h incubation, confirming earlier flow cytometry and cytotoxicity data. Possible liposome uptake was studied by labeling the liposomal bilayer with Rhod-PE, a stable bilayer marker. Liposome uptake by the tumor cells did not occur as evidenced by the red fluorescence from Rho-labelled liposomes surrounding the cells in the medium, which was neither associated with the cells nor internalized, in contrast to the NBD-GalCer and MTO.

In addition, pre-treating SKBR3 breast carcinoma cells with empty SCS enriched-liposomes followed by a washing and subsequent incubation with non-enriched MTOL demonstrated increased MTO uptake that they did not display upon single treatment (Fig 6A), suggesting that SCS transfer occurs independent on the drug influx (Fig. 6B).

Intratumoral fate of MTO

Intratumoral MTO delivery after i.v. administration of SCS-MTOL was compared to MTOL to study whether presence of SCS in the formulation affected MTO accumulation in the tumor and the intratumoral fate of the liposomes. MCF-7 tumor-bearing mice were treated with MTOL, SCS-MTOL or free MTO at 5 $mg \cdot Kg^{-1}$ after which tumors were isolated 24h after liposome administration and analyzed for intratumoral presence of liposomal drug. Slices of snap-frozen tumor tissue were prepared and analyzed directly for MTO fluorescence by confocal microscopy. Subsequently slices were fixed and stained for tumor vessels and macrophages and imaged to study possible localization of MTO in these different cell types.

For all MTOL formulations, non-enriched (Fig. 7A.1), C_8-GluCer (Fig. 7A.2) and C_8-GalCer (Fig. 7A.3), rather similar heterogeneous drug distribution patterns within the tumor were observed. Confocal

A

	Treatment						
MTO	+	-	-	-	-	-	-
MTOL	-	+	+	+	+	+	-
C_8-GluCer	-	-	+	-	-	-	-
C_8-GalCer	-	-	-	+	+	+	-
NBD-PE	-	-	-	-	+	+	-
Rhod	-	-	-	-	-	+	-
Medium	-	-	-	-	-	-	+

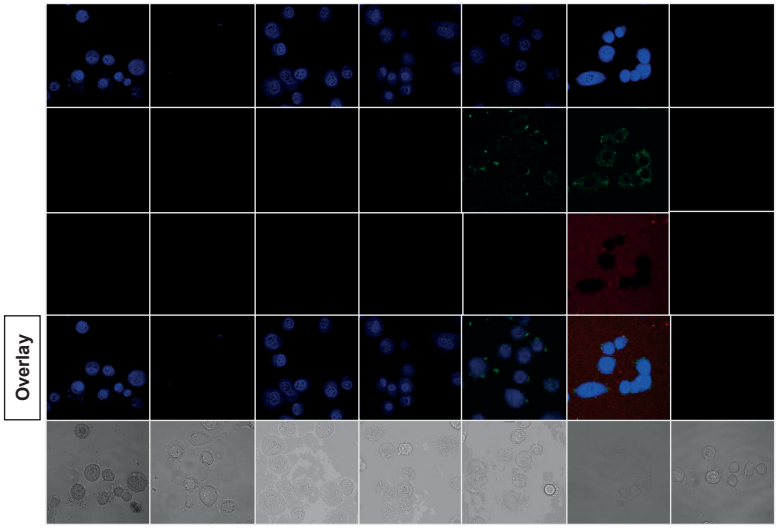

B

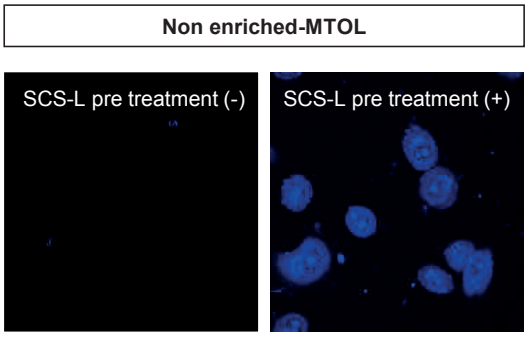

Figure 6 - Cellular localization of fluorescent NBD-C6-GluCer or NBD-C6-GalCer and MTO studied by confocal microscopy (A). SKBR3 breast carcinoma cells were treated for 2h at 37°C with NBD labeled-GalCer (5 μM) liposomes containing MTO (10 μM), the green fluorescent labeled-GalCer was imaged separately from MTO. The SCS accumulates in the plasma membrane and MTO accumulates in the nucleus and cytoplasm. Intracellular-localization of Rhodamine labeled liposomes (red) wasn't seen. (B) Pre-incubating cells with C_8-GalCer liposomes not containing MTO for 1h followed by washing and treatment with MTOL (10 μM), resulted in intracellular drug levels comparable to direct treatment with C_8-GalCer-MTOL (10 μM)

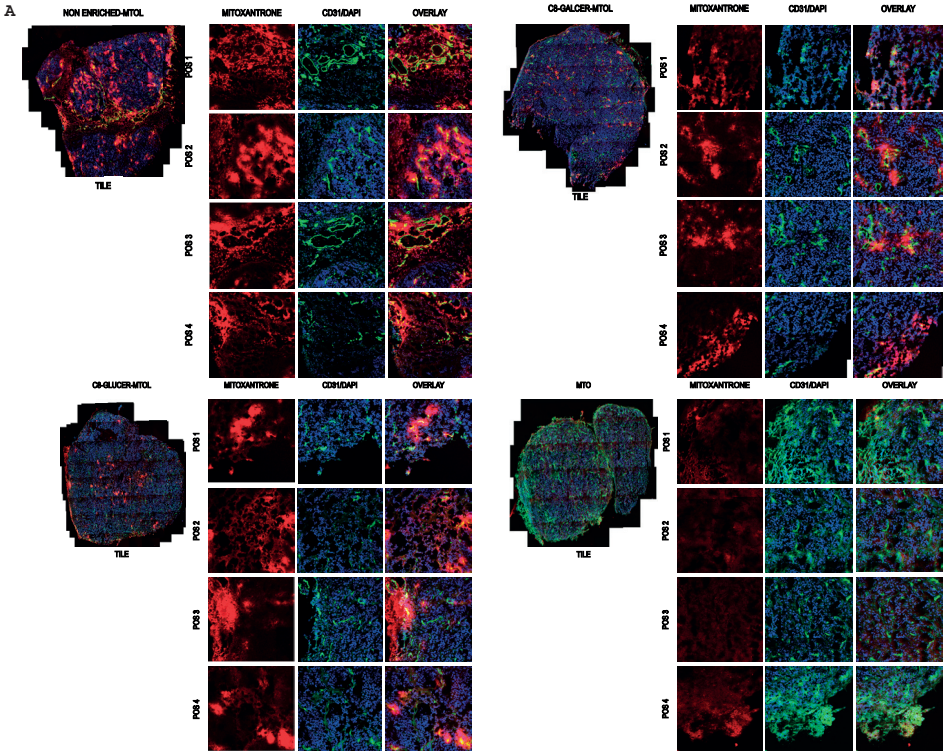

micrographs showed that liposomal-MTO delivery clearly correlated with CD31-positive tumor vessels, mainly in the tumor periphery (Fig. 7A). Further, nuclear uptake of MTO was observed in tumor tissue, surrounding the leaky tumor vessels. Occasionally, more centrally located regions with MTO fluorescence were observed. For free MTO treatment only marginal MTO fluorescence was observed in the tumor periphery (Fig. 7A.4) suggesting an important improvement in tumor drug delivery by liposomal formulation. Co-localization of liposomal MTO with CD11b positive cells (Fig. 7B), tumor associated macrophages (TAM) and in the stroma was observed to a minor extent and mainly in the better vascularized tumor periphery for all liposome-based treatments.CD11b positive cells were observed throughout the tumor in locations devoid of MTO fluorescence.

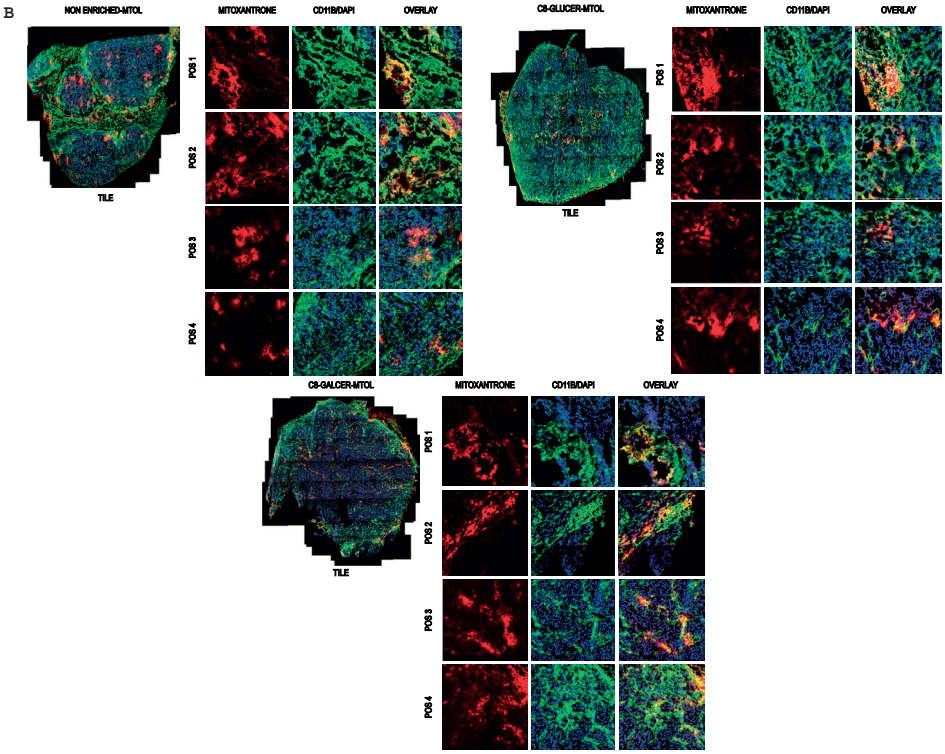

Figure 7 - Fluorescence micrographs of orthotopic MCF-7 breast carcinoma frozen sections, obtained from NMRI-nude female mice 24h after i.v injection of MTO (5 mg·Kg^{-1}) in form of standard MTOL and SCS-MTOL (C_8-GluCer and C_8-GalCer). After MTO imaging, frozen sections were stained for (A) anti-CD31, macrophages and (B) anti-CD11b antibody (vessels)

DISCUSSION

Although MTO has been developed as a less toxic alternative for anthracycline chemotherapy, side effects are not absent and remain an important reason for inadequate dosing for tumor treatment. Liposomal encapsulation is a clinically proven strategy to further decrease toxic side effects of chemotherapeutic drugs [14] and is successfully applied in this study. Whereas liposomal encapsulation positively affects drug toxicity, it is less beneficial for effective delivery of bioavailable drug into tumor cells [19, 20, 22]. To overcome the latter obstacle we applied a novel drug delivery strategy targeting tumor cell membrane composition by insertion of short chain sphingolipids (SCS) to improve chemotherapeutic drug uptake [24-28]. To optimally combine both strategies to the benefit

of MTO chemotherapy, we developed novel liposomal MTO formulations carrying the drug inside and the SCS in their bilayer. Homogeneous and stable formulations of SCS-MTOL were prepared with small size (<100 nm) and high MTO content, which upon remote loading was found in nanocrystalline form intraliposomally. SCS, upon their transfer to tumor cell membranes, strongly improved the drug delivery capacity of MTOL as was observed by live cell confocal imaging and flow cytometry, resulting in strongly improved *in vitro* anti-tumor activity toward human breast carcinoma. Remarkably, this drug delivery process displayed selectivity for tumor cells over normal cells. Both endothelial cells and especially fibroblasts appeared much less affected upon treatments with this novel SCS-MTOL. On-going studies focus on the underlying mechanism of this cell type specificity for SCS-mediated tumor cell membrane permeabilization. Liposomal formulations were able to deliver detectable drug quantities to orthotopic human breast carcinoma tumors, in contrast to free MTO treatment. SCS modification of the MTOL did not notably affect intratumoral distribution patterns of MTO. This combined with the demonstrated improvements that SCS add to the intracellular drug delivery process make us conclude that these novel SCS-MTOL formulations hold promise for further improvement in MTO cancer chemotherapy.

Remote loading of chemotherapeutic drugs into small unilamellar vesicles (SUVs) offers advantages of high entrapment levels and safety in the preparation procedure and has been applied for multiple anti-cancer drugs [30]. Such loading procedure requires a pH or ammonium sulphate gradient and both were applied for MTO encapsulation. The pH gradient method using intraliposomal citrate buffer of pH 4 yielded unstable aggregating particles with low drug entrapment. The ammonium sulphate method however yielded higher drug entrapment levels observed as a precipitate in the liposome core and did not induce aggregation. Liposomes containing MTO were uniformly round shaped independently on the presence of SCS in the liposomal bilayer. Interestingly, these findings differ from those we obtained with SCS-enriched liposomes loaded with Doxorubicin, on which we previously reported [27]. These SCS-Doxorubicin liposomes were to some extent rod-shaped when co-formulated with SCS, while non-enriched liposomes were uniformly round-shaped [27]. For both amphiphilic drugs, the presence of SCS improved

drug-loading efficiency in relation to non-enriched liposomes. However, the mechanism to form the intraliposomal precipitates differs. In the liposomal core, MTO and Doxorubicin associate to sulphate anions by double and single NH-groups, respectively. Additionally, Doxorubicin is able to self-stack into fibers through hydrophobic interactions which are bridged by the sulphate anions [38], inducing higher levels of intraliposomal drug, which may deform the liposomes to rod-shaped structures. In fact, optimal drug:lipid ratio for loading of MTO was lower than for Doxorubicin.

For MTO-loading a D:PL ratio of 0.07 (w/w) was determined optimal for non-enriched and SCS-enriched-MTOL, resulting in maximal drug loading efficiency. SCS-enriched nanoliposomes reached a higher MTO loading efficiency close to 100% against 75% for non-enriched nanoliposomes. Likely, the presence of SCS, C_8-GluCer and C_8-GalCer in the liposomal bilayer helped to improve MTO entrapment. The exposed hydroxyl groups of the sugar moiety of the hydrophilic SCS head group may promote MTO interaction through hydrogen binding thereby increasing the loading efficiency [39].

Concerning stability (Fig. 1 and Fig. 2), both MTOL and SCS-MTOL had similarly low levels of MTO release, presenting characteristics of an optimal formulation from a pharmaceutical point of view: maximum drug content and high stability together with maintenance of physical properties, such as size <100 nm and pdi <0.1. The initial drug release, which was observed both during storage and in the first hour at 37°C of incubation, can be explained by the release of MTO associated to the phospholipid bilayer. Considering that HSPC is neutral and PEG-DSPE is negatively charged and that MTO has a tendency to associate with negatively charged lipids at a pH between 5 and 8 could explain its presence in and drug release from the liposomal membrane at 37°C for all liposomal formulations, especially in the presence of serum. In the presence of 50% human serum, non-enriched liposomes continuously released MTO, indicating a contribution from the intraliposomal MTO pool. Instead, SCS-MTOL initially released MTO, but after that retained their intraliposomal MTO content. Therefore it can be assumed that SCS when inserted in the liposomal bilayer, together with improving drug loading efficiency also contributed to the stability profile of the nanoliposomes, improving MTO retention at high density serum better than non-enriched-MTOL.

Although SCS did not affect MTO release, they synergistically acted with liposomal MTO to improve its intracellular delivery and efficacy towards breast carcinoma cells. 24h incubation of tumor cells with SCS-MTOL markedly increased cytotoxicity compared to non-enriched MTOL. Previous studies demonstrated the potency of SCS as drug uptake enhancers for Doxorubicin when using nanoscale liposomal drug delivery systems [24, 26-28]. Here, we confirm this for MTO. Remarkably, SCS mediated drug uptake displayed a clear selectivity for tumor cells when compared to normal cells, such as endothelial cells and fibroblasts that were much less affected by SCS-MTOL. When comparing C_8-GluCer and C_8-GalCer we learned that different short chain glycoceramides can affect cellular drug uptake differently in the same tumor cell line. C_8-GalCer-MTOL caused much higher MTO uptake in SKBR3 cells than C_8-GluCer-MTOL as quantified by flow cytometry subsequently causing more toxicity towards this cell line. These observations are well in line with previous findings with SCS-liposomal Doxorubicin [27]. Also in that study, SCS provided specificity of Doxorubicin delivery to tumor cell membranes in comparison to normal cells and more subtly also showed that different SCS displayed preferential activity in some tumor cell lines compared to others. These observations suggest that responsiveness to SCS mediated drug delivery is not only (tumor) cell type specific, but is also dependent on the nature of the SCS. Optimal combinations of drugs and SCS may be available for particular tumor cell types. Such combinations can be obtained by extensive screening of lipids and drugs that will be part of future studies in which also the importance of the lipid composition of the receiving cell membrane will be investigated. Figure 8 illustrates the proposed mechanism of action for SCS as intracellular drug uptake enhancers.

Previous studies already indicated SCS transfer to the cell membrane precedes Doxorubicin transfer and cellular influx [27, 28]. As shown by confocal microscopy (Fig. 6), MTO is transported across the cell membrane and through the cytoplasm reaching the nucleus where it is retained and active [10, 40]. Upon labelling liposomes with Rhodamine-PE, a stable bilayer marker, we could prove that liposomes are not taken up by the cells. Yet, SCS are transferred from the liposomal bilayer to the cell membrane, via a process which is not related to cellular nanoparticle uptake.

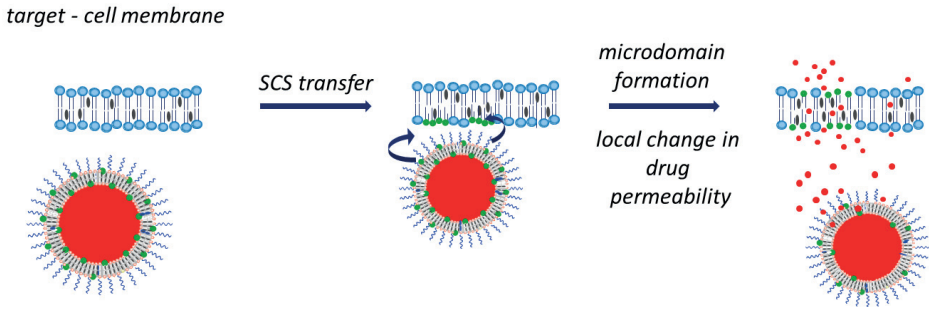

Figure 8 - Illustration of SCS mechanism of action. SCS (green) in the liposome bilayer are transferred to tumor cell membrane creating enhanced permeabilized specific areas improving intracellular drug (red) uptake. Drug influx occurs at a later stage and is transferred from the liposome core to the tumor cell independent on previous lipid transfer

Interestingly SCS delivered to tumor cell membranes by non-drug containing liposomes could similarly promote MTO uptake from non SCS-containing MTOL (Fig. 6B) indicating that SCS transfer and MTO uptake act independent of the liposomal carrier and synergize at the cell membrane level.

Although the *in vitro* drug delivery route for the novel SCS-MTOL could be elucidated, the *in vivo* situation is much more complex with the presence of various tumor physiological barriers and multiple cell types within a tumor. To gain further understanding of *in vivo* tumor drug delivery we investigated the intratumoral fate of MTO when administered as MTOL, C_8-GluCer or C_8-GalCer-MTOL or free drug. Detectable MTO levels, 24h after i.v. administration were only observed upon treatment with liposomal formulations and not upon free MTO administration demonstrating that nanoparticle mediated drug delivery can help to extend tumor drug exposure. Low tumor drug levels after free MTO treatment correlate to the large volume of distribution of the free drug and its rapid clearance from circulation [41]. Liposomal encapsulation is known to extend drug circulation time [17] and this in combination with immature, more leaky tumor vasculature can lead to liposome extravasation and interstitial accumulation of both carrier and drug [42, 43]. Here, all liposomal formulations delivered their MTO content mainly perivascularly in a rather heterogeneous manner throughout the tumor correlating with the tumor vascular make-up. Certainly not all vessels were characterized by MTO presence suggesting that not all tumor vessels allow liposome extravasation and subsequent drug

delivery. Tumor vasculature is very heterogeneous and permeability of a specific tumor vessel does not only depend on perfusion of the vessel, but also on the intrinsic profile of the endothelial lining and the surrounding microenvironment [44]. Strategies to induce increased vascular permeability using for instance biological vascular modifiers as TNF-α or physical treatments with for instance hyperthermia may further improve interstitial nanoparticle-mediated drug delivery [19, 20, 45].

From our observations in an orthotopic human breast carcinoma tumor, in presence or absence of SCS, fluorescent MTO is observed intracellularly as well as extracellularly. Upon interstitial localization drug release may involve gradual release from the liposomes and subsequent cellular uptake as in the *in vitro* situation. Tumor tissue is, in addition to tumor cells, composed of stromal cells, which may also take up the drug. Importantly, SCS *in vitro* clearly displayed a preference to enhance MTO delivery into tumor cells and to a much lesser extent in fibroblasts and endothelial cells (Fig.5).

Whereas some studies concluded a role of tumor associated macrophages (TAM) in drug release from liposomes [46], others have described that tumor uptake of liposomal drugs does not correlate with the presence of TAM [47, 48]. It was proposed that the respective improvement in drug delivery may be related to an alternative TAM-mediated processes that increases tumor vasculature permeability and liposome localization in TAM-rich areas. These findings are in accordance with Banciu et al. [48] who reported that the anti tumor effect of liposomal Doxorubicin (Doxil) does not depend on the presence of functional TAM in tumors. In the present study, MCF-7 tumors had a considerable TAM content localized in particular zones in the tumor. Although liposomal MTO was also delivered in these tumor regions, drug delivery was not solely restricted to macrophage enriched areas, but also occurred in different regions lacking TAM presence. As no major differences were found in tumor drug delivery patterns between non-enriched MTOL and SCS-MTOL it is likely that SCS do not promote co-localization of the SCS-MTOL with macrophages.

CONCLUSION

In conclusion, a novel nanoliposomal formulation of MTO with bilayer inserted SCS has been developed that displayed tumor cell specific, enhanced drug delivery. Whereas liposomal formulation improved tumor drug delivery compared to free MTO, SCS improved cellular MTO uptake preferentially in tumor cells. This new concept of drug delivery by targeting tumor cell membrane composition, modulating its permeability constitutes a promising direction to improve MTO chemotherapy efficacy.

AKNOWLEDGEMENTS

This work was financed by the Dutch Cancer Society. The authors thank Thomas Soullié for technical assistance with various aspects of histology and data processing and Sabine Barnert for performing cryo-TEM analyses.

REFERENCES

1. Dunn CJ, Goa KL. Mitoxantrone: a review of its pharmacological properties and use in acute nonlymphoblastic leukaemia. Drugs Aging.1996;9(2):122-47.
2. White RJ, Durr FE. Development of mitoxantrone. Investigational New Drugs.1985; 3(2):85-93.
3. Koutinos G, Stathopoulos GP, Dontas I et al. The effect of doxorubicin and its analogue mitoxantrone on cardiac muscle and on serum lipids: an experimental study. Anticancer Res.2002;22(2A): 815-20.
4. Chungun A, Uchide T, Tsurimaki C et al. Mechanisms Responsible for Reduced Cardiotoxicity of Mitoxantrone Compared to Doxorubicin Examined in Isolated Guinea-Pig Heart Preparations. J Vet Med Sci.2008;70:255-264.
5. Murray TJ. The cardiac effects of mitoxantrone: do the benefits in multiple sclerosis outweigh the risks? Expert Opin Drug Saf.2006; 5(2):265-274.
6. Cristofanilli M, Holmes F, Esparza L et al. Phase I/II trial of high dose mitoxantrone in metastatic breast cancer: the M.D. Anderson Cancer Center experience. Breast Cancer Res Treat.1999;54(3): 225-233.
7. Pusztai L, Holmes FA, Fraschini G, Hortobagyi GN. Phase II study of mitoxantrone by 14-day continuous infusion with granulocyte colony-stimulating factor (GCSF) support in patients with metastatic breast cancer and limited prior therapy. Cancer Chemother Pharmacol.1999; 43(1):86-91.
8. Cook AM, Chambers EJ, Rees GJG. Comparison of mitozantrone and epirubicin in advanced breast cancer. Clin Oncol.1996;8:363-366.
9. Faulds D, Balfour J, Chrisp C, Langtry D. Mitoxantrone. A review of its pharmacodynamic and pharmacokinetic properties, and therapeutic potential in the chemotherapy of cancer. Drugs. 1991;41(3):400-449.
10. Fox EJ. Mechanism of action of mitoxantrone. Neurology.2004;63(12 suppl 6):S15-S18.
11. Feofanov A, Sharonov S, Kudelina I, Fleury F, Nabiev I. Localization and molecular interactions of mitoxantrone within living K562 cells as probed by confocal spectral imaging analysis. Biophys J.1997; 73(6):3317-27.
12. Hajihassan Z, Rabbani-Chadegani A. Studies on the binding affinity of anticancer drug mitoxantrone to chromatin, DNA and histone proteins. J Biomed Sci.2009;16(31).
13. van Dalen EC, van der Pal HJH, Bakker PJM, Caron HN, Kremer LCM. Cumulative incidence and risk factors of mitoxantrone-induced cardiotoxicity in children: a systematic review. Eur J Cancer.2004; 40(5):643-652.
14. Allen TM, Cullis PR. Liposomal drug delivery systems: from concept to clinical applications. Adv Drug Deliv Rev.2013;65(1):36-48.
15. Paliwal SR, Paliwal R, Agrawal GP, Vyas SP. Liposomal nanomedicine for breast cancer therapy. Nanomedicine (Lond).2011;6(6):1085-100.

16. Koning GA, Krijger GC. Targeted multifunctional lipid-based nanocarriers for image-guided drug delivery. Anticancer Agents Med Chem.2007;7(4):425-40.
17. Mattheolabakis G, Rigas B, Constantinides PP. Nanodelivery strategies in cancer chemotherapy: biological rationale and pharmaceutical perspectives. Nanomedicine (Lond).2012;7(10):1577-90.
18. Deshpande PP, Biswas S, Torchilin VP. Current trends in the use of liposomes for tumor targeting. Nanomedicine (Lond).2013;8(9): 1509-28.
19. Seynhaeve AL, Dicheva BM, Hoving S, Koning GA, Ten Hagen TL. Intact Doxil is taken up intracellularly and released doxorubicin sequesters in the lysosome: Evaluated by in vitro/in vivo live cell imaging. J Control Release.2013;172(1);330-340.
20. Seynhaeve ALB, Hoving S, Schipper D et al. Tumor Necrosis Factor Î± Mediates Homogeneous Distribution of Liposomes in Murine Melanoma that Contributes to a Better Tumor Response. Cancer Res.2007;67(19): 9455-9462.
21. O'Brien MER, Wigler N, Inbar M et al. Reduced cardiotoxicity and comparable efficacy in a phase III trial of pegylated liposomal doxorubicin HCl (CAELYX/DOXIL) versus conventional doxorubicin for first-line treatment of metastatic breast cancer. Ann Oncol.2004; 15(3):440-449.
22. Laginha KM, Verwoert S, Charrois GJR, Allen TM. Determination of Doxorubicin Levels in Whole Tumor and Tumor Nuclei in Murine Breast Cancer Tumors. Clin cancer Res.2005;11(19 Pt1):6944-6949.
23. Visani G, Isidori A. Doxorubicin variants for hematological malignancies. Nanomedicine (Lond).2011;6(2):303-6.
24. van Lummel M, van Blitterswijk WJ, Vink SR et al. Enriching lipid nanovesicles with short-chain glucosylceramide improves doxorubicin delivery and efficacy in solid tumors. Faseb J.2009;25 (1):280-289.
25. Veldman RJ, Zerp S, van Blitterswijk WJ, Verheij M. N-hexanoyl-sphingomyelin potentiates in vitro doxorubicin cytotoxicity by enhancing its cellular influx. Br J Cancer.2004;90(4):917-925.
26. Veldman RJ, Zerp S, van Blitterswijk WJ et al. Coformulated N-Octanoyl-glucosylceramide Improves Cellular Delivery and Cytotoxicity of Liposomal Doxorubicin. J Pharmacol Exp Ther.2005; 315(2):704-10.
27. Pedrosa LRC, Hell A, Suss R, et al. Improving Intracellular Doxorubicin Delivery Through Nanoliposomes Equipped with Selective Tumor Cell Membrane Permeabilizing Short-Chain Sphingolipids. Pharm Res.2013;30(7):1883-1895.
28. van Hell AJ, Melo MN, van Blitterswijk WJ et al. Defined lipid analogues induce transient channels to facilitate drug-membrane traversal and circumvent cancer therapy resistance. Sci Rep.2013; 3,1949.
29. Siskind LJ, Fluss S, Bui M, Colombini M. Sphingosine Forms Channels in Membranes That Differ Greatly from Those Formed by Ceramide. J Bioenerg Biomembr.2005; 37(4):227-236.
30. Haran G, Cohen R, Bar LK, Barenholz Y. Transmembrane ammonium sulfate gradients in liposomes produce efficient and stable

entrapment of amphipathic weak bases. Biochim Biophys Acta.1993; 1151(2):201-215.
31. Pinto AC, Moreira JN, Simões S. Liposomal imatinib-mitoxantrone combination: Formulation development and therapeutic evaluation in an animal model of prostate cancer. The Prostate.2011;71(1):81-90.
32. Li C, Cui J, Wang C et al. Encapsulation of mitoxantrone into pegylated SUVs enhances its antineoplastic efficacy. Eur J Pharm Biopharm.2008;70(2):657-665.
33. Lim HJ, Masin D, Madden TD, Bally MB. Influence of Drug Release Characteristics on the Therapeutic Activity of Liposomal Mitoxantrone. J. Pharmacol. Exp. Ther.1997; 281(1):566-573.
34. Rouser G, Fkeischer S, Yamamoto A. Two dimensional thin layer chromatographic separation of polar lipids and determination of phospholipids by phosphorus analysis of spots. Lipids.1970;5(5): 494-496.
35. Jaffe EA, Nachman RL, Becker CG, Minick CR. Culture of human endothelial cells derived from umbilical veins. Identification by morphologic and immunologic criteria. J. Clin. Invest.1973;52(11): 2745-2756.
36. Skehan P, Storeng R, Scudiero D et al. New Colorimetric Cytotoxicity Assay for Anticancer-Drug Screening. J. Natl Cancer Inst.1990; 82(13):1107-1112.
37. Li L, ten Hagen TLM, Schipper D et al. Triggered content release from optimized stealth thermosensitive liposomes using mild hyperthermia. J Control Release.2010;143(2):274-279.
38. Li X, Hirsh DJ, Cabral-Lilly D et al. Doxorubicin physical state in solution and inside liposomes loaded via a pH gradient. Biochim. Biophys. Acta.1998;1415(1):23-40.
39. Law SL, Chang P, Lin CH. Characteristics of mitoxantrone loading on liposomes. Int. J. Pharm.1991;70:1-7.
40. Durr FE, Wallace RE, Citarella RV. Molecular and biochemical pharmacology of mitoxantrone. Cancer Treat Rev.1983;10(Suppl B): 3-11.
41. Orthmann A, Zeisig R, Suss R et al. Treatment of Experimental Brain Metastasis with MTO-Liposomes: Impact of Fluidity and LRP-Targeting on the Therapeutic Result. Pharm Res.2012;29(7):1949-1959.
42. Maeda H, Nakamura H, Fang J. The EPR effect for macromolecular drug delivery to solid tumors: Improvement of tumor uptake, lowering of systemic toxicity, and distinct tumor imaging in vivo. Adv Drug Deliv Rev.2013;65(1):71-9.
43. Yuan F, Leunig M, Huang SK, Berk DA, Papahadjopoulos D, Jain RK. Microvascular Permeability and Interstitial Penetration of Sterically Stabilized (Stealth) Liposomes in a Human Tumor Xenograft. Cancer Res.1994;54(13):3352-3356.
44. Nakasone ES, Askautrud HA, Kees T et al. Imaging Tumor-Stroma Interactions during Chemotherapy Reveals Contributions of the Microenvironment to Resistance. Cancer Cell.2012;21(4):488-503.
45. Li L, ten Hagen TLM, Schipper D et al. Improved intratumoral nanoparticle extravasation and penetration by mild hyperthermia. J Control Release.2013;167(2): 130-137.

46. Storm G, Steerenberg PA, Emmen F, van Borssum WM, Crommelin DJ. Release of doxorubicin from peritoneal macrophages exposed in vivo to doxorubicin-containing liposomes. Biochim Biophys Acta.1988; 965(2-3):136-45.
47. Mayer LD, Dougherty G, Harasym TO, Bally MB. The Role of Tumor-Associated Macrophages in the Delivery of Liposomal Doxorubicin to Solid Murine Fibrosarcoma Tumors. J Pharmacol Exp Ther.1997;80(3): 1406-1414.
48. Banciu M, Schiffelers RM, Storm G. Investigation into the Role of Tumor-Associated Macrophages in the Antitumor Activity of Doxil. Pharm Res.2008;25(8):1948-1955.

CHAPTER 4

Plasma membrane targeting by short chain sphingolipids inserted in nanoliposomes improves anti-tumor activity of mitoxantrone in an orthotopic breast carcinoma xenograft model

Lília R. Cordeiro Pedrosa, Olaf van Tellingen, Thomas Soullié, Ann L Seynhaeve, Alexander M.M Eggermont, Timo L.M. ten Hagen, Marcel Verheij, Gerben A. Koning

J Control Release, submitted

ABSTRACT

Mitoxantrone (MTO) is clinically used for treatment of various types of cancers providing an alternative for similarly active, but more toxic chemotherapeutic drugs like anthracyclines. To further decrease its toxicity MTO was encapsulated into nanoliposomes. Although nanoliposomal drugs can accumulate in target tumor tissue, they still face the plasma membrane barrier for effective intracellular delivery. Aiming to improve MTO tumor cell bioavailability, we used short chain lipids to target and modulate the tumor cell membrane, promoting MTO plasma membrane traversal. MTO was encapsulated in nanoliposomes containing the Short Chain Sphingolipid (SCS), C_8-Glucosylceramide (C_8-GluCer) or C_8-Galactosylceramide (C_8-GalCer) in their bilayer. These new SCS-nanoliposomes containing MTO (SCS-MTOL) were tested *in vivo* for tolerability, pharmacokinetics, biodistribution, tumor drug delivery by intravital microscopy and efficacy, and compared to standard MTO-liposomes (MTOL) and free MTO.

Liposomal encapsulation decreased MTO toxicity and allowed administration of higher drug doses. SCS-MTOL displayed increased clearance and lower skin accumulation compared to standard MTOL. Intratumoral liposomal drug delivery was heterogeneous and rather limited in hypoxic tumor areas, yet SCS-MTOL showed faster MTO bioavailability than MTOL. The increased MTO bioavailability correlated well with the improved antitumor activity of SCS-MTOL in a MDA-MB-231 breast carcinoma model. Multiple dosing of liposomal MTO strongly delayed tumor growth compared to free MTO and prolonged mouse survival, whereas among the liposomal MTO treatments, C_8-GluCer-MTOL was most effective. Targeting plasma membranes with SCS improved MTO tumor bioavailability and thereby therapeutic activity and represents a promising approach to improve MTO-based chemotherapy.

INTRODUCTION

Breast cancer is the second most commonly diagnosed cancer among women after non-melanoma skin cancer, and is the second leading cause of cancer death after lung cancer [1, 2]. Chemotherapy is frequently part of the treatment and is applied prior to surgery (neoadjuvant) to decrease tumor size or after surgery (adjuvant) to eliminate possibly remaining or metastasized tumor cells. Chemotherapy is also applied in advanced and recurrent disease. Anthracyclines are often used in breast cancer chemotherapy, next to taxanes, cyclophosphamide, methotrexate, fluorouracil, carboplatin and more recently introduced targeted drugs [3]. Mitoxantrone (MTO) has gained importance in the treatment of metastatic breast cancer as compared to anthracyclines [4, 5] due to its similar therapeutic activity and lower drug toxicity at equal doses [6, 7].

Nuclear DNA is the major target for MTO. Binding of MTO to DNA causes DNA condensation and inhibition of replication and RNA transcription. MTO is also a potent inhibitor of topoisomerase II, an enzyme involved in control of DNA topology through breaking and rejoining double-stranded DNA [8, 9].

MTO, like other amphiphilic drugs crosses the cell membrane by a relatively slow process involving a flip-flop [10]. Next, MTO preferentially associates to the inner leaflet of the membrane among the phospholipid head groups, rather than inside the lipid bilayer [10]. However, the complex and heterogeneous composition of the plasma membrane and the presence of caveolae and lipid rafts, make the plasma membrane a mosaic-like patchwork [11] with a differentiated lipid distribution that may reduce or prevent drug passage [12]. Poor accumulation of cytotoxic drugs in tumor cells is a major limitation in cancer therapy and membrane lipid and proteins play an important role in drug resistance. At the cellular level resistance can be caused by drug pumps such as the transmembrane P-glycoprotein that compete actively with passive drug transport across the membrane, limiting intracellular drug uptake and efficacy [13]. In addition, more and more evidence suggests that tumor cell membrane lipid composition and its biophysical state contributes to multidrug resistance [12]. To overcome these barriers, we questioned whether the membrane barrier function could be modulated to specifically enhance drug membrane traversal and

increase its intracellular accumulation and thus its therapeutic efficacy. Here we aim to apply our previously described concept of targeting the plasma membrane lipid composition using short chain sphingolipids (SCS) [14] as novel drug delivery strategy to improve MTO chemotherapy for breast cancer. To achieve this we made use of a nanovesicle platform with bilayer-inserted SCS and MTO encapsulated in its aqueous core [14]. Whereas liposomal encapsulation prolongs systemic circulation and decreases drug toxicity, it is less beneficial for effective delivery of bioavailable drug into tumor cells limiting therapeutic efficacy [15]. However, inserting SCS, like C_8-Glucosylceramide (C_8-GluCer) or C_8-Galactosylceramide (C_8-GalCer) in the nanoliposomal bilayer improves drug co-delivery to tumor cells through membrane permeabilization [16-19]. This approach combines reduced toxicity through nanoliposomal encapsulation with the advantage of enhanced intracellular drug delivery by SCS-mediated tumor cell membrane traversal.

Here, we present efficacy studies in an orthotopic breast cancer model using SCS-liposomal based MTO chemotherapeutic treatment in comparison to free MTO and optimized standard MTOL. Pharmacokinetics and biodistribution of the MTO formulations were studied. Intratumoral drug delivery was imaged by intravital microscopy.

MATERIAL AND METHODS

Lipids and Chemical Reagents

Hydrogenated soy phosphatidylcholine (HSPC) and distearoylphosphatidylethanolamine (DSPE)-PEG_{2000} were from Lipoid (Ludwigshaven, Germany). Short chain sphingolipids, D-glucosyl-ß-1,1' N-octanoyl-D-erythro-sphingosine (C_8-GluCer), D-galactosyl-ß-1,1' N-octanoyl-D-erythro-sphingosine (C_8-GalCer) and 1,2-dipalmitoyl-sn-glycero-3-phosphatidylethanolamine-N-(lissamine rhodamine B sulfonyl) (ammonium salt) (Rho-PE) were from Avanti Polar Lipids (Alabaster, AL, USA).

Polycarbonate filters were from Northern Lipids (Vancouver, BC, Canada) and PD-10 Sephadex columns were from GE Healthcare (Diegem, Belgium). Cholesterol, HEPES (2-[4-(2-hydroxyethyl)piperazin-1-

yl] ethanesulfonic acid) were from Sigma Aldrich (Zwijndrecht, The Netherlands). Hoechst was from Molecular Probes (Leiden, The Netherlands). Phosphate-buffered-saline was from Boom and FACS flow fluid from BD Biosciences. Mitoxantrone-dihydrochloride, 2mg·Kg^{-1} (OnKotrone) was from Baxter. Hormonal pellets, 1.5mg β estradiol 17-Acetate from Innovative Research of America, Sarasota, Florida, USA. Matrigel membrane Matrix was from BD Biosciences. Hypoxia specific marker HP3-1000 Kit Pimonidazole Hydrohloride, Hypoxyprobe-1 Omni Kit PAb2627AP and Rabbit antisera were from HPI (Burlington, MA, USA) Goat anti Rabbit AF488 and DAPI were purchased from Invitrogen, Carlsbad, CA, USA. Fluoromount-G was from SouthernBiotech, AL, USA.

Nanoliposome preparation

Nanoliposomes were composed of HSPC/ cholesterol/ DSPE-PEG$_{2000}$ in a molar ratio of 1.85: 1: 0.15. To the mixture of lipids 0.1 mole of SCS was added per mole of total amount of lipid (including cholesterol). Standard nanoliposomes and SCS-enriched nanoliposomes containing MTO were prepared by lipid film hydration and extrusion method using a thermobarrel extruder (Northern Lipids, Vancouver, Canada) at 65°C [20]. Lipids were dissolved in chloroform methanol (9:1 v/v), and a lipid film was created under reduced pressure on a rotary evaporator and subsequently dried under a stream of nitrogen. Lipid film was hydrated by addition of 250 mM of $(NH_4)_2SO_4$, pH 5.5 and liposomes were sized by sequential extrusion through 100-, 80-, and 50 nm polycarbonate filters (Northern Lipids, Vancouver, Canada). Non-encapsulated $(NH_4)_2SO_4$ was removed by gel filtration chromatography using PD-10 Sephadex column, eluted with 135 mM NaCl, 10 mM Hepes buffer, pH 7.4 and drug loading was performed for 1 h at 65°C, at a drug to phospholipid ratio (D:PL) of 0.07 (w/w) [14]. Size and polydispersity index (PDI) were determined by dynamic light scattering using a Zetasizer Nano ZS (Malvern Instruments, Worcestershire, UK). Lipid concentration was measured by phosphate assay [21].

After separation of free non-encapsulated MTO from liposome-encapsulated MTO, the amount of entrapped drug was measured by fluorimetry ($\lambda_{excitation}$ 607 nm; $\lambda_{emission}$ 684 nm) and measured after entire liposome solubilization with 1% (v/v) Triton in water in relation to a MTO calibration curve.

Fluorescent labelled liposomes were prepared using fluorescent lipid Rhodamine at 0.1 mol% of total amount of lipid.

Mitoxantrone quantification in plasma and tissue by HPLC-UV

A high performance liquid chromatography (HPLC) assay was developed and validated for the quantification of MTO in mouse plasma and tissue samples of liver, spleen, kidney, heart, lungs and tumor to determine *in vivo* MTO pharmacokinetics and biodistribution after 4 and 24h [22]. The HPLC separations were performed on a stainless steel analytical GraceSmart RP18 column, 150mm × 2.1mm packed with internal diameter 5µm particle size C-18 material, preceded by a guard column holding an AJ0-A286 C18 cartridge (Phenomenex, Torrance, CA, USA). The isocratic mobile phase was 27:73 (v/v) acetonitrile:ammonium formate (160 mM) with hexanesulfonic acid (35 mM), adjusted to pH 2.7 with formic acid and running at a flow rate of 0.2 ml/min. UV absorption at 655 was monitored using a SF757 UV/VIS detector (Kratos, NJ, USA). Peak detection and integration was done with a Chromeleon data system version 6.8 (Dionex, Sunnyvale, CA, USA).

Standard of MTO, 1000 ng/ml was prepared by dilution of MTO stock solution 2 mg/ml in water/acetonitrile (80:20), aliquoted and stored at –20°C.

To determine MTO plasma levels, fresh calibration standards of 30, 100, 300, 1000, 3000 and 10 000 ng/ml were prepared in human plasma for each analytical run in duplicate. Quality control (QC) samples in plasma were prepared by appropriate dilution of a stock solution of MTO 2 mg/ml in human plasma to a final concentration of 50, 500 and 5000 ng/ml and respective MTO quantification was analyzed at same run time as calibration standards and samples in order to validate the MTO quantification.

To determine MTO levels in tissue homogenates, fresh calibration standards of 30, 100, 300, 1000, 3000 and 10000 ng/ml were prepared in respective blank tissue homogenates for each analytical run in duplicate. QC samples were also prepared by appropriate dilution of a stock solution in respective stock tissue homogenates to a final concentration of 50, 500 and 5000 ng/ml. Calibration curves were calculated by linear regression analysis of the peak surface areas.

Standards and sample pretreatment involved a protein precipitation step. To 100 µl of plasma sample or tissue homogenate, 400 µl of extraction buffer (methanol containing 0.5M HCl:acetonitrile (90/10, v/v) was added. The resulting mixture was vortexed and kept on melting-ice for 15 min. After centrifugation at 14000 rpm, 4°C for 15 min, 200 µl of supernatant was separated and mixed with 200 µl MilliQ water and 50 µl was subjected to HPLC.

Mitoxantrone quantification in tumor by LC-MS/MS

MTO levels in tumors of mice treated with standard, C_8-GluCer or C_8-GalCer-MTOL and free MTO were evaluated 4 h after administration by liquid chromatography-tandem mass spectrometry (LC-MS/MS) [23] using an API3000 detector (ABSciex, USA). Detector settings: MTO 445.3→88.1; MTO-d8 453.3→92.1; each 150 ms; nebulizer gas 12 l/min; curtain gas 8 l/min and Collision gas 8 l/min; ESI source: 5000V at a temperature of 400°C ; DP 60; FP 180; EP 10; CE 42 and CXP 7 V. A Symmetry C18 column (150mm x 2.1mm, 3.5 µm) (Waters) was used. Chromatographic separations were accomplished by using a 2 min gradient from 5 to 90% methanol in 0.1% formic acid in water, maintained at 90%B for an additional 2 min. MTO-d8 (Toronto Research Chemicals, Canada) 1 ug/ml in water was used as internal standard (IS) solution.

Calibration standards of 0.5, 1, 2, 10, 50, 250, 500 ng/ml were prepared in duplicate fresh in plasma for each analytical run. Quality control samples (QC) were prepared by appropriate dilution of a stock solution of MTO 2 mg/ml in tumor tissue to a final concentration of 1.0, 10, 500 and 400 ng/ml. Samples of 100 µl were mixed with 50 µl of IS and 100 µl of borate buffer pH11. MTO extraction was performed by mixing for 5 min with 1 ml of diethyl ether : dichloromethane (3:2) (v/v). After centrifugation at 13000 rpm for 10 min the aqueous layer was frozen using carbon dioxide/ethanol and the organic supernatant layer was decanted into a clean vial and reconstituted in methanol: formic acid 5:95. After brief vortex-mixing and sonication for 5 min, samples were analyzed after injection of 50 µl.

Mice and Tumor models

Human basal epithelial MDA-MB-231 and luminal-epithelial MCF-7 breast carcinoma cells [24] were kindly provided by Dr. John WM

Martens, (Erasmus Medical Center, Rotterdam, NL) and cultured in Dulbeccos's modified Eagle medium, supplemented with 10% fetal calf serum and 4 mM L-glutamine (Lonza, Belgium) and incubated at 37°C in a humidified environment of 95% air and 5% CO_2.

NMRI nu/nu female mice (Charles River, USA) were used for the human basal-epithelial MDA-MB-231 and luminal-epithelial MCF-7 breast carcinoma tumor model. All mice were housed at 20–22°C, humidity of 50–60%, and 12 hour light–dark cycles. Sterile rodent food and acidified vitamin C-fortified water were given *ad libitum*.

The MDA-MB-231 orthotopic tumor model was established by first generating a bulk tumor by subcutaneous (s.c) injection of $1x10^6$ cells in the flank of mice. From this bulk fragments of 3-4 mm3 were used for transplantation in the mammary fatpad. Mice were used for experiments after ~ 4 weeks when tumors reached a volume of approximately 25 mm^3, determined following the equation *(length*width*d*0,4)* [25]. For MCF-7, human breast carcinoma xenografts, tumor growth was stimulated by hormonal pellets 1.5 mg β estradiol 17-Acetate. A hormonal pellet was implanted s.c 2 days before tumor inoculation. Cells ($1x10^6$) mixed in matrigel were inoculated in the mammary fatpad. After approximately 5 weeks when tumor reached a minimum volume of 25 mm^3 mice were used for experiments. All animal studies were done in accordance to protocols approved by the committee on Animal Research of Erasmus MC, Rotterdam, The Netherlands.

Maximum Tolerated Dose (MTD)

Tolerability studies were performed in female NMRI nu/nu mice with free MTO, standard-MTOL, C_8-Glucer-MTOL and C_8-Galcer-MTOL. A single dose of $5mg \cdot Kg^{-1}$ was injected i.v. via the lateral tail vein. During the experimental period, the mice were monitored for weight loss and other signs of pain and distress in accordance to the code of practice for animal experiments in cancer research by FELASA (1994), such as altered eating and drinking habits; abnormal growth or drop in body weight; abnormal body temperature; altered consistency, amount and colour of faeces; lack of inquisitive behaviour and isolation; abnormal posture and locomotion; altered depth and frequency of breathing and abnormal reactions to external stimuli. Body weight of individual mice was measured every 2-3 days over the course of the study. The MTD of the different

formulations was estimated as the highest dose of MTO that could be safely administered in non-tumor bearing mice without unacceptable toxicity, meaning less than 20% loss of initial body weight or any other signs as described above.

Pharmacokinetics and biodistribution studies

Plasma pharmacokinetics and biodistribution analysis were performed in a human MCF-7 xenograft model when the tumor reached a minimum volume of 25 mm^3. For pharmacokinetics study, mice received a single i.v dose of 5 $mgKg^{-1}$ MTO in free or liposomal form (standard MTOL, C_8-GluCer-MTOL and C_8-GalCer-MTOL), via lateral tail vein. At different time points, 0.1, 4, 8 and 24h after injection, blood samples were taken via tail vein bleeding and collected in eppendorf tubes containing heparin as an anti-coagulant. Blood samples were centrifuged at 13 000 rpm, at 4°C for 10 min to separate the plasma. Plasma samples were stored at –20°C until further analysis. Pharmacokinetic parameters such as half-life (T1/2), volume of distribution (V_{ss}), area under the plasma concentration versus time (0-24h) curve (AUC), Maximum Concentration (C_{max}) and Clearence (Cl) were determined for MTO in plasma by PKSolver add-in in Microsoft Excel [26].

For biodistribution studies, mice were euthanized at 4 or 24h after drug administration. Liver, spleen, kidneys, lungs, heart and tumor were isolated, rinsed in ice-cold saline, collected, weighed and homogenized in 1 ml ice-cold sucrose medium (0.25 M sucrose, 25 mM KCl, 5 mM $MgCl_2$, 10 mM Tris, pH 7.4) using a FastPrep bead assisted homogenizer (MP Bio), equipped with a 7 mm probe. Homogenates were stored at –20°C until further analysis. MTO concentrations in plasma organs and tumor tissue samples were determined by HPLC-UV as described at section *2.3*. MTO levels in the tumor after 4 h post administration were determined by LC-MS/MS measurements.

Therapeutic activity

In vivo anti-tumor efficacy was studied in orthotopically implanted MDA-MB-231 tumors. The treatment groups consisted of PBS, free MTO, standard, C_8-GluCer and C_8-GalCer enriched MTO-nanoliposomes. A single dose of 5 $mg \cdot Kg^{-1}$ MTO was administered i.v for free and respective nanoliposomal MTO formulations. Tumor growth and body

weight were measured every 2-3 days for 16 days. Tumor growth was evaluated by measurement of tumor volume (*section 2.5*) represented after normalization for the initial tumor volume at day zero of treatment. In addition, a multi dosing schedule study was performed in the MDA-MB-231 model by weekly administering MTO formulations i.v. for maximally 5 weeks at a dose of 5 mg·Kg^{-1} MTO for nanoliposomes and for reasons of toxicity at 2.5 mg·Kg^{-1} for free MTO. Tumor growth and body weight were monitored every 2-3 days until two weeks after last injection. Mice were sacrificed when tumor size exceeded 2 cm^3 or upon appearance of signs of distress as outlined in *2.6*, and chosen as a human endpoint for the experiment and used to obtain survival plots.

Intratumoral MTO uptake by intravital microscopy

For intravital microscopy the dorsal skinfold model was used [27, 28]. Briefly, mice were anesthetized and after dissecting the skin leaving the fascia and opposing the skin fold of the mouse was sandwiched between two frames fixed with two light metal bolds and sutures. A small viable tumor piece (approximately 1 mm^3) was taken from a bulk tumor and transplanted in the fascia and on both sides the window was closed with a 12-mm diameter cover glass of 0.13 to 0.16 mm thick [27, 28]. Mice were housed individually in an incubation room with an ambient temperature of 30°C and 60% humidity. Between 10-14 days, when tumors reached a diameter of approximately 4 mm, mice were used for experiments. Four different treatments free MTO, standard MTOL, C_8-GluCer and C_8-Galcer enriched MTO nanoliposomes were administrated i.v, at a MTO concentration of 5 mg·Kg^{-1} and imaging was performed before injection and at 15 min, 2h, 4h, 8h and 24 h after injection. Mice were anesthetized and fixed to a heated microscope stage of a Leica SP5-multiphoton microscope.

Intratumoral accumulation of MTO

Intratumoral MTO delivery was evaluated 24h after single i.v administration of 5 mg·Kg^{-1} MTO, formulated in standard, C_8-GluCer and C_8-GalCer-MTOL in mice bearing an orthotropic MCF-7 tumor. To investigate drug location in relation to tumor hypoxia Pimonidazole Hydrochloride was injected i.p. (2.5 mg/mouse) 4h before sacrifice. Tumors with a diameter of 6 to 8 mm were excised, immediately

snap-frozen in liquid nitrogen and stored at –80°C until further analysis.

Five µm slices were cut and, without fixation to prevent degradation of MTO, examined for MTO fluorescence using a 633 nm laser and 670 long pass filter with a Zeiss LSM microscope. After imaging MTO fluorescence, the same cryostat sections were air dried and fixed in acetone for 5 min and washed with Tris Buffered Saline. The sections were blocked in PBS/BSA 1% goat serum 10% and incubated with Hypoxyprobe-1 Omni Kit PAb2627 (AP) Rabbit antisera. Thereafter the sections were incubated with Alexa fluor goat anti rabbit 488 and mounted with Fluoromount-G DAPI 1:1000 was included for nuclear staining and imaging was performed with a Leica SP5 MP microscope.

Statistical analysis

Statistical analysis was performed by the non-parametric Kruskal-Wallis and Mann Whitney *U* test. P-values less than 0.05 were considered statistically significant. Calculations were performed using GraphPad Prism v5.0 and SPSS v.20 for Windows 2000.

RESULTS

Maximum Tolerated Dose

The maximum tolerated dose of standard and SCS enriched-MTOL (C_8-GluCer and C_8-GalCer) was determined in female NMRI nu/nu mice and compared to free MTO. At a dose of 5 mg·Kg^{-1}, none of the liposomal MTO formulations caused body weight loss for a period of 14 days (Fig. 1). By contrast, free MTO induced a decrease in body weight, which remained less than 20% of pretreatment values. When administrating 10 mg·Kg^{-1} of MTO in free or liposomal form the treatment had to be interrupted after 6 days due to the exclusion of mice showing more than 20% of body weight loss, hypothermia and lethargy (data not shown). This was most pronounced in the free MTO treatment group. Also nanoliposomal MTO formulations induced considerable toxicity at this high dose as evidenced by increasing weight loss over time, which reached > 20% in some mice between day 6 and 8 in all three liposomal MTO treatment groups. Due to these observations the MTD of MTO in free or liposomal form was

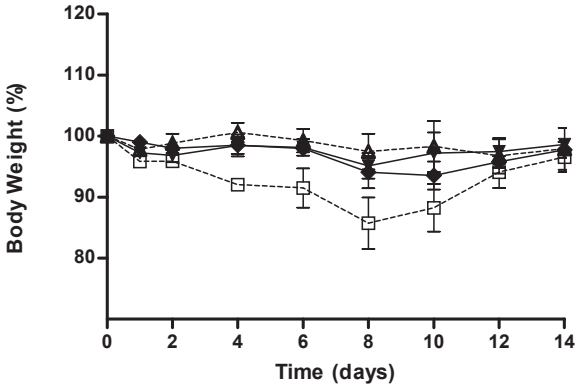

Figure 1 - Maximum tolerated dose (MTD) was determined by monitoring weight loss of mice after a single i.v administration of 5 mg·Kg^{-1} in form of standard MTOL (△), C_8-GluCer (▼),C_8-GalCer-MTOL (◆) or free MTO (□). Mice with body weight loss exceeding 20% of initial body weight were sacrificed and taken out of the experiment. A Dose of 5 mg·Kg^{-1} didn't induce toxicity for liposomal treatment groups. All data represent the mean ± SD for at least 3 mice per treatment group

defined at 5 mg·Kg^{-1} for single administrations. Remarkably, in these studies as well as in the efficacy studies standard-MTOL at a dose of 5 or 10 mg·Kg^{-1} caused visible MTO accumulation in the skin (data not shown). The skin of MTO-L treated mice became blue in a dose-dependent manner (MTO has a dark blue color) in contrast to mice treated with SCS-MTOL or free MTO.

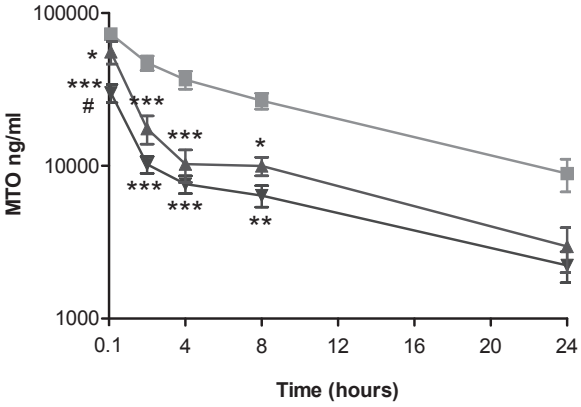

Figure 2 - MTO plasma concentration versus time of standard MTOL (■), C_8-GluCer enriched MTOL (▲) and C_8-GalCer-MTOL (▼). NMRI:nu/nu mice were injected with 5 mg·Kg^{-1} MTO as encapsulated in liposomes at t=0. MTO concentration was determined by HPLC as described in Materials and Methods . All data represent the mean ± SEM for at least 7 samples. (*) $p<0.05$ against MTOL; (**) $p<0.01$ against MTOL; (***) $p<0.001$ against MTOL; # $p<0.05$ versus C_8-GluCer-MTOL

Table 1 – PK parameters for MTO plasma distribution

Parameter	Units	MTOL	C_8-GluCer-MTOL	C_8-GalCer-MTOL
T1/2	h	10.97	10.51	11.06
Cmax	µg/ml	70.88	55.75	30.03
AUC $_{0-24}$	µg/ml*h	557	247	156
Cl	ml/h	0.18	0.43	0.65
Vss	ml	2.50	4.87	8.48

Pharmacokinetic parameters were determined by non-compartmental analysis of plasma MTO concentration time profiles. The mean plasma MTO concentration values at various time points after administration from n= 7 to 8 mice were used to calculate the pharmacokinetic parameter using PK Solver Excel add-in was employed. T1/2: half-life time; Cmax: maximum concentration; AUC: area under the curve; Cl: clearance; Vss: Volume of distribution.

Pharmacokinetics and biodistribution of MTO

The pharmacokinetics of MTO after a single 5 mg·Kg^{-1} i.v. administration of free or liposomal formulations was monitored in nude mice. MTO plasma levels from C_8-GluCer and C_8-GalCer MTO-L treated mice declined more rapidly than standard MTOL treated mice (Fig. 2). Yet, free MTO, could not be detected at the chosen time points due to ultrafast elimination rates.

Early after administration at 0.1, 2, 4 and 8h post injection MTO levels in circulation were significantly lower for both SCS-enriched-MTOL compared to MTOL ($p<0.05$). Differences at 24h were not significant. Remarkably, maximum MTO plasma concentration (C_{max})

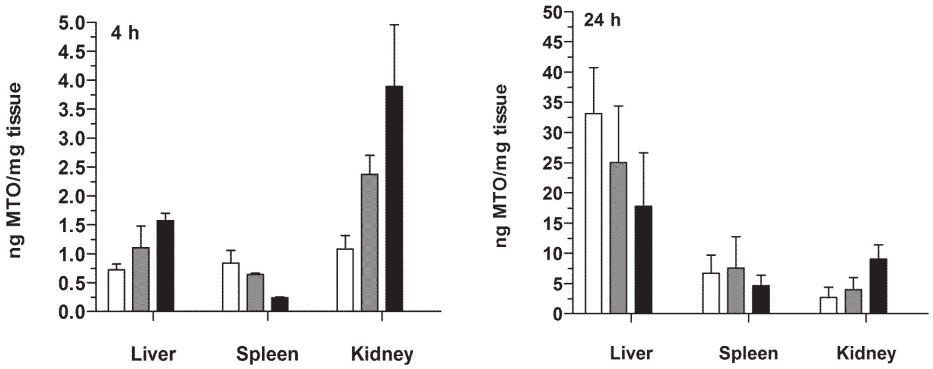

Figure 3 - Distribution of MTO at 4 and 24h from different MTO formulations: MTOL (white), C_8-GluCer enriched MTOL (dark-grey) and C_8-GalCer-MTOL (black) in liver, spleen and kidney. At 4 or 24h free MTO drug levels were below the detection limit. NMRI:nu/nu mice bearing a human orthotopic model of MCF-7 breast carcinoma were injected i.v with 5 mg·Kg^{-1} MTO encapsulated in nanoliposomes and sacrificed at 4 or 24h. MTO concentration was determined by HPLC as described in Materials and Methods. MTO concentration was determined per mg tissue. All data represent the mean ± STDEV for at least 3 animals. *, $p<0.001$ C_8-GalCer-MTOL versus non MTOL in same tissue.

measured at the first time point after C_8-GalCer-MTOL administration was nearly 2 times lower than for C_8-GluCer-MTOL ($p<0.001$), which on its turn was lower than MTOL (Fig 2, table 1).

Based on a non-compartmental pharmacokinetic analysis MTOL and SCS-MTOL displayed similar MTO plasma half-lifes ($t_{1/2}$), of around 11 h. The lower C_{max} for the SCS-MTOL is consistent with a faster clearance and increased distribution volume (Vss) resulting in an AUC of standard MTOL that was 2 and 4-fold higher than for C_8-GluCer-MTOL and C_8-GalCer-MTOL, respectively.

MTO biodistribution at 4h revealed low MTO levels in liver, spleen and kidney for MTOL, C_8-GluCer and C_8-GalCer-MTOL compared to 24h. MTO levels in liver and kidney were somewhat higher for C_8-GalCer-MTOL (Fig. 3). After 24 h MTOL injected mice had the highest drug levels in the liver, whereas spleen and kidney MTO levels were comparable in all treatment groups. After 4h kidney MTO levels for C_8-GalCer-MTOL treated mice were greater than MTOL ($p<0.001$) and comparable to C_8-GluCer-MTOL, (Fig. 3). MTO levels measured by HPLC in the heart, lungs and tumor at 4 and 24h post injection were below the lower detection limit for all treatment groups (data not shown).

Enhanced intratumoral MTO delivery by SCS

To evaluate intratumoral fate of liposomes and MTO after administration of MTOL, C_8-GluCer or C_8-GalCer-MTOL high resolution intravital microscopy was performed in NMRI nu/nu mice bearing a window chamber with implanted MDA-MB-231 tumors. Intratumoral liposome and MTO accumulation were imaged at 15 min, 2; 4, 8 and 24h after administration of 5 $mg \cdot Kg^{-1}$ MTO in free form or formulated in Rho-PE labeled liposomes with or without SCS. Intratumoral MTO fluorescence after free MTO administration could not be detected at any of the analyzed time points (data not shown). By contrast, SCS-liposomal formulations all delivered clearly detectable MTO (purple) to tumor tissue (Fig. 4). The nanoliposomes (red) appeared in tumor vasculature directly after injection and remained visible both in the vasculature as well in tumor tissue up to 24h. For all formulations liposomal fluorescence levels in the tumor increased up to 8h and showed a slight decline between 8 and 24h. At 15 min after liposome administration MTO fluorescence was low and clearly co-localized with liposomal fluorescence in the

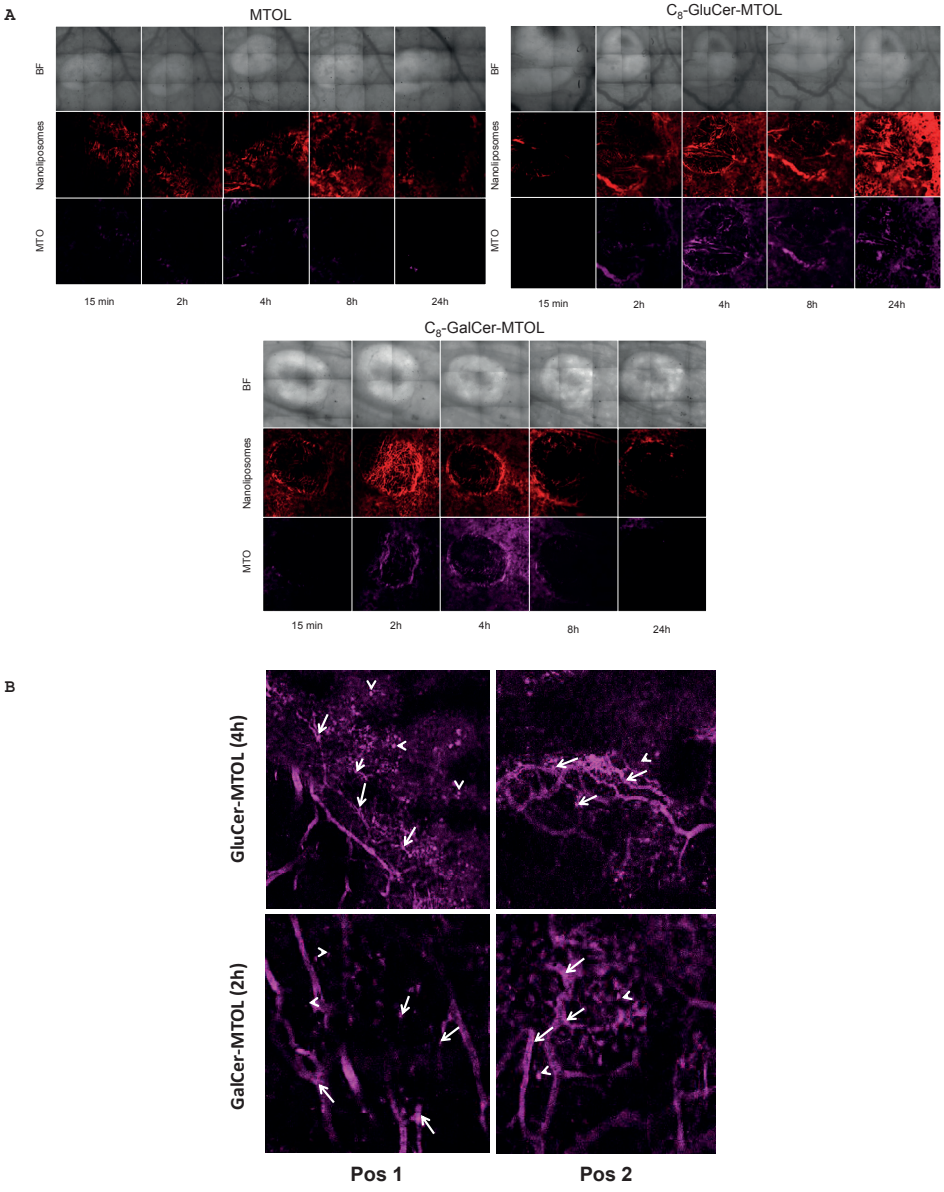

Figure 4 - (A) Intratumoral MTO uptake from standard MTOL, C_8-GluCer-MTOL and C_8-GalCer-MTOL imaged by intravital microscopy. NMRI:nu/nu mice bearing MDA-MB-231 breast carcinoma were injected with 5 mg·kg^{-1} MTO encapsulated in liposomes at t=0. MTO (purple) and fluorescently RhoPE labeled nanoliposomes (red) were followed within the tumor and imaging was performed 15 min, 2h, 4h, 8h and 24h post injection. (B) MTO uptake by tumor cells (arrowhead) and endothelial cells (arrow) are observed at high magnification imaging (10x objective with 3x digital zoom) for SCS-enriched-MTOL (C_8-GluCer-MTOL at 4h and C_8-GalCer-MTOL at 2h post injection)

vasculature, representing liposome-encapsulated MTO. Delivery of MTO, visible from increasing fluorescence mainly in the tumor rim, increased in the first hours after liposome administration and was more abundant for both SCS-MTOL (C_8-GluCer and C_8-GalCer) than for MTOL. Treatment with C_8-GluCer or C_8-GalCer-MTOL resulted in optimal MTO levels at around 4h post-administration after which MTO fluorescence decreased gradually, although detectable levels remained up to 24h.

Higher magnification images (Fig. 4B) clearly indicate MTO from SCS-enriched nanoliposomes present inside as well as outside the tumor vasculature. Punctuated fluorescent appearance is indicative of cellular MTO accumulation in vascular endothelial cells (arrows) and tumor cells (arrowheads). This was not observed for standard-MTOL (data not shown).

MTO distributes heterogeneously in the tumor

Next, we explored the effect of i.v. administration of SCS enriched-MTOL or MTOL on intratumoral MTO delivery in relation to hypoxic tumor areas in an orthotopic MCF-7 breast carcinoma model by immunohistochemistry (Fig. 5). MTO delivery by MTOL treatment was observed in limited areas (Fig. 5A, Position 3) within the tumor and hardly associated with hypoxic regions. On the other hand, C_8-GluCer-MTOL (Fig. 5B, Position 1 and 4) and C_8-GalCer-MTOL (Fig. 5C, Position 1 and 4) seemed to deliver MTO to some extent into hypoxic tumor areas mainly in the tumor periphery, although heterogeneously (Fig. 5C). Treatment with free MTO resulted in low MTO accumulation and a heterogeneous distribution as well (Fig. 5D, Position 4).

Efficacy of single dose administration

The efficacy of a single i.v. administration of SCS enriched-MTOL (C_8-GluCer and C_8-GalCer) and standard-MTOL was compared to free MTO in a MDA-MB-231 orthotopic breast carcinoma model at the MTD of 5 $mg \cdot Kg^{-1}$. There is a trend toward all MTO treatments inducing a tumor growth delay, however differences with buffer treated control mice remained non-significant (Fig. 6A).

In contrast to liposomal formulations, free MTO induced considerable toxicity with nearly 20% of body weight loss at day 7 and 9 post injection, after which mice recovered (Fig. 6B).

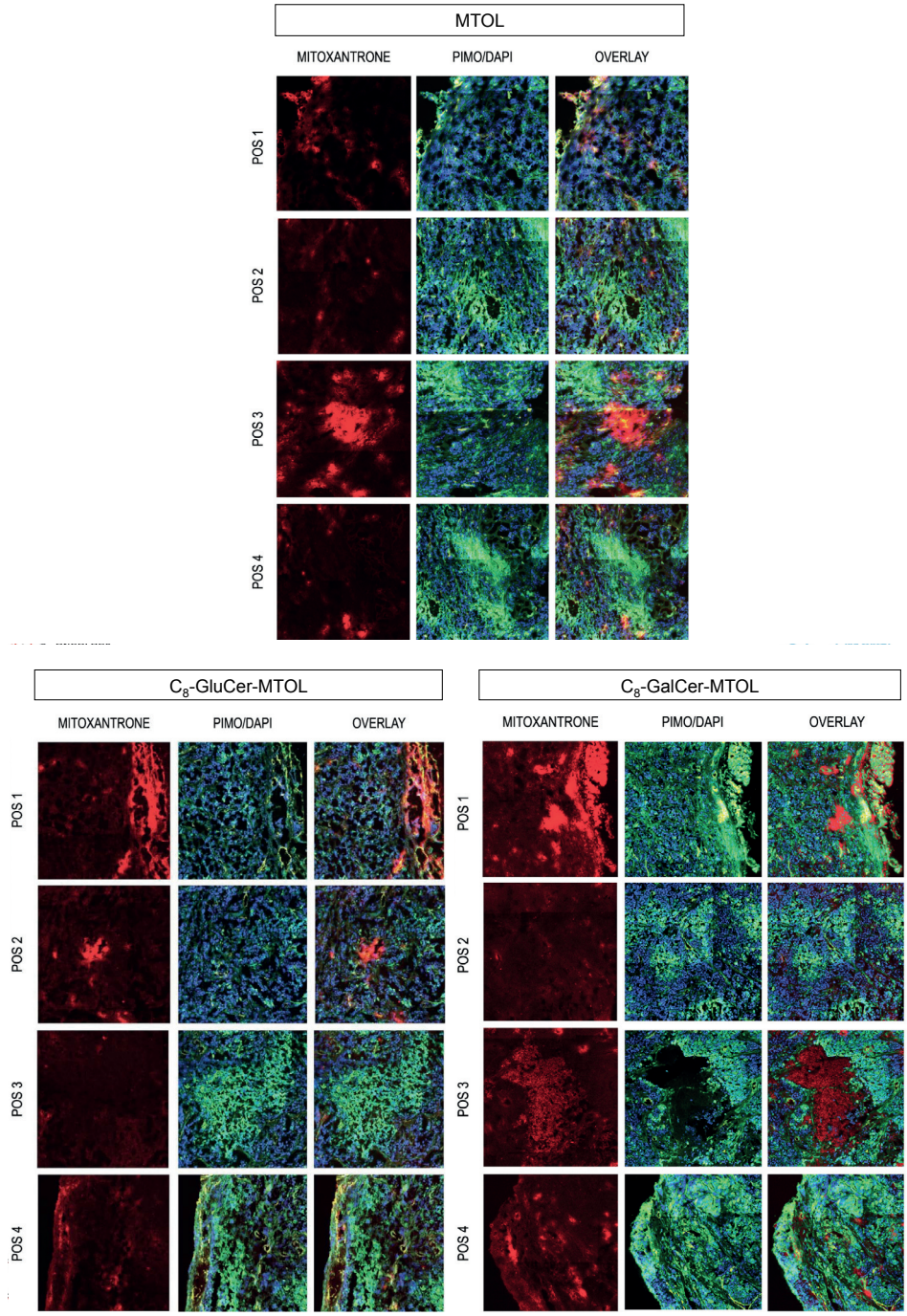

Figure 5 – Intratumoral MTO localization related to hypoxic tumor regions (green) 24h post treatment with (A) standard-MTOL, (B) C_8-Glucer-MTOL (C) C_8-GalCer-MTOL and (D) Free MTO

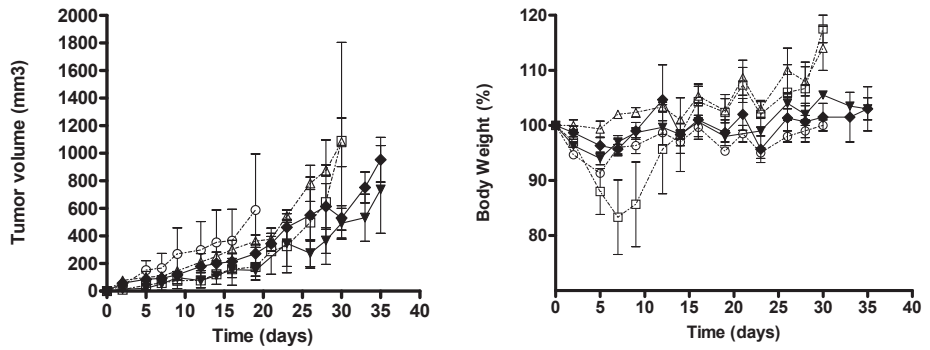

Figure 6 – Efficacy after a single i.v administration of standard MTOL (△), C_8-GluCer-MTOL (▼) C_8-GalCer-MTOL (◆) and free MTO (□). Saline was administered i.v in control groups (○). NMRI:nu/nu mice bearing an orthotopic MDA-MB-231 tumor were injected with 5 mg·kg^{-1} MTO when tumors reached a palpable size > 25 mm^3. After treatment we followed (A) tumor growth (mm^3), and (B) % change in body weight. For tumor growth analysis following respective treatments, tumor volumes were normalized for initial tumor size. All data represent the mean ± SD for at least 3 mice per treatment group

Administering MTO in nanoliposomal form, either as standard-MTOL or SCS-MTO-L caused minor changes in body weight and did not differ from the PBS treatment group, confirming observations in non-tumor bearing mice (Fig. 1). Due to the significant toxicity observed upon single administration of 5 mg·Kg^{-1} free MTO in tumor bearing animals, which was most pronounced at day 7 post injection, the free MTO dose had to be lowered for the multiple dose administration studies.

Efficacy study of multiple dosing

A multiple dosing schedule was applied in which a dose of 5 mg·kg^{-1} liposomal MTO was administered weekly for 5 weeks. The dose of free MTO was reduced to 2.5 mg·Kg^{-1} based on the toxicity observed in the single dose study. Tumor growth and body weight were followed up to 2 weeks after the last dose.

Free MTO in the multi-dosing schedule delayed tumor growth up to 19 days, however thereafter tumors quickly resumed growth similarly to buffer treated animals (Fig. 7A). In contrast, liposomal MTO formulations strongly reduced tumor growth during the whole study period up to 44 days in comparison to saline group ($p<0.05$). Of the liposomal formulations C_8-GluCer-MTOL showed the strongest anti-tumor activity compared to standard-MTOL ($p=0.01$) (Fig 7A insert). Although C_8-GalCer-MTOL treatment also displayed a trend

toward higher anti-tumor activity than standard-MTOL, differences were not significant.

Cumulative doses of liposomal MTO hardly affected body weight of treated mice (Fig. 7B). All treated animals remained at body

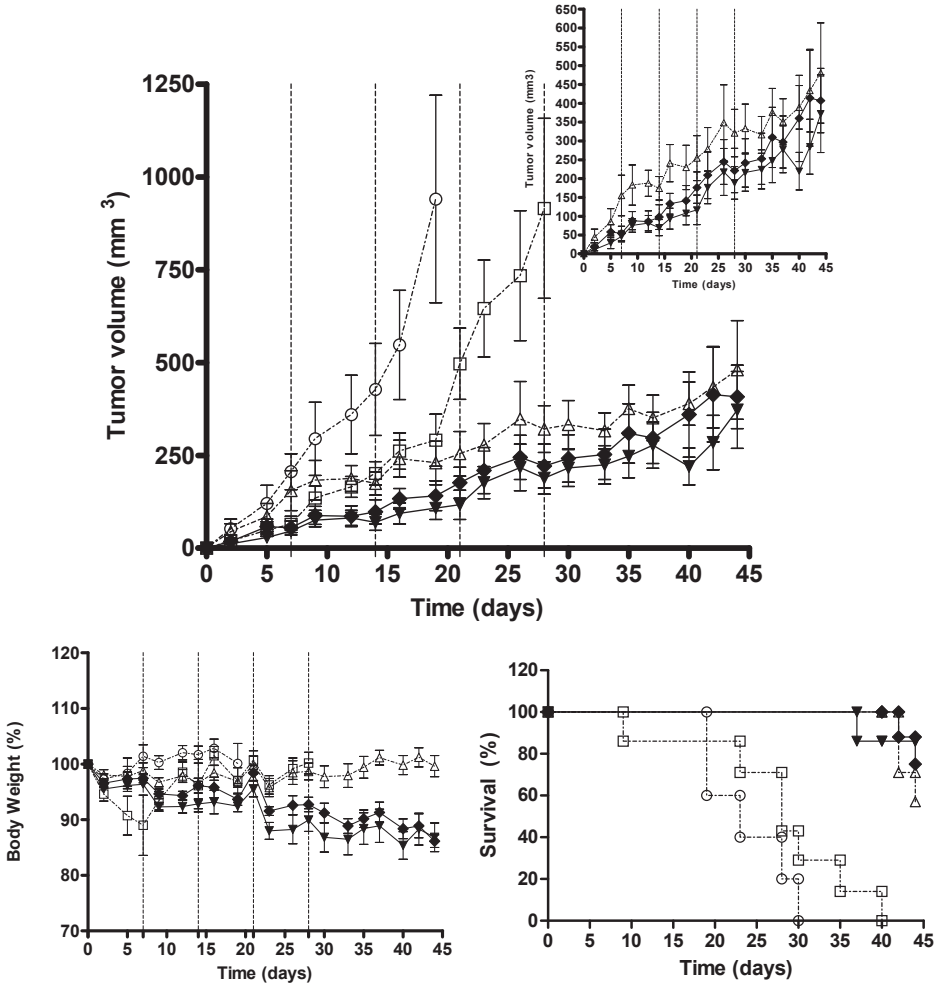

Figure 7 - Efficacy study of multiple dosing schedule of i.v. administered standard MTOL (△), C_8-GluCer-MTOL (▼), C_8-GalCer-MTOL (◆) and free MTO (□). Saline i.v administration was performed in control groups (○). Mice bearing an orthotopic MDA-MB-231 tumor were injected at their MTD with 5 mg·Kg^{-1} MTO for liposomal formulations and 2.5 mg·Kg^{-1} for free MTO every 7 days for 5 weeks. Dotted vertical lines represent subsequent i.v administration days after first treatment at day 0. (A) Tumor growth (mm^3) and (B) % of body weight was followed up to 2 weeks after last administration. Mice with tumor sizes exceeding 1700 mm^3 or presenting body weight loss higher than 20% of initial body weight were sacrificed and taken out of the experiment. (C) Survival of tumor-bearing mice is represented in a Kaplan-Meier plot. All data represent the mean ± SEM for at least 5 mice per treatment group

weights similar to the day of treatment. SCS-MTOL showed a slight decrease in body weight of approximately 10% starting after day 21. Free MTO treated mice showed a decrease in body weight early after treatments started. All liposomal MTO treated mice showed a survival of 80% or more in comparison to free MTO with 0% survival after 40 days of treatment due to tumor size ($p<0.01$) (Fig. 7C). Control mice did not survive longer than 30 days due to tumor size. In a similar multi-dosing schedule empty nanoliposomes (standard, C_8-GluCer and C_8-GalCer enriched liposomes) did not affect tumor growth when compared to PBS treated mice (Supplemental Fig. 1A). Body weight changes for all treated mice were minimal and comparable between treatment groups (Supplemental Fig. 1B).

DISCUSSION

In breast cancer chemotherapy anthracyclines are being used extensively. The use of MTO, an anthracenedione closely related to anthracyclins, however, has gained importance in the treatment of metastatic breast cancer [4, 5] to decrease toxicity at similar therapeutic activity [6]. Nonetheless, MTO still exerts considerable toxicity [29], which should be further minimized while maintaining or even improving its therapeutic activity. To this end we encapsulated MTO in liposomes. These nanocarriers are known to decrease toxicity of their encapsulated drugs [20] and to deliver their contents in tumors through extravasation from leaky tumor vasculature [30]. In this study, MTO encapsulation in PEGylated HSPC and cholesterol-containing liposomes indeed limited toxicity, which allowed administration of higher MTO doses in the treatment of breast carcinoma-bearing mice. In addition, we applied short chain sphingolipid (SCS) based membrane-targeting to lower the tumor cell membrane barrier function toward MTO traversal. SCS upon their insertion into cell membranes exert drug transport enhancing properties to amphiphilic drugs such as Doxorubicin (Dox) and MTO [14, 16-19, 31] (Chapter 2, 3). SCS preferentially exert these properties toward tumor cell membranes, a phenomenon which is likely related to an aberrant make up of these membranes in comparison to those of normal cells [14, 18, 19] (Chapter 2, 3). Tumor cell selectivity has been observed for

the drug uptake enhancing effect of SCS [18, 32]. Studies toward the mechanism described rapid SCS delivery from the liposomal to the tumor cell membrane independent of liposomal uptake, which preceded enhanced liposomal drug influx [14, 18]. Considering the maintenance of vehicle stability profile [14], it is expected that SCS-MTOL enhance intracellular MTO influx by a fast SCS transfer to the tumor cell membrane followed by a rearrangement of the lipid bilayer of the nanocarrier, possible enhanced MTO release and subsequent modulation of tumor cell membrane permeability. Nanoliposomal co-delivery of SCS and MTO *in vitro* showed increased intracellular drug delivery and cytotoxic activity preferentially toward tumor cells [14]. Here this novel SCS-nanoliposomal MTO drug delivery system first decreased MTO toxicity over free drug and second increased tumor drug delivery and therapeutic activity compared to non-SCS-containing MTO-liposomes in an orthotopic breast carcinoma model.

In single MTO administration studies a MTD of 5 $mg \cdot kg^{-1}$ was determined for both free and liposomal MTO. Free MTO however exerted considerable toxicity, as evidenced by a 10-20% decrease in body weight in both normal (Fig. 1) and tumor-bearing mice (Fig. 6B), which lasted up to 12 days post-treatment. None of the liposomal MTO formulations exerted significant toxicity at 5 $mg \cdot kg^{-1}$. Due to free drug toxicity upon cumulative doses, MTO dose had to be reduced to 2.5 $mg \cdot kg^{-1}$ in a weekly repeated multi-dosing study. Even at the reduced dose free MTO caused some decrease in body weight > 10% early after initiating multi-dose treatment (Fig. 7.B), where liposomal formulations did not affect mouse body weight. It is clear from these observations that nanoliposomal encapsulation indeed clearly improved toxicity profile of MTO chemotherapy which confirms similar reports by others [33, 34].

Whereas nanoliposomal drug encapsulation ameliorates toxicity, it may hamper effective delivery of bioavailable drug into tumor cells, thereby limiting therapeutic efficacy [27, 35]. Cell membrane traversal of chemotherapeutic drugs can be strongly enhanced by targeting tumor cell membrane lipid composition. This approach involving the use of truncated (sphingo)lipids is particularly effective for amphiphilic drugs that pass membranes passively, and thus relatively slowly and inefficient. This was demonstrated for a range of drugs [31] and studied in detail for Dox [16-18]

and more recently also for MTO *in vitro* [14]. Here we combined nanoliposomal delivery of MTO with two different SCS, C_8-GalCer and C_8-GluCer, and demonstrated the benefits of this novel combination *in vivo* toward breast carcinoma.

Pharmacokinetics of MTO administered in free or nanoliposomal form was studied during 24h in mice. In contrast to free MTO, which could not be detected at the chosen time points due to very short half-life [36-38], liposomal formulations strongly improved MTO circulation half-life and thus lowered apparent V_{ss}. Decrease of drug toxicity for nanoliposomal MTO likely reflects these changes in MTO pharmacokinetics and distribution. MTO from SCS-MTOL displayed a different pharmacokinetic profile compared to standard MTOL. MTO in the SCS-containing formulations displayed a lower C_{max} and AUC and a higher Cl and V_{ss}, all representing an increased MTO clearance, especially in the first moments after administration as evidenced by a lower C_{max} in comparison to MTOL. The two SCS-MTOL differed in their pharmacokinetics; C_8-GluCer-MTOL had pharmacokinetic parameters closer to MTOL than C_8-GalCer-MTOL.

Previous *in vitro* release studies showed a gradual and continuous release of 25-30% MTO from MTOL during 24h while SCS-MTOL showed an initial release of around 20% followed by a phase with minimal release up to 24h [14]. Such release from the liposomes most likely also occurred *in vivo* and influenced MTOL and SCS-MTOL pharmacokinetics. Liposomal MTO formulations reported here compare positively to other formulations for which MTO release rates of approximately 50% in 24h in the presence of 50% serum have been reported [37].

The faster MTO elimination from plasma for SCS-MTOL treated mice coincided with increased liver and kidney levels at 4h after administration suggesting enhanced cellular uptake by liver macrophages [39]. MTO levels in liver and spleen at 24h post treatment were much higher than after 4h, reflecting ongoing liposome clearance through these organs. The role of liver and spleen in clearance of liposomes by cells of the Reticuloendothelial System (RES) are well documented [40]. In addition, clearance of free MTO occurs to considerable extent through liver [8] followed by biliary and fecal excretion [39, 41], a route that may also be involved in clearance of MTO released from liposomes upon cellular processing in the RES.

The differences in pharmacokinetic profile between SCS-MTOL and MTOL caused differences in skin accumulation. MTOL accumulated to a high extent in the skin, whereas this was not observed for SCS-MTOL. Palmar-plantar erythrodysesthesia (PPE) also called hand-foot syndrome is a dose-limiting side effect commonly reported for PEGylated liposomal Doxorubicin (PLD) (Doxil or Caelyx) [42], which is driven by skin accumulation of liposomes containing drug and subsequent slow drug release, causing local toxicity. Similarly to PLD, MTOL have slow clearance determining their accumulation in skin, in contrast to SCS-MTOL.

Although release from liposomes may occur to some extent, liposomal encapsulation limits drug bioavailability [27, 35]. Combining SCS with MTOL improved drug efficacy specifically in tumor cells by enhancing intracellular drug levels, in comparison to standard-MTOL [14]. Accordingly, intravital microscopy in a breast carcinoma tumor model showed higher intratumoral MTO fluorescence for C_8-GalCer-MTOL and C_8-GluCer-MTOL much earlier than MTOL. MTO delivery within the tumor was very limited for standard-MTOL up to 24h. Therefore we conclude that SCS improved MTO bioavailabilty in the tumor. Quantification of these findings in tumor tissue by HPLC-UV and LC-MS/MS was not successful. As, in general, detected MTO levels were low in isolated tumor tissue, we hypothesize that measuring tumor drug levels is hampered by inefficient drug extraction of MTO from cellular material. Although different extraction buffers such as methanol-acetonitrile or diethyl ether dichloromethane were used this did not increase detection levels in tumor. Similar observations confirming inefficient drug extraction were done in *in vitro* studies to extract MTO from tumor cells (data not shown). The difficulty of MTO extraction is also confirmed by other studies and explained by the strong affinity of MTO to chromatin [9].

In addition to tumor cells, MTO uptake by tumor-vascular lining was also observed confirming previously reported data on co-localization of MTO and CD31 positive cells in a breast carcinoma tumor model [14] and delivery of Dox to tumor vascular endothelial cells using SCS-enriched Dox-liposomes [17]. It is likely, that SCS-MTOL exert cytotoxicity toward tumor cells as well as tumor vasculature, adding to its anti-tumor effect.

Tumor hypoxia results from low levels of oxygen delivery in poorly perfused regions of a tumor and oxygen consumption by

tumor cells with high metabolic activities [43, 44]. Hypoxia is associated with limited chemotherapeutic efficacy and increased drug resistance [45] and hypoxic regions, due to their limited perfusion, are difficult to reach with chemotherapy. Here we analyzed MTO bioavailability in hypoxic areas in a human MCF-7, breast carcinoma tumor model 24h after administration of SCS-MTOL, standard MTO and free MTO. Liposomal drug delivery was heterogeneous within the tumor, for MTO liposomes, standard or SCS-enriched MTOL. Intratumoral accumulation of liposomal chemotherapeutics not only depends on perfusion, but also on the intrinsic characteristics of the endothelial lining and the surrounding microenvironment [46]. These factors contribute to the heterogeneity in drug delivery, whereas the favorable pharmacokinetics of liposomes contributed to increased tumor accumulation in comparison to free MTO, as was also observed by intravital imaging. Upon arrival in the tumor liposomal SCS exert their favorable drug uptake enhancing properties improving MTO bioavailability, as confirmed by intravital microscopy.

A single administration of MTO, 5 $mg \cdot Kg^{-1}$, showed limited effectiveness on tumor growth in all MTO treatment groups (free MTO, standard-MTOL, C_8-GluCer and C_8-GalCer-MTOL) compared to control group. Multiple dosing to achieve higher cumulative tumor drug doses and more homogeneous exposure to the tumor was chosen as an alternative. Nanoliposomal treatments (standard and SCS-enriched-MTOL) with 5 doses administered in a weekly interval strongly inhibited tumor growth and increased survival over free MTO. Importantly, C_8-GluCer-MTOL treatment was the most effective of all three liposomal formulations and outperformed MTOL ($p=0.009$). Although C_8-GalCer-MTOL showed a similar trend to improved outcome, differences were not significant. Remarkably, SCS-MTOL displayed an early tumor response directly after treatment onset, whereas MTOL treated tumors responded later. These results support the ability of SCS-MTOL to improve drug bioavailability more quickly than MTOL as observed by intravital microscopy. Enhanced Dox bioavailability by C_8-Glucer-PLD was also confirmed by intravital optical imaging in experimental animals with orthotopically implanted B16 melanoma and this formulation showed corresponding enhancement in antitumor activity in an A431 xenograft mouse model [17]. This concept of enhanced drug delivery by modulating tumor cell membrane permeability provides promising opportunities for cancer

chemotherapy. In contrast to reports by others on ceramides [32], their glycosylated counterparts C_8-GluCer or C_8-GalCer had no clear anti-tumor effect and exert their activity only in concert with a chemotherapeutic drug at the level of the tumor cell membrane.

Cancer type and tumor physiological characteristics are determinants for outcome after chemotherapy [46]. Here, SCS-MTOL were successfully applied to breast carcinoma treatment showing an improved therapeutic effect in comparison to free MTO and MTOL. Different liposomal formulations containing MTO have been developed [37, 38], which thusfar did not reach clinical application. The lack of clinical translation is probably due to critical pitfalls on formulation or adverse effects such as skin toxicity [37]. The latter can be circumvented by SCS-liposomal MTO formulations. This novel and advanced MTO nanoliposomal formulation not only holds promise for breast cancer treatments but also for other cancer types, such as pancreatic cancer, which showed high susceptibility to MTO treatment [47], prostate carcinoma [48] and leukemia [49]. In conclusion, SCS-MTOL provide a promising approach to improve the therapeutic window of MTO chemotherapy by improving MTO bioavailability to tumor cells.

AKNOWLEDGMENTS

This work was financed by the Dutch Cancer Society. The authors thank Levi Buil for technical assistance with HPLC. The microscopy facilities used are part of the Erasmus Optical Imaging Center and we like to thank the OIC for their assistance.

REFERENCES

1. A.C. Society, *Cancer Facts & Figures 2013.* American Cancer Society, Atlanta, 2013.
2. J. Ferlay, E. Steliarova-Foucher, J. Lortet-Tieulent, S. Rosso, J.W. Coebergh, H. Comber, D. Forman, F. Bray, *Cancer incidence and mortality patterns in Europe: Estimates for 40 countries in 2012.* Eur J Cancer, 49(6) (2013)1374-1403
3. M.S. Hassan, J. Ansari, D. Spooner, S.A. Hussain, *Chemotherapy for breast cancer (Review).* Oncol Rep, 24(5) (2010) 1121-31
4. M. Cristofanilli, F.A. Holmes, L. Esparza, V. Valero, A. Buzdar, J.A. Neidhart, G.N. Hortobagyi, *Phase I/II trial of high dose mitoxantrone in metastatic breast cancer: the M.D. Anderson Cancer Center experience.* Breast Cancer Res Treat, 54 (3) (1999) 225-233
5. L. Pusztai, F.A. Holmes, G. Fraschini, G.N. Hortobagyi, *Phase II study of mitoxantrone by 14-day continuous infusion with granulocyte colony-stimulating factor (GCSF) support in patients with metastatic breast cancer and limited prior therapy.* Cancer Chemother Pharmacol. 43 (1) (1999) 86-91
6. A.M. Cook, E.J. Chambers, G.J. Rees. *Comparison of mitozantrone and epirubicin in advanced breast cancer.* Clin Oncol, 8 (1996) 363-366
7. L.A. Smith, V.R. Cornelius, C.J. Plummer, G. Levitt, M. Verrill, P. Canney, A. Jones, *Cardiotoxicity of anthracycline agents for the treatment of cancer: systematic review and meta-analysis of randomised controlled trials.* BMC Cancer, 10 (2010) 337
8. E.J. Fox, *Mechanism of action of mitoxantrone.* Neurology, 63(12 suppl 6) (2004) S15-S18
9. Z. Hajihassan, A. Rabbani-Chadegani, *Studies on the binding affinity of anticancer drug mitoxantrone to chromatin, DNA and histone proteins.* J Biomed Sci, 16 (2009) 31
10. R. Regev, D. Yeheskely-Hayon, H. Katzir, G.D. Eytan, *Transport of anthracyclines and mitoxantrone across membranes by a flip-flop mechanism.* Biochem Pharmacol, 70(1) (2005)161-9
11. G.L. Nicolson, *The Fluid—Mosaic Model of Membrane Structure: Still relevant to 3 understanding the structure, function and dynamics of biological 4 membranes after more than 40 years.* Biochim Biophys Acta, 1838(6) (2014) 1451-66
12. A.B. Hendrich, K. Michalak, *Lipids as a target for drugs modulating multidrug resistance of cancer cells.* Curr Drug Targets, 4(1) (2003) 23-30
13. U.A. Germann, I. Pastan, M.M. Gottesman, *P-glycoproteins: mediators of drug resistence.* Semin Cell Biol, 4 (1) (1993) 63-76
14. L.R.C. Pedrosa, T.L.M ten Hagen, R. Süss, A. van Hell, A.M.M. Eggermont, M. Verheij, G.A. Koning, *Short-chain glycoceramides promote intracellular mitoxantrone delivery from novel nanoliposomes into breast cancer cells.* Submitted.
15. T.M. Allen, P.R. Cullis, *Liposomal drug delivery systems: from concept to clinical applications.* Adv Drug Deliv Rev, 65(1) (2013)36-48

16. R.J. Veldman, G.A. Koning, A. van Hell, S. Zerp, S.R. Vink, G. Storm G, M. Verheij, W.J. van Blitterswijk, *Coformulated N-Octanoyl-glucosylceramide Improves Cellular Delivery and Cytotoxicity of Liposomal Doxorubicin*. J Pharmacol Exp Ther, 315(2) (2005) 704-10
17. M. van Lummel, W.J. van Blitterswijk, S.R. Vink, R.J. Veldman, M.A. van der Valk, D. Schipper, B.M. Dicheva, A.M.M Eggermont, T.L.M. ten Hagen, M. Verheij, G.A. Koning, *Enriching lipid nanovesicles with short-chain glucosylceramide improves doxorubicin delivery and efficacy in solid tumors.* FASEB J, 25(1) (2011) 280-289
18. L.R.C. Pedrosa, A. van Hell, R. Suss, W. Blitterswijk, A. Seynhaeve, W. Cappellen, A.M.M. Eggermont, T.L.M Hagen, M. Verheij, G.A.Koning, *Improving Intracellular Doxorubicin Delivery Through Nanoliposomes Equipped with Selective Tumor Cell Membrane Permeabilizing Short-Chain Sphingolipids.* Pharm Res, 30(7) (2013) 1883-1895
19. A. J. van Hell, M.M. Melo, W.J. van Blitterswijk, D.M. Gueth, T.M. Braumuller, L.R.C. Pedrosa, J.Y. Song, S.J. Marrink, G.A. Koning, J. Jonkers, M. Verheij, *Defined lipid analogues induce transient channels to facilitate drug-membrane traversal and circumvent cancer therapy resistance.* Sci Rep, 3 (2013) 1949
20. G. Haran, R. Cohen, L.K. Bar, Y. Barenholz, *Transmembrane ammonium sulfate gradients in liposomes produce efficient and stable entrapment of amphipathic weak bases.* Biochim Biophys Acta, 1151(2) (1993) 201-215
21. G. Rouser, S. Fkeischer, A. Yamamoto, *Two dimensional thin layer chromatographic separation of polar lipids and determination of phospholipids by phosphorus analysis of spots*, Lipids, 5(5) (1970) 494-496
22. J.L. Johnson, A. Ahmad, S. Khan, Y.F. Wang, A.W. Abu-Qare, J.E. Ayoub, A. Zhang, I. Ahmad, *Improved liquid chromatographic method for mitoxantrone quantification in mouse plasma and tissues to study the pharmacokinetics of a liposome entrapped mitoxantrone formulation.* J Chromatogr B Analyt Technol Biomed Life Sci, 799(1) (2004) 149-55
23. P. Zhang, G. Ling, J. Sun, Y. Sun, X. Pu, Z. Wang, Z. He, *Determination of mitoxantrone in rat plasma by liquid chromatography–tandem mass spectrometry method: Application to a pharmacokinetic study,* J Chromatogr B Analyt Technol Biomed Life Sci, 878(24) (2010) 2260-5
24. A. Hollestelle, J.H. Nagel, M. Smid, S. Lam, F. Elstrodt, M. Wasielewski, S. S. Ng, P.J. French, J.K. Peeters, M.J. Rozendaal, M. Riaz, D.G. Koopman, T.L.M. ten Hagen, B.H. de Leeuw, E.C. Zwarthoff, A. Teunisse, P.J. van der Spek, J.D. Klijn, W. N. Dinjens, S.P. Ethier, H. Clevers, A. G. Jochemsen, M.A. den Bakker, J.A. Foekens, J.W. Martens, M. Schutte, *Distinct gene mutation profiles among luminal-type and basal-type breast cancer cell lines.* Breast Cancer Res Treat, 121(1) (2010) 53-64
25. A.M. Attia, D.W. Weiss, *Immunonoly of spontaneous mammary carcinomas in mice: V. aquired tumor resistenceand enhancement in strain A mice infectedwith mamarry tumor virus.* Cancer Res, 26(8) (1966)1787-1800

26. Y. Zhang, M. Huo, J. Zhou, S. Xie, *PKSolver: An add-in program for pharmacokinetic and pharmacodynamic data analysis in Microsoft Excel.* Comput Methods Programs Biomed, 99(3) (2010) 306-14
27. A.L.B. Seynhaeve, S. Hoving, D. Schipper, C.E. Vermeulen, G. aan de Wiel-Ambagtsheer, S.T. van Tiel, A.M.M. Eggermont, T.L.M. ten Hagen, *Tumor necrosis factor alpha mediates homogeneous distribution of liposomes in murine melanoma that contributes to a better tumor response.* Cancer Res, 67(19) (2007) 9455-62
28. L. Li, T.L.M. ten Hagen, D. Schipper, T.M. Wijnberg, G.C. van Rhoon, A.M.M. Eggermont, L.H. Lindner, G.A. Koning, *Triggered content release from optimized stealth thermosensitive liposomes using mild hyperthermia.* J Control Release, 143(2) (2010) 274-9
29. A. Wundes, G.H. Kraft, J.D. Bowen, T.A. Gooley, R.A. Nash, *Mitoxantrone for worsening multiple sclerosis: tolerability, toxicity, adherence and efficacy in the clinical setting.* Clin Neurol Neurosurg, 112(10) (2010) 876-82
30. H. Maeda H, H. Nakamura, J. Fang, *The EPR effect for macromolecular drug delivery to solid tumors: Improvement of tumor uptake, lowering of systemic toxicity, and distinct tumor imaging in vivo.* Adv Drug Deliv Rev, 65(1) (2013) 71-9
31. R.J. Veldman, S. Zerp,W.J. van Blitterswijk, M. Verheij, *N-hexanoyl-sphingomyelin potentiates in vitro doxorubicin cytotoxicity by enhancing its cellular influx.* Br J Cancer, 90(4) (2004) 917-925
32. M.A. Tran, C.D. Smith, M. Kester, G.P. Robertson, *Combining Nanoliposomal Ceramide with Sorafenib Synergistically Inhibits Melanoma and Breast Cancer Cell Survival to Decrease Tumor Development*. Clin Cancer Res, 14(11) (2008) 3571-3581.
33. C. Li, J. Cui, C. Wang, J. Wang, Y. Li, L. Zhang, L. Zhang, W. Guo, Y. Wang, *Lipid composition and grafted PEG affect in vivo activity of liposomal mitoxantrone.* Int J Pharm, 362(1-2) (2008) 60-6
34. A. Orthmann, R. Zeisig, R. Süss, D. Lorenz, M. Lemm, I. Fichtner, *Treatment of Experimental Brain Metastasis with MTO-Liposomes: Impact of Fluidity and LRP-Targeting on the Therapeutic Result.* Pharm Res, 29(7) (2012) 1949-59
35. K.M. Laginha, S. Verwoert, G.J. Charrois, T.M. Allen, *Determination of Doxorubicin Levels in Whole Tumor and Tumor Nuclei in Murine Breast Cancer Tumors*. Clin Cancer Res, 11(19 Pt 1) (2005) 6944-9
36. K.M. Rentsch, D.H. Horber, R.A. Schwendener, H. Wunderli-Allenspach, E. Hänseler, *Comparative pharmacokinetic and cytotoxic analysis of three different formulations of mitoxantrone in mice.* Br J Cancer, 75(7) (1997) 986-92
37. C. Li, J. Cui, C. Wang, Y. Li, H. Zhang, J. Wang, Y. Li, L. Zhang, L. Zhang, W. Guo, Y. Wang, *Encapsulation of mitoxantrone into pegylated SUVs enhances its antineoplastic efficacy.* Eur J Pharm Biopharm,70(2) (2008) 657-65
38. H.J. Lim, D. Masin, N.L. McIntosh, T.D. Madden, M.B. Bally, *Role of Drug Release and Liposome-Mediated Drug Delivery in Governing the Therapeutic Activity of Liposomal Mitoxantrone Used to Treat Human A431 and LS180 Solid Tumors*. J Pharmacol Exp Ther, 292(1) (2000) 337-45

39. K.J. Patel, O. Trédan, I.F. Tannock, *Distribution of the anticancer drugs doxorubicin, mitoxantrone and topotecan in tumors and normal tissues.* Cancer Chemother Pharmacol, 72(1) (2013) 127-38
40. A. Gabizon, H. Shmeeda, Y. Barenholz, *Pharmacokinetics of Pegylated Liposomal Doxorubicin:Review of animal and human studies.* Clin Pharmacokinet, 42(5) (2003) 419-36
41. D.S. Alberts, Y.M. Peng, G.T. Bowden, W.S. Dalton, C. Mackel, *Pharmacology of mitoxantrone: mode of action and pharmacokinetics.* Invest New Drugs, 3(2) (1985) 101-7
42. K.P. Farr, A. Safwat, *Palmar-plantar erythrodysesthesia associated with chemotherapy and its treatment.* Case Rep Oncol, 4(1) (2011) 229-35
43. E. Lord, L. Harwell, C.J. Koch, *Detection of Hypoxic Cells by Monoclonal Antibody Recognizing 2-Nitroimidazole Adducts.* Cancer Res, 53(23) (1993) 5721-6
44. A.J. Primeau, A. Rendon, D. Hedley, L. Lilge, I.F. Tannock, *The Distribution of the Anticancer Drug Doxorubicin in Relation to Blood Vessels in Solid Tumors.* Clin Cancer Res, 11(24 Pt 1) (2005) 8782-8
45. J.P. Cosse, C. Michiels, *Tumour hypoxia affects the responsiveness of cancer cells.* Anticancer Agents Med Chem, 8(7) (2008) 790-7
46. E.S. Nakasone, H.A. Askautrud, T. Kees, J.H. Park, V. Plaks, A.J. Ewald, M. Fein, M.G. Rasch, Y.X. Tan, J. Qiu, J. Park, P. Sinha, M.J. Bissell, E. Frengen, Z. Werb, M. Egeblad, *Imaging Tumor-Stroma Interactions during Chemotherapy Reveals Contributions of the Microenvironment to Resistance.* Cancer Cell, 21(4) (2012) 488-503
47. V. Yagublu, N. Caliskan, A.L. Lewis, R. Jesenofsky, L. Gasimova, J.M. Löhr, M. Keese, *Treatment of experimental pancreatic cancer by doxorubicin-, mitoxantrone-, and irinotecan-drug eluting beads.* Pancreatology, 13(1) (2013) 79-87
48. D.J. Taylor, C.E. Parsons, H. Han, A. Jayaraman, K. Rege, *Parallel screening of FDA-approved antineoplastic drugs for identifying sensitizers of TRAIL-induced apoptosis in cancer cells.* BMC Cancer, 11 (2011) 470
49. C. Parker, R. Waters, C. Leighton, J. Hancock, R. Sutton, A.V. Moorman, P. Ancliff, M. Morgan, A. Masurekar, N. Goulden, N. Green, T. Révész, P. Darbyshire, S. Love, V Saha. *Effect of mitoxantrone on outcome of children with first relapse of acute lymphoblastic leukaemia (ALL R3): an open-label randomised trial.* Lancet, 376 (9757) (2010) 2009-17

CHAPTER 5

C_8-glycosphingolipids preferentially insert into tumor cellmembranes and promote chemotherapeutic drug uptake

Lília R. Cordeiro Pedrosa, Wiggert A. van Cappellen, Barbara Steurer, Dalila Cicero, Timo L.M. ten Hagen, Alexander M.M Eggermont, Marcel Verheij, Felix María Goñi, F.-Xabier Contreras, Gerben A. Koning

In preparation

ABSTRACT

Insufficient drug delivery into tumor cells severely limits the therapeutic efficacy of chemotherapy. Co-delivery of liposome-encapsulated drug and synthetic short chain sphingolipids (SCS) greatly improved drug bioavailability by enhancing intracellular drug uptake. However, the molecular mechanism used by SCS to improve drug uptake is still enigmatic. We hypothesize that after relocation from the liposomal to the plasma membrane SCS have a tendency to self-associate into specific microdomains with improved drug permeability.

Live cell imaging was used to follow the intracellular fate of fluorescent C6-NBD-GalCer incorporated in liposomes in SKBR-3, breast carcinoma and BLM, melanoma and non-tumor endothelial cells and fibroblasts to compare cell membrane lipid transfer differences. Additionally click chemistry was applied post SCS-treatment to stain and image native SCS in cell membranes by confocal microscopy and quantify lipid transfer by thin layer chromatography (TLC). SCS-mediated flip-flop was investigated in model membranes. SCS-enriched liposomes containing the chemotherapeutic drug Doxorubicin (Dox) were incubated at 4°C and 37°C to study intracellular drug uptake in MDA-MB-231, breast carcinoma and BLM melanoma cells in comparison to standard liposomes without SCS and free Dox.

SCS transfer to cell membrane was independent of liposomal uptake and that the majority of the transferred lipid remained in the plasma membrane whereas a smaller fraction was detected in lysosomes. The transfer of SCS was tumor cell specific as 3-fold higher levels in tumor cells compared to non-tumor cells. These results were by click chemistry, confocal imaging and TLC. SCS when transferred to the plasma membrane, induced a transbilayer flip-flop of pyrene-SM, but pore formation was not observed. Imaging of drug uptake at 4°C revealed that SCS enhanced the interaction of Dox with the outer leaflet of the plasma membrane of tumor cells, augmenting the subsequent transmembrane flip-flop of the drug, which only occured at 37°C. Our results demonstrate that SCS preferentially insert into tumor cell plasma membranes and there enhance a cells intrinsic capacity to translocate amphiphilic drugs such as Dox across the membrane via a biophysical process.

INTRODUCTION

Ineffective outcome of chemotherapy is often due to dose limiting toxic side effects of free drug and to poor drug bioavailability in tumor cells. Liposomal drug carrier technology is extensively described as an effective means to prevent drug toxicity by minimizing drug interaction with healthy tissue [1-3]. Caelyx or Doxil, a formulation of doxorubicin (Dox) encapsulated in PEGylated, 85-100 nm liposomes (PLD) [4, 5] is approved by EMEA in Europe and by FDA in USA, for treatment of AIDS-related Kaposi's sarcoma [6], refractory ovarian cancer [7], myeloma [8] and metastatic breast cancer [6, 9]. Although PLD, due to its favorable pharmacokinetic profile and small particle size accumulates in tumors [10], its high stability prevents optimal drug accumulation in tumor cells [11, 12]. PLD's low drug bioavailability remains a main issue limiting therapeutic efficacy [2, 13]. A novel approach to enhance intracellular drug delivery in tumor cells was developed and involves insertion of short chain sphingolipids (SCS), like C_8-glucosylceramide (C_8-GluCer) or C_8-galactosylceramide (C_8-GalCer) in the tumor cell membrane, increasing its permeability to various anti-cancer drugs [14]. Co-delivery of SCS and drugs to tumor cells using liposomes as a nanocarrier caused higher levels of intracellular drug delivery specifically in tumor cells [15-18]. The mechanism underlying this SCS mediated drug uptake enhancement and its preference for tumor cells remained underexposed thusfar and is the subject of this study.

Sphingolipids contain a sphingosine backbone where the functional amino group at position C2 is acylated with a fatty acid (Fig. 1). One of the most investigated sphingolipids, ceramide has a free functional hydroxy group (-OH) at position C1, whereas in more complex sphingolipids this position is linked to a polar head group. In the particular case of glycosphingolipids, the head group corresponds to a sugar residue (i.e. glucose or galactose). It has been described that long-chain ceramides, but not short chain, have membrane remodeling properties when externally added or *in situ* generated in model membranes [19, 20]. For instances, ceramides induce transbilayer lipid motion and increase membrane permeability in LUVs. Generation of non-lamellar structures by ceramide creates transitory lipid-packaging defects between lamellar

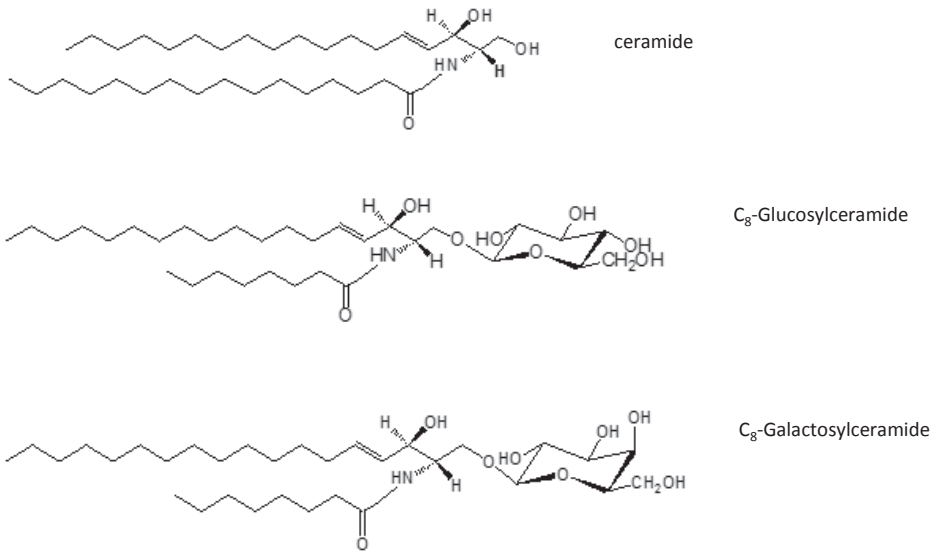

Figure 1 - Molecular structures of ceramide and short chain sphingolipids (C_8-Glucosyl and C_8-Galactosyl). Molecular structures were design by Chem Draw Ultra 8.02

and non-lamellar phases that account for the lipid scrambling and membrane permeability effects observed. In addition, it has been reported that both short (C2) and long chain (C16) ceramides spontaneously form large stable pores in the outer mitochondrial membrane contributing to cytochrome C release during initiation of apoptosis [21]. Spontaneous formation of ceramide channels occurs by lateral segregation of ceramide chains parallel to the plane of the membrane with channel diameters of 0.8 nm for short chain and up to 11 nm for long chain ceramides [21]. Further, Soumya *et al.* were able to visualize C16-ceramide channels in a phospholipid membrane by transmission electron microscopy [22]. These channels consisted of columns of four to six ceramides H-bonded via amide groups and arranged as staves in either a parallel or antiparallel manner. Differences in the biophysical interactions between ceramides and phospholipids are described to be dependent on the N-acyl chain length and the intra- and intermolecular hydrogen bonds between sphingolipids and surrounding lipids and lead to the formation of specific membrane domains, lipid sorting and create signaling platforms [20, 23]. Yet, for glycosphingolipids little is known about their behavior in membranes and possible mechanisms for domain formation and their role in enhancing drug transport. It's also known that C6-ceramide doesn't enhance intracellular Dox

uptake [14, 17] lining off the importance of the hydrophilic head group of SCS such as C_8-GluCer or C_8-GalCer in the properties of SCS as drug uptake enhancers.

Based on the known behavior of ceramides and sphingosine and the tendency of certain sphingolipids to self-associate [24-26] our prevalent hypothesis is that upon spontaneous relocation of liposome-incorporated SCS to the tumor cell membrane upon cellular contact they self-organize into specific micro-or nano-domains with increased drug permeability. The SCS contribute to imperfect lipid packing, hence creating local differences in membrane fluidity and lipophilicity. This sequence of events likely leads to formation of transitory nanoscale membrane channels [17] that alter membrane permeability and transmembrane diffusion of amphiphilic drugs [27] with a preference for tumor cells [18].

In the present study, we aim at investigating the molecular mechanisms underlying SCS-mediated cellular drug uptake and to study the cell type specificity of such mechanisms. To this end, the cellular fate of liposomes and SCS is investigated by confocal microscopy using fluorescently labeled SCS (C6-NBD-GalCer) and a stable liposomal bilayer marker (DiD). Studies are performed in tumor cells and normal cells to determine a possible preference of SCS transfer to tumor cells. In addition, post treatment click chemistry is applied in order to disturb as little as possible the original molecular structure of the lipid (C_8-GluCer) and SCS incorporation in cell membranes is imaged by microscopy and quantified by TLC. Finally new insights on SCS mechanism of action as Dox uptake enhancers to tumor cells are studied at 4°C and biophysical features of SCS are investigated using model membrane systems.

MATERIAL AND METHODS

Materials

Hydrogenated soy phosphatidylcholine (HSPC) and distearylphosphatidylethanolamine (DSPE)-PEG_{2000} were from Lipoid (Ludwigshaven, Germany). Short chain sphingolipids, C_8 Glucosyl(ß) Ceramide (d18:1/8:0) D-glucosyl-ß-1,1' N-octanoyl-D-erythro-sphingosine (C_8-GluCer), C_8 Galactosyl(ß) Ceramide (d18:1/8:0)

D-galactosyl-ß-1,1' N-octanoyl-D-erythro-sphingosine (C_8-GalCer), C_6-NBD Galactosyl Ceramide N-[6-[(7-nitro-2-1,3-benzoxadiazol-4-yl)amino]hexanoyl]-D-galactosyl-ß1-1'-sphingosine, egg-Phosphatidylcholine (PC), Phosphatidylethanolamine (PE), egg-sphingomyelin, liver phosphatidylinositol and brain PS were from Avanti Polar Lipids (Alabaster, AL, USA). DiD, from Invitrogen, (Carlsbad, USA).

Polycarbonate filters were from Northern Lipids (Vancouver, BC, Canada) and PD-10 Sephadex columns were from GE Healthcare (Diegem, Belgium). Cholesterol, HEPES (2-[4-(2-hydroxyethyl)piperazin-1-yl] ethanesulfonic acid). Hoechst was from Molecular Probes (Leiden, The Netherlands). PBS was from Boom and FACS flow fluid from BD Biosciences. Dox-HCl (Dox) was from Pharmachemie (Haarlem, The Netherlands). Cholesterol, HEPES (2-[4-(2-hydroxyethyl)piperazin-1-yl] ethanesulfonic acid) were from Sigma Aldrich (Zwijndrecht, The Netherlands). Pyrenebutyroyl-Sphingomyelin (pyr-SM) was synthesised as described in Contreras et al (2012).

Standard and SCS-enriched liposomal formulations

Standard and SCS-enriched liposomes were formulated of HSPC/ cholesterol/ DSPE-PEG_{2000} in a molar ratio of 1.85: 1: 0.15. To the mixture of lipids, 0.1mol of SCS was added per mole of total amount of lipid (including cholesterol).

Liposomes of 85-100nm in diameter were prepared by lipid film hydration and extrusion method using a thermobarrel extruder, Northern Lipids, Vancouver, Canada at 65°C [27].

Lipids were dissolved in chloroform methanol 9:1 (v/v) mixed and a lipid film was created under reduced pressure on a rotary evaporator and subsequently dried under a stream of nitrogen. Finally, lipid film was hydrated by 135 mM NaCl, 10 mM Hepes buffer, pH 7.4 and liposomes were sized by sequential extrusion through 100-, 80-, and 50 nm polycarbonate filters (Northern Lipids, Vancouver, Canada).

Fluorescently labeled liposomes and fluorescently labeled SCS liposomes were prepared using the lipophilic tracer DiD (Invitrogen, Carisbad, USA) and C6-NBD Galactosyl Ceramide at 0.25 mol% of total amount of lipid.

Hydration of the lipid film with $(NH_4)_2SO_4$ allowed loading of liposomes with Dox by a transmembrane ammonium sulphate gradient.

Liposomes were loaded with Dox in a drug to phospholipid ratio of 0.1:1 (w/w) for 1 h at 65°C [34]. Non-encapsulated Dox was removed by ultracentrifugation at 29000 rpm for 1h at 4°C in a Beckman ultracentrifuge (Ti50.2 rotor). The liposome pellet was resuspended in HEPES buffer (135 mM NaCl, 10 mM HEPES, pH 7.4). Size and polydispersity index (pdi) were determined by light scattering using a Zetasizer Nano ZS (Malvern Instruments, Malvern, UK). Lipid concentration was measured by phosphate assay [28].

Large unilamellar liposomes (LUV's) formulation

Large unilamellar liposomes (LUV's) mimicking plasma membrane lipid composition were composed of 17.5% (mol) PC, 5% (mol) PS, 5% (mol) PI, 10% (mol) PE, 50% (mol) cholesterol and 12.5% (mol) Egg- SM and formulated as described elsewhere [29]. Lipids were dissolved in chloroform: methanol 2:1 (v/v) at the desired molar ratio and lipidic mixture was dried under a stream of nitrogen. To eliminate remaining traces of organic solvent, lipid mixture was placed in an excicator for 30 min under vaccum. Resuspension of lipids was performed in Hepes Buffer (5 M KOH, 100 mM HEPES, pH 7.4) and then vigorously shaken with a vortex mixer to form multilamelar vesicles. The liposomes suspension was frozen and thawed for ten cycles. A single freeze-thaw cycle consisted of freezing for 2 min at liquid nitrogen temperature (–196°C) and thawing for 5 min in a water bath at 50°C. Liposomes were extruded by 10 passages through two filters of 100 nm (Nucleopore, Pleasanton CA) at room temperature. LUV's were kept on ice and used immediately after preparation.

Cell culture

All tumor cell lines (BLM melanoma, MDA-MB-231 and SKBR-3 breast carcinoma, HeLa cervix carcinoma) were cultured in Dulbeccos's modified Eagle medium, supplemented with 10% fetal calf serum and 4 mM L-glutamine. HUVEC were isolated by collagenase digestion using the method described by Jaffe *et al.* [30] and cultured in HUVEC medium containing human endothelial serum free medium (Invitrogen), 20% heat inactivated newborn calf serum (Cambrex), 10% heat inactivated human serum (Cambrex), 20 ng/ml human recombinant epidermal basic fibroblast growth factor (Peprotech EC Ltd) and 100 ng/ml human recombinant epidermal growth factor (Peprotech EC

Ltd) in fibronectin (Roche Diagnostics) coated flasks. Fibroblasts (3T3) were cultured in Dulbeccos's modified Eagle medium containing nutrient mixture F12, supplemented with 10% fetal calf serum and 4 mM L-glutamine. All serum supplements were heat inactivated at 56°C for 30 min. Cells were subcultured twice a week by trypsinization when a confluency of 80-90% was reached, and maintained in a water saturated atmosphere of 5% CO2 at 37°C. Tumor cells were seeded on a coating of 0.1% collagen (Invitrogen, Carlsbad, USA) in culture medium and HUVEC were seeded on a coating of 1mg/ml fibronectin in PBS (Roche, Rotkreuz, Switzerland) for microscopic imaging.

Liposomal, SCS and drug fate by confocal microscopy

Laser Scanning Confocal Microscopy (Zeiss LSM 510 META) was used to study the *in vitro* fate of fluorescently labeled liposomes with DiD and fluorescently labeled SCS (C_6-NBD-GalCer) in SKBR3, breast carcinoma cell after 2h at 37°C. C_6-NBD-GalCer was excited with the 488 nm line from an Argon ion laser, emission was detected between 505 nm and 550 nm. Dox was excited with a 543 nm Helium-Neon laser. Dox emission was detected between 560 and 615 nm. The lipophilic tracer DiD was excited at 563 nm and infrared emission was detected with a longpass 650 nm filter. The LysoTracker® Red DND-99 (Invitrogen, Carlsbad, USA) was incubated with cells in a concentration of 50 nM for 1h at 37°C. The dye was excited with 543 nm and emission was detected with a bandpass filter from 585 to 615 nm. Cells were imaged with a 63x planachromat oil (n.a. 1.4) objective lens. For confocal experiments $1x10^5$ cells were seeded on glass coverslides one day prior to imaging. For time lapse experiments 10 positions on a slide were selected and images were taken every 15 min in 4 focal planes for up to 14h. The 633 nm He-Ne laser line was used for autofocus adjustments.

For confocal microscopy experiments at 4°C precooled cells were treated with 40 µM Dox in form of free drug, standard liposomes or 10% (mol) C_8-GalCer enriched liposomes diluted in cold culture medium and incubated for 2h at 4°C. Cells were imaged before and after washing with ice cold culture medium. Cells were kept on ice during experimental handling. Subsequently cells were further incubated for 2h at 37°C and 5% CO_2 and were imaged again before and after washing with culture medium.

C_8-GluCer cellular distribution and quantification by click chemistry

A C_8-GluCer containing an omega-terminal alkyne in the fatty acid was synthesized as described by Thiele *et al.* [28]. Addition of the omega-terminal alkyne maintains the original chemical properties of C_8-GluCer and allows lipid detection by click chemistry with an azide-labeled fluorophore to localize and quantify the C_8-GluCer transferred to the cell. The alkyne group is accessible to the azide once the lipid is inserted in the cell. Non-inserted lipid is washed off before fixation and labeling. 10^5 HeLa cells were seeded in 3.5 cm glass bottom dishes. After treatment with 2 µM of C_8-GluCer in ethanol/ de-lipidated medium, cells were incubated for 1 and 2h at 37°C, 5% CO_2. Cells were washed twice in PBS and fixed at RT for 10 min with 4% PFA in PBS 4% glucose and 4 mM EDTA. After fixation, click chemistry was performed for 1h at RT by adding a mixture of 0.1mM TBTA, 1mM TCEP, 1mM CuSO4 and 10 µM Cy3-azide in PBS. Cells used as control were treated in absence of $CuSO_4$ that catalyze the click chemistry reaction. After washing in PBS cells were stored at 4°C until further imaging by confocal microscopy. To localize the lipid in the cell by fluorescence microscopy, additional nuclear and plasma membrane staining were performed. For C_8-GluCer quantification, cells were scraped and collected in 300µl of PBS and centrifuged at 6500 rpm for 5 min at RT. Lipid extraction and quantification was performed as described in Thiele *et al.*, (2012). Fluorescence images were acquired with a digital UV Chromato-Vue cabinet (UVP, LLC).

Transbilayer redistribution of pyrene SM by SCS

The extent of transbilayer lipid motion or flip-flop was measured in LUV's composed of 17,5 mol% PC; 5 mol% PS; 5 mol% PI; 10 mol% PE; 50 mol% cholesterol; 12.5 mol% SM [29], by a method described by Muller *et al.* [30]. This method consists of an asymmetric incorporation of pyrene fluorescent SM analogue (Pyr-SM) inserted in the outer leaflet of the membrane and further dilution of the probe within the inner and outer leaflet of the membrane upon a transbilayer redistribution induced by SCS membrane interaction. Pyr-SM can be present in form of excimers (I_E) when in high concentration in the outer leaflet or monomers (I_M) upon dilution of the probe to the inner leaflet of the cytoplasmic membrane

displaying different emission at 465 nm or 395 nm, respectively. Redistribution of pyr-SM from the outer to the inner leaflet can be followed by a decrease of excimer and increase in monomer fluorescence, decreasing the ratio I_E/I_M. The transbilayer movement of pyr-SM in pure phospholipid vesicles is described as very slow causing a constant I_E/I_M. Experiments were performed at 37°C in a spectrofluorometer AMINCO Bowman Series2. Lipid concentration was 300 µM for LUV's to which 15 µM of Pyr-SM was added and incubated for 10 min at 37°C prior to addition of 15 µM of SCS (C_8-GluCer or C_8-GalCer). Immediately after Pyr-SM incorporation in the outer leaflet of the membrane, before any redistribution, I_E/I_M was set to 1. SCS-induced flip-flop is represented by I_E/I_M ratio of pyr-SM upon incorporation of SCS in the outer leaflet of the membrane. Control experiments were performed by adding ethanol, which was used as vehicle to deliver SCS.

Leakage assay

Leakage of vesicular 8-aminonaphtalene-1,3,6-trisulfonate (ANTS)/ p-xylene bispyridinium bromide (DPX) was assayed, as explained by Ellens *et al.* [31]. ANTS and DPX are water soluble anion/cation fluorophore quencher pair. ANTS fluorescence in the liposome (plasma membrane like LUVs) is quenched by collisional energy transfer to DPX. When both ANTS and DPX are trapped in the lumen of a vesicle, they exist in the form of a non-fluorescent complex. When vesicle efflux occurs, ANTS and DPX become diluted, the complex dissociates and free ANTS emits fluorescence. ANTS fluorescence spectrum has an excitation maximum at 350 nm and emission maximum at 530 nm. A cut of filter of 450 nm was placed between the sample and the emission monochromator to avoid scattering interferences. Liposomes were prepared as described at section 2.2. Non-encapsulated ANTS-DPX complex is removed by passing the liposomes through a Sephadex G-75 column. LUVS were prepared freshly for each experiment. A spectrofluorimeter Aminco Bowman Series 2 with fluorescence set at 355 nm for excitation and 520 nm for emission in presence of a filter of 450 nm to eliminate possible noise from the presence of liposomes, was used to measure differences in fluorescence of ANTS-DPX complex under constant mixing at 37°C. The basal signal of fluorescence was set to 0% before adding 15 µM of C_8-GluCer to 0,3 mM of the LUV's suspension. The fluorescence for 100% release was

set after solubilizing liposomal membrane by adding Triton X-100 (10 mM final concentration in the cuvette).

RESULTS

Liposome characterization

Dox-loaded or empty liposomes with and without SCS were prepared and characterized. Liposomes were obtained with a size between 85 and 95 nm, a polydispersity index (pdi) of <0.1 and Dox-loading efficiency of >80%. Values for liposome size and pdi before (emptyL) and after loading with Dox, drug concentration, loading efficiency and phospholipid (PL) recovery after ultracentrifugation (UC) are represented in Table 1.

Table 1 – Liposomes characterization

	Empty-L		Dox-L			
	size (nm)	pdi	size (nm)	pdi	Loading (%)	PL recovery (%)
Standard-L	87.5 ± 2.1	0.05 ± 0.02	89.5 ± 1.1	0.06 ± 0.03	88 ± 2.0	68 ± 3.0
C8-Glucer-L	89.4 ± 1.4	0.05 ± 0.03	91.3 ± 1.2	0.05 ± 0.04	86 ± 2.0	72 ± 2.0
C8-GalCer-L	88.4 ± 1.8	0.06 ± 0.01	89.4 ± 1.7	0.07 ± 0.03	85 ± 1.0	73 ± 3.0

More than 3 independent batches were formulated for each formulation and each measurement was performed in triplicate

SCS transfer to cell membrane

SCS are described to enhance intracellular drug uptake from liposomes into tumor cells. To investigate the behaviour of SCS incorporated in liposomal bilayer when in contact with tumor cell membranes, live cell imaging was performed in SKBR3, breast carcinoma cells, incubated for 2h at 37°C with 20 µM of fluorescently labelled C_6-NBD-GalCer (Fig. 2A) inserted in the liposomal bilayer. SCS from SCS-liposomes in the medium surrounded the tumor cells and were inserted throughout the plasma membrane. Within the plasma membrane SCS tended to accumulate in distinct areas with filopodia or lamellopodia like cellular protrusions (Fig. 2B). Intracellular SCS uptake was minor in comparison to the high levels of lipid in the cell membrane. In cytoplasm SCS fluorescence intensity varied between 0 and 2000 AU. In contrast, lipid fluorescence reached a maximum of intensity of 15000 AU in cell membrane (Fig. 2B). An

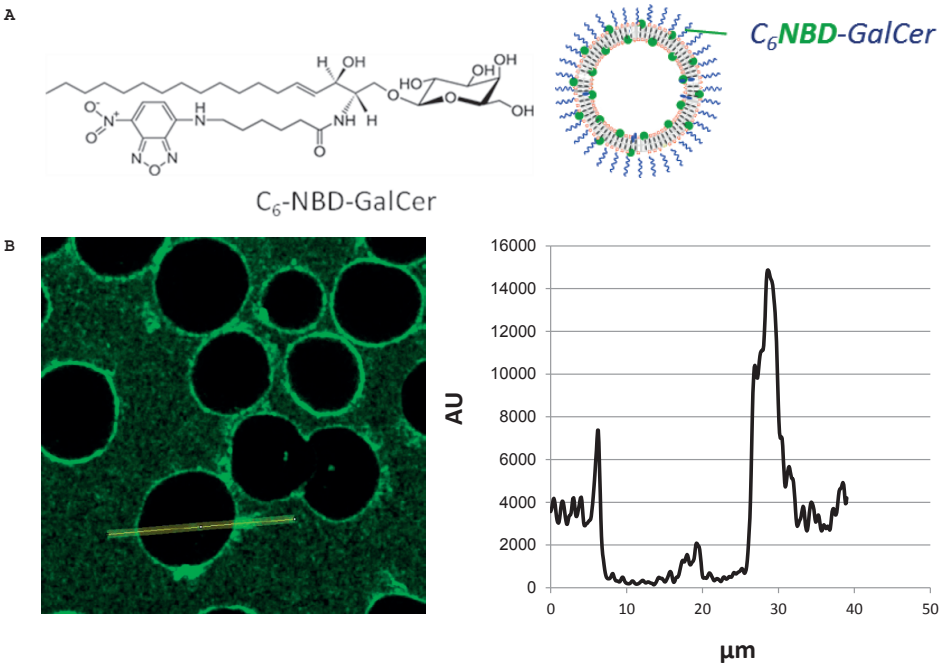

Figure 2 - Live cell confocal microscopy images of SKBR3 human breast carcinoma cells incubated with liposomes containing the SCS marker C_6-NBD-GalCer (green) (A) for 2h at 37°C. Single cell lipid transfer quantification was performed by following the fate of C_6-NBD-GalCer fluorescence which increases significantly in the cell membrane and is minor in cytoplasm, referring to a preferential lipid transfer to cellular membrane with higher accumulation in defined plasma membrane areas (B). Cells were imaged with a 63x plan-apochromat oil (n.a. 1.4) objective lens

illustration of transfer of fluorescently labelled NBD-C6-GalCer from liposomes in suspension (green) to the cell membrane is presented as supplemental movie 1 (Supplemental data - digital version). The massive accumulation of the lipid in cell membrane (red) is observed to occur in irregular structures that surrounded the cell surface. Fluorescence intensity was quantified by Image J by separating two classes of fluorescence intensity (green as low and red as higher intensity) applying a high threshold .

SCS insertion into cell membrane is reversible

To address the question of possible SCS internalization, live cell microscopy was performed. BLM cells were incubated with C_6-NBD-GalCer liposomes and fluorescence was detected using a Zeiss ELYRA PS1 microscope equipped with a LSM 780 scanhead with high sensitivity GAsP detectors. Figure 3 shows ascendant focal

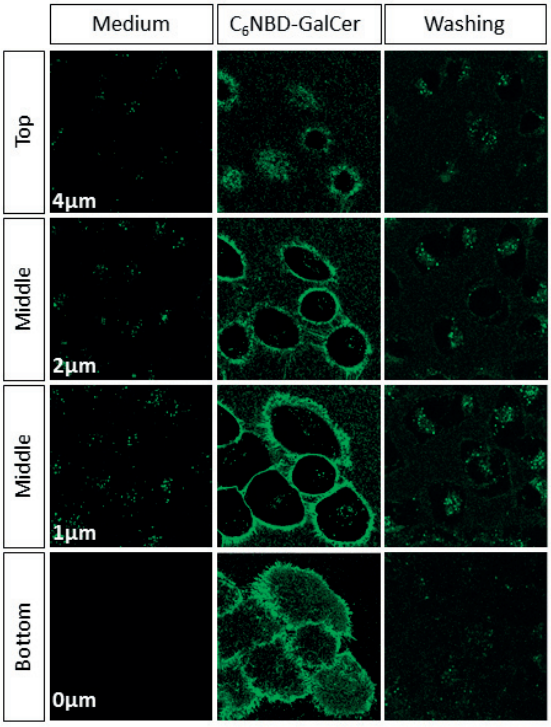

Figure 3 - BLM cells incubated for 2h at 37°C with medium or C6-NBD-GalCer liposomes imaged before and after washing. Cells were imaged with a 63x planapochromat oil (n.a. 1.4) objective lens

planes with a slide interval of 0.4 µm of BLM cells treated with 60 µM fluorescently labelled C6-NBD-GalCer incorporated in liposomes (middle panel) for 2 hours at 37°C showing massive lipid accumulation in the cell membrane with higher incidence at specific areas. Control BLM cells without SCS treatment (left panel) showed some intracellular auto fluorescent signal. Intense washing of SCS-liposome-treated cells with cold-PBS could remove a major part of the SCS from the membrane (right panel) pointing to a reversible membrane interaction in the outer layer of the cell membrane. After washing some SCS fluorescence remained associated with the cells.

Cellular fate of SCS and liposome

To unravel the mechanism of action of SCS as cellular drug uptake enhancers we monitored the intracellular fate of fluorescently labelled liposomes in SKBR3 human breast carcinoma cells in relation to the fluorescent SCS (Fig. 4). Dual labelled liposomes were used

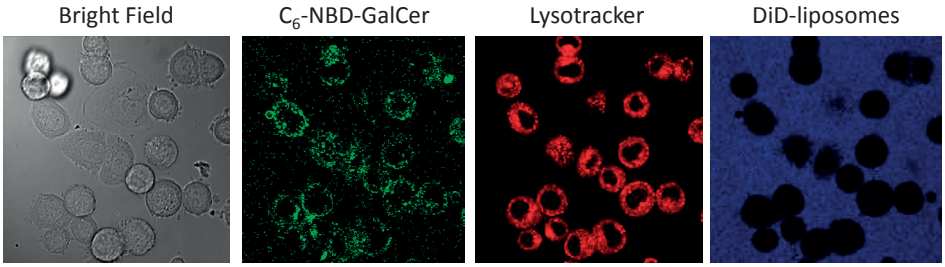

Figure 4 - Live cell confocal microscopy images of SKBR3 human breast carcinoma incubated with liposomes containing the SCS marker C_6-NBD-GalCer (green) and the lipophilic tracer DiD marking the phospholipid bilayer of the liposomes (blue). Colocalization of C_6-NBD-GalCer and lysotracker was performed incubating cells with a red lysotracker for 1h, washed and further incubated with liposomes containing the SCS marker C_6-NBD-GalCer. Cells were imaged with a 63x planapochromat oil (n.a. 1.4) objective lens

containing the blue lipophilic tracer DiD as a stable marker for the liposomal phospholipid bilayer and green fluorescent lipid analogue C_6-NBD-GalCer as a SCS marker. After a 2h incubation at 37°C liposomal nanoparticles (DiD, blue) remained solely outside the cell, whereas SCS (C_6-NBD-GalCer, green) accumulated in the plasma membrane and to some extent intracellularly.

Intracellular colocalization of C_6-NBD-GalCer (green) and lysotracker red, labelling acidic organelles was observed.

SCS transfer is tumor cell specific

The plasma membrane undergoes continuous rearrangements through endo- and exocytosis therefore we studied the fate of C_6-NBD-GalCer in tumor and non tumor cells and possible differences between those cells in handling of the SCS. Liposomes containing the fluorescent SCS C_6NBD-GalCer were used to treat BLM melanoma cells, 3T3 fibroblasts and HUVEC endothelial cells and the lipid fate was followed in living cells for 14 hours (Fig. 5A). Shortly after start of treatment the fluorescent SCS analogue, C_6-NBD-GalCer, accumulated in the plasma membrane of BLM cells. After 1h of incubation fluorescence intensity reached a maximum and remained constant throughout the 14h time span of the experiment. BLM melanoma cells displayed little intracellular fluorescence before liposome treatment but not in the cell membrane. During the 14h incubation intracellular fluorescence increased suggesting lipid internalization and processing. In contrast to BLM tumor cells, 3T3 fibroblasts and HUVEC endothelial cell incubations resulted in lower levels of membrane uptake of C_6-NBD-GalCer during a 14h

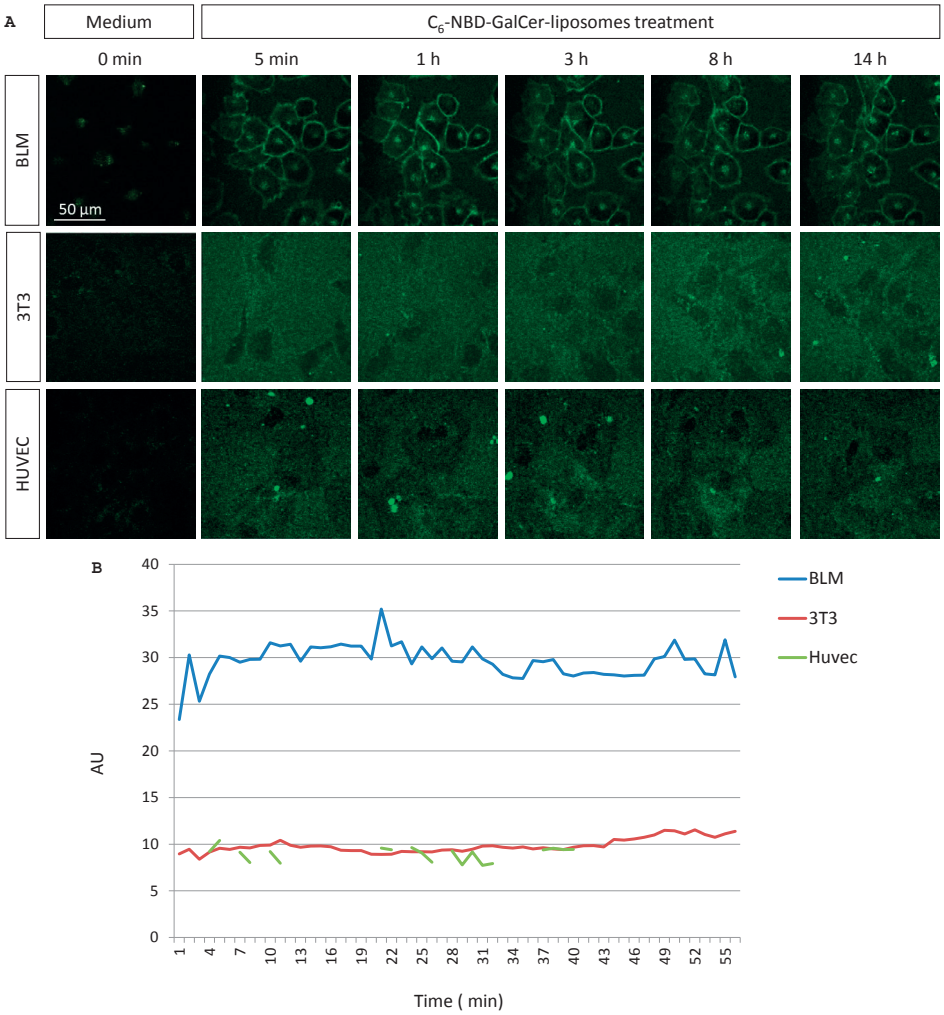

Figure 5 - (A) Time lapse live cell confocal microscopy of BLM melanoma, 3T3 fibroblast and HUVEC endothelial cells before treatment and at different time points after treatment with C_6-NBD-GalCer liposomes for a total of 14h. (B) Intensity of lipid fluorescence was quantified considering mean intensity of cell membrane by Image J. Cells were imaged with a 63x planochromat oil (n.a. 1.4) objective lens

incubation period. For non-tumor cells, C_6-NBD-GalCer fluorescence remained mainly extracellular most likely liposome associated. Quantification of cell-associated fluorescent lipid analogue using Image J software, yielded a 3 fold higher amount of fluorescence from C_6-NBD-GalCer enriched liposomes measured in the cell membrane of BLM melanoma cells in comparison to HUVEC or 3T3 (Fig. 5B). The mean fluorescence intensity of number of cells in the field of view was considered and subtracted for the background fluorescence,

which was the same in all images of all cell lines considered. A mask was made as a tresholded area of a Gaussian blur image and was applied to select the cell membrane of the cells. Mean fluorescence intensities are compared within tumor and non-tumor cell membranes in time.

Native SCS transfer imaged by post incubation click chemistry

The transfer and incorporation of SCS into the membrane of tumor and non-tumor cells was monitored by click chemistry using a clickable C_8-GluCer analogue, as proof of concept for the data obtained with fluorescently C6-NBD-labeled SCS. The extension of the transfer and respective incorporation of the lipid analogue into tumor and non-tumor cells was evaluated based on the fluorescence properties of the azide-labeled fluorophore, which by click chemistry fluorescently labels the cell-associated omega alkyl-SCS lipid analogue.

When imaging omega alkyne-SCS (Cy3 Azide, Fig. 6) after 2h at 37°C, transferred lipid localized into distinct cell compartments accordingly to previous results with fluorescent labelled lipid, C6-NBD-GalCer, after cell washing. Untreated cells were imaged at same conditions as SCS-treated cells and displayed no Cy3-fluorescent staining.

Lipid transfer quantification in tumor and non-tumor cells

In HeLa cells, it was observed by post treatment click chemistry that SCS incorporation into cell membranes is time and concentration dependent. After 2h at 37°C, SCS levels in cell membranes were higher than after 1h, at same initial SCS concentrations. Increasing SCS concentration (in free form) from 10 to 40 μM, increased cell membrane associated SCS levels (Fig. 7A).

Upon treatment of BLM, MDA-MB-231 and 3T3 fibroblast cells with SCS (alkyl-C_8-GluCer) added either in free form (Fig. 7C) or co-inserted in liposomes (Fig. 7D) incorporation of the glycosphingolipids into the cells was quantified by TLC and fluorescence imaging. After lipid extraction, the clickable analogue was subjected to click chemistry reaction and the amount of SCS inserted into the different cells was quantified. As total insertion, the initial concentration of clickable SCS added to the cells was loaded and the fluorescence value obtained was set to

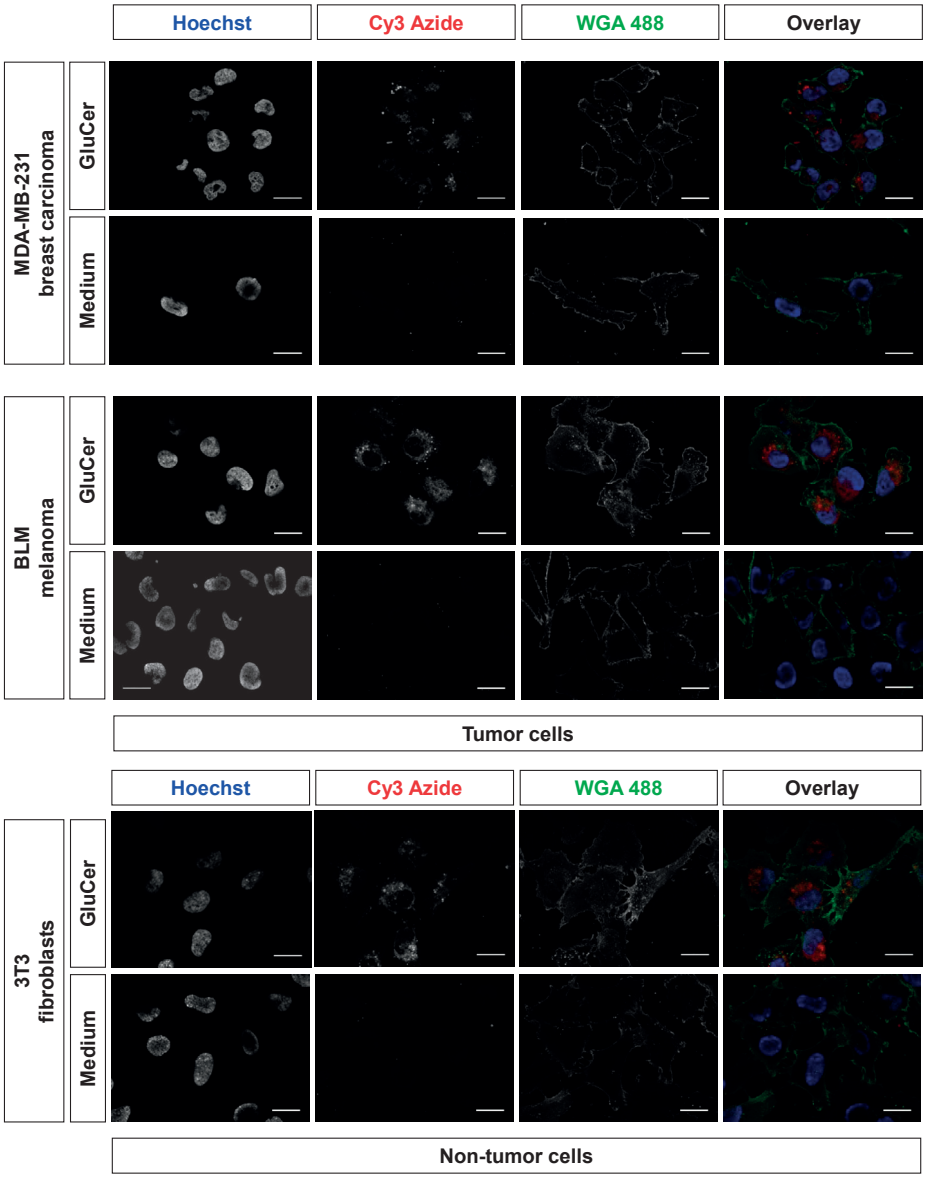

Figure 6 – C_8-GluCer transfer to plasma membrane of tumor cells, BLM, melanoma and MDA-MB-231 breast carcinoma cells and non-tumor cells, 3T3 fibroblasts. (A) Confocal imaging of fluorescently labelled alkyl-C_8-GluCer (red) incorporation into plasma membrane (green). Hoechst staining was performed for nucleus observation (blue)

100%. After normalization, BLM and MDA-MB-231 tumor cells showed higher incorporation of SCS (C_8-GluCer) than non-tumor cells, 3T3 fibroblasts (p= 0.044 and p=0.019, respectively) (Fig. 7B). An illustration of lipid measurement including the peaks of the

A

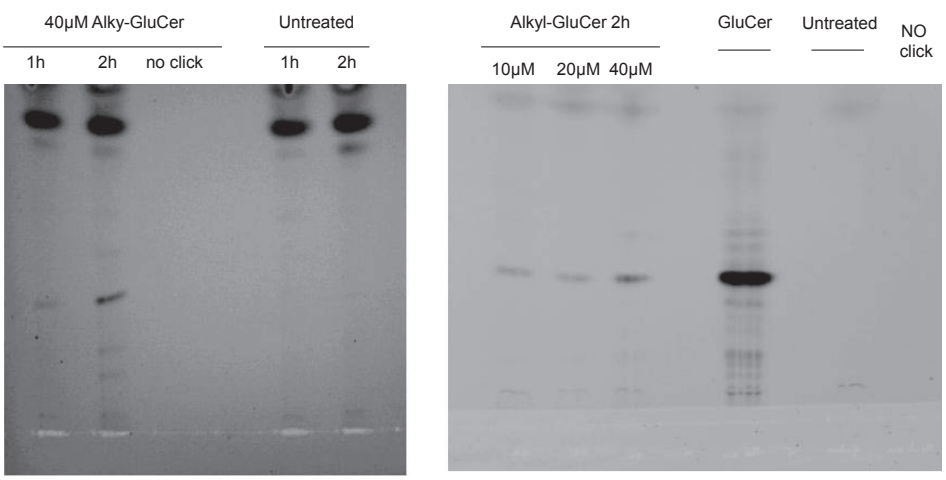

B

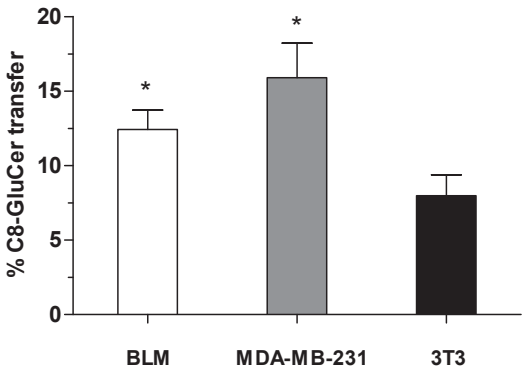

C

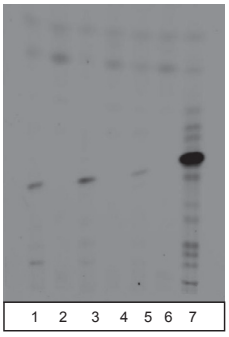

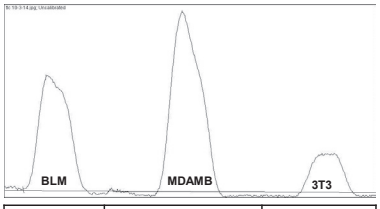

	Area	% Transfer
BLM	25748,844	290,450
MDA-MB	39385,844	444,270
3T3	8865,146	100,000

1. BLM +10μM Alkyl-GluCer 2h
2. BLM untreated
3. MDA-MB +10μM Alkyl-GluCer 2h
4. MDA-MB untreated
5. 3T3 +10μM Alkyl-GluCer 2h
6. 3T3 untreated
7. Control 100% alkyl-GluCer

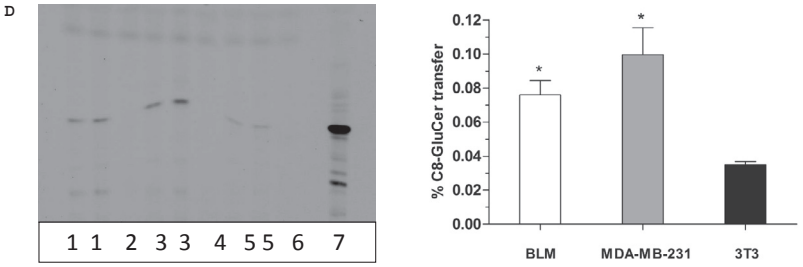

1. BLM +100µM Alkyl GluCer liposomes 2h
2. BLM untreated
3. MDA-MB +100µM Alkyl GluCer liposomes 2h
4. MDA-MB untreated
5. 3T3 +100µM Alkyl GluCer lipososmes 2h
6. 3T3 untreated
7. Control 100% alkylGluCer

Figure 7 - (A) C_8-GluCer lipid analogue insertion is concentration and exposure time dependent. (B) C_8-GluCer lipid analogue insertion into plasma membranes was quantified by click chemistry. Lipid transfer in tumor cells was higher than in non tumor cells ($p<0.05$). (C) C_8-GluCer transfer to plasma membrane was quantified by TLC. (D) Liposome co-inserted C_8-GluCer transfer to plasma membrane was quantified by TLC. Control was set as 100% of lipid transfer in plasma membrane. Six independent experiments were performed. * $p \leq 0.05$ in comparison to 3T3, fibroblasts

covered lipid area in different cell lines and respective TLC is represented in figure 7C.

SCS induce transbilayer redistribution (flip-flop) of pyr-SM in model membranes

Under normal conditions the diffusion of lipids across lipid bilayers is very slow. Here we studied the effect of SCS on transbilayer lipid redistribution by using model membranes. LUV's mimicking plasma membrane like lipid composition were loaded initially with pyr-SM, which inserts in the outer leaflet, [29]. The lipid transbilayer diffusion assay is based on the measurement of the intrinsic properties of the fluorescence pyrene-SM upon redistribution between the inner and outer membrane monolayers. Here pyrSM was used to monitor the transbilayer redistribution of the SM in the membrane induced by SCS (C_8-GluCer or C_8-GalCer). Redistribution of the fluorescent probe from the outer to the inner leaflet leaded to a decrease of the eximer and an increase of the monomer concentrations. This reflects a SM transbilayer distribution from the outer to the inner leaflet caused by addition

of SCS. Ethanol was used as negative control. Addition of SCS to LUV's caused 30% of SM transbilayer redistribution, 3-fold higher than the control (p=0.0109).

Formation of aqueous pores

To investigate whether drug-permeable domains formed by SCS represent physical aqueous pores, model membranes encapsulating hydrophilic low molecular weight compounds were investigated for possible SCS-induced permeability. Membrane passage of hydrophilic ANTS-DPX complexes upon incubation with SCS-liposomes was investigated. These water soluble complexes exist as a non-fluorescent complex when entrapped in the LUV's core. Upon formation of a hydrophilic pore, vesicle efflux occurs, causing dilution of the complex and subsequent ANTS-DPX dissociation, which can be assessed by measuring ANTS fluorescence. 100% leakage of ANTS-DPX was set by total disruption of LUV's in presence of detergent. Incubation of C_8-GluCer liposomes with ANTS-DPX entrapped in LUV's, did not display changes in fluorescence demonstrating that ANTS remained associated to DPX in the vesicle core. As positive control, tetanolysin a cholesterol-binding dependent toxin was used to create pores in the bilayer. Based on these results, transient pore formation induced by SCS is excluded as a possible mechanism used by SCS to boost drug binding and uptake in cells.

Influence of temperature on function of SCS as intracellular drug uptake enhancers

To address the mechanism of SCS as drug uptake enhancers, SCS enriched liposomes containing Dox were used to treat MDA-MB-231 breast carcinoma and BLM melanoma cells. Using the autofluorescent properties of Dox, intracellular drug uptake was followed by confocal microscopy and drug uptake levels of SCS-enriched liposomes were compared to standard liposomes without incorporation of SCS in the liposomal bilayer and free drug. Cellular incubation at 4°C causes a more laterally ordered lipid bilayer and increases cell membrane rigidity [37]. It also inhibits energy dependent drug transport across the cell membrane. Dox was imaged in MDA-MB-231, breast carcinoma or BLM, melanoma cells by live cell confocal microscopy after 2h of incubation at 4°C before and after washing (Fig. 9 left panels). After cold imaging these cells were further incubated

for 2h at 37°C after which imaging before and after washing was performed (Fig. 9 right panels).

No cellular uptake of free Dox was observed in MDA-MB-231 carcinoma and BLM melanoma cells at 4°C. Signal from free Dox is visible as reddish background in the extracellular space. More abundant Dox fluorescence is found associated with MDA-MB-231 and BLM cells incubated with SCS enriched Dox-liposomes (C_8-GalCer-DoxL) at 4°C. Treatment with standard liposomes at 4°C results in hardly detectable intracellular drug levels. In all incubations Dox signal is almost completely lost after washing, indicating that fluorescent signal before washing resulted from membrane-associated drug. After additional incubation at 37°C for 2h (third column) both cell lines showed nuclear uptake of free Dox. Most of Dox signal remains after washing confirming intracellular presence, especially in the nucleus, whereas some cytoplasmic or membrane associated Dox is also removed upon washing. After treatment with SCS-enriched liposomes for 2h at 4°C and 2h at 37°C Dox is found intracellular in the nucleus as well as cytoplasmic and membrane associated. After washing the cytoplasmic/membrane associated drug fraction is almost completely removed from cells. After crossing the cell membrane, intracellular Dox is naturally directed to the nucleus where it exerts its cytotoxic action. At 37°C, when cells were treated with SCS enriched liposomes Dox reached the nucleus where it is retained. For standard liposomes cytoplasmic nuclear Dox uptake is minimal and is mainly cytoplasmic or membrane bound.

DISCUSSION

Our working hypothesis is based on a spontaneous transfer of the SCS from the liposomal bilayer to the cell membrane, causing cell membrane permeability modulation and subsequent enhanced intracellular amphiphilic drug influx, improving therapeutic efficacy of applied cytostatic drug in cancer treatment [15, 16, 18]. Here we investigated the mechanism of action underlying liposomal SCS as cellular drug uptake enhancer.

In this study we were able to proof that upon cellular contact SCS are transferred from the liposomal bilayer to the plasma membrane, most likely into the exoplasmatic leaflet (Fig. 2)

where Dox membrane interaction and transmembrane transport are facilitated [27]. The C6-NBD-GalCer used to demonstrate lipid transfer has an NBD-fluorescent label covalently attached to the SCS lipid analogue in the N-acyl short chain, thereby elongating its truncated chain (Fig. 2A) and possibly interfering with intermolecular interactions and changing the fate of the truncated lipid chain in the cell membrane permeability modulation. Via an omega alkylation of C_8-GluCer it was possible to follow the fate of the lipid without interfering with its original and native structure. Transfer of this C_8-GluCer was demonstrated as well to occur to a higher extent in tumor cells and its cellular accumulation was found concentration dependent (Fig. 6). Although differences exist between the two used tracers, similar transfer behavior was observed. The fluorescently labelled SCS analogue C6-NBD-GalCer present in the liposomal bilayer (Fig. 2A) is transferred and re-distributed throughout the plasma membrane with seemingly increased levels in filopodia or lamellopodia like cellular protrusions (Fig. 2B). Biomembranes are non-equilibrium structures, in which lipid asymmetry is maintained by active transbilayer lipid transport [32, 33]. When lipid transfer occurs in one direction it is naturally compensated by the simultaneous transfer of other lipids in the reciprocal direction so mass conservation in each monolayer, is maintained. The opposite situation, namely the net transfer of mass (lipid molecules), would lead to higher lateral pressure and bilayer collapsing. It is also known that maintenance of membrane asymmetry in the resting state is energy dependent and flip-flop of lipids cannot occur by itself [33]. Transbilayer lipid motion triggered by external agents has been shown only for long chain ceramides [20]. Here however, we have shown a transbilayer lipid movement or flip-flop by external glycosylated short chain ceramides, C_8-GluCer or C_8-GalCer, which induced a pyrene-SM movement from the outer to the inner leaflet in higher extent than short chain ceramides (C6 or C2-ceramide) [20] (Fig. 8). Likely, the increased flip-flop induced by glycosylceramides such as C_8-Glucer and C_8-GalCer is also related to the additional sugar moiety of these SCS, upon incorporation in the outer leaflet.

It has been described that only long N-acyl chain (more than 12 C) ceramides and not N-acyl short chain ceramides, were able to induce formation of stable lipid microdomains [34]. Here, possible

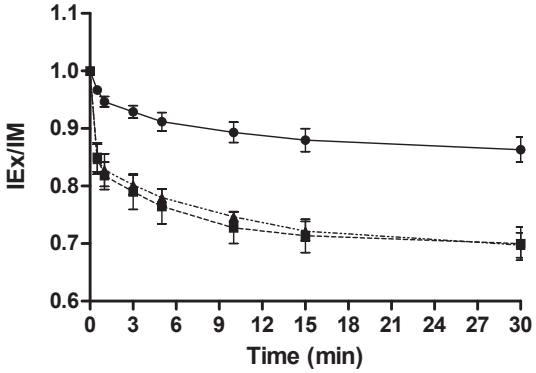

Figure 8 - Transbilayer lipid motion induced by short chain sphingolipids, C_8-GluCer (■) or C_8-GalCer (▲) in LUV (300 mM). Ethanol was used as control (●). Both SCS in free form induced similar flip-flop of pyridine-SM and higher than control group (p=0.0109)

pore domain formation induced by SCS transfer to model membranes was also studied (Fig. 9). Leakage of hydrophilic compounds was however not observed confirming previously reported data by co-workers in cellular studies [14], where it was proved that C6-SM didn't increase membrane permeability of a hydrophilic marker (AF488-hydrazine) or a cytosolic protein (LDH) [15]. Seemingly, SCS induce rearrangement of the cell membrane enhancing intracellular drug uptake by processes that do not include aqueous pore domain formation.

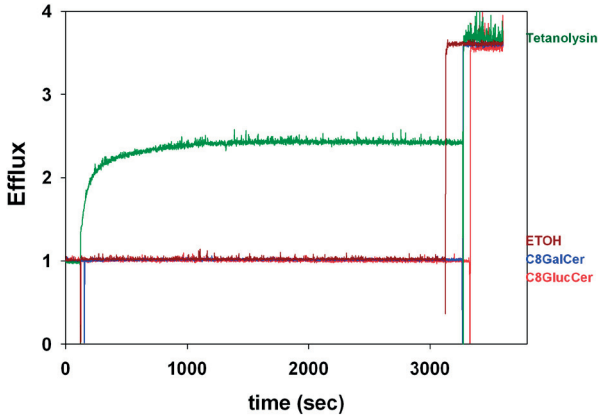

Figure 9 - Time course of ANTS/DPX release. The effect of different SCS on the release of vesicular ANTS/DPX content. 15 µM of C_8-GalCer (blue) or C_8-GluCer (red) were externally added to freshly prepared plasma membrane like LUVs (300 µM) and ANTS/DPX efflux monitored over time. Ethanol (µl) and tetanolysin (10 ng) were used as negative and positive controls, respectively

It was also shown by others that a sugar moiety in the polar head group weakens intermolecular interactions by reducing packing efficiency [35]. In case of glycosylsphingolipids, such as C_8-GluCer and C_8-GalCer containing relatively small polar head groups the increase of molecular order acquired by close packing is unfavorable because it cannot be compensated by release of enough molecules of water from the polar head group hydration shell [35]. Partly, this supports the rearrangement of the plasma membrane structure by the transfer of SCS (Fig. 8) and subsequently increased permeability to drug traversal (Fig. 10). SCS insertion in the cell membrane might lower packing density, promoting Dox insertion and Dox-SCS interaction [17] or enhancing exposure Dox to binding lipids (e.g. PE) in the plasma membrane improving intracellular drug uptake [36].

SCS-plasma membrane transfer was found to be reversible as observed after extensive cell washing (Fig. 3). These findings suggest SCS accumulate to a large extent in the outer leaflet of the PM. Whereas lipid transfer to the plasma membrane occurred substantially this occurred without intracellular uptake of the nanoliposomes (Fig. 4) confirming previous data on enhanced drug uptake by non-fluorescently labelled-SCS enriched liposomes containing Dox in MCF-7, breast carcinoma cell line [18] (*Chapter 2*). Besides a massive transfer to plasma membrane (Fig. 2B) part of the lipid remained associated with the liposomal bilayer. The transfer phenomenon occurs from filled to empty SCS membranes, a concentration gradient that requires only SCS enriched liposome versus plasma membrane contact. Although massive membrane accumulation was observed for prolonged periods (Fig. 3) also intracellular presence of C_6-NBD-GalCer was observed especially after extensive washing, which removed the majority of membrane associated SCS (Fig. 3 and 4). Live cell imaging with NBD-SCS and click chemistry lipid tracking and quantification, in which extensive washing was also applied, on TLC's from isolated cell membranes of tumor and non-tumor cells demonstrated a preferential transfer and incorporation of SCS into tumor cell membranes. This result nicely corresponds to earlier observations showing the drug uptake enhancing properties of SCS and subsequent induction of cytotoxicity which was specific for various tumor cell lines and much less in normal cells [1]. Other groups reported on plasma membrane lipid

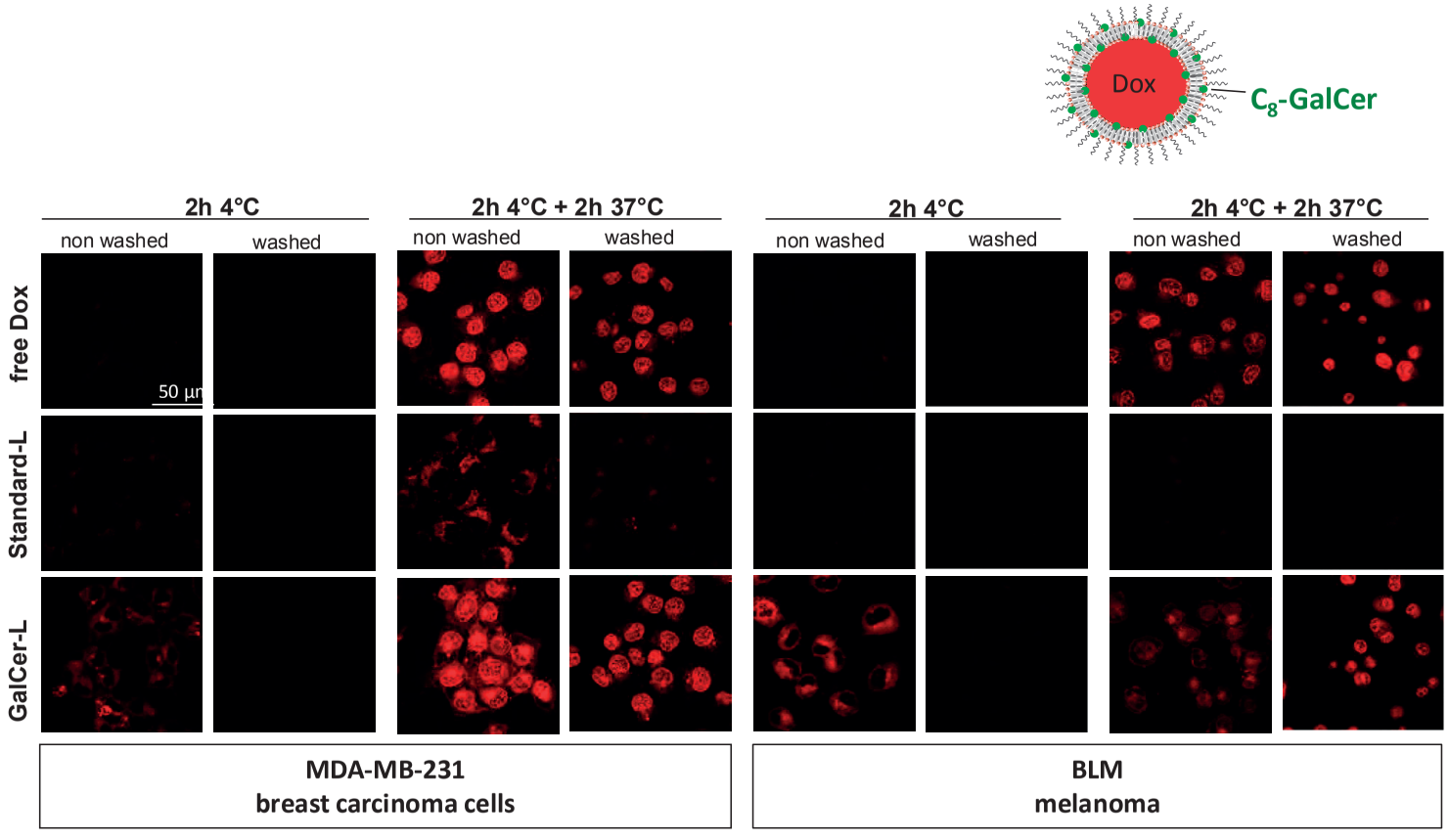

Figure 10 - Dox uptake in MDA-MB-231 breast carcinoma cells and BLM melanoma cells after incubation at 4°C before and after washing and after further incubation at 37°C before and after washing. Red fluorescence represents Dox. Cells were imaged with a 63x planapochromat oil (n.a. 1.4) objective lens

composition differences mainly at the level of phosphatidylcholine (PC), phosphatidylethanolamine (PE), phosphatidylserine, sphingomyelin (SM) and phosphatodylinositol (PI) in tumor and non-tumor cells lipidome [37]. Differences in phospholipid patterns are described to decrease membrane permeability of tumor cells by an increased rigidity [17, 38]. Recently, it has been reported that faster proliferating cells modulate and rearrange their lipidome [39] supporting the differential phospholipid composition between tumor and non-tumor cells. In addition, lower cholesterol levels are described to increase membrane fluidity in tumor cells [17, 38]. The lipidome of tumor cells is also associated to multidrug resistance phenomenon influencing the ability of tumor cells to respond to chemotherapy [37]. Likely the specific cellular lipidome determines the affinity for SCS membrane insertion and subsequently causes enhanced drug uptake specifically in tumor cells. The SCS targeting, preferentially to tumor cell membrane modulating its permeability to drug uptake, constitutes a promising direction to chemotherapy efficacy.

Live cell imaging and co-staining with lysotracker confirmed lysosomal localization of NBD-C6-GC. Likely, SCS associated to lysosomes might be subject to degradation or alternatively be redistributed from there to other organelles [40]. Naturally occurring glycosphingolipids, which almost exclusively reside in the outer membrane leaflet are ultimately delivered to the late endosomal pathway [41]. Nevertheless, we should be cautious in drawing conclusions on the intracellular trafficking as this may be affected to some extent by the NBD fluorophore [42]. The similarity in intracellular localization in distinct cell compartments observed in live cell imaging with NBD-GC and click chemistry-based imaging seems in favor of similar intracellular trafficking behavior, however in the latter assay lysosomal staining could not be performed as fixation procedures are not compatible with lysosomal co-staining.

The process by which Dox normally crosses the plasma membrane involves spontaneous adsorption by insertion of the molecule's hydrophobic anthraquinone into the exoplasmic leaflet of the lipid bilayer, followed by an energetically unfavorable flip-flop of the drugs hydrophilic sugar moiety between the outer and the inner membrane leaflet. At physiological conditions, this flip-

flop is extremely slow with a half-life of 0.7 min [27]. The cellular uptake of free Dox at 4°C (Fig. 10) is therefore virtually impossible for thermodynamic reasons. The marginal cell-associated signal of free Dox at 4°C in figure 10 hence results from membrane associated Dox molecules, but not from uptake of free Dox occurred at 4°C in MDA-MB-231 or BLM tumor cells. Relating the results from figure 4 on absence of liposomal uptake, with figure 10 reveals that Dox fluorescence in figure 10 originates from Dox in the free and not liposomal form, since liposomes are not taken up and remain extracellularly. Membrane associated Dox can easily be washed away, explaining complete loss of fluorescent signal after washing cells treated with free Dox at 4°C. In addition cells treated with Dox in form of SCS enriched liposomes show a more intense signal for membrane associated Dox even at 4°C with transmembrane transport blockage. Washing reveals that Dox is mostly membrane co-associated with SCS. At 4°C the presence of SCS in the liposome membrane greatly enhances Dox-plasma membrane interaction, compared to non-enriched liposomes. This suggests that at 4°C, SCS exert their effect on the outer membrane leaflet. Yet, at 4°C the reduced membrane fluidity leads to stabilization of lipid microdomains, blocking intracellular transport and perhaps slowing down flip-flop process. After additional incubation at 37°C for 2h, of MDA-MB-231 or BLM cells, intracellular uptake of Dox delivered as free drug was comparable to Dox delivered from SCS enriched liposomes, whereas uptake from non-enriched liposomes is marginal. Here, we conclude that SCS exert their effect on the outer membrane leaflet, where they enhance the Dox-membrane influx by a biophysical process and consequently facilitate Dox membrane traversal. By the reversible association of Dox molecules at 4°C and of SCS molecules as observed in figure 3 we may speculate on the molecular association of Dox molecules and SCS at the level of the outer leaflet. This is supported by van Hell who has reported, by modeling experiments, molecular assembly of SCS and Dox when the latter associates to hydrophobic core of the bilayer [17].

In summary, important insights on the mechanism by which SCS enhance drug uptake are described. SCS are able to transfer spontaneously to plasma membrane preferentially in tumor cells modulating plasma membrane permeability to cytostatic drugs, enhancing its influx and efficacy. Yet, membrane-restructuring

effects within the plasma membrane induced by SCS were determined as the driving force for enhanced intracellular drug influx which might ultimately also affect chemotherapy resistance.

AKNOWLEDGMENTS

This work was financed by the Dutch Cancer Society. The authors thank to the OIC for their assistance.

REFERENCES

1. Gabizon A, Shmeeda H, Barenholz Y, *Pharmacokinetics of Pegylated Liposomal Doxorubicin:Review of animal and human studies.* Clin Pharmacokinet. 2003;42(5):419-36.
2. Allen TM, Cullis PR, *Liposomal drug delivery systems: from concept to clinical applications.* Adv Drug Deliv Rev. 2013;65(1):36-48.
3. Koning GA, Krijger GC, *Targeted multifunctional lipid-based nanocarriers for image-guided drug delivery.* Anticancer Agents Med Chem. 2007;7(4):425-40.
4. Gabizon AA, *Pegylated Liposomal Doxorubicin:Metamorphosis of an old drug into a new form of chemotherapy.* Cancer Invest. 2001;19(4): 424-36.
5. O'Brien ME, Wigler N, Inbar M, Rosso R, Grischke E, Santoro A, Catane R, Kieback DG, Tomczak P, Ackland SP, Orlandi F, Mellars L, Alland L, Tendler C; CAELYX Breast Cancer Study Group, *Reduced cardiotoxicity and comparable efficacy in a phase III trial of pegylated liposomal doxorubicin HCl (CAELYX/Doxil®) versus conventional doxorubicin for first-line treatment of metastatic breast cancer.* Ann Oncol. 2004;15(3):440-9.
6. Northfelt DW, Dezube BJ, Thommes JA, Miller BJ, Fischl MA, Friedman-Kien A, Kaplan LD, Du Mond C, Mamelok RD, Henry DH, *Pegylated-liposomal doxorubicin versus doxorubicin, bleomycin, and vincristine in the treatment of AIDS-related Kaposi's sarcoma: results of a randomized phase III clinical trial.* J Clin Oncol. 1998;16(7): 2445-51.
7. Tejada-Berges T, Granai CO, Gordinier M, Gajewski W, *Caelyx/Doxil for the treatment of metastatic ovarian and breast cancer.* Expert Rev Anticancer Ther. 2002;2(2):143-50.
8. Hussein MA, Anderson KC, *Role of liposomal anthracyclines in the treatment of multiple myeloma.* Semin Oncol. 2004;31(6 Suppl 13): 147-60.
9. Alberts DS, Muggia FM, Carmichael J, Winer EP, Jahanzeb M, Venook AP, Skubitz KM, Rivera E, Sparano JA, DiBella NJ, Stewart SJ, Kavanagh JJ, Gabizon AA, *Efficacy and safety of liposomal anthracyclines in phase I/II clinical trials.* Semin Oncol. 2004;31(6 Suppl 13):53-90.
10. Maeda H, Nakamura H, Fang J, *The EPR effect for macromolecular drug delivery to solid tumors: Improvement of tumor uptake, lowering of systemic toxicity, and distinct tumor imaging in vivo.* Adv Drug Deliv Rev. 2013;65(1):71-9.
11. Laginha KM, Verwoert S, Charrois GJ, Allen TM, *Determination of Doxorubicin Levels in Whole Tumor and Tumor Nuclei in Murine Breast Cancer Tumors.* Clin Cancer Res. 2005;11(19 Pt 1):6944-9.
12. Seynhaeve AL, Hoving S, Schipper D, Vermeulen CE, de Wiel-Ambagtsheer Ga, van Tiel ST, Eggermont AM, Ten Hagen TL, *Tumor Necrosis Factor Î± Mediates Homogeneous Distribution of Liposomes in Murine Melanoma that Contributes to a Better Tumor Response.* Cancer Res. 2007;67(19):9455-62.

13. Laginha KM, Moase EH, Yu N, Huang A, Allen TM, *Bioavailability and therapeutic efficacy of HER2 scFv-targeted liposomal doxorubicin in a murine model of HER2-overexpressing breast cancer.* J Drug Target. 2008(7):605-10.
14. Veldman RJ1, Zerp S, van Blitterswijk WJ, Verheij M, *N-hexanoyl-sphingomyelin potentiates in vitro doxorubicin cytotoxicity by enhancing its cellular influx.* Br J Cancer. 2004 ;90(4):917-25.
15. Veldman RJ, Zerp S, van Blitterswijk WJ, Verheij M, *Coformulated N-Octanoyl-glucosylceramide Improves Cellular Delivery and Cytotoxicity of Liposomal Doxorubicin*. Br J Cancer. 2004;90(4): 917-25.
16. van Lummel M, van Blitterswijk WJ, Vink SR, Veldman RJ, van der Valk MA, Schipper D, Dicheva BM, Eggermont AM, ten Hagen TL, Verheij M, Koning GA, *Enriching lipid nanovesicles with short-chain glucosylceramide improves doxorubicin delivery and efficacy in solid tumors.* FASEB J. 2011;25(1):280-9.
17. van Hell AJ, Melo MN, van Blitterswijk WJ, Gueth DM, Braumuller TM, Pedrosa LR, Song JY, Marrink SJ, Koning GA, Jonkers J, Verheij M, *Defined lipid analogues induce transient channels to facilitate drug-membrane traversal and circumvent cancer therapy resistance.* Sci Rep. 2013;3:1949.
18. Pedrosa LR, van Hell A, Süss R, van Blitterswijk WJ, Seynhaeve AL, van Cappellen WA, Eggermont AM, ten Hagen TL, Verheij M, Koning GA, *Improving Intracellular Doxorubicin Delivery Through Nanoliposomes Equipped with Selective Tumor Cell Membrane Permeabilizing Short-Chain Sphingolipids.* Pharm Res. 2013;30(7):1883-95.
19. Contreras FX, Villar AV, Alonso A, Kolesnick RN, Goñi FM, *Sphingomyelinase Activity Causes Transbilayer Lipid Translocation in Model and Cell Membranes.* J Biol Chem. 2003;278(39):37169-74.
20. Contreras FX, Basañez G, Alonso A, Herrmann A, Goñi FM, *Asymmetric Addition of Ceramides but not Dihydroceramides Promotes Transbilayer (Flip-Flop) Lipid Motion in Membranes.* Biophys J. 2005;88(1):348-59.
21. Siskind LJ, Colombini M, *The lipids C2- and C16- Ceramide Form Large Stable Channels Implications for apoptosis.* J Biol Chem. 2000; 275(49):38640-4.
22. Samanta S1, Stiban J, Maugel TK, Colombini M, *Visualization of ceramide channels by transmission electron microscopy.* Biochim Biophys Acta. 2011;1808(4):1196-201.
23. Sot J, Bagatolli LA, Goñi FM, Alonso A, *Detergent-resistant, ceramide-enriched domains in sphingomyelin/ceramide bilayers.* Biophys J. 2006;90(3):903-14.
24. Siskind LJ, Fluss S, Bui M, Colombini M, *Sphingosine Forms Channels in Membranes That Differ Greatly from Those Formed by Ceramide.* J Bioenerg Biomembr. 2005;37(4):227-36.
25. Elrick MJ, Fluss S, Colombini M, *Sphingosine, a product of ceramide hydrolysis, influences the formation of ceramide channels.* Biophys J. 2006;91(5):1749-56
26. Goñi FM, Alonso A., *Effects of ceramide and other simple sphingolipids on membrane lateral structure.* Biochim Biophys Acta. 2009;1788(1):169-77

27. Regev R, Yeheskely-Hayon D, Katzir H, Eytan GD, *Transport of anthracyclines and mitoxantrone across membranes by a flip-flop mechanism.* Biochem Pharmacol. 2005;70(1):161-9.
28. Thiele C, Papan C, Hoelper D, Kusserow K, Gaebler A, Schoene M, Piotrowitz K, Lohmann D, Spandl J, Stevanovic A, Shevchenko A, Kuerschner L, *Tracing fatty acid metabolism by click chemistry.* ACS Chem Biol. 2012;7(12):2004-11.
29. Temmerman K, Nickel W, *A novel flow cytometric assay to quantify interactions between proteins and membrane lipids.* J Lipid Res. 2009;50(6):1245-54.
30. Müller P, Schiller S, Wieprecht T, Dathe M, Herrmann A, *Continuous measurement of rapid transbilayer movement of a pyrene-labeled phospholipid analogue.* Chem Phys Lipids. 2000;106(1):89-99.
31. Ellens H, Bentz J, Szoka FC, *H+- and Ca2+-induced fusion and destabilization of liposomes.* Biochemistry. 1985;24(13):3099-106.
32. Daleke DL, *Regulation of transbilayer plasma membrane phospholipid asymmetry.* J Lipid Res. 2003;44(2):233-42.
33. Pomorski T, Hrafnsdóttir S, Devaux PF, van Meer G, *Lipid distribution and transport across cellular membranes.* Semin Cell Dev Biol. 2001;12(2):139-48.
34. Megha, Sawatzki P, Kolter T, Bittman R, London E., *Effect of ceramide N-acyl chain and polar headgroup structure on the properties of ordered lipid domains (lipid rafts).* Biochim Biophys Acta. 2007;1768(9):2205-12.
35. Maggio B, Fanani ML, Rosetti CM, Wilke N, *Biophysics of sphingolipids II. Glycosphingolipids: An assortment of multiple structural information transducers at the membrane surface.* Biochim Biophys Acta. 2006 ;1758(12):1922-44.
36. Speelmans G, Staffhorst RWHM, de Kruijff B., *The anionic phospholipid-mediated membrane interaction of the anti-cancer drug doxorubicin is enhanced by phosphatidylethanolamine compared to other zwitterionic phospholipids.* Biochemistry. 1997;36(28):8657-62.
37. Peetla C, Vijayaraghavalu S, Labhasetwar V, *Biophysics of cell membrane lipids in cancer drug resistance: Implications for drug transport and drug delivery with nanoparticles.* Adv Drug Deliv Rev. 2013;65(13-14):1686-98.
38. Hendrich AB, Michalak K., *Lipids as a target for drugs modulating multidrug resistance of cancer cells.* Curr Drug Targets. 2003;4(1): 23-30.
39. Atilla-Gokcumen GE, Muro E, Relat-Goberna J, Sasse S, Bedigian A, Coughlin ML, Garcia-Manyes S, Eggert US, *Dividing cells regulate their lipid composition and localization.* Cell. 2014;156(3):428-39.
40. Kolter T, Sandhoff K, *Lysosomal degradation of membrane lipids.* FEBS Lett. 2010;584(9):1700-12.
41. Hannun YA, Obeid LM., *Principles of bioactive lipid signalling: lessons from sphingolipids.* Nat Rev Mol Cell Biol. 2008;9(2):139-50.
42. Mazères S, Schram V, Tocanne JF, Lopez A, *7-nitrobenz-2-oxa-1,3-diazole-4-yl-labeled phospholipids in lipid membranes: differences in fluorescence behavior.* Biophys J. 1996 Jul;71(1):327-35.

CHAPTER 6

General Discussion

DISCUSSION

The aim of the research described in this thesis was to improve chemotherapy bioavailability to tumor cells by applying a novel drug delivery strategy that uses short chain sphingolipids (SCS) co-formulated with liposome-encapsulated drugs to promote increased cell-membrane drug passage.

The ability of liposomes to entrap and carry cytotoxic compounds in their hydrophilic core through the blood stream until further accumulation at the target tissue – the tumor, is well described and makes liposomal drug delivery a promising strategy in cancer therapy [1, 2]. Yet a main challenge remains to render liposome-entrapped drugs bioavailable. Numerous attempts have been made to overcome the limited intracellular accumulation of liposome-encapsulated drug in tumor cells by application of different strategies, merely focusing on inducing drug release from liposomes at the tumor site using local or remote triggers as referred to in the introduction [1]. However, upon tumor accumulation and possible release from the nanocarrier, intracellular drug delivery still requires the passage of one final hurdle, the tumor cell membrane. The work described in this thesis has been aimed at the development and application of strategies targeting the tumor cell membrane using SCS making this barrier more permeable to chemotherapeutic drugs delivered by liposomal vehicles. The amphiphilic chemotherapeutic agents, doxorubicin (Dox) and mitoxantrone (MTO) have been entrapped in novel 85 nm SCS-enriched liposomes for the treatment of solid tumors. This approach combines the benefits of reduced toxicity and improved tumor accumulation of drugs through nanoliposomal encapsulation with enhanced intracellular drug delivery by SCS-mediated tumor cell membrane permeabilization.

SCS-enriched liposomes containing amphiphilic drugs

This thesis covers the application of SCS-liposomal delivery of two main chemotherapeutic drugs: Dox and MTO. Both are amphiphilic drugs that combine hydrophilic characteristics allowing for solubility in aqueous solutions with hydrophobic characteristics enabling some partitioning into biomembranes. Especially at the latter level, SCS are expected to influence drug behavior, promoting delivery across these biomembranes.

In previous studies an array of fluorescent chemotherapeutic drugs was tested for SCS enhanced drug uptake properties using N-hexanoyl-sphingomyelin (C6-SM), a synthetic SCS. A clear correlation was found between the octanol-water partitioning behavior, reflecting compound lipophilicity, and SCS-mediated drug uptake enhancement, which appeared to be optimal for amphiphilic drugs, such as Dox, epirubicin, topotecan, camptothecin and daunarubicin, but was not observed for hydrophilic or lipophilic compounds [3]. Conveniently, many amphiphilic compounds are optimally suited for liposomal drug delivery as they can be loaded remotely into preformed liposomes by crossing the phospholipid liposomal bilayer and subsequent trapping in the hydrophilic core of the nanocarrier.

SCS-enriched liposomes containing Dox

PEGylated SCS-enriched liposomes containing Dox were firstly described by Veldman et al. using *N*-octanoyl-glucosylceramide (C_8-GluCer) inserted in a liposomal bilayer [4]. Although C_8-GluCer and C6-SM in free form had similar Dox uptake enhancing properties [3], C_8-GluCer was chosen for liposomal formulation as C_6-SM in free form under free serum conditions significantly affected cell membrane integrity, as demonstrated by a dose-dependent leakage of the cytosolic enzyme lactate dehydrogenase (LDH) into the extracellular medium. C_8-GluCer did not induce this phenomenon up to concentrations as high as 100 µM [4].

C_8-GluCer-enriched liposomes were prepared by lipid film hydration and extrusion and subsequent remote loading using an ammonium sulphate method [5]. Initially, mixtures of DPPC, cholesterol, PEG_{2000}-DSPE, and C_8-GluCer were prepared for liposomal formulation [4]. However, at a later stage and also in this thesis, lipid mixtures for C_8-GluCer-enriched liposomes were made similar to Doxil or Caelyx using HSPC, cholesterol, and PEG_{2000}-DSPE at a molar ratio of 1.85:1:0.15 to which an optimal amount of 10 mol% C_8-GluCer was added [6]. Although formulations were optimal regarding *in vitro* efficacy and also exerted improved anti-tumor activity *in vivo* [6], further pharmaceutical optimization of the formulation and preparation process was needed and is described in *Chapter 2* of this thesis. Optimization and detailed characterization regarding drug loading, liposome size, pdi, drug entrapment efficiency, morphology and stability was performed, all representing important

criteria for translation of this formulation towards future clinical application. C_8-GluCer-Dox-liposome formulations with efficient drug loading and high stability under physiological and storage conditions were achieved. Additionally different synthetic glycosphingolipids, *N*-octanoyl-galactosylceramide (C_8-GalCer) and *N*-octanoyl-lactosylceramide (C_8-LacCer), that in free form also displayed strong Dox uptake enhancing properties [3], were inserted in the liposomal bilayer for liposomal Dox delivery. In liposomal form, C_8-GalCer provided drug uptake enhancing properties for Dox similar to C_8-GluCer enriched-liposomes at the same optimal 10 mol% of incorporated lipid analog, high loading efficiency and optimal physicochemical characteristics such as size <100 nm and stability. Although C_8-LacCer-enriched liposomes were successfully prepared, sufficient drug loading was not achieved. Likely, the more complex sugar moiety of C_8-LacCer in comparison to C_8-GluCer or C_8-GalCer interfered with the liposomal membrane preventing a stable transmembrane ammonium sulfate gradient for efficient Dox loading. Successful loading of LacCer liposomes will require alternative drug loading methods, which were not employed in this thesis.

With respect to the optimal amount of SCS incorporated in the liposomal bilayer a saturation in drug uptake enhancement was observed upon cellular treatment with higher quantities of liposomal C_8-GluCer [6] and C_8-GalCer (*Chapter 2*). In addition, liposomal formulations with lower Dox:Phospholipid (Dox:PL) mass ratios, thus carrying more SCS molecules per Dox molecule, did not induce additional cytotoxicity. This correlates well with the finding that cytotoxicity is related to Dox treatment and not to the SCS toxicity, which was found upon treating cells with free lipids [3] or with empty SCS-liposomes (*Chapter 4*). Upon Dox loading, deformation of liposomes from round to a more rod-shaped morphology was observed and appeared more pronounced for SCS (C_8-GluCer or C_8-GalCer) formulations than standard Dox-liposomes. Deformation to rod-shaped morphology has been described upon Dox-loading [7] and reflects the high amount of loaded Dox in individual liposomes. Dox is able to self-stack into fibers through hydrophobic interactions, which are bridged by the sulphate anions [8], inducing high levels of intraliposomal drug, which may deform the liposomes to rod-shaped structures (*Chapter 2*). The seemingly increased deformation

of SCS-Dox-liposomes may be caused by increased loading efficiency of SCS-liposomes compared to standard liposomes (table 2, *Chapter 2*) as well as by an increase in liposomal membrane elasticity. Nonetheless, SCS-enriched Dox-liposomes were highly stable and size and pdi were not affected by SCS incorporation.

SCS-enriched liposomes containing MTO

MTO, an anthracenedion is a synthetic chemotherapeutic similar to anthracyclines, designed to cause less gastrointestinal toxicity, cardiotoxicity and alopecia at equally myelosuppressive doses [9]. Yet, clinical studies also indicate significant remaining toxicity of MTO-based chemotherapy [10-12], which may be circumvented by liposomal encapsulation.

Several liposomal formulations containing MTO have been described [13-17], but clinical development has been limited to one study, which involved a short-circulating formulation [18]. To broaden the application of the SCS-liposomal drug delivery and to combine reduced toxicity with improved delivery of MTO, we set out to formulate MTO in SCS-liposomes. Similar to previously described Dox-liposomes, a mixture of HSPC, cholesterol, and PEG_{2000}-DSPE at a molar ratio of 1.85:1:0.15 composed the liposomal bilayer. For SCS-enriched liposomes, 10 mol% of the lipid analogue C_8-GluCer or C_8-GalCer was added. In this thesis (*Chapter 3*), the liposomal MTO loading method was optimized using a transmembrane ammonium sulphate gradient reaching drug loading efficiency higher than 90%. A drug to phospholipid (D:PL) mass ratio of 0.07, slightly lower than what is described in literature for liposomes containing MTO [16], was found to provide optimal size, a loading efficiency above 90% and an optimal stability profile during long term storage and at physiological conditions (37°C in presence of serum). Co-incorporation of SCS improved MTO entrapment in the liposomal core in comparison to non-enriched (standard) liposomes. Also the stability profile in serum of SCS-MTO-liposomes was slightly improved compared to standard liposomes. The exposed hydroxyl groups of the sugar moiety of the hydrophilic SCS head group may promote MTO interaction through hydrogen bonding thereby increasing loading efficiency. In addition, the low level of MTO release, which is only observed in the first minutes upon exposure to serum, may reflect release of liposomal bilayer associated MTO (*Chapter*

3). On the other hand, standard liposomes showed a slow, but continuous drug release, likely from the aqueous core. In contrast to SCS-enriched Dox-liposomes morphology of both standard and SCS-enriched-MTO-liposomes was similar displaying a round shape with an intraliposomal drug precipitate. Apparently, MTO forms an intraliposomal crystal with different characteristics than Dox. While MTO associates to sulphate anions by single NH-groups, Dox associates by double NH-groups in addition to a self-structured association. In addition, the higher D:PL ratios obtained for Dox liposomes compared to MTO-liposomes may also affect liposomal deformation. An optimized liposomal formulation of standard and SCS (C_8-GluCer or C_8-GalCer)-enriched MTO-loaded liposomes was developed that - from a pharmaceutical point of view - fulfilled all criteria to undergo *in vitro* and *in vivo* evaluation.

SCS improve liposomal drug bioavailability: *in vitro* and *in vivo*

A higher drug cytotoxicity *in vitro* was explicitly seen for C_8-GluCer and C_8-GalCer enriched-liposomes loaded with Dox in BLM, Mel 57 melanoma, MCF-7 and SKBR3 breast carcinoma, ASPC-1 and Panc-1 pancreatic carcinoma cell lines of human origin (*Chapter 2*) as well as for MTO in MCF-7 and SKBR3 breast carcinoma cell lines (*Chapter 3*), in comparison to standard liposomes. This paramount effect was correlated to an enhanced amount of drug able to reach the intracellular compartment (*Chapter 2* and *3*). Studies in this thesis demonstrate that C_8-GluCer or C_8-GalCer by itself is innocuous to cells, as empty SCS-liposomes did not cause tumor cell cytotoxicity (*Chapter 2*). In our formulations the antitumor activity is merely related to co-formulated MTO or Dox. This contrasts with reports on C2 and C6-ceramides co-inserted in nanoliposomes that displayed cytotoxicity by itself and a synergistic effect with co-administrated drugs on tumor growth [19, 20]. Additionally, it was previously shown by co-workers that C6-ceramide did not enhance drug uptake [3], proving that C_8-GluCer or C_8-GalCer differentially potentiate chemotherapy as compared to short chain ceramides. The latter are toxic by themselves as was also found for C6-SM [3]. On the other hand, C_8-GluCer or C_8-GalCer remain largely ineffective by themselves, but are able to strongly potentiate amphiphilic drugs such as Dox and MTO. Apparently, the

sugar moiety on SCS molecular structure plays an important role in the mechanism of action regarding drug uptake enhancing properties and in terms of toxicity.

Remarkably, SCS drug uptake enhancing effect appeared to be tumor cell specific. In non-tumor cells such as HUVEC, endothelial cells and 3T3, fibroblasts SCS were not able to induce intracellular drug influx to the same extent as in tumor cells and induced only limited toxicity. In addition, different tumor cell types responded differently to C_8-GluCer and C_8-GalCer enriched drug-liposomes, outlining a more subtle cell type specificity for SCS-enhancing drug uptake properties (*Chapter 2 and 3*). *In vivo* studies also indicated tumor–selectivity for the drug uptake enhancing properties of SCS. Previous studies described that C_8-GluCer-enriched Dox-liposomes displayed an anti-tumor activity superior to standard liposomes in a human A431 squamous cell carcinoma xenograft mouse model [6] and spontaneous invasive lobular carcinoma [21] confirming the improved intratumoral drug bioavailability induced by the presence of the short chain lipid analogue. Although tumor micro environmental and other tumor pathophysiological differences between these models cannot be excluded in their effect on therapeutic outcome, the existence of a possible tumor type specificity for the improved efficacy of Dox in SCS-liposomes may also play a role [22, 23] as we also found *in vitro* (*Chapter 2*). However, when considering the drug pharmacokinetic profile of SCS-enriched liposomes [21], i.e. their faster clearance from circulation lowering chances of intratumoral accumulation, it remains remarkable that SCS-Dox-liposomes achieved improved therapeutic outcome compared to standard liposomes and strongly supports the idea that SCS contributed to improve drug bioavailability [6,21]. Remarkably, similar results were obtained in a MDA-MB-231 breast carcinoma tumor model treated with C_8-GluCer enriched MTO-liposomes, which were more effective than standard MTO-liposomes (*Chapter 4*). In that study C_8-GalCer-enriched MTO-liposomes had similar therapeutic activity as standard liposomes. These findings support *in vitro* observations that different SCS differently affected drug uptake in the same cell type (cell type selectivity). In addition we hypothesize that responses of certain SCS also preferentially depend on the chemotherapeutic compound itself and that optimal SCS – drug combinations may exist for various tumor cell types. At this point additional studies

are required to further understand the SCS working mechanism and especially how cell type selectivity plays a role in optimal SCS drug uptake enhancing properties. High throughput screenings of different SCS in combination with different drugs and cell types are required to further substantiate such suggestions and identify ideal SCS - drug combinations.

Liposomal drug delivery *in vivo* is complex due to the presence of various tumor physiological barriers and multiple cell types within a tumor [23]. For example, tumor vasculature providing access of the circulating liposomes to the tumor tissue is very heterogeneous and the permeability of a specific tumor vessel does not only depend on perfusion of the vessel, but also on the intrinsic profile of the endothelial lining and the surrounding microenvironment [22]. Tumor tissue, in addition to tumor cells, is composed of endothelial and stromal cells, which may also take up the liposomes and/or drug. The role of tumor-associated macrophages (TAM) in drug release from liposomes is still under debate (*Chapter 1, 3*) [24-26]. The results presented in this thesis, do not indicate a major role of TAM in liposomal MTO delivery, nor showed major differences in tumor drug delivery patterns between standard and SCS-enriched liposomes (*Chapter 3*). Intravital microscopic imaging on intratumoral MTO accumulation in the MDA-MB-231 breast carcinoma tumor model confirmed the potential of liposomal SCS to enhance intratumoral MTO levels. MTO was found to be associated with both tumor cells and cells lining tumor-vasculature within a few hours post treatment. Standard MTO-liposomes were not able to deliver visible levels of bioavailable drug within the same time-frame, confirming improvement of bioavailability (*Chapter 4*). The observation of MTO delivery to tumor vasculature by SCS-enriched liposomes, but not standard liposomes (Fig.4B, *Chapter 5*), matches with previous work on SCS-Dox-liposomes by *van Lummel et al.* underlining the potential of dual targeted drug delivery to tumors using SCS [6].

Co-formulation with SCS markedly affected drug pharmacokinetics of both MTO and Dox. C_8-GluCer and C_8-GalCer increase the clearance rate of MTO (*Chapter 4*) and Dox [21] lowering circulating drug levels and the plasma concentration-time AUC. An increased volume of distribution was observed for SCS enriched-liposomes in comparison to standard liposomes (table 2, *Chapter 4*) which might

be related to a faster nanoparticle clearance or to a premature drug leakage from liposomes. The latter seems unlikely in view of the high stability of SCS-MTO-liposomes observed in serum exposure studies (Fig. 2, *Chapter 3*). On this topic, further studies on particle, drug and SCS (C_8-GluCer or C_8-GalCer) pharmacokinetics are pivotal to understand *in vivo* SCS-liposome behaviour. MTO fluorescence visualized by intravital microscopy in a MDA-MB-231 breast carcinoma tumor model reached its maximum at around 4h after treatment while intratumoral bioavailable drug levels were still minor for standard liposomes 24h after treatment (Fig. 4, *Chapter 4*). Unfortunately quantifying MTO levels in the tumor turned out to be unreliable and unsuccessful thus far (*Chapter 4*). MTO accumulation in the tumor was determined by HPLC and MS after extraction from homogenized cellular material using various extraction media such as methanol-acetonitrile or diethyl ether dichloromethane. Only very low levels of MTO were measured, which was likely due to incomplete extraction. Similar *in vitro* studies on MTO cellular extraction confirmed incomplete extraction from especially tumor cell nuclei, which remained visibly blue after the procedure. The difficulty of MTO extraction is explained by the strong affinity of MTO to chromatine, DNA and histone proteins [27]. MTO-chromatin complexes result in very compact structures that prevent quantitative MTO extraction. MTO-chromatin interactions were proven to be stronger than Dox-chromatin interaction. The latter binds to less condensed structure of chromatin having more affinity to DNA, whereas in case of MTO the affinity of drug to chromatin is higher than to DNA [27].

The *in vivo* fate of the SCS has not yet been investigated. It has been described that C6-ceramide has different and independent pharmacokinetics from the respective liposomal drug [28], suggesting that such short chain lipids may exchange to cell membranes and serum proteins upon systemic administration [20]. However, a PK study for C_8-GluCer or C_8-GalCer is required to provide evidence. Such lipid shedding would imply liposomal membrane disturbance and promote drug leakage, and seems unlikely for SCS enriched-liposomes, which had a high stability profile in presence of serum (*Chapter 3*).

SCS mechanism of action

Our working hypothesis on the mechanism of action of SCS mediated drug uptake enhancement is based on a spontaneous transfer of the liposomal bilayer inserted SCS to the cell membrane, modulating cell membrane permeability and enhancing intracellular influx of amphiphilic drugs, as well as their therapeutic effect on tumor cells [3, 4, 6].

Upon cellular contact SCS are transferred from the liposomal bilayer to the plasma membrane, most likely the exoplasmatic leaflet (*Chapter 2*, *3*, *5*). The fluorescence-tagged lipid analogue is transferred to and re-distributed throughout the plasma membrane displaying specific defined areas with more intense lipid accumulation, which may resemble specific microdomains with higher permeability to drugs. However, the exact nature of the structures formed in the outer leaflet of plasma membrane by the accumulation of SCS, remains unclear. In this thesis it was proven that SCS-plasma membrane association is independent on liposomal cellular uptake and based on a biophysical process related to a weak intermolecular SCS bonding, which was reversible by washing (*Chapter 5*). Additionally, quantifying the SCS transferred to the cell membrane by click chemistry and thin layer chromatography (TLC) demonstrated a concentration and time dependency with higher cell-associated lipid analogue concentrations observed with increasing time and lipid concentration (Fig. 7, *Chapter 5*). Yet, to render more evidence for SCS membrane microdomains different super-resolution imaging techniques were applied. These are structured-illumination microscopy (SIM) described and able to resolve a focal area to 50 nm in the lateral dimension [29], photoactivated localization microscopy (PALM) combined with total internal resolution microscopy (TIRF) described as ideal to visualize single molecule fluorescence near the plasma membrane [30, 31] and scanning electron microscopy (SEM) which can achieve resolutions higher than 1 nm [32]. Unfortunately several setbacks were encountered in these studies. During SIM imaging the sample was illuminated on large scale with patterned laser light, which required a fluorophore with good quantum yield and a high bleaching resistance. Here the applied fluorophore, C6-NBD-GalCer was bleached rapidly. For PALM and TIRF analysis, the photostability of C6-NBD-GalCer turned out to be too low to allow

super resolved single molecular imaging. Finally for SEM, cells needed to be fixed and dehydrated hampering localization of NBD-C6-GalCer fluorescence drastically. Furthermore, the fluorescent NBD-C6-GalCer label requires optimization for successful application in super-resolution microscopic techniques.

Previously reported insights on the mechanism Dox uptake enhancing properties of SCS in model membranes showed to be independent on membrane proteins, but closely correlated to membrane lipidic structure [21]. In addition, the SCS effect was associated to Dox insertion and translocation in the membrane. In the bilayer's hydrophobic core of the membrane the SCS and Dox self-assemble into a temporary nano-sized channel. At the end, SCS were recycled to the cell membrane surface to sequester new Dox molecules to transverse the membrane [21]. In absence of Dox, this phenomenon did not occur [21].

It is well described that ceramides in bilayers are able to induce membrane permeabilization, transbilayer lipid movements (flip-flop) and transition to nonlamellar phases [33]. For glycosphingolipids the sugar moiety in the polar head group is described to weaken intermolecular bilayer interactions with membrane phospholipids reducing membrane packing efficiency since a considerable amount of water can associate to its polar head group affecting molecular packing areas and surface compressibility [34]. Thus the membrane micropolarity would increase by the presence of glycosphingolipids in comparison to pure phospholipid membrane composition. However, it is also described that for more complex glycosphingolipids the order of their molecular structure might be increased by a compressibility molecular factor releasing the water in favour of the system's entropy and thus membrane packing. In case of glycosphingolipids containing relative small polar head groups, such as C_8-GluCer and C_8-GalCer the increase in molecular order acquired by close packing with phospholipids in the membrane is thermodynamically unfavourable because it cannot be compensated by release of enough water molecules from the polar head group hydration shell translating into a different phase state [34].

In parallel, transbilayer lipid movement of pyrene labelled-phospholipid analogues induced by external agents has been shown for C6 and C2 ceramides [36]. Here it was shown that a transbilayer lipid movement or flip-flop of pyrene-SM from the outer to the inner

membrane leaflet of plasma membrane mimicking vesicles could be induced by addition of C_8-GluCer or C_8-GalCer in free to a level that was 3-fold higher than short chain ceramides (C6 or C2-ceramide) (*Chapter 5*). Glycosphingolipids such as C_8-GluCer and C_8-GalCer thus cause significant membrane rearrangements upon insertion in the outer leaflet as evidenced by the induction of flip-flop of phospholipids. Partly, this supports the rearrangement of the plasma membrane structure by the transfer and assembling of SCS in domains. Again, the sugar moiety of SCS seems to provide important differences between SCS and short chain ceramides in their membrane rearrangement capacity. This phenomenon may be correlated to the formation of specific microdomains in the cell membrane where drug membrane interaction and transmembrane transport is facilitated as proved by modelling [22]. Tumor cell specificity is described for the drug uptake enhancing properties of SCS (*Chapter 2* and *3*). This was proven to correlate with a preferential SCS transfer to tumor cells compared to non-tumor cells as observed by confocal microscopy when following fluorescently labelled C6-NBD-GalCer enriched liposomes or a C_8-GluCer omega alkylated lipid analogue in free form visualized by click chemistry. Quantification of the latter by TLC and click chemistry on isolated cell membranes confirmed the preference for SCS to accumulate into tumor cell membranes over membranes of normal cells (*Chapter 5*).

Initially our working hypothesis for the SCS enhancing drug uptake properties involved possible formation of pores by the SCS transferred from the liposomal bilayer to the outer leaflet of the cell membrane, as reported for sphingosine and ceramides which form specific channels of 2 and 10 nm, respectively in planar lipid bilayers [35]. The existence of pore formation would allow passage of hydrophilic compounds across the membrane. Involvement of such channels could be excluded using a leakage assay with model membranes (LUV's) entrapping a hydrophilic ANTS-DPX complex. Possible membranous pores would cause efflux of the complex and dissociation of ANTS and DPX rendering ANTS fluorescence. Upon addition of C_8-GluCer in free or liposomal form, ANTS remained complexed to DPX in the vesicle core and did not leak from the LUV's. Based on this, possible pore formation induced by SCS is excluded as a mechanism of SCS drug uptake enhancement. This result is nicely in accordance with previous data showing no cellular

uptake enhancement of hydrophilic fluorescent compounds such as AF 488-hydrazine [3].

The mechanism by which SCS enhance drug uptake is well directed to a full understanding since important allusions are already described by modelling [21] and living cell experiments (*Chapter 2, 3, 4*). It is known that SCS transfer to cell membrane is independent on liposomal cellular uptake and precedes drug influx. Together it is described that SCS do not induce nonspecific membrane damage or induce drug structure modification and that endocytic processes or ABC transporter proteins or natural lipid rafts are not involved in the enhancing drug uptake properties of SCS [3]. In living cell experiments at 4°C Dox transmembrane transport was not observed for free Dox. By contrast, cells treated with Dox in form of SCS-enriched liposomes showed an intense fluorescent Dox signal representing membrane associated Dox, which could be removed by washing. Dox insertion into the membrane was possible when promoted by the presence of SCS, but transmembrane transport of Dox at 4°C is prohibited by itself [36]. After additional incubation at 37°C intracellular Dox uptake occurred for free drug or SCS-enriched liposomal forms, whereas uptake from standard liposomes was marginal. Seemingly, SCS exert their effect on the outer membrane leaflet, where they enhance the Dox-membrane influx by a biophysical process after which they facilitate Dox membrane traversal. The latter is likely explained by the assembly of SCS-Dox complexes in the hydrophobic bilayer which is in line previous findings following a modelling approach [21].

This novel approach for improved drug delivery and therapeutic outcome in chemotherapy by modulating tumor cell membrane using SCS reveals a promising strategy to improve drug bioavailability. Thus far, SCS drug uptake enhancing properties were observed *in vivo*, in breast carcinoma (*Chapter 3, 4*) [21] melanoma and squamous cell carcinoma [6] tumor models. To further broaden the application additional studies in different tumor types and at different stages of tumor development involving additional drugs are required to reveal the full potential of this technology. At this point, SCS membrane targeted drug delivery refers to a chemotherapeutic design that can open new directions on chemotherapy considering monotherapy or in combinations applied clinically as chemotherapeutic cocktails.

CONCLUSION

The ultimate goal of the thesis was the application of SCS enriched liposomes to improve chemotherapy outcome, by enhancing drug bioavailability in target cells.

C_8-GluCer enriched liposomes containing Dox were optimized and characterized regarding size, loading efficiency, drug to lipid ratio and stability to advance pharmaceutical development of this formulation toward clinical application. A new lipid analogue, C_8-GalCer co-inserted in the liposomal bilayer was used to develop an optimal novel liposomal Dox formulation. Additionally to Dox, MTO chemotherapy was tested for the enhancing drug uptake properties of SCS, C_8-GluCer or C_8-GalCer enriched liposomes containing MTO were developed into novel liposomal formulations. For SCS enriched liposomes containing Dox or MTO, drug bioavailability was evaluated *in vitro* by assessing drug cytotoxicity and intracellular drug uptake in a panel of tumor and non-tumor cell lines. Remarkably, the SCS drug uptake enhancing and cytotoxic properties were displayed preferentially in tumor cells. Intratumoral bioavailable drug levels for SCS-liposomal treatment exceeded standard liposomal treatment in a MDA-MB-231 tumor model. Stromal cells did not seem to play an important role in intratumoral drug uptake, yet, drug co-localized with tumor cells and tumor vasculature. It was also found that drug pharmacokinetics and biodistribution is substantially affected by C_8-GluCer or C_8-GalCer incorporation. However, study of liposome and lipid analogue pharmacokinetics is still required to determine the exact processes taking place upon SCS-drug-liposome administration. In an orthotopic breast cancer model, following a multiple dosing schedule, C_8-GluCer enriched liposomes containing MTO provided improved therapeutic outcome compared to standard MTO-liposomes. On the other hand, C_8-GalCer liposomes did not increase the drug therapeutic outcome in relation to standard liposomes.

SCS enriched liposomal chemotherapy may provide an optimal treatment with low toxicity profiles and a high accumulation rate at the tumor site through application of liposomes and improved drug bioavailability by SCS tumor cell membrane permeability modulation. This lipid-drug combined chemotherapy shows high potential to be assigned to a multitude of solid tumors. Yet the drug uptake enhancing properties of SCS in the tumor must be vastly

explored considering different tumor models and different lipid-drug combinations to determine optimal chemotherapeutic outcome. The mechanism of action by which SCS enhance drug bioavailability was revealed to involve a biophysical process at the outer leaflet of the cell membrane preferentially to tumor cells. In this direction, normal cells are protected while the tumor is being challenged with more drug uptaketo the benefit of chemotherapy outcome.

REFERENCES

1. Allen TM, Cullis PR, *Liposomal drug delivery systems: from concept to clinical applications.* Adv Drug Deliv Rev, 2013. 65(1):36-48.
2. Deshpande PP, Biswas S, Torchilin VP, *Current trends in the use of liposomes for tumor targeting.* Nanomedicine (Lond), 2013; 8(9): 1509-28.
3. Veldman RJ, Zerp S, van Blitterswijk WJ, Verheij M, N-hexanoyl-sphingomyelin potentiates in vitro doxorubicin cytotoxicity by enhancing its cellular influx. Br J Cancer, 2004; 90(4):917-925.
4. Veldman RJ, Koning GA, van Hell A, Zerp S, Vink SR, Storm G, Verheij M, van Blitterswijk WJ, Coformulated N-Octanoyl-glucosylceramide Improves Cellular Delivery and Cytotoxicity of Liposomal Doxorubicin. J Pharmacol Exp Ther, 2005;315(2):704-10.
5. Haran G, Cohen R, Bar LK, Barenholz Y, *Transmembrane ammonium sulfate gradients in liposomes produce efficient and stable entrapment of amphipathic weak bases.* Biochimica et Biophysica Acta (BBA) - Biomembranes, 1993;1151(2):201-215.
6. van Lummel M, van Blitterswijk WJ, Vink SR, Veldman RJ, van der Valk MA, Schipper D, Dicheva BM, Eggermont AM, ten Hagen TL, Verheij M, Koning GA, *Enriching lipid nanovesicles with short-chain glucosylceramide improves doxorubicin delivery and efficacy in solid tumors.* FASEB J, 2009; 25(1):280-289.
7. Barenholz, Y, *Doxil®-the first FDA-approved nano-drug: lessons learned.* J Control Release, 2012;160(2):117-34.
8. Li X, Hirsh DJ, Cabral-Lilly D, Zirkel A, Gruner SM, Janoff AS, Perkins WR, *Doxorubicin physical state in solution and inside liposomes loaded via a pH gradient.* Biochimica et Biophysica Acta (BBA) - Biomembranes, 1998;1415(1):23-40.
9. Cook AM, Chambers EJ, Rees GJ,*Comparison of mitozantrone and epirubicin in advanced breast cancer.* Clin Oncol, 1996;8:363-366.
10. Smith LA, Cornelius VR, Plummer CJ, Levitt G, Verrill M, Canney P, Jones A, *Cardiotoxicity of anthracycline agents for the treatment of cancer: systematic review and meta-analysis of randomised controlled trials.* BMC Cancer, 2010; 10:337.
11. Gharib MI, Burnett AK, *Chemotherapy-induced cardiotoxicity: current practice and prospects of prophylaxis.* Eur J Heart Fail, 2002;4(3): 235-42.
12. Dunn CJ, Goa KL, *Mitoxantrone: a review of its pharmacological properties and use in acute nonlymphoblastic leukaemia.* Drugs Aging, 1996;9(2):122-47.
13. Pinto AC, Moreira JN, Simões S, *Liposomal imatinib–mitoxantrone combination: Formulation development and therapeutic evaluation in an animal model of prostate cancer.*Prostate, 2011;71(1):81-90.
14. Li C, Cui J, Wang C, Wang J, Li Y, Zhang L, Zhang L, Guo W, Wang Y, *Lipid composition and grafted PEG affect in vivo activity of liposomal mitoxantrone.* Int J Pharm. 2008. 362(1-2):60-66.
15. Li C, Cui J, Wang C, Li Y, Zhang H, Wang J, Li Y, Zhang L, Zhang L, Guo W, Wang Y, *Encapsulation of mitoxantrone into pegylated SUVs enhances its antineoplastic efficacy.* Eur J Pharm Biopharm, 2008;70(2):657-665.

16. Lim HJ, Masin D, Madden TD, Bally MB, *Influence of Drug Release Characteristics on the Therapeutic Activity of Liposomal Mitoxantrone*. J Pharmacol Exp Ther, 1997;281(1):566-73.
17. Lim HJ, Masin D, McIntosh NL, Madden TD, Bally MB, *Role of Drug Release and Liposome-Mediated Drug Delivery in Governing the Therapeutic Activity of Liposomal Mitoxantrone Used to Treat Human A431 and LS180 Solid Tumors*, J Pharmacol Exp Ther, 2000;292(1): 337-45.
18. Chang HI, Yeh MK, *Clinical development of liposome-based drugs: formulation, characterization, and therapeutic efficacy.* Int J Nanomedicine, 2012;7:49-60.
19. Stover TC, Sharma A, Robertson GP, Kester M, *Systemic Delivery of Liposomal Short-Chain Ceramide Limits Solid Tumor Growth in Murine Models of Breast Adenocarcinoma*. Clin Cancer Res, 2005; 1;11(9): 3465-74.
20. Tran MA, Smith CD, Kester M, Robertson GP, *Combining Nanoliposomal Ceramide with Sorafenib Synergistically Inhibits Melanoma and Breast Cancer Cell Survival to Decrease Tumor Development*. Clin Cancer Res, 2008;14(11):3571-81.
21. van Hell AJ, Melo MN, van Blitterswijk WJ, Gueth DM, Braumuller TM, Pedrosa LR, Song JY, Marrink SJ, Koning GA, Jonkers J, Verheij M, *Defined lipid analogues induce transient channels to facilitate drug-membrane traversal and circumvent cancer therapy resistance.* Sci Rep, 2013; 3:1949.
22. Nakasone ES1, Askautrud HA, Kees T, Park JH, Plaks V, Ewald AJ, Fein M, Rasch MG, Tan YX, Qiu J, Park J, Sinha P, Bissell MJ, Frengen E, Werb Z, Egeblad M, *Imaging Tumor-Stroma Interactions during Chemotherapy Reveals Contributions of the Microenvironment to Resistance*. Cancer Cell, 2012;21(4):488-503.
23. Brown JM, Giaccia AJ, *The Unique Physiology of Solid Tumors: Opportunities (and Problems) for Cancer Therapy*, Cancer Res, 1998; 58(7):1408-16.
24. Storm G, Steerenberg PA, Emmen F, van Borssum Waalkes M, Crommelin DJ, *Release of doxorubicin from peritoneal macrophages exposed in vivo to doxorubicin-containing liposomes. Biochim Biophys Acta. 1988;965(2-3):136-45.*
25. Mayer LD, Dougherty G, Harasym TO, Bally MB, *The Role of Tumor-Associated Macrophages in the Delivery of Liposomal Doxorubicin to Solid Murine Fibrosarcoma Tumors*. J Pharmacol Exp Ther, 280(3): 1406-14.
26. Banciu M, Schiffelers RM, Storm G, *Investigation into the Role of Tumor-Associated Macrophages in the Antitumor Activity of Doxil.* Pharm Res, 2008;25(8):1948-55.
27. Hajihassan Z, Rabbani-Chadegani A, *Studies on the binding affinity of anticancer drug mitoxantrone to chromatin, DNA and histone proteins.* J Biomed Sci, 2009;16:31.
28. Zolnik BS, Stern ST, Kaiser JM, Heakal Y, Clogston JD, Kester M, McNeil SE, *Rapid Distribution of Liposomal Short-Chain Ceramide in Vitro and in Vivo*. Drug Metab Dispos, 2008 ;36(8):1709-15.

29. Gustafsson M, *Surpassing the lateral resolution limit by a factor of two using structured illumination microscopy.* J Microsc, 2000. 198(Pt2):82-7.
30. Hess ST, Girirajan TP, Mason MD, *Ultra-high resolution imaging by fluorescence photoactivation localization microscopy.* Biophys J, 2006; 91(11):4258-72.
31. Ha T, Tinnefeld P, *Photophysics of fluorescent probes for single-molecule biophysics and super-resolution imaging.* Annu Rev Phys Chem, 2012; 63:595-617.
32. Egerton R, *Physical principles of electron microscopy : an introduction to TEM, SEM, and AEM.* Springer 2005; 202.
33. Goñi FM, Alonso A, *Biophysics of sphingolipids I. Membrane properties of sphingosine, ceramides and other simple sphingolipids.* Biochim Biophys Acta, 2006;1758(12):1902-21.
34. Maggio B, Fanani ML, Rosetti CM, Wilke N, *Biophysics of sphingolipids II. Glycosphingolipids: An assortment of multiple structural information transducers at the membrane surface.* Biochim Biophys Acta, 2006;1758(12):1922-44.
35. Siskind LJ, Fluss S, Bui M, Colombini M, *Sphingosine Forms Channels in Membranes That Differ Greatly from Those Formed by Ceramide.* Journal of Bioenergetics and Biomembranes, 2005;37(4):227-236.
36. Regev R, Yeheskely-Hayon D, Katzir H, Eytan GD, *Transport of anthracyclines and mitoxantrone across membranes by a flip-flop mechanism.* Biochem Pharmacol, 2005; 70(1):161-9.

CHAPTER 7

Summary / Samenvatting

SUMMARY

Nanotechnology has attracted much attention in the past years as a means to improve drug delivery in cancer therapy. The entrapment of drugs in nanoliposomes, small lipid vesicles, prolongs drug retention in circulation and prevents severe toxicity observed in normal chemotherapeutic regimes administering free drugs. However, liposomal drug delivery still needs to overcome remaining hurdles such as specific drug accumulation in the tumor and drug bioavailability. Short chain sphingolipid (SCS) are a special class of lipids with recently identified capacity to make tumor cell membranes more permeable to chemotherapeutic drugs.

The aim of the work described in this thesis is to develop and investigate short chain sphingolipid (SCS)-enriched liposomal formulations containing doxorubicin (Dox) or mitoxantrone (MTO) and apply them as a new therapeutic approach to enhance drug bioavailability and improve chemotherapy through modulation of plasmamembrane permeability of tumor cells.

The background of liposomal drug delivery, SCS membrane modulation and the possible benefits of combining both approaches for chemotherapy improvement is introduced in the first chapter. **Chapter 2** describes the development of optimal liposomal formulations of C_8-glucosylceramide (C_8-GluCer) and introduces novel C_8-galactosylceramide (C_8-GalCer)-enriched liposomes containing Dox. Co-formulation of SCS induced deformation of liposomal bilayer upon Dox-loading from a round to a more enlongated rod-shaped morphology. This did not affect stability and even improved liposomal drug loading efficiency. The performed pharmaceutical optimization is important for future translation of these formulations toward clinical application. These formulations enhanced intracellular drug levels, which nicely correlated with a strongly improved therapeutic drug response in comparison to standard Dox-liposomes without SCS. Importantly, a tumor cell type specificity was demonstrated for the SCS-mediated drug uptake enhancing properties, as non-tumor cells were much less sensitive to liposomal SCS-Dox treatment than tumor cells. New insights in the mechanism of action of SCS-mediated drug delivery described a cellular routing of the SCS into the membrane, which differs from the liposomal nanocarrier that remained outside and its drug content that efficiently reached the nucleus. Based on

these findings we concluded that a transfer of the SCS to the tumor cell membrane preceeds and promotes cellular Dox uptake.

Chapter 3 describes novel SCS (C_8-GluCer or C_8-GalCer) enriched liposomal formulations containing MTO as a promising formulation for breast cancer therapy. Stable SCS-MTO-liposomes (MTOL) were developed that strongly increased MTO delivery and cytotoxicity to breast carcinoma cells compared to standard MTOL. Again,non tumor cells appeared to be much less affected by this combined drug delivery approach confirming the tumor-cell type selectivity of SCS-enriched liposomes. The drug delivery mechanism involved a transfer of SCS to the cell membrane, which occured independently nanoliposome internalization and drug transfer. The latter was demonstrated by separate administration of SCS and MTO by pretreatment of cells with non-drug loaded SCS-liposomes and subsequent drug treatment by MTOL administration, which also clearly enhanced cellular MTO uptake. This demonstrates that SCS transfer and MTO uptake act independent of the liposomal carrier and synergize at the cell membrane level. In experimental tumor modelstumor drug delivery by nanoliposomal formulations was strongly improved relative to free drug. Nanoliposomal MTO delivery and cellular uptake was heterogeneous throughout the tumor and clearly correlated with CD31-positive tumor vessels. Yet, MTO uptake by CD11b positive macrophages in tumor stroma was minor.

Further in vivo testing of SCS-enriched nanoliposomes containing MTO (SCS-MTOL) is described in chapter 4. Pharmacokinetics and efficacy were compared to free MTO and standard MTOL in single and multiple dose schedules in an orthotopic MDA MB-231 human breast carcinoma mouse model. Liposomal encapsulation decreased MTO toxicity and allowed administration of higher drug doses. SCS-MTOL displayed increased MTO clearance and lower skin accumulation compared to standard MTOL. Intratumoral liposomal drug delivery was heterogeneous and rather limited in hypoxic tumor areas, yet SCS-MTOL showed faster MTO bioavailability than MTOL. The increased MTO bioavailability correlated well with the improved antitumor activity of SCS-MTOL in the breast carcinoma model compared to MTO-liposomes without SCS. Multiple dosing of liposomal MTO strongly delayed tumor growth compared to free MTO and prolonged mouse survival, whereas among the liposomal MTO treatments, C_8-GluCer-MTOL was most effective.

Liposomal encapsulation combined with targeting plasma membranes with SCS improved MTO tumor bioavailability and thereby therapeutic activity and represents a promising approach to improve MTO-based chemotherapy.

Research focused on the mechanisms underlying SCS-mediated drug uptake enhancement is described in chapter 5. It was found that upon cellular contact SCS are transferred from the liposome bilayer to the plasma membrane, most likely into the exoplasmic leaflet, where they enhance drug-membrane interaction and in turn facilitate transmembrane transport and subsequently improve cytotoxic potential of the drug.

Live cell imaging revealed that SCS transfer to cell membrane was independent of liposomal uptake and that the majority of the transferred lipid remained in the plasma membrane, whereas a smaller fraction was detected in lysosomes. Higher levels of fluorescent SCS were found in tumor cells compared to non-tumor cells proving that the transfer of SCS is tumor cell specific. These results were confirmed for native SCS that were labeled by post treatment click chemistry, imaged by confocal imaging and quanitied by thin layer chromatography Also these studies revealed that SCS transfer and incorporation in the cell membrane was higher for BLM, melanoma and MDA MB-231, breast carcinoma than 3T3, fibroblasts. These findings provide a clear explanation for the preferential cytotoxicity of SCS-DoxL and SCS-MTOL to tumor cells over non-tumor cells (chapter 2 and 3).

Studies in celmembrane mimicking model membranes demonstrated that SCS, when transferred from the liposome bilayer to the plasma membrane, induced membrane rearrangements as evidenced by a transbilayer flip-flop of pyrene-SM. Pore Formation of aqueous pores, measured as leakage of hydrophilic fluorescent probes was however not observed. Imaging of drug uptake at 4°C revealed that SCS enhanced the interaction of Dox with the outer leaflet of the plasma membrane of tumor cells, augmenting the subsequent transmembrane flip-flop of the drug, which only occured at 37°C. Our results demonstrate that SCS preferentially insert into tumor cell plasma membranes and there enhance a cells intrinsic capacity to translocate amphiphilic drugs such as Dox across the membrane via a biophysical process.

Chapter 6 discusses the significance of the results described in this thesis and future perspectives.

The main goal of the thesis was the application of SCS enriched liposomes to improve chemotherapy outcome, by enhancing drug bioavailability in target tumor cells. Development of SCS (C_8-GluCer or C_8-GalCer) enriched liposomes containing Dox and MTO was successfully achieved with optimal characteristics from a pharmaceutical point of view, for use in vitro and vivo studies and to advance pharmaceutical development of such formulations toward clinical application, which is currently ongoing for C_8-GluCer-Dox-liposomes.

In vitro studies revealed that the SCS drug uptake enhancing and cytotoxic properties were displayed preferentially in tumor cells. Mechanistic studies demonstrated that this was related to preferential accumulation of SCS in tumor cell membranes.

Intravital microscopic imaging proved that intratumoral bioavailable drug levels for SCS-liposomal treatment exceeded standard liposomal treatment in a MDA MB-231 tumor model. Therapeutic studies in an orthotopic breast cancer model demonstrated improved therapeutic efficacy of C_8-GluCer enriched MTO-liposomes compared to standard MTO-liposomes.

SCS-enriched liposomal chemotherapy represents a novel attractive drug delivery approach, which combines the benefits of reduced toxicity and improved tumor accumulation of drugs through nanoliposomal encapsulation with enhanced intracellular drug delivery by SCS-mediated tumor cell membrane permeabilization. In these studies we've broadened the application using different glycosphingolipids to formulate two chemotherapeutic drugs. Given their proven therapeutic potential, the performed pharmaceutical optimization of formulations will contribute to ultimate near future clinical application. Next to a translational direction, future studies will aim at further broadening of this drug delivery platform to include novel chemotherapeutic drugs, new SCS lipids and the search for optimal SCS – drug combinations for improved drug delivery. A further understanding of the working mechanism, especially in relation to the tumor cell membrane lipid composition will help to find efficient tumor cell-specific drug delivery routes for various chemotherapeutic drugs.

SAMENVATTING

De toepassing van nanotechnologie voor verbetering van geneesmiddel afgifte in de behandeling van kanker is de laatste jaren sterk in opkomst. Het verpakken van cytostatica in nanoliposomen, minuscule vetblaasjes, verlengt de verblijftijd in circulatie, en vermindert de ernstige bijwerkingen van conventionele chemotherapie waardoor de therapeutische breedte toeneemt. Echter, liposomale chemotherapie afgifte aan tumoren en uiteindelijk in tumorcellen moet nog verder worden verbeterd. Kort-ketenige sfingolipiden (SCS) vormen een specifieke klasse van lipiden waarvan recent ontdekt is dat deze tumorcel membranen meer permeabel maken voor chemotherapeutica.

Het doel van het onderzoek dat in dit proefschrift is beschreven, is de ontwikkeling van liposomen met kort-ketenige sfingolipiden in de lipide bi-laag en de chemotherapeutica doxorubicine (Dox) of mitoxantrone (MTO) binnenin het vetblaasje en de toepassing daarvan om de werkzaamheid van de chemotherapie te verbeteren door de permeabiliteit van tumorcel membranen te moduleren.

De achtergrond van het gebruik van liposomen voor geneesmiddel afgifte, de toepassing van SCS voor het moduleren van celmembranen en de mogelijke voordelen van het combineren van beide strategieën voor verdere verbetering van chemotherapie, worden geïntroduceerd in het eerste hoofdstuk.

Hoofdstuk 2 beschrijft de ontwikkeling van optimale liposomale formuleringen van C8-glucosylceramide (C8-GluCer) en introduceert nieuwe C8-galactosylceramide (C8-GalCer) bevattende liposomen met Dox. De aanwezigheid van SCS in de bi-laag veroorzaakte een vormverandering in de liposomen na belading met Dox van een ronde naar een meer langwerpige staafvormige structuur. Dit had echter geen effect op de stabiliteit en leidde zelfs tot een verbetering in de Dox beladingsgraad. De uitgevoerde farmaceutische optimalisatie van de bereiding van deze liposomen is van groot belang voor toekomstige klinische toepassing.

Deze nieuwe formuleringen waren in staat intracellulaire Dox niveaus te verhogen, wat leidde tot een verhoogde therapeutische respons in vergelijking met Dox-liposomen zonder SCS. Een belangrijke waarneming was dat de SCS-gemedieerde Dox opname bij voorkeur in tumorcellen plaatsvond. Normale cellen bleken veel minder gevoelig te zijn voor liposomale SCS-Dox behandeling dan tumorcellen. Uit

een studie naar het achterliggende mechanisme bleek dat het SCS zich in het tumorcelmembraan nestelt en een andere route volgt dan het liposoom, dat buiten de cel blijft, en Dox, dat efficiënt naar de celkern wordt getransporteerd. Op basis van deze resultaten is geconcludeerd dat de overgang van het SCS naar de tumorcel membraan vooraf gaat aan een verhoogde cellulaire Dox opname.

In hoofdstuk 3 worden nieuwe veelbelovende SCS-bevattende liposomale MTO-formuleringen beschreven voor toepassing in borstkanker chemotherapie. Stabiele formuleringen zijn ontwikkeld die een sterk verhoogde cellulaire MTO opname en cytotoxische werking veroorzaakten bij borstkanker cellen in vergelijking met standaard MTO-liposomen zonder SCS. Opnieuw bleken normale cellen veel minder gevoelig voor deze gecombineerde chemotherapie aanpak, wat een bevestiging is van de tumorcel selectiviteit van SCS-bevattende liposomen. In het mechanisme van verhoogde MTO afgifte speelde de overgang van SCS naar tumorcel membranen een belangrijke rol en bleek deze overgang onafhankelijk van opname van het hele liposoom en het MTO. Dit laatste werd aangetoond door de waarneming dat een voorbehandeling van tumorcellen met lege SCS-liposomen gevolgd door een behandeling met MTO-liposomen zonder SCS ook leidde tot een verhoging van cellulaire MTO opname. Dit laat zien dat de SCS overgang en MTO opname onafhankelijk is van opname van het liposoom en dat deze elkaar versterken op het niveau van het celmembraan. In experimentele tumormodellen veroorzaakten liposomale MTO formuleringen een sterke verbetering in MTO ophoping in de tumor. Liposomale MTO afgifte was heterogeen in het tumorweefsel en sterk gecorreleerd met de aanwezigheid van (CD31-positieve) tumorbloedvaten. Opname van MTO in CD11b-positieve macrofagen in tumor stroma daarentegen was gering.

Verder in vivo onderzoek naar SCS-MTO-liposomen is beschreven in hoofdstuk 4. Farmacokinetiek en therapeutische werking zijn vergeleken met vrij toegediend MTO en MTO-liposomen zonder SCS in enkelvoudige en meervoudige toedieningsschema's in een orthotoop MDA MB-231 humaan borstkanker model in muizen. Liposomale insluiting verlaagde de toxische bijwerkingen van MTO en maakte het mogelijk om hogere doseringen te geven. SCS-MTO-liposomen gaven een versnelde MTO klaring en verlaagde ophoping in de huid in vergelijking met MTO-liposomen zonder SCS. Opname in de tumor was heterogeen en beperkt in hypoxische gebieden. Opvallend was dat SCS-MTO-liposomen

betere en snellere biologische beschikbaarheid van het MTO gaven dan formuleringen zonder SCS. Deze verbetering in cellulaire beschikbaarheid werd bevestigd door de verbeterde therapeutische werkzaamheid van de SCS-MTO-liposomen in het borstkanker tumor model in vergelijking met MTO-liposomen. Meervoudige toediening van liposomaal MTO gaf een sterke remming van de tumorgroei in vergelijking met vrij MTO en gaf een verlengde overleving. Van de liposomale MTO behandelingen was die met C8-GluCer-MTO-liposomen het meest effectief.

De gecombineerde aanpak van liposomale insluiting van MTO en het sturen van SCS naar tumorcel membranen, verbeterde de cellulaire beschikbaarheid van MTO en daardoor de therapeutische werkzaamheid. Hiermee is een veelbelovende verbetering bereikt in MTO-gebaseerde chemotherapie.

Nader onderzoek naar het onderliggend werkingsmechanisme van SCS-gemedieerde verbetering van cellulaire opname van chemotherapie is beschreven in hoofdstuk 5. SCS gaan tijdens interactie met tumorcellen over van de liposomale bi-laag naar de exoplasmatische laag van het plasmamembraan. Daar verbeteren deze de interactie van het chemotherapeuticum met het membraan, vergemakkelijken het transport over deze barrière, en dragen zodoende bij tot een toegenomen cytotoxiciteit.

Het microscopisch afbeelden van de interactie van fluorescerende SCS-liposomen met levende cellen liet duidelijk zien dat de liposomen niet de cel binnen gaan, maar wel flinke hoeveelheden fluorescent gelabeld SCS aan het tumorcel membraan overbrengen. Een kleiner deel daarvan werd intracellulair aangetroffen in lysosomen.

SCS gingen in veel sterkere mate over naar tumorcel membranen dan naar membranen van normale cellen wat overeenkomt met de eerder waargenomen preferentiële afgifte van chemotherapie aan tumorcellen door SCS-liposomen. Deze resultaten zijn ook gevonden voor het gewone, niet fluorescent gelabelde, SCS door deze pas na behandeling en fixatie van de cellen fluorescent te labelen door middel van click chemie. Daarna zijn de cel gebonden lipiden zichtbaar gemaakt met confocale microscopie en gekwantificeerd door middel van dunne laag chromatografie. Ook in die experimenten werd veel hogere opname van de SCS gevonden in BLM melanoma cellen en MDA MB-231 borstkanker cellen dan in 3T3, fibroblasten. Deze bevindingen geven een zeer duidelijke verklaring voor de

preferentiële toxiciteit van Dox of MTO-bevattende SCS-liposomen voor tumorcellen in vergelijking met normale cellen (hoofdstuk 2 en 3).

Studies met modelmembranen die celmembranen nabootsen, lieten zien dat SCS opname in celmembranen herschikking veroorzaakt van lipiden in dat membraan. Dit werd aangetoond door een sterk toegenomen flip-flop van fluorescent pyrene-SM in de model membranen onder invloed van SCS. In vergelijkbare studies kon de vorming van kleine water-bevattende poriën worden uitgesloten omdat hydrofiele fluorescente moleculen niet werden vrijgegeven door de modelmembranen.

Studies bij een temperatuur van 4°C lieten zien dat SCS de interactie van Dox met het celmembraan van tumorcellen versterken om vervolgens bij 37°C de transmembraan flip-flop van Dox te stimuleren.

De resultaten van deze studies naar het mechanisme laten zien dat SCS preferentieel overgaan naar het membraan van tumorcellen en daar de intrinsieke capaciteit van de cel om Dox of MTO over het membraan te transporteren, verhogen via een biofysisch proces.

In hoofdstuk 6 worden de resultaten van het onderzoek in een breder kader geplaatst en nader bediscussieerd en worden mogelijke toekomstige ontwikkelingen beschreven.

Het hoofddoel van het onderzoek beschreven in dit proefschrift was de toepassing van SCS-bevattende liposomen voor het verbeteren van chemotherapie, door beschikbaarheid van de chemotherapie voor tumorcellen te vergroten. Ontwikkeling van SCS (C8-GluCer or C8-GalCer) bevattende liposomen met Dox of MTO als inhoud was succesvol, en deze formuleringen hadden optimale farmaceutische eigenschappen voor in vitro en in vivo studies en voor de verdere farmaceutische ontwikkeling van deze formuleringen voor klinische toepassing, een proces dat op dit moment gaande is voor GluCer-Dox-liposomen.

In vitro studies hebben laten zien dat SCS-gemedieerde chemotherapie opname en cytotoxische werking vooral optrad bij tumorcellen. Mechanistische studies toonden aan dat dit werd veroorzaakt door preferentiële opname van SCS in tumorcel membranen.

Intravitale beeldvorming toonde aan dat de biologische beschikbaarheid van MTO voor tumorcellen in MDA MB-231 borst tumoren hoger was na behandeling met SCS-liposomen dan met standaard MTO-liposomen. Therapeutische studies in een orthotoop borstkanker

model lieten een duidelijke verbetering zien na behandeling met C8-GluCer-MTO-liposomen in vergelijking met MTO-liposomen zonder SCS.

SCS-bevattende liposomale chemotherapie is een nieuwe en aantrekkelijke aanpak voor verbetering van chemotherapie afgifte aan tumoren. Het combineert de voordelen van verminderde toxiciteit en toegenomen ophoping van chemotherapie in tumoren door gebruik te maken van liposomen en de toename van cellulaire chemotherapie opname door SCS-gemedieerde permeabilisatie van het tumorcel membraan. In deze studies hebben we de toepassing van deze technologie verder uitgebreid door verschillende SCS te testen in combinatie met twee verschillende chemotherapeutica. Gezien de bewezen therapeutische werkzaamheid zal de uitgevoerde farmaceutische optimalisatie nader bijdragen tot uiteindelijke klinische toepassing in de nabije toekomst. Naast deze translationele richting zullen toekomstige studies zich ook richten op het verder verbreden van dit chemotherapie afgifte platform, waarbij nieuwe chemotherapeutica, nieuwe SCS zullen worden bestudeerd en studies worden gedaan naar optimale SCS-chemotherapie combinaties voor verbeterde afgifte aan tumorcellen. Het nog beter begrijpen van de onderliggende werkingsmechanismen en in het bijzonder het belang van de lipide samenstelling van tumorcel membranen, zal verder bijdragen aan het vinden van meer en nog betere manieren voor tumorcel specifieke afgifte van verschillende cytostatica.

CHAPTER 8

Acknowledgments

PhD Portfolio

Publications/Awards

About the author

ACKNOWLEDGEMENTS

I would like to express my deepest gratitude to my supervisor Dr. Gerben Koning for his trust, daily guidance and encouragement. I sincerely thank you for your patience and cordiality in the innumerous discussions we have had. Thank you for helping me to scientifically sprout and grow, but also for your friendly attitude when I most needed.

My appreciation to my promoters Prof.dr. Alexander Eggermont and Prof.dr. Marcel Verheij. To Prof.dr. Alexander Eggermont, thank you for the opportunity to work at LECO but also for the fruitful discussions and support on my research. It's a honor to have you as my promoter. To Prof.dr. Marcel Verheij, thank you for the scientific input, criticism and priceless support in making this project a whole.

To Dr. Timo ten Hagen, thank you for helping to carry out my research.

My indebted gratitude to Dr. Olaf van Tellingen for embracing me at his friendly Lab in the Department of Diagnostic Oncology, The Netherlands Cancer Institute - Antoni van Leeuwenhoek Hospital. Thank you for your daily base support and motivating good mood, patience, scientific criticism and handy lab work.

Thank you to Dr. Gert van Cappellen, for the great technical support on Optical Imaging and for the steadfast availability for new and unplanned experiments with a peaceful presence.

My appreciation to Prof.dr. Regine Suss for hosting me at Department of Pharmaceutical Technology and Biopharmacy, Albert-Ludwigs University, in Freiburg, Germany to learn on Cryo-Transmission Electron Microscopy. Thank you for the opportunity but also for critically reading related articles.

I am also extremely grateful to Prof.dr. Felix Goñi and Dr. Xabier Contreras, from Biophysics Unit in Bilbao. To Prof.dr. Felix Goñi, thank you for the approach at Sphingolipids Club Meeting and criticism on my work. I am very glad that I took the opportunity to

work at your department even for a short but very intensive time during the last month of my PhD. To Dr. Xabier I am very grateful for all the expertise and handy lab work to unveil more on the mysterious fate of short chain sphingolipids and biomembranes.

My acknowledgement to Thomas Sollié for all experimental work performed to my project but also to Joost, Cindy, Gisela and Debbie for daily practical support.

To my LECO colleagues, thank you all in a peculiar way to each of you, for the daily companionship, work discussions and unique memories that I will take with my graduation.

To my compatriot friends, thank you for the *family* feeling.

To my paranymphs, Andrea and Rui thank you for the friendship which I greatly cherish.

To Miguel, who exceptionally supported and encourage me I would like to express my most sincere gratitude. Your presence was certainly an immeasurable source of motivation for me to accomplish this thesis. Thank you for the love. Thank you for being "there".

To my dearest family my gratitude is unutterable and everlasting.

To my brother, Pedro thanks for the support and love and your constant listening and wise words.

To my mother Maria José and father José Nicolau I would like to express my gratitude for all their unwavering support, encouragement and love, for their unflinching belief in me and for always inspiring me. I have been truly blessed for sharing my life with you.

À minha querida família a minha gratidão é inestimável e eterna.

Ao meu irmão, Pedro, obrigada pelo carinho e apoio permanente. Obrigada pelo ouvir constante e as melhores palavras de conforto.

À minha mãe, Maria José e pai, José Nicolau quero expressar a minha gratidão pelo apoio incondicional, coragem e carinho. Obrigada por acreditarem em mim inabalavelmente e por desde sempre me inspirarem. Sinto me abencoada por vos ter comigo.

PhD PORTFOLIO

Lília Raquel Cordeiro Pedrosa
Laboratory of Experimental Surgical Oncology
Department of Surgical Oncology, Erasmus MC
Molecular Medicine Postgraduate School
PhD period: 20th April 2009 to 31st December 2013
Promotor: Prof. Alexander M.M. Eggermont
Co-promotor: Prof. Marcel Verheij
Supervisor: Dr. Gerben A. Koning

	Year	ECTS
Courses and Workshops		
Animal Experimentation Article 9 Course	2009	3.0
Radiation Course: Stralingsbeschermings-deskundigheidsniveau 5B	2010	1.7
Animal Imaging Workshop by AMIE	2010	1.4
Basic and Translational Oncology Course	2010	1.8
The Basic Introduction Course on SPSS	2010	0.5
Molecular Medicine Course	2010	0.7
Advanced Drug Delivery & Drug Targeting Course, Leiden/Amsterdam Center of Drug Research, Leiden, The Netherlands	2011	1.8
The research management for PhD students workshop	2011	1.0
In vivo Imaging "From Molecule to Organism"	2011	1.8
Quantitative Pharmacology and PK/PD for Drug Discovery & Development Scientists, LAKEMEDELSAKADEMIN, Munich, Germany	2012	3.0
Workshop on Photoshop and Illustrator CS5	2013	0.3
Oral presentations		
20th Annual International Workshop on Liposomes Ameland, NL	2009	1.0
9th Sphingolipid Club Meeting, Favignana, Italy	2011	1.0
10th Sphingolipid Club Meeting, Assisi, Italy	2013	1.0
Annual Presentation Scientific meetings at JNI	2009-13	2.0
Poster Presentations		
ILS 2009 Annual Meeting - Liposome Advances: Progress in Drug and Vaccine Delivery, London, UK	2009	0.3
16th International Charles Heidelberger Symposium on Cancer Research,	2010	0.3
ILS 2011 Annual Meeting - Liposome Advances: Progress in Drug and Vaccine Delivery	2011	0.3
Gordon's Conference: Cancer Nanotechnology, West Dover VT, USA	2013	0.3
Molmed Day	2010-13	0.9

International Conferences

ILS 2009 Annual Meeting - Liposome Advances: Progress in Drug and Vaccine Delivery, London, UK	2009	1.0
16th International Charles Heidelberger Symposium on Cancer Research, Coimbra, Portugal	2010	1.0
26th Annual meeting of the European Society of Hyperthermic Oncology, Rotterdam, The Netherlands	2010	1.0
ILS 2011 Annual Meeting - Liposome Advances: Progress in Drug and Vaccine Delivery, London, UK	2011	1.0
9th Sphingolipids Club Meeting, Favignana, Italy	2011	1.0
10th Sphingolipid Club Meeting, Assisi, Italy	2013	1.0
Gordon's Conference: Cancer Nanotechnology, West Dover VT, USA	2013	1.0

Seminars and Workshops

20th Annual Meeting of Liposomes Ameland	2009	1.0
Annual Molmed Day	2010-13	1.2
Annual LabSience Day	2009-13	1.5
Annual SurgeryStaff Day	2009-12	1.2
Weekly JNI Oncology lectures	2009-13	2.5
Visiting Scientist at Faculty of Pharmaceutical Sciences in Freiburg, Germany for training with Cryo-Transmission Electron Microscopy technique, under the supervision of Prof. Regine Suss (1 week)	2011	2.5
Visiting Scientist at The Netherlands Cancer Institute - Antoni van Leeuwenhoek Hospital, Amsterdam, The Netherlands for training on High Pressure Liquid Chromatography at Department of Diagnostic Oncology, under the supervision of Dr. Olaf van Tellingen (6 months).	2013	8
Visiting Scientist at Unit of Biophysics, CSIC-UPV/EHU University of Basque Country, Spain for research on tumor cell membrane modulation with Dr. Xabier Contreras and Prof. Felix Goñi (2 weeks)	2013	5

Teaching Activities: Supervising practicals

Supervision of Technician student internship: B. Duijndam (9 months)	2010-11	8
Supervision of Technician student internship: S.Hoogendoorn (3 months)	2012	8
Supervision of Master student from Molecular Medicine School: B. Steurer (9 months)	2012-13	8

PUBLICATIONS/AWARDS

Publications

- Pedrosa LRC, van Hell A, Suss R, Blitterswijk W, Seynhaeve A, Cappellen W, Eggermont AMM, Hagen TLM, Verheij M, Koning GA, **Improving Intracellular Doxorubicin Delivery Through Nanoliposomes Equipped with Selective Tumor Cell Membrane Permeabilizing Short Chain Sphingolipids**, Pharm Res, July 2013, Volume 30, Issue 7, pp 1883-1895.

- Pedrosa LRC, Hagen TLM, Suss R, van Hell A, Eggermont AMM, Verheij M, Koning GA, **Short chain glycoceramides promote intracellular mitoxantrone delivery from novel nanoliposomes into breast cancer cells**, Submitted.

- Pedrosa LRC, Hagen TLM, Tellingen O, Soullié T, Eggermont AMM, Verheij M, Koning GA, **Plasma membrane targeting of short chain sphingolipids inserted in nanovesicles improves anti tumor activity of mitoxantrone in an orthotopic breast carcinoma xenograft**, Submitted.

- Pedrosa LRC, Hagen TLM, Goñi F, Eggermont AMM, Verheij M, Koning GA, Contreras X, **Short Chain Sphingolipids enhance intracellular drug uptake preferentially in tumor cells**, In preparation.

- van Hell AJ, Melo MN, van Blitterswijk WJ, Gueth DM, Braumuller TM, Pedrosa LRC, Song JY, Marrink SJ, Koning GA, Jonkers J, Verheij M., **Defined lipid analogues induce transient channels to facilitate drug-membrane traversal and circumvent cancer therapy resistance**, Sci Rep. 2013;3:1949

- Azadeh Haeri, Lília R.C. Pedrosa, Timo L.M. ten Hagen, Simin Dadashzadeh, Gerben A. Koning, **A novel combined approach of short chain sphingolipids and thermosensitive liposomes for improved tumor delivery of anticancer drugs**, In preparation.

Awards

- **Travel grant Award** by Avanti Polar Lipids at Sphingolipid Club Meeting, September 29-02nd October, Favignana-Italy, 2011.

- **Best Presentation Award**: Improving doxorubicin efficacy through nanoliposomes equipped with selective tumor cell membrane permeabilizing short chain sphingolipids at Sphingolipid Club Meeting, 27th June- 01st July, Asissi-Italy, 2013.

- **Journal Cover** for Pharm Res, July 2013, Volume 30, Issue 7.

ABOUT THE AUTHOR

Lília Raquel Cordeiro Pedrosa was born on 19th May, 1981 in Coimbra, Portugal. She attended secondary school at Dr. Joaquim Carvalho Liceum in Figueira da Foz. In 2000 she started a 6-year degree on Pharmaceutical Sciences at University of Coimbra studying, in between, 1-year abroad at University of Barcelona, Spain and obtaining a Pharm-D degree in 2006. In 2007 she followed a Post-Graduation in "Pharmacy and the Medicine Law", Biomedical Law centre of the Faculty of Law of the University of Coimbra starting in parallel her first job as PharmD - Regularity Affairs Officer. Aiming for scientific knowledge on Pharmaceutical Technology in 2008 she started a scholarship for Scientific Research in the project "The increase in the bioavailability of oral insulin through the nanoencapsulation into polysaccharides". After her mother's relapse on breast cancer her determination was to contribute on cancer research and at 20th April 2009 she started her PhD at the Department of Surgical Oncology at Erasmus Medical Center in Rotterdam, The Netherlands. Lília is currently working as a Scientist at to-BBB, a clinical stage biotechnology company in Leiden, The Netherlands.

ADDENDUM

Supplemental Data

CHAPTER 2

Supplemental Table 1. *In vitro* IC_{50} values toward tumor cells BLM, melanoma and SKBR3, breast carcinoma, after treatment with C_8-GluCer-DoxNL following different drug to phospholipid ratios: 0.25:1; 0.2:1; 0.15:1; 0.1:1 (w/w).

D:PL ratio*	IC_{50} (µM)	
	BLM	MCF-7
0.25:1	6.7 ± 3.6	6.3 ± 6.0
0.2:1	7.5 ± 2.6	18.7 ± 9.3
0.15:1	13.2 ± 5.7	9.1 ± 9.8
0.1:1	10.6 ± 4.6	10.9 ± 1.6

* P > 0.05, no significant difference between considered D:PL ratios

Supplemental Table 2 - Stability after 6 months at 4°C of different glycoceramide-enriched liposomes

D:PL (w/w) ratio	SCS-PLD	Size (nm) ± SEM	Pdi ± SEM
0.1:1	Non-enriched	99 ± 1.80	0.03 ± 0.002
	10% C_8-GluCer	91 ± 0.96	0.08 ± 0.04
	10% C_8-GalCer	92 ± 1.6	0.06 ± 0.05

Supplemental Table 3. *In vitro* IC_{50} values of doxorubicin in different cell lines, following different densities for C_8-GalCer-DoxNL

	IC_{50} (µM)		
	MCF-7	BLM	ASPC
0% C_8-GalCer-DoxNL	228.5 ± 60.7	184.8 ± 30.1	180.2 ± 17.1
5% C_8-GalCer-DoxNL	177.6 ± 61.1	253.7 ± 35.8	99.5 ± 17.5
10% C_8-GalCer-DoxNL*	5.3 ± 1.8	10.1 ± 1.14	10.3 ± 1.7
15% C_8-GalCer-DoxNL*	20.6 ± 8.0	10.6 ± 2.76	7.7 ± 2.8

* P< 0.05 versus 0% C8-GalCer-PLD (non enriched liposomes containing doxorubicin) and 5% C8-GalCer-DoxNL

A

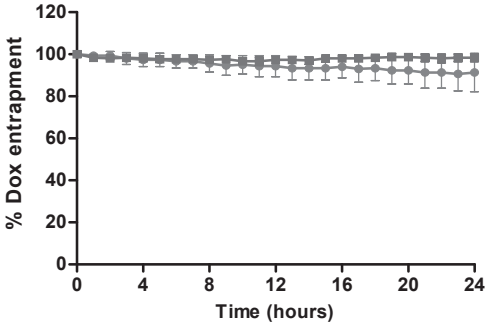

B

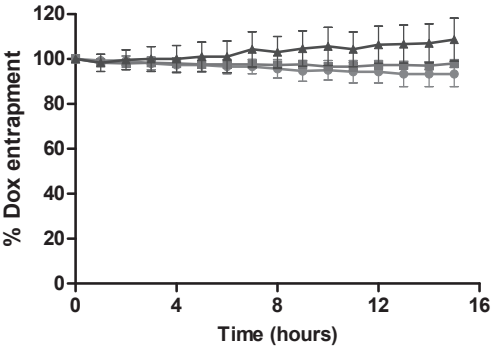

Supplemental Figure 1. (A) Stability at 37°C in the presence of 10%FCS of enriched C_8-GluCer-DoxNL (■) for 24h and (B) enriched C_8-GalCer-PLD (▲) for 15h. Measurements were based on doxorubicin fluorescence following time and were performed continuously. Both enriched-DoxNL presented a better stability profile than non-enriched-DoxNL (●)

A)

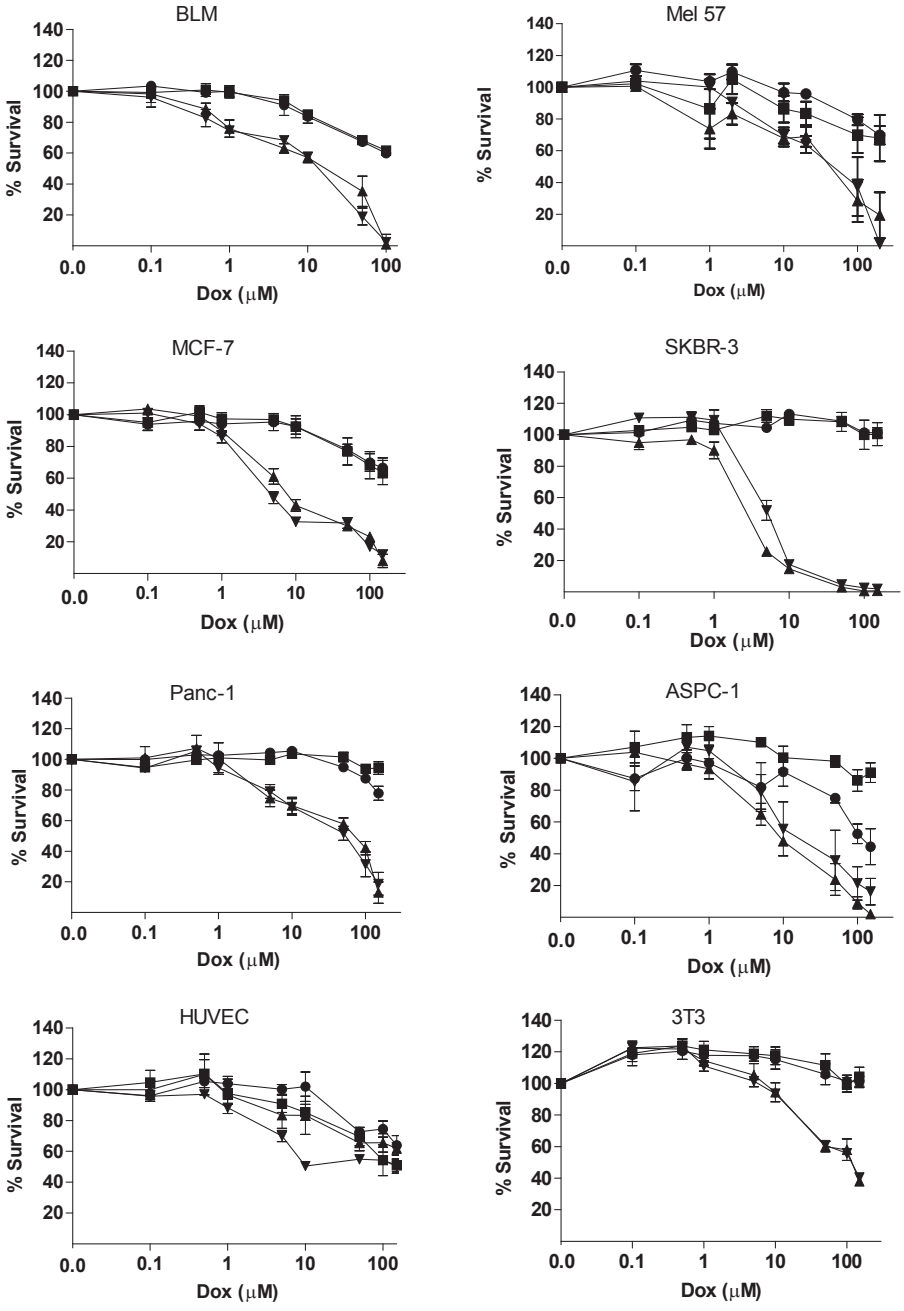
BLM
Mel 57
MCF-7
SKBR-3
Panc-1
ASPC-1
HUVEC
3T3
% Survival
Dox (μM)
0.0
0.1
1
10
100
20
40
60
80
100
120
140

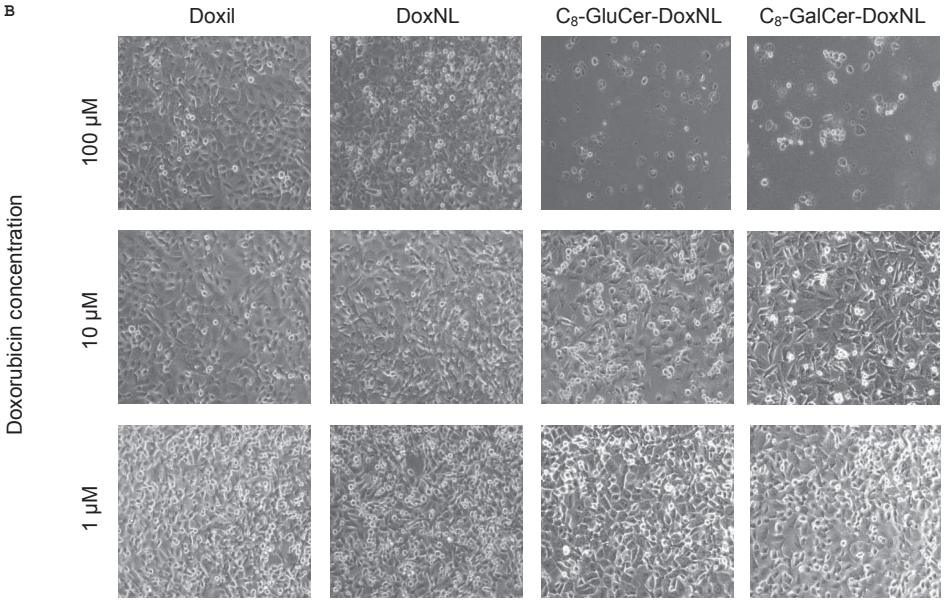

Supplemental Figure 2. *In vitro* drug efficacy toward tumor cells (BLM, Mel 57 melanoma, MCF-7 and SKBR-3 breast carcinoma, Panc-1 and ASPC-1 pancreatic carcinoma) and non-tumor cells (HUVEC, endothelial cells and 3T3, fibroblasts). (A) Cells were treated with Doxil (●), non-enriched-DoxNL (■), 10% C_8-GluCer-DoxNL (▲) and 10% C_8-GalCer-DoxNL (▼) for 24h at 37°C. Cell survival was quantified by colorimetric SRB assay. (B) Cellular morphology was analyzed by microscopy. Values represent the mean ± SEM of at least 3 experiments

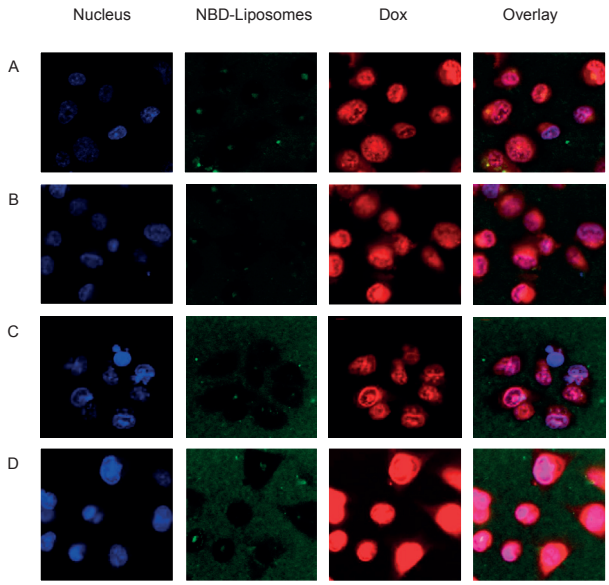

Supplemental Figure 3. Co-localization of NBD-PE labeled liposomes (green) and Dox (red) by Confocal Microscopy. After nucleus staining with Hoechst (blue), BLM melanoma

cell line was treated with 10 µM Dox in form of C_8-GluCer-DoxNL (A) and C_8-GalCer-PLD (B). ASPC-1 pancreatic carcinoma cells were equally treated with 10 µM Dox in form of C_8-GluCer-DoxNL (C) and C_8-GalCer-DoxNL (D). After treatment cells were incubated for 4h at 37°C. Nuclear and cytoplasmatic drug uptake was analyzed

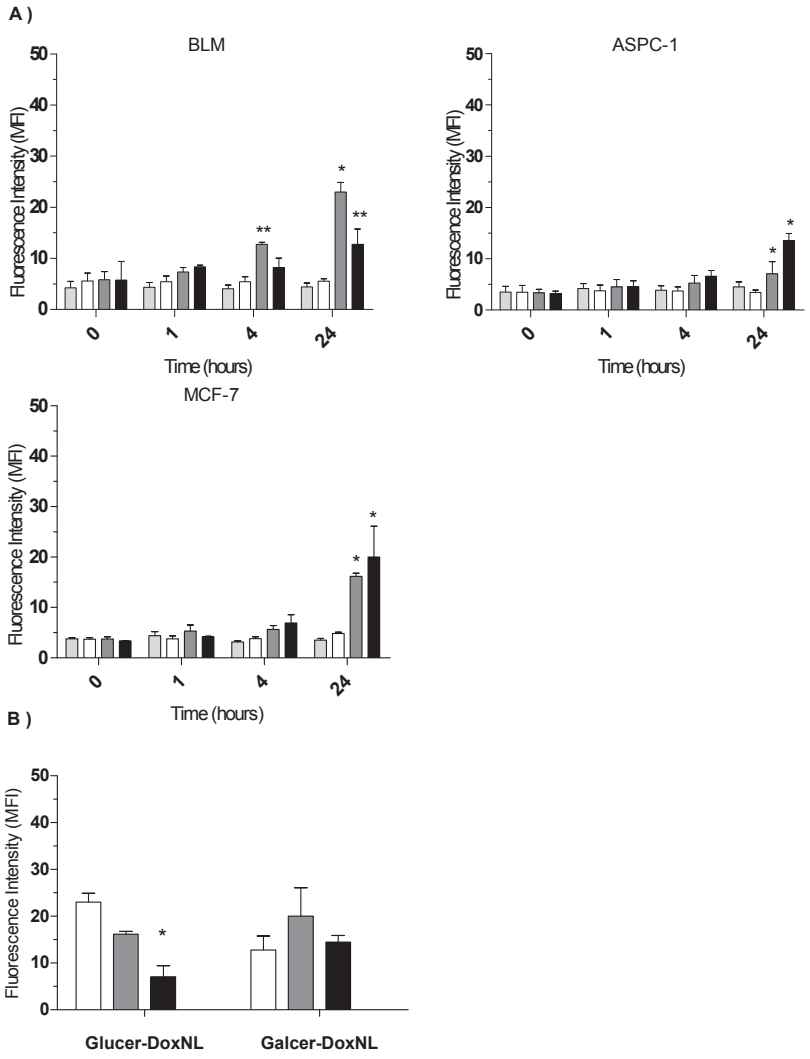

Supplemental Figure 4. Intracellular Dox uptake after treatment with DoxNL, 1 µM was quantified by flow cytometry in BLM melanoma, MCF-7 breast carcinoma and ASPC-1 pancreatic carcinoma (A). Doxorubicin was formulated in non-enriched-DoxNL (open), 10% C_8-GluCer-DoxNL (dark grey) and 10% C_8-GalCer-DoxNL (black). Fluorescence of non-treated cells was measured as a control (light grey).
At least three independent experiments were performed and values represent the mean ± SEM; *, P<0.001; **, P<0.01 and #, P<0.05 versus non enriched-DoxNL at the same time point. (B) Overview of Dox uptake by 3 different tumor cell lines incubated with 1 µM C_8-GluCer or C_8-GalCer-DoxNL after 4 h of incubation. C_8-GluCer seemed to increase Dox uptake in BLM (open) cells when compared to MCF-7 (grey) and ASPC-1 (black) cells. C_8-GalCer-DoxNL gives similar results in all three cell lines

CHAPTER 3

Supplemental Table 1. MTO loading with different gradients

		% Drug Loading		
D:PL(w/w)	Hydration buffer	MTOL	C_8-GluCer-MTOL	C_8-GalCer-MTOL
0.08	Citrate	8	3	2.5
0.08	Ammomium Sulphate	27	20	47
0.036	Ammonium Sulphate	51	70	71

More than 3 independent batches were formulated for each formulation and each measurement was performed in triplicate

CHAPTER 4

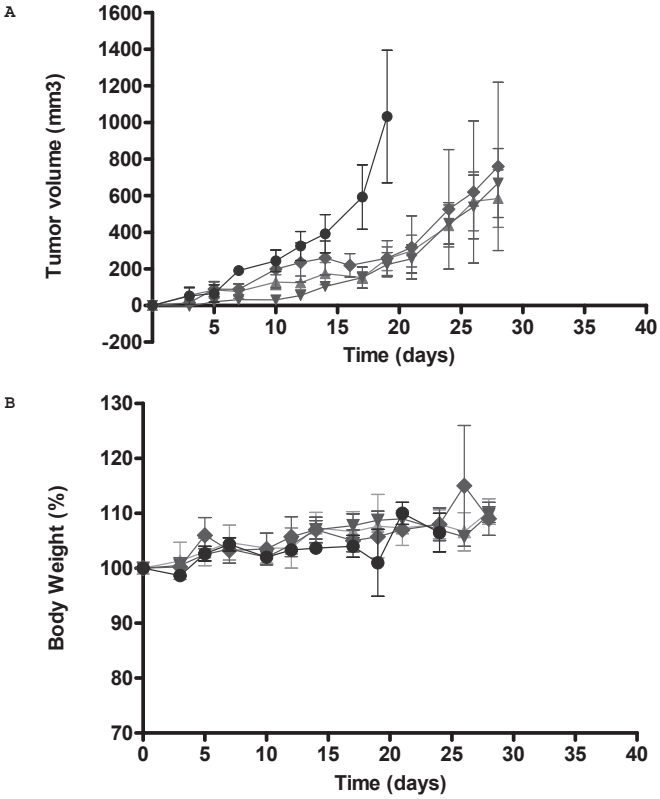

Supplemental Figure 1. Efficacy study of multiple dosing schedule of i.v. administered Liposomes : Standard-L (△), C_8-GluCer-L (▼), C_8-GalCer-L (◆). Saline i.v administration was performed in control groups (○). NMRI:nu/nu mice bearing a orthotopic MDA-MB-231 breast carcinoma tumor model were injected at same lipid concentration as efficacy study for MTOL, 5 mg·Kg^{-1} MTO every 7 days for 5 weeks. (A) Tumor growth (mm^3) and (B) % of body weight was followed up for 2 weeks after last administration. Mice presenting body weight loss superior to 20% of initial body weight were sacrificed and removed from the experiment. All data represent the mean ± STDEV for at least 3 mice